

20th century minimum and maximum temperature variations analysed on a regional scale in Switzerland

Statistical analyses of observational data

INAUGURAL – DISSERTATION

Zur Erlangung der Würde eines *Doctor rerum naturalium*
der Mathematisch-Naturwissenschaftlichen Fakultät
der Universität Freiburg in der Schweiz

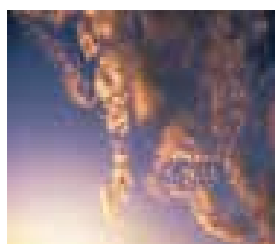
vorgelegt von

Patricia Jungo

aus (Heimatort): Düdingen und Fribourg

Dissertation Nr. 1365 – Mécanographie Universität Freiburg

Oktober 2001

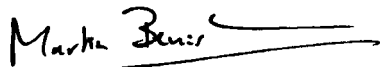


Die vorliegende Arbeit wurde von der Mathematisch–Naturwissenschaftlichen Fakultät der Universität Fribourg in der Schweiz im Dezember 2001 aufgrund der Gutachten von Prof. Martin Beniston, Prof. Claude Collet, Dr. Christoph Frei und Prof. Heinz Wanner angenommen.

The present work was accepted as dissertation by the Faculty of Mathematics and Science of the University of Fribourg in Switzerland in December 2001 based on the experts' reports of Prof. Martin Beniston, Prof. Claude Collet, Dr. Christoph Frei and Prof. Heinz Wanner.

Fribourg, 21. Dezember 2001

Der Leiter der Doktorarbeit:
Prof. Martin Beniston



Der Dekan:
Prof. Alexander von Zelewsky



Adresse der Autorin (Authors address):

Dr. Patricia Jungo
Bundesamt für Statistik
place de l'Europe 10
2010 Neuchâtel
E-mail: patricia.jungo@bfs.admin.ch

Zitierung (Citation):

Jungo P., 2001: 20th century minimum and maximum temperature variations analysed on a regional scale in Switzerland – statistical analyses on observational data. Ph.D. Thesis No. 1365, University of Fribourg, Switzerland. 221 pp.

Zu beziehen bei der Autorin (Available from the author)

Abstract:

The principal aim of this study is to establish a regional and seasonal assessment of the secular trend and the decadal-scale variability in the 20th century minimum and maximum temperature warming.

Through the principal achievements of this study I could provide a better understanding of regional climate trends in Switzerland, which is essential in order to assess the relation between climate change, natural hazards and the resulting potential risk for certain areas of this country.

CONTENTS

SUMMARY	1
ZUSAMMENFASSUNG	5
1. INTRODUCTION.....	9
1.1. GENERAL ASPECTS AND LARGE TO GLOBAL-SCALE BACKGROUND.....	9
1.2. PRINCIPAL OBJECTIVES OF THIS THESIS.....	13
1.3. CONTEXTUAL INFORMATION.....	18
1.3.1. Observed temperature fluctuations in the recent past and the present at different scales and various mountain regions.....	18
a.) <i>Mean temperature variations at the hemispheric scale</i>	18
b.) <i>Mean temperature variations on the European scale</i>	18
c.) <i>Mean temperature variations in mountain regions</i>	19
d.) <i>Mean temperature variations in Alpine countries</i>	19
e.) <i>Tmin and Tmax variations</i>	21
1.3.2. Switzerland.....	21
a.) <i>Geographical situation</i>	21
b.) <i>Importance of regional studies</i>	22
c.) <i>Sensitivity of mountain regions</i>	23
1.3.3. Changing temperature and environmental impacts.....	24
2. SOURCE DATA.....	27
2.1 GENERAL DESCRIPTION OF THE DATA NETWORK.....	27
2.2. QUALITY AND HOMOGENEITY OF THE DATA SETS.....	29
2.3. METHODOLOGICAL PROCEEDING LINKED TO THE NUMBER OF DATA TIME SERIES.....	31
3. CLIMATOLOGICAL REGIONALISATION.....	33
3.1 CHAPTER OUTLINE.....	34
3.2. DATA PREPARATION.....	36
3.3. STATISTICAL METHODS.....	37
3.3.1 Principal Component Analysis (PCA).....	37
3.3.2. Cluster Analysis (CA).....	40
3.3.3. Tests.....	41

3.4. RESULTS.....	42
3.4.1. Establishing clusters in winter.....	42
a.) PCA on winter Tmin.....	42
b.) CA on winter Tmin.....	43
c.) PCA on winter Tmax.....	45
d.) CA on winter Tmax.....	46
3.4.5. Establishing clusters in spring.....	48
a.) PCA on spring Tmin.....	48
b.) CA on spring Tmin.....	49
c.) PCA on spring Tmax.....	50
d.) CA on spring Tmax.....	50
3.4.3. Establishing clusters in summer.....	53
a.) PCA on summer Tmin.....	53
b.) CA on summer Tmin.....	54
c.) PCA on summer Tmax.....	56
d.) CA on summer Tmax.....	57
3.4.4. Establishing clusters in autumn.....	58
a.) PCA on autumn Tmin.....	58
b.) CA on autumn Tmin.....	59
c.) PCA on autumn Tmax.....	61
d.) CA on autumn Tmax.....	62
3.5. REPRESENTATIVE STATIONS PER CLUSTER.....	63
3.6. DISCUSSION.....	63
4. SECULAR TRENDS AND INTERANNUAL TO DECADEAL SCALE FLUCTUATIONS IN REGIONAL MEAN TIME SERIES.....	69
4.1 CHAPTER OUTLINE	69
4.2 PRELIMINARY ANALYSES.....	70
4.2.1. Computation of the regional mean time series.....	70
4.2.2. Limitation of the result description.....	71
4.3. PAPER BY JUNGO AND BENISTON (2001).....	72
CHANGES IN THE ANOMALIES OF EXTREME TEMPERATURES IN THE 20 TH CENTURY AT SWISS CLIMATOLOGICAL STATIONS LOCATED AT DIFFERENT LATITUDES AND ALTITUDES.....	72
Summary.....	73
1. Introduction.....	73

2. Data.....	75
2.1. Quality.....	75
2.2. Treatment.....	76
3. Methods.....	78
4. Results.....	79
4.1. Winter.....	80
4.1.1. Linear regression over three time spans.....	80
4.1.2. Anomaly fluctuations.....	81
4.1.3. 9 Periods.....	82
4.2 Spring, summer, autumn.....	85
5. Discussion.....	87
6. Conclusion.....	88
4.4. COMPARISON WITH EXISTING TEMPERATURE TREND STUDIES IN ALPINE COUNTRIES.....	90
5. VARIATIONS IN TEMPERATURE EXTREMES.....	93
5.1. CHAPTER OUTLINE.....	93
5.2. METHODS.....	96
5.3. RESULTS.....	97
5.3.1. Winter.....	97
5.3.2. Spring.....	99
5.3.3. Summer.....	101
5.3.4. Autumn.....	104
5.4. DISCUSSION.....	105
6. LINKS BETWEEN TMIN/TMAX, THE NAOI AND ALPINE WEATHER TYPES.....	109
6.1. PAPER BY BENISTON AND JUNGO (2001).....	109
SHIFTS IN THE DISTRIBUTIONS OF PRESSURE, TEMPERATURE AND MOISTURE AND CHANGES IN THE TYPICAL WEATHER PATTERNS IN THE ALPINE REGION IN RESPONSE TO THE BEHAVIOR OF THE NORTH ATLANTIC OSCILLATION.....	109
Abstract.....	109
1. Introduction.....	110
2. The influence of the NAO on Alpine climate.....	112
2.1 Influence on means.....	112
2.2 The influence on the probability density functions of climate variables.....	114

2.3 The influence on climatological weather types over the alpine region.....	120
3. Discussion.....	126
4. Conclusions.....	130
6.2. DISCUSSION INCLUDING WEATHER TYPES IN SPRING, SUMMER AND AUTUMN.....	132
7. ADDITIONAL APPLICATION OF THE REGIONALISATION METHODS (PCA AND CA) ON WIND GUST DATA.....	137
7.1. PAPER BY JUNGO, GOYETTE AND BENISTON (2001).....	137
DAILY WIND GUST SPEED PROBABILITIES OVER SWITZERLAND ACCORDING TO THREE TYPES OF SYNOPTIC CIRCULATION.....	137
Abstract.....	137
1. Introduction.....	138
2. Data.....	143
3. Methods.....	143
3.1 Wind gust probability.....	144
3.2 Synoptic weather types.....	145
3.3 Classification of Swiss climatological stations.....	146
4. Results.....	147
5. Example and Discussion.....	155
6. Conclusion.....	160
8. SYNTHESIS.....	163
REFERENCES.....	169
ACKNOWLEDGEMENTS.....	177
APPENDIX A.....	179
APPENDIX B.....	207
APPENDIX C.....	221
APPENDIX D.....	231
Curriculum Vitae.....	235

SUMMARY

The major aim of this study is to describe in a detailed manner the 20th century minimum and maximum temperature variations in Switzerland and to assess whether the magnitude of the secular warming and its interannual to interdecadal fluctuations show common seasonal patterns in different climatological regions.

In a first step different climatological regions could successfully be established for all four seasons applying a statistical clustering method (Cluster Analysis) to the minimum and maximum temperature time series of a maximum number of climatological stations situated in different parts of the country. A Principal Component Analysis is preceding the actual clustering method which allows to compare the climatological station time series based on minimum and maximum temperature variations as well as on specific station related characteristics. Each of the resulting clusters aggregates a number of climatological stations, which follow a similar temporal development in the temperature data and own comparable station related characteristics. These clusters can therefore be considered as representative of a certain climatological region, which however is not necessarily geographically uniform.

The clustering is carried out separately for two different climatological parameters in all four seasons, namely minimum and maximum temperatures in winter, spring, summer and autumn. The resulting clustering patterns reflect a strong dependency upon these climatological parameters as well as upon the seasons. Typical seasonal night-time and day-time temperature distributions over complex terrain have a determining influence on the emerging clustering patterns, which are similar in winter and autumn and in spring and summer. The classic fog and stratus areas combined with the particular cold air drainage over complex terrain have a determining influence on the clustering pattern in winter and autumn and thus the clusters are mainly specified through altitudinal stages. In spring and summer the clustering patterns are still related to the altitude they show however an additional dependency on specific geographical areas. Out of each of the eight clustering patterns three main regions emerged which could be related to the three most contrasting climatic areas in Switzerland and identified as “low altitudes, north”, “high altitudes”, and “low altitudes, south”. The description of the following analyses is restricted to these three regions.

The quantitative analyses of the minimum and maximum temperature trends and fluctuations over the 20th century are carried out on regional mean time series computed for each cluster. A new and very detailed description for the seasonal minimum and

maximum temperature variations during the 20th century in Switzerland results. Secular warming trends are detected for both, minimum and maximum temperatures. The magnitudes differ mostly between the seasons. The minimum temperatures show generally higher trend estimates than the maximum temperatures with a more pronounced secular warming in winter and autumn. Analysing the temperatures on a decadal scale an abrupt warming is detected during the 1990s, which is especially emphasised for winter minimum temperatures in the region “high altitudes”. A further warm period during the 20th century occurred from 1940 to 1950. In contrast to the warming at the end of the century this mid-century warming is most evident in maximum temperatures during spring and summer in the regions “low altitudes, north” and “high altitudes”. The long-term decadal trend shows that minimum and maximum temperatures in all regions and seasons except for autumn are persistently increasing since 1980. The autumn temperatures play a special role since their secular warming trend is principally related to rather cold temperatures in the beginning of the century and a mild period during the 1980s, which, however, is not extended into the 1990s. These observations lead to the conclusion that a change in the seasonal warming pattern occurred during the last few decades.

Analyses of minimum and maximum temperature extremes are supporting the conclusions formulated above. The warming trends as well as the mild phases, which are observed in minimum and maximum temperatures, can generally be related to a warming in both tails of the distribution (warm and cold).

The described results can be linked to the 20th century evolution of large and small scale synoptic systems. The North Atlantic Oscillation exerts a high influence on winter weather types in Switzerland. The increasingly positive North Atlantic Oscillation Index during the last two decades most probably generated a changed frequency pattern of the alpine weather types in winter. In the 1990s this is expressed with a higher frequency of warm winter weather types (convective high-pressure and western advective) on the expenses of a major cold type (eastern advective). The frequency analysis of the alpine weather types for the other seasons does not yield as obvious results as for winter. It was found however, that the main warm periods occurring in different seasons during the century (mid-century summer warming; autumn mild phase in the 1980s) can principally be related to an elevated number of convective high-pressure weather types which usually generate milder temperatures.

In an additional chapter the climatological regionalisation method, previously used with temperature data is applied to wind gust data. The analyses show that the gust factor between maximum and mean daily wind speeds over complex terrain follow a lognormal

distribution. This knowledge in combination with the climatological regionalisation serves to estimate wind gust speed probabilities over the complex terrain of Switzerland according to three types of synoptic weather situations.

ZUSAMMENFASSUNG

Das Hauptziel dieser Studie ist eine möglichst detaillierte Beschreibung der Variationen der Minimum- und Maximumtemperaturen während des 20. Jahrhunderts, wobei es von Interesse ist abzuklären, ob der Umfang der Jahrhundertwärmung sowie die annuellen und dekadalen Schwankungen in verschiedenen Regionen der Schweiz übereinstimmende saisonale Muster aufweisen.

In einem ersten Schritt wurde eine möglichst hohe Anzahl von Minimum- und Maximumtemperaturzeitreihen der Landesklimastationen mit einer statistischen Gruppierungsmethode (Clusteranalyse) erfolgreich nach Jahreszeit geordnet. Vor der eigentlichen Gruppierungsmethode wird eine Hauptkomponentenanalyse durchgeführt, die es erlaubt, einen Vergleich der Klimastationen anhand der Variationen in Minimum- und Maximumtemperaturen sowie spezifischen stationsbezogenen Eigenschaften vorzunehmen. In jeder dieser so erhaltenen Gruppen werden Klimastationen vereint, welche ähnliche zeitliche Temperaturvariationen aufweisen und deren stationsbezogenen Eigenschaften vergleichbar sind. Somit können diese Gruppen als jeweilige Vertreter einer bestimmten Klimaregion, deren Gebiet jedoch nicht unbedingt geographisch zusammenhängt, angenommen werden.

Die Clusteranalyse wird jeweils auf Minimum- und Maximumtemperatur in den vier verschiedenen Jahreszeiten Winter, Frühling, Sommer und Herbst angewendet. Die daraus resultierenden verschiedenen Gruppierungsmuster widerspiegeln eine starke Abhängigkeit von den Klimaparametern und den Jahreszeiten. Die saisontypische Nacht- und Tagestemperaturverteilung über komplexem Terrain übt einen bestimmenden Einfluss aus auf die sich bildenden Gruppierungsmuster, welche im Winter und im Herbst sowie im Frühling und im Sommer am ähnlichsten sind. Während den kühlen Jahreszeiten wird die Gruppierung der Klimastationen von den typischen herbstlichen und winterlichen Nebel- und Stratusgebieten wie auch vom Absinkverhalten der Kaltluft über komplexem Terrain am stärksten beeinflusst. Das Gruppierungsmuster ist daher eng verbunden mit der Höhe über Meer, auf welcher sich eine Klimastation befindet. Während den warmen Jahreszeiten ist die Verbindung zur Höhe immer noch zu finden, die Zugehörigkeit zu einer geographischen Region ist jedoch genauso massgebend. Drei bestimmte Klimaregionen, welche mit den drei gegensätzlichsten Klimazonen in der Schweiz in Verbindung gebracht werden können, treten innerhalb der acht erhaltenen Gruppierungsmuster regelmässig auf. Die drei Regionen werden dementsprechend benannt als: „tiefere Lagen, Nord“, „hohe Lagen“ und „tiefere Lagen, Süd“. Die

Beschreibung der Analysen beschränkt sich im weiteren Verlauf der Arbeit auf diese drei Regionen.

Die weiteren quantitativen Analysen, welche der Erfassung des Trends in den Minimum- und Maximumtemperaturen und deren Schwankungen während des 20. Jahrhunderts dienen, basieren auf mittleren regionalen Zeitreihen, die für jede einzelne Gruppe berechnet werden. Daraus geht eine neue und sehr detaillierte Beschreibung der saisonalen Minimum- und Maximumtemperaturvariationen während des 20. Jahrhunderts hervor. Die Minimum- sowie die Maximumtemperaturen unterliegen einer allgemeinen Erwärmung, welche sich in ihrem Ausmass zwischen den verschiedenen Jahreszeiten am meisten unterscheidet. Die Minimumtemperaturen weisen eine grundsätzlich grössere Erwärmung als die Maximumtemperaturen auf, was sich am stärksten im Winter und im Herbst äussert. Eine dekadal skalierte Untersuchung der Temperaturen lässt darauf schliessen, dass die 90er Jahre einer abrupten Erwärmung unterlagen, welche in den winterlichen Minimumtemperaturen in der Region „hohe Lagen“ besonders nachdrücklich ist. Zwischen 1945 und 1950 ist eine weitere Warmphase zu finden, welche im Gegensatz zur Warmphase in den 90er Jahren vor allem in den Maximumtemperaturen des Frühlings und des Sommers in den Regionen „tiefere Lagen, Nord“ und „hohe Lagen“ ermittelt werden kann. Der dekadal skalierte Langzeittrend weist für alle Regionen und Jahreszeiten, ausser dem Herbst, von 1980 an kontinuierlich ansteigende Temperaturen auf. Die Herbsttemperaturen nehmen eine etwas spezielle Rolle ein, da sie nicht von einer Erwärmung in den 90er Jahren geprägt werden. Die starke Erwärmung, die ihnen über das Jahrhundert hinweg eigen, ist kann vor allem auf kalte Werte am Anfang des Jahrhunderts und eine milde Phase während den 80er Jahren zurückgeführt werden. Diese Beobachtungen lassen auf einen Wandel des jahreszeitlichen Erwärmungsmusters über die letzten Dekaden hinweg schliessen.

Die bisher beschriebenen Resultate können auf den Ergebnissen aus der Analyse der Minimum- und Maximumtemperaturextreme abgestützt werden. Die gefundenen Erwärmungstrends sowie die verschiedenen Warmphasen stehen in enger Verbindung mit einer Erwärmung der Extremwerte in beiden Enden (extrem warm und extrem kalt) der Minimum- und Maximumtemperaturverteilung.

Die Ergebnisse können in einen direkten Zusammenhang mit der Entwicklung diverser klein- und grossräumiger synoptischer Systeme im 20. Jahrhundert gebracht werden. Die Nordatlantische Oszillation übt einen grossen Einfluss auf die Wetterlagen in der Schweiz während des Winters aus. Mit grosser Wahrscheinlichkeit ist der über die letzten zwei Jahrzehnte hinweg zunehmend positive Nordatlantische Oszillationsindex bezeichnend

für einen Wandel im Frequenzenmuster der winterlichen Wetterlagen. Es steht fest, dass während der 90er Jahre ein vermehrtes Auftreten von sogenannten „warmen“ winterlichen Wetterlagen, wie konvektive Hochdrucklagen und advektive Westlagen, einhergeht mit einem markanten Rückgang der sogenannten „kalten“ winterlichen Wetterlagen wie sie die advektiven Ostlagen darstellen. Die Frequenzanalyse der Wetterlagen in den anderen Jahreszeiten ergibt keine so klaren Resultate. Die grossen Warmphasen während des Jahrhunderts (Sommer Mitte Jahrhundert, Herbst in den 80er Jahren) können jedoch in Verbindung gebracht werden mit einem erhöhten Auftreten von konvektiven Hochdrucklagen, welche für mildere Temperaturen bedeutend sind.

In einem zusätzlichen Kapitel wird die klimatologische Regionalisierungsmethode wie sie im vorhergehenden Teil an Temperaturdaten angewendet worden ist an Windgeschwindigkeitsdaten getestet. In der Analyse wird aufgezeigt, dass über komplexem Terrain, der Faktor zwischen den täglichen maximalen und mittleren Windgeschwindigkeiten eine lognormale Verteilung annimmt. In Verbindung mit einer klimatologischen Regionalisierung, welche für drei Arten von synoptischen Wetterlagen vorgenommen wird, dient diese Erkenntnis dazu, die Wahrscheinlichkeit der Windböengeschwindigkeit über dem komplexen Terrain der Schweiz abzuschätzen.

1. INTRODUCTION

1.1. GENERAL ASPECTS AND LARGE TO GLOBAL-SCALE BACKGROUND

During the past two decades the issue of the influence of human activities on natural systems on earth has gained a lot of importance and climate change is one of the central terms used within this context. Prior to the industrial era, climate variability was induced essentially by natural forcings like volcanism or the solar activity. The amount of greenhouse gas (GHG) in the atmosphere like carbon dioxide (+30%), methane (+145%) and nitrous oxide (+15%) has considerably increased since the pre-industrial times, i.e. about 1750 (IPCC, 1996, p.3). The amplification of these anthropogenic forcing factors is mainly due to the growing rate of fossil fuel combustion, land-use change and agriculture. The description of climate variations on different spatial and temporal scales and their link to natural or anthropogenic forcing factors are two main concerns in climate research. Statistical methods applied to observational data records are the principal tool for the description of climate variations whereas it is a major aim of the climate modelling to attribute these observations to either anthropogenic or natural forcing.

The present study is of purely statistical nature with the basic idea to describe the space time variations in minimum and maximum temperatures during the 20th century in Switzerland. The methods used serve the purpose to detect changes and trends in temperature variability rather than to relate observed changes to climate change, i.e. make attributions to anthropogenic or natural forcings. Even though the signal of the global climate change can be reflected in regional trends it is impossible to relate them to either one of the forcings without the necessary quantitative information about expected changes due to, e.g. greenhouse gas, volcanic or solar forcing, which can only be estimated by a regional climate model (Schönwiese et al., 1994; Easterling et al., 1997).

It was found reasonable for the present study to concentrate on the parameters minimum and maximum temperature and to bring their temporal variation into relation with changes in warm and cold temperature extremes as well as with alpine weather types. Temperature and/or precipitation are frequently used parameters in climate studies. These are two of the most often measured climatological variables with a generally high spatial coverage and, as mentioned in Beniston et al. (1994), temperature is together with precipitation, one of the principal controlling factors on a wide range of climate-dependent environmental and ecological systems. In the report of the Intergovernmental Panel of

Climate Change (IPCC) it is declared, referring to analyses of worldwide 20th century observational data records, that the response to a general warming is likely to lead to a decrease in days with extremely low temperatures (IPCC, 1996, chapter 3.5). New results of modelling studies since the IPCC report 1996 showed that especially in the Northern Hemisphere midlatitudes extremes are significantly modified through changes in the daily temperature variability, which was found to generally decrease in winter and increase in summer (Meehl et al., 2001).

Most of the current information on the climate is based on trends made on observational data for the 20th century. Regular and spatially corresponding measurements of different climatic variables have only been recorded during this period. However, the trends should not be evaluated without considering some general information about the further past. Pfister (1999) sees an inconvenience in assessing climate tendencies by referring only to the trends of the 20th century, which for the climate history represents a rather brief time interval. A full climatic cycle is possibly ongoing over a millennial or even longer time scale and we cannot know with certainty on which point in a long natural cycle we are at the actual. Further, climate warming is not particular to the 20th century, a number of warm epochs with temperatures in the Northern Hemisphere situated well above today's have been detected through analyses on paleoclimatic data (Ahrens, 1994; Bradley and Jones, 1995). The Pliocene climatic optimum (3.3 – 4.3 mio years BP), the Eemian interglacial optimum (130'000 years BP) and the mid-Holocene optimum (5'000 – 6'000 years BP) are the 3 warmest epochs of the past. The latter period is often used as an analogue to the climate expected in the first half of the 21st century. However, the transition to the mid-Holocene climatic optimum took far longer than what is expected from greenhouse gas forcing for the next century in some regions (IPCC, 1996, chapter 3.6). In addition, Bradley (2000) reminds that the 20th century warming was preceded by the period of the Little Ice Age (approx. 1450-1850), which was exceptionally cold for the late Holocene. Thus, large parts of the world have experienced a fluctuation from very cold annual mean temperatures to very warm annual mean temperatures within a range of only 200 years. In consequence, these analogues for warm periods are not a direct parallel for the future and therefore, the debate on the normality of the present changes and their predictability is relevant.

There is increasing evidence that changes in climate are taking place in an accelerated manner over the last few decades; the global mean temperature is currently about 0.7°C above its 1900 value (IPCC, 1996, chapter 3.2; WMO, 1999). Mann et al. (1999)

concluded in a study considering a paleoclimatic data set that the Northern Hemispheric warming in the latter 20th century is anomalous in the context of at least the last millennium. The authors support this conclusion by the finding that the decade of the 1990s was, with a moderately high level of confidence, the warmest decade since the year 1000 and 1998 the warmest year.

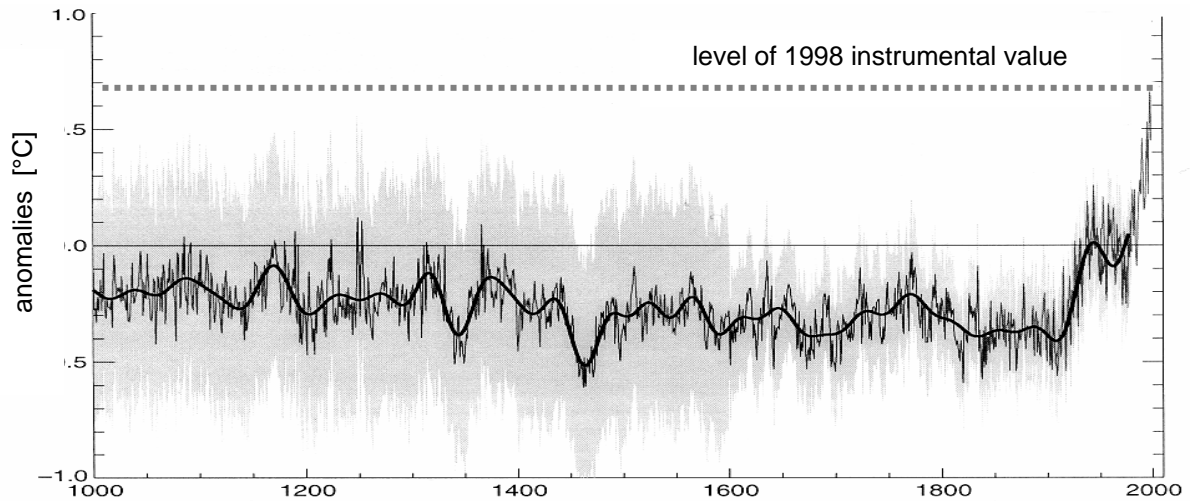


Figure 1.1: Northern Hemisphere annual mean temperature anomalies (relative to 1961 to 1990) reconstructed from paleoclimatic data (since 1902 instrumental data is included) for the period AD 1000 to 1999. The light-grey surface indicates the standard error limits, the black line is a 40 year smoothed curve. Source: IPCC TR (2001).

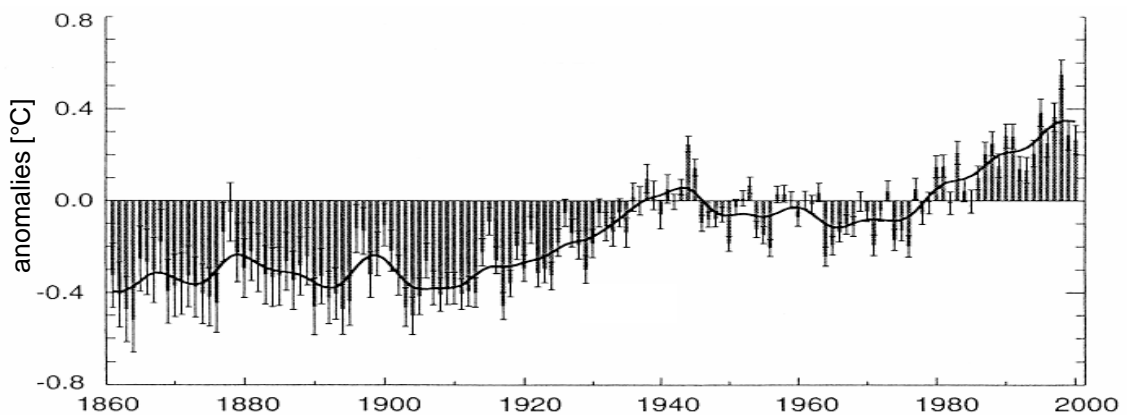


Figure 1.2: Observed global annual mean temperature anomalies (relative to 1961 to 1990) from 1861 to 2000. The annual means are combinations of land-surface air and sea surface temperatures. The standard errors are indicated as bars on each annual series. Source: IPCC TR (2001).

For completion of the general information two recent studies discussing the influence of the anthropogenic forcing on the observed 20th century global to hemispheric scale mean temperature warming are cited in the following. Stott et al. (2001) show through an optimal detection method (seasonal and annual model data compared to observational data) that on a global scale both, anthropogenic and natural effects have contributed to the warming in the first half of the 20th century. The principal cause for the warming in the latter half, in contrast, was found to be mainly anthropogenic due to increases in GHG. In a study conducted by Crowley (2000) sufficient agreement was found between model results and observations for the past 1000 years to conclude that the anthropogenic increase in GHG explains most of the 20th century climate change observed in the Northern Hemisphere. The author further states that the natural variability, considering solar irradiance and volcanism as forces, has minor effects on the decadal-scale 20th century temperature variations while in times before 1850 between 41 and 64% of the variations could still be explained by these forces. These results provide evidence that on a global or hemispheric scale anthropogenic influences on the climate system can unmistakably be detected for the 20th century.

According to the Milankovitch astronomical theory described in Berger (1992), a climate model, under absence of other natural and of all anthropogenic influences, shows that the climate should be tending towards another Ice Age in about 60'000 years, with the first climax of colder climate occurring around 3'000 – 7'000 years from now. The net effect of the increase of all trace substances in the atmosphere as a result of man's activities is apparently counteracting this natural cooling trend and is tending towards a generalised warming.

1.2. PRINCIPAL OBJECTIVES OF THIS THESIS

Various studies discussing the topic of temperature changes, analysing present day or paleoclimatic and paleoecologic climate records linked to environmental, societal or economic systems, have already been carried out (discussed in the IPCC reports 1996, 1996a, 1996b, 1998). However, most of these studies using the Swiss temperature data set are based on the time series of a limited number of climatological stations, which are, without further testing, considered as representative for particular and extensive regions. This leaves us with isolated sets of information and important knowledge may be lost due to a lack of coherence. Further, there has been little extensive work done on the specificity of regional climate itself in Switzerland and consequently, a better understanding of regional climate trends is essential to assess the relation between climatic change, natural hazards and the resulting potential risks for certain areas.

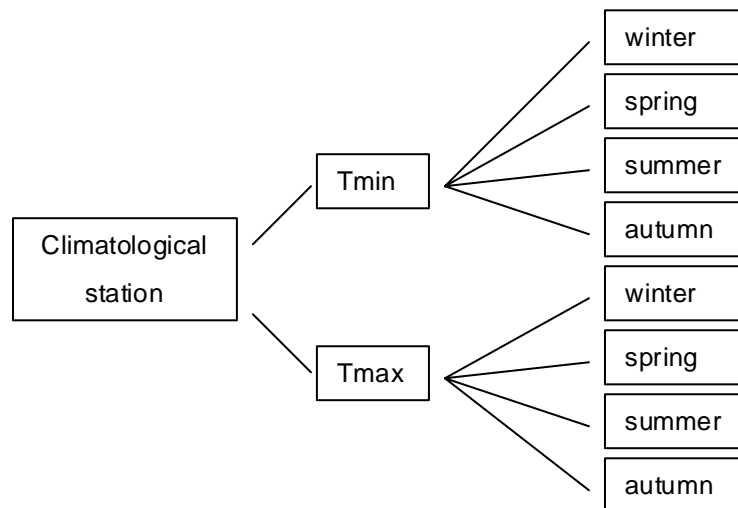
The objective of the present study is to describe and quantify the decadal-scale variations and secular trends of minimum and maximum temperatures in 4 separate seasons during the 20th century for several climatological regions in Switzerland. The secular trends in temperature extremes (minima and maxima exceeding a certain threshold) and the decadal frequency of alpine weather types since the middle of the century are analysed and brought into relation with the temporal variations found in both, minimum and maximum temperatures. Some focus will be placed on variations during the 1990s. These results constitute an important basis for assessing the possible climatic influence for concurrent variations of ecosystems, glacier, water levels and natural hazards.

Additionally Swiss wind speed data series are analysed on a daily basis. The aim is to calculate the probability of exceeding a gust speed based on the mean wind in relation to the prevailing synoptic weather type. This analysis represents a further application of the statistical regionalisation method used with minimum and maximum temperatures.

At this stage precision concerning a few basic assumptions and frequently used terms and should be provided:

- Minimum and maximum temperature will hereafter be referred to as Tmin and Tmax.
- The abbreviation “Tmin/Tmax” signifies “both parameters, Tmin as well as Tmax”.
- The term region does not refer to a closed geographical area as such but rather to single points in the geographical space, which are linked to clusters by the means of a statistical method.
- The terms region, group and cluster are used as synonyms.

- T_{min} and T_{max} will be analysed as separate parameters in the 4 seasons: winter (DJF), spring (MAM), summer (JJA) and autumn (SON), which yields in 8 separate data sets. This could be expressed as organigram:



Organigram 1.1: Type and amount of data sets analysed per climatological station

In order to attain the objective of this thesis, several working steps have been defined:

- I. Choosing a period during which a maximum number of Swiss climatological stations are in operation and evaluate their quality by analysing the meta data. *Chapter 3.*
- II. Through Principal Component Analysis reduction of data by extracting a number of components explaining the major part of the variance in the original data matrix and assignment of typical characteristics (physical, surrounding environment of climatological stations) to these components. *Chapter 3.*
- III. Through Cluster Analysis definition of a number of regions per season as a function of the daily T_{min}/T_{max} time series of the selected climatological stations and the extracted components. *Chapter 3.*
- IV. Selection of representative stations for each region. *Chapter 3.*

- V. Creation of regional mean time series based on the representative stations. *Chapter 4.*
- VI. Analysing the secular, the recent 60-year and 40-year trends as well as the interannual and interdecadal variations in Tmin/Tmax for the 20th century on regional mean time series. *Chapter 4.*
- VII. Comparing of the observed regional scale trends and tendencies to results of existing studies carried out on the regional to global scale. *Chapter 4.*
- VIII. Analysing the secular trend in the warm and cold temperature extremes, exceeding a given threshold within Tmin/Tmax in specific regions. *Chapter 5.*
- IX. Relating the results found for the temperature extremes of Tmin/Tmax to the temporal variation of Tmin/Tmax. *Chapter 5.*
- X. Analysing the interdecadal changes in the frequency of alpine weather types since the middle of the 20th century for each season. *Chapter 6.*
- XI. Relating the observations of the weather type frequency to the temporal variation of Tmin/Tmax. *Chapter 6.*
- XII. Repeating Principal Component and Cluster Analysis on wind speed data. Defining a number of regions for different synoptic circulation patterns over the alpine region in function of wind gust data and the extracted components. *Chapter 7.*
- XIII. Calculating regional exceeding probabilities for wind gusts. *Chapter 7.*

The following section describes the topic treated in each chapter:

Chapter 1, Section 1.3: In this section, a general description of the temperature evolution on the European and regional scale is given and regional scale background information on the area analysed as well as on the issue of temperature changes is provided.

Chapter 2: This chapter comprises a general description of the data set upon which all analyses are based. For statistical analyses of time series, it is essential that the time span of the data series is of sufficient duration. Further, the quality of the data in terms of

accuracy of the observations and homogeneity is essential for the quality of the results. 132 climatological stations distributed throughout Switzerland have been evaluated, reviewing the meta data (description of the stations' history) and collecting information about the placement and geographical orientation of the stations. Additional information about the data homogeneity of Swiss climatological stations is provided in the existing literature and has been summarised in this chapter. In Chapter 3 (Section 3.5.) a comparison with homogenised data sets of Norm90 (MeteoSwiss) is made for the T_{min}/T_{max} time series of the climatological stations which were selected as representative and therefore to use for the further analyses in Chapter 4.

Chapter 3: With the purpose of subdividing a high number of climatological stations as a function of T_{min}/T_{max} for each season separately a Cluster Analysis is used (CA). In order to reduce the amount of data and to assure a more robust CA the time series are processed using Principal Component Analysis (PCA). The resulting regions are clusters of climatological stations, which exhibit a comparable variability in their temperature data time series. Similar station-related descriptive characteristics as for example the geographical location, the altitude, special site characteristics, topography and population density can be assigned to them.

It should be emphasised again that the term region in this case refers to a subject related, spatially incoherent area based on single points that are represented by single climatological stations.

The regionalisation offers the major advantage that a number of representative climatological stations, which meet certain quality measures, can be selected per region. Consequently, the following analyses can be carried out on the time series of either only one single representative station per region or on one mean time series for the region as a whole, which is based on all representative stations. This results in a high quality data set for an entire region.

Chapter 4: The topic of this chapter is on the one hand to present 20th century trends and variations of T_{min}/T_{max} in Switzerland for the period 1901-1999, referring to the regions constructed on a seasonal basis. On the other hand it is to highlight the unusually fast and important temperature rise that has taken place since the end of the 1980s and its seasonal and regional dependency. The results are placed into a context with existing studies carried out in Switzerland (which often suffer of limitations mentioned in the first section of 1.2.) and are compared to findings of other regions in different countries.

Chapter 5: Since the environment generally reacts nonlinearly to extremes, it is important to analyse the tails of the Tmin/Tmax distribution in relation to the entire distribution. A rise or drop in the temperature trend can be due to a change in either tail or only one tail of the distribution. This is a non-neglecting question to be answered in order to be able to assess regional ecological and economic consequences. Based on the results of Chapter 3 and 4, secular trends in warm and cold extremes within Tmin/Tmax are analysed and systematically compared between regions, Tmin and Tmax and seasons. The monthly 10% mean value for both temperature extremes (3 warmest and coldest values within Tmin/Tmax) are used as thresholds.

Chapter 6: The increasingly strong positive anomalies in the North Atlantic Oscillation Index (NAOI) since the end of the 1970s have a considerable influence on the alpine weather, especially during the winter season (Beniston et al., 1994; Wanner et al. 1997, 2000; Stefanicki et al., 1998). Thus, the variations in climatological parameters respond to a certain degree to the forcing of the NAOI. This relation is tested for Tmin/Tmax among other parameters and the occurrence of typical alpine weather types during the second half of the century is analysed for each season based on 5 equal periods from 1945 to 1999.

Chapter 7: This chapter serves the purpose to test whether the regionalisation method used for Tmin/Tmax is also valid for wind speed data during different synoptic circulation patterns over the alpine region. In addition a method developed for a rather uniform terrain in the USA in order to predict the expected value of the daily maximum wind gust speed knowing the mean wind is now applied to the complex terrain of Switzerland (objective f). The results could have value for predictions of high wind speeds over complex terrain.

1.3. CONTEXTUAL INFORMATION

1.3.1. Observed temperature fluctuations in the recent past and the present at different scales and various mountain regions.

a.) Mean temperature variations at the hemispheric scale

Referring to Jones and Briffa (1992), who analysed world-wide seasonal and annual mean temperature anomalies (relative to 1951-70) on observational data during 1850 to 1990 the continental mid-to-lower latitude areas of the Northern Hemisphere were subject to some of the greatest warming during the 20th century. Analysing world-wide interdecadal mean temperature anomalies (relative to 1951-80) on observational data over the period 1881 to 1990 Parker et al. (1994) describe a generally cold end of the 19th century and start to the 20th century, together with a substantial warming between about 1920 and 1940. According to these authors, a slight cooling of the Northern Hemisphere took place between the 1950s and the mid-1970s, whereas the Southern Hemisphere was subject to a progressive warming. They state further that recent warming has been most marked over the northern continents in winter and spring, with the exception of Greenland, the north-western Atlantic and the midlatitude north Pacific.

b.) Mean temperature variations on the European scale

Based on historical records, Lamb (1995) states that it was not until the late 19th or the early 20th century that a more lasting warm period was established in Europe after the Little Ice Age (approx. early 16th to late 19th century). The author indicates that around the 1920s and 1930s, the climatic warming finally became noticeable to most people due to obvious changes as for example in Spitzbergen, where the open season for shipping was extended from three months per year before 1920 to over seven months per year by 1939. At the same time, the average total area of the arctic sea ice declined by between 10% and 20%. Additionally, the growing season in temperate latitudes increased in duration over this period of time. The last frost in spring was recorded at increasingly earlier dates and the first frost in late autumn correspondingly later. Analysing the seasonal mean temperature anomalies (relative to 1961-90) on observational data from 1891 to 1990, Schoenwiese et al. (1994) found a strong winter warming in Eastern Europe, a moderate one in Western Europe and further a strong spring warming in

Northeastern Europe and a moderate autumn warming over the entire continent. Some of the regions analysed show a seasonal cooling, which is never as strong as the warming trends, however. An Italian study (Southern Europe) conducted by Maugeri et al. (1998) on monthly mean temperatures over the period of 1867 – 1993 indicates strongest linear warming trends in winter followed by autumn. The authors believe that the significant trend values, which they report, are more closely related to the high temperatures of the last 5 years of the period analysed than to a continuous positive trend.

c.) Mean temperature variations in mountain regions

Diaz and Bradley (1997) have undertaken a study concerning the temperature variations at high elevation sites during the 20th century. Analysing annual mean temperature anomalies (relative to 1951-70) on observational data over the period 1880 to 1990, they conclude that in recent decades, the strongest warming at high elevations principally occurred in Western Europe, with the exception of the Scandinavian region. According to the authors, the Caucasus mountains do not exhibit the recent warming observed in the West European mountains. The temperature series for the Asian high altitude regions and the North American continent, however, confirm the same general warming features as in Western Europe. In an analysis of annual surface temperature anomalies, Villalba et al. (1997) have analysed tree-ring records in the Andes of northern Patagonia at altitudes between 1200 and 1750m. The reconstruction of annual mean temperatures since 1750 shows substantially higher temperatures in the 1980s compared to the past 250 years. Other warm periods in this region also occurred during the 1910s and during the second half of the 18th and the early 19th centuries. 20th century cold episodes in the Patagonian Andes were found between 1950 to 1955 and 1965 to 1976.

d.) Mean temperature variations in Alpine countries

During the period of the Little Ice Age two warmer periods have been detected in a 240 year long time series (combination of instrumental records and proxydata between 1760 and 1998) in the alpine region (Böhm et al., 2000). The first lasted from the 1790s to the 1820s and the second from the 1860s to the early 1870s. Further, they confirm a temperature rise during the entire 20th century with a first maximum in the 1950s and a second one in the 1990s, which was the strongest in the whole period analysed. In the alpine countries glaciers are a common source for proxydata. In Barry (1992) a

description of the most recent advances and recessions shows that many alpine glaciers were still advancing after the Little Ice Age until about the 1920s. In the 1890s this was found to be mainly due to cool and cloudy summers which were coupled later on with cool and snow rich winters. During the period 1945-54 a maximum recession, which can be associated to higher temperatures, an increased sunshine duration and reduced precipitation, was observed. A slight re-advance, in relation with cooler summers, was noticeable during the late 1960s to the early 1980s. According to Haeberli (1994) alpine glacier and permafrost signals of recent warming trends constitute some of the clearest evidence available concerning past and present changes in the climate system. The glacier changes in particular indicate that the secular changes in surface energy balance may well be in accordance with the estimated anthropogenic greenhouse forcing.

Based on historical records Pfister (1999) presents three major temperature patterns having strongly affected the Swiss climate of the past 500 years with analogues detected in the climate of the 20th century. In this study monthly mean temperatures are expressed relative to the 1901-1960 averages.

1. *Great fluctuations in the variability.* Decades with either a very high or low frequency in anomalies were numerous in the 16th and 17th century. Some were characterised through uniquely negative or positive temperature anomalies which has only re-occurred in the decade 1986-95.

2. *Slow changes (regarding to the 500-year time scale).* Since the beginning of the 20th century, cold temperature anomalies are tending to disappear. A similar event can be found in the 17th century.

3. *Sudden changes.* Changes from a warm to a cold climate or vice versa have taken no longer than a few decades during the last glaciation and the subsequent era. The Little Ice Age also started with a sudden change in the middle of the 16th century. A comparable climatic flip into the other direction started in the late 1980s.

It is observed that the annual mean temperature warming in Switzerland has not taken place in a gradual and continuous manner since the beginning of the 20th century, but rather in separate periods with substantial warming in the 1920s, the 1940s and in the 1980s (Beniston et al., 1994, Wanner et al., 1997). The 1920 and 1980 warmth can be associated to a higher frequency of the mild westerly weather type during winter, which is linked to a positive North Atlantic Oscillation Index whereas the 1940s warmth in contrast is principally related to warmer summers (Wanner et al., 1997). In a study, analysing the annual mean temperatures anomalies (relative to 1951-80) for the period 1901-95 of 8 Swiss climatological stations situated at altitudes between 570 and 2500m, Diaz and

Bradley (1997) state that the warming experienced since the 1980s in the Alps is stronger than what has been observed for the same period on the global scale. The authors indicate that analyses on climatic records in the Austrian and Bavarian Alps resulted in comparable conclusions.

e.) T_{min} and T_{max} variations

On a hemispheric scale a generally asymmetric evolution since the late 1950s, expressed in terms of a stronger increase in T_{min} than in T_{max} has been observed by Karl et al. (1993) who analysed monthly mean T_{min} and T_{max} records. More recent work by Dai et al. (1999), based on observational records of worldwide monthly mean T_{min} and T_{max}, supports this conclusion. Even though regional temperature fluctuations are spatially very varied this evolution has been widely confirmed on the Swiss scale by results from several analyses on the fluctuation of annual or monthly mean T_{min} and T_{max} during the 20th century (Beniston et al., 1994; Baeriswyl and Rebetez, 1996; Weber et al., 1994, 1997, Heino et al. 1999).

More exhaustive information on T_{min} and T_{max} trends in the 20th century are provided in Section 4.4 where the results of the present study are compared to similar studies undertaken in Europe.

1.3.2. Switzerland

a.) Geographical situation

Switzerland is characterised by a very complex topography; the country can be divided into four main regions. The Jura is a mountain range in the northwest, the Plateau includes a plain stretching from the west to the northeast, the Alps are situated in the southwestern, central and eastern part of the country and the South covers the region from the southern slopes of the Alps to the Po basin. (Figure 1). The Alps traverse the country from SW to NE separating the Jura and the Plateau from the South. Being under the influence of mediterranean weather systems, the climatic conditions south of the Alps can be quite different to those north of the Alps, which are under atlantic or continental influence. The Alps exert a shielding effect against advances of cold air originating from

the north or northeast for areas on the southern side of the Alps, which are thus found to be 2 – 4 °C warmer than areas on the northern side (Schär et al, 1998).

Hereafter the term “Alps” always refers to the Swiss Alps only.

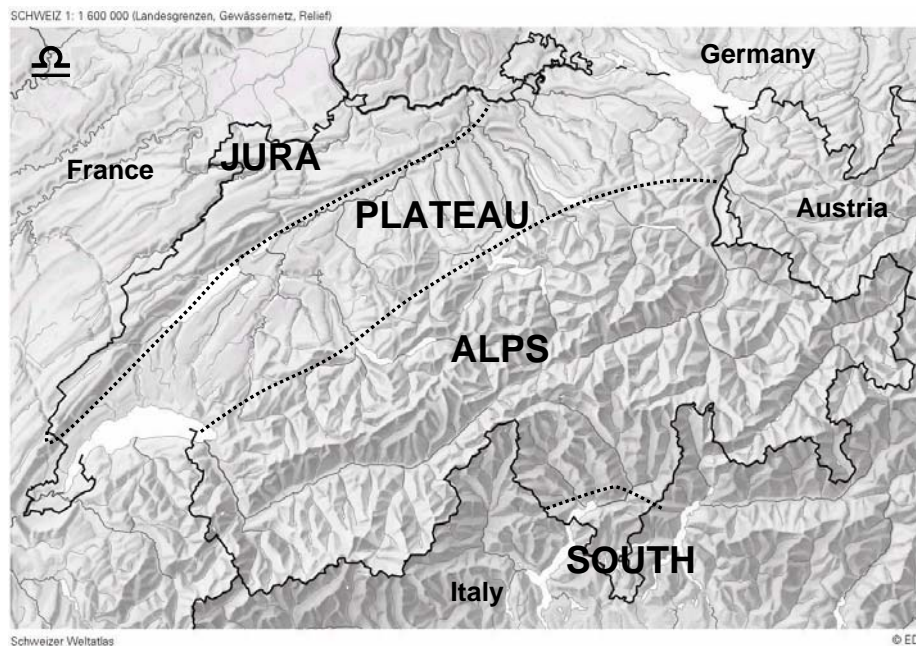


Figure 1.3: Map of Switzerland. The four main regions based on topography (Jura, Plateau, Alps and South) are indicated in an approximate manner.

Source map: <http://www.educeth.ch/geographie> (12.09.2001)

b.) Importance of regional studies

Regional studies on climatic variations have been seriously discussed only since a few years, even though they are of major importance. The quantitative analysis and description of regional climate variations serve as a basis for a more complex understanding of the influence the climate exerts on natural systems. This kind of study is crucial in order to obtain better estimates of the sensitivity of natural systems towards the climate. Having more accurate information about the sensitivity of natural systems may help to take precautionary measures early enough to prevent disasters involving human and material losses that could occur because of possible changes in the natural environment. In Switzerland, mainly alpine communities will be concerned with these

types of problems in the future, since the high altitude regions are likely to be the most exposed to temperature changes (IPCC, 1996, chapter 5).

In most cases the observational data records on a regional level are much denser and therefore more reliable than on a global or hemispheric basis. Even if it is not certain that every region follows the observed large-scale temperature trends and fluctuations, which are described in earlier sections of this study, long term studies of the climate system on different scales rely on this type of analyses. As stated in Zengh et al. (1997) regional studies on observational data provide an important basis to test trend signatures predicted by regional climate models.

c.) Sensitivity of mountain regions

Even though the present study does not uniquely concentrate on the Alps they occupy a special position in the climate change discussion. The IPCC has identified mountain regions as one of the important global systems, which require attention in terms of fundamental climate processes and for the impacts of climate change (IPCC, 1996b, chapter 5).

Baeriswyl et al. (1997) have shown that the anomalies of winter T_{min} can be related to altitude. The higher a site is, the stronger are the anomalies. Therefore, the alpine part of Switzerland is likely to undergo the most intense changes of all regions in a changing climate. It represents an environment mostly free of direct anthropogenic influences and in addition, the very high altitudes are closest to the conditions of the free atmosphere, where the global and long-term signals of climate change can be detected. Beniston and Rebetez (1996) conclude, that significant long-term climatic fluctuations on a large scale can therefore be more clearly identified at higher elevations. These results are conform with a regional climate model simulation of the current climate which shows a more pronounced warming at high elevations during winter and spring related to the depletion of the snowpack and a modified albedo feedback (Giorgi et al., 1997). The authors reason that high elevation sites can therefore serve for an earlier detection of the global warming. Several results from the Swiss National Science Foundation Program 31 on "Climate change and natural hazards" (NFP 31) showed how important environmental changes in the alpine regions can be, especially for economic activities in areas that are subject to natural hazards. The final report emphasises that the costs of such activities are already high and are likely to continue to rise. With the ongoing climate fluctuations it is increasingly inevitable to build extensive safety constructions (NFP 31, 1998). Further,

land-use planning generally takes only known (current and past) risks into consideration thus it is most probable for exceptional incidents to affect the socioeconomic system very strongly. Mountain communities have certainly reason to be concerned about climatic change, in some cases however, there may also be room for new opportunities (Price, 1994).

1.3.3. Changing temperature and environmental impacts

There is much evidence that on different scales a warming has taken place in an accelerated manner over the last two decades. This fact is a challenge to the ecosystem since the living conditions can be changing in an abrupt way. It is very likely that several plant species will be endangered or become subject to extinction because of their failure to either migrate or adapt fast enough to new environmental conditions (Grabherr et al. 1994). Haeberli and Beniston (1998) showed that simulations for a double-CO₂ scenario using regional climate models (RCM) with a 20-km horizontal grid produce conditions under which the Alps would lose major parts of their glacier cover within decades. The generally expected warmer winter and summer temperatures, notably at higher elevations, also cause a warming of cold firn areas and the lower limits of permafrost occurrence in the Alps would be expected to rise by several hundred meters. In addition the evidence is growing stronger that climate warming is accompanied by an increasing frequency of intense precipitation events, as well as by droughts, depending on the region (Rebetez, 1999; Frei et al., 2000). It is probable then, that soils and rocks which are now still frozen solid, will lose their equilibrium and end up as soil- or rockslides endangering mountain villages. Different studies led within the NFP 31, also point out that the frequency and the usual annual rhythm of extreme events will probably change with increasing temperatures (NFP 31, 1998). Presumably, the debris flow season will start earlier in the year and end later in fall. This can be attributed to a shorter period of snow cover during winter, which normally has the function to retain water until spring as well as to a general change in the proportions of rain and snowfall during winter which is related to warmer temperatures (Frei et al., 2000). With these kinds of changes, expected in temperature, precipitation and vegetation, the hydrological system can be disturbed, which in turn may have consequences for water and energy supply.

At this point, it seems obvious that variations in extreme temperatures can disrupt both natural and the socio-economic systems. A key problem is that human interference with

natural systems e.g. the construction of settlements and infrastructure in remote areas can lead to an increase of risks. A long-term interdisciplinary project, funded by the Swiss National Science Foundation, with the focal point on Alpine related climate and environmental change (Climate and Environment in Alpine Research CLEAR) was recently completed in co-operation of several Swiss research institutes. The aim is to generate a more accurate information platform concerning the link between changes in natural systems and concurrent socio-economic reactions.

2. SOURCE DATA

In this Chapter only the general information valid for the source data set used in each chapter is given. A more detailed description of the data set and its transformations specific to the quantitative analyses undertaken in each chapter is provided separately within the chapter in question. To provide a better overview of the type and the amount of data used in each chapter linked to the methodological proceeding an organigram is depicted in Section 2.3

2.1 GENERAL DESCRIPTION OF THE DATA NETWORK

The data analysed in this investigation is provided by the Swiss Meteorological Institute (MeteoSwiss), which manages a dense network of different types of climatological and weather stations distributed throughout Switzerland. For the analyses of the present study exclusively data recorded by so called “conventional climatological stations” is used. Currently, their network is composed of 98 stations, however there were periods with less but also with more stations in operation. The conventional climatological stations work on a traditional semi-automatic mode, where observers read the data daily and the records of the earliest conventional stations installed go back to the end of the 19th century. Two thirds of these stations, however, were installed only after 1965. Therefore only about 20% of the stations currently in operation are providing continuous data for over 40 years. Figures 2.1 and 2.2 depict the spatial and altitudinal distribution of the 132 climatological stations described in *Appendix A* (see Section 2.2.). In the present study, information concerning the altitude is always given in meters above sea level (m).

The MeteoSwiss guidelines to determine T_{min} and T_{max} recordings from 1901 until today are listed below (Bantle 2001):

- 1901 to 1970:
Observers read the T_{min} and T_{max} thermometer 4 times during a day (21:30 previous day, 7:30, 13:30, 21:30 (UTC)) and reset the instrument after every checking. The extreme values out of the 4 measurements are the resulting minimum and maximum values.
- since 1971:
As above except for changes in the reading time: T_{min}: 19:00 previous day, 7:00, 13:00, 19:00 (UTC) and T_{max}: 7:00, 13:00, 19:00, 7:00 next day (UTC)

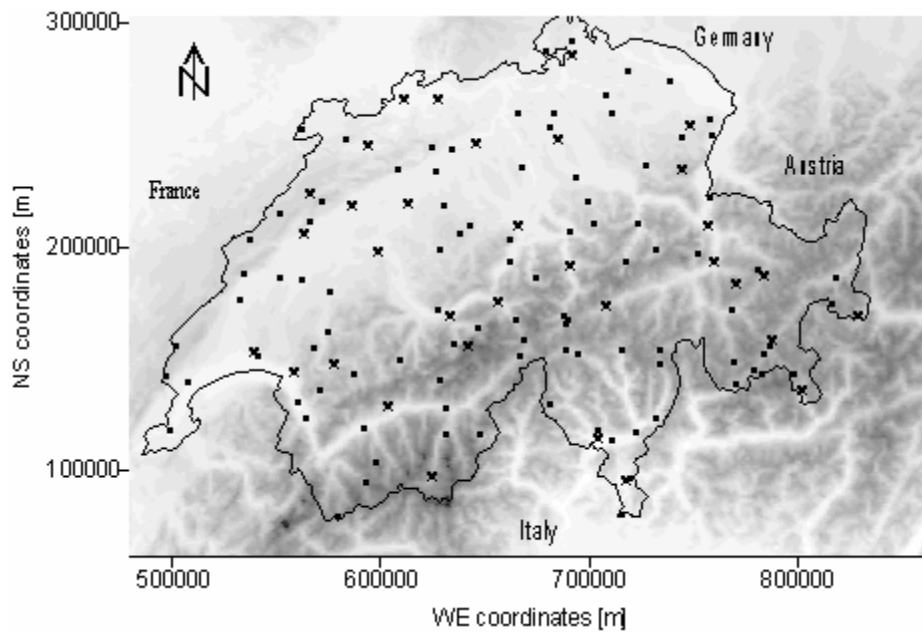


Figure 2.1: Spatial distribution of 132 conventional climatological stations in Switzerland. Depicted as “x” are stations which were/are in operation and recording T_{min} and T_{max} for 40 years or more.

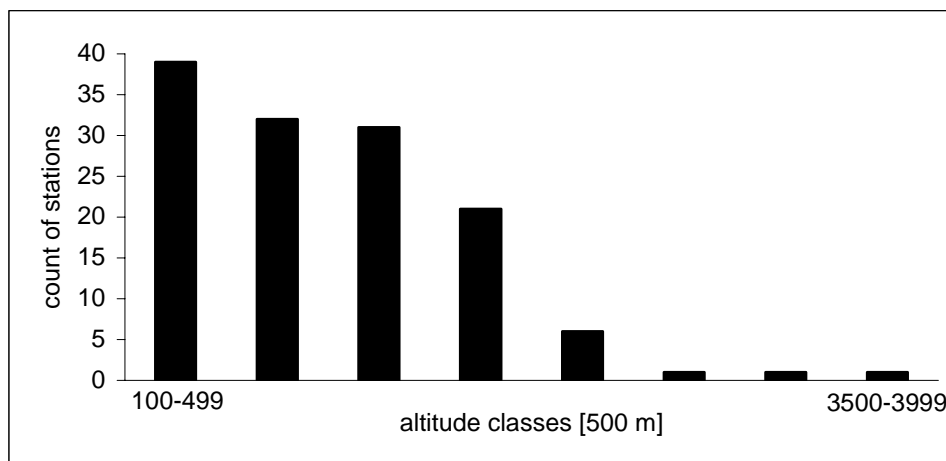


Figure 2.2: Altitudinal distribution of 132 conventional climatological stations in Switzerland depicted as number of stations included in different classes of 500m difference in height.

2.2. QUALITY AND HOMOGENEITY OF THE DATA SETS

In the present study the Tmin and Tmax data sets are used as such, without any adjustment applied to the data. If a time series is found to be unsatisfactory in terms of data quality and homogeneity it is excluded from the analyses.

Data quality depends primarily on the position of a climatological station and its immediate surroundings. MeteoSwiss has regulations on where and how to install a climatological station; occasionally, though, the possibilities to place a station are limited and compromising solutions must be found. Long-term data of climatological stations often contains breaks in the continuity of the time series, because of a variety of modifications that might occur. Often encountered inconveniences in terms of data homogeneity are changes in the immediate surroundings over time as well as changes of the station location and exchanges of the observers. Additionally, new regulations about the exact observation time, changes or replacements of the instrumentation or different averaging methods on the data can cause artificial discontinuities. In most cases however, if changes are undertaken by MeteoSwiss, overlapping measurements are made over a certain period in order to ensure the data homogeneity. The data is not homogenised by MeteoSwiss, although, the following tests of plausibility are applied automatically to the daily data of Tmin, Tmax and morning (T07), noon (T13) and evening (T19) temperatures:

- $T_{\min} \leq \{T07, T13, T19\} \leq T_{\max}$
- $\{T_{\min}, T07, T13, T19, T_{\max}\} \in [-40^{\circ}\text{C}, +40^{\circ}\text{C}]$
- $(T_{\min} - \max \{T07, T13, T19\}) \leq 10^{\circ}\text{C}$
- $(\min \{T07, T13, T19\}) - T_{\min} \leq 5^{\circ}\text{C}$
- $(T_{\max} - T_{\min}) \leq 20^{\circ}\text{C}$

The thresholds noted in the 5 tests are empirical values thus they possibly differ between regions and seasons. Whenever a tested temperature value exceeds these threshold they are examined manually and if a reason for a correction is found, then the data series are treated manually (Konzelmann, pers. com. June 23, 2000; Gisler et al., 1997).

Considerable work has been done to assess the quality of Swiss data sets with important conclusions to take into consideration for further studies. The data homogeneity of the Swiss Tmin and Tmax time series has been discussed in several publications (Montmollin, 1993; Beniston et al., 1994; Weber et al., 1994; Baeriswyl and Rebetez, 1996, 1997; Rebetez and Beniston, 1998, 1998a; Heino et al., 1999). In these studies few inhomogeneities have been found and the Swiss climatological database is considered to be reliable enough for a treatment as such. In 1970, changes in the time of data

observation were made; yet, no discontinuity, which could have been caused by these observation changes, can be detected in the 20th century temperature time series (Montmollin, 1993). In a study conducted by Baeriswyl et al. (1997), the homogenised morning (07h), noon (13h) and evening (19h) temperature time series of Geneva and Bern (Gisler et al., 1997) are compared to the non-homogenised ones considering monthly means over the period from 1901 to 1990. The findings show that differences in data variability are rarely significant and in the few dissimilarities that have been found did not invalidate the final results of this study. Weber et al. (1994) tested the temperature bias due to urbanisation for climatological stations close to Swiss cities and found that it is negligible. In any case, it is not ideal to filter extreme data too rigorously, since real (non-spurious) values would in some instances be eliminated because of the great temporal and spatial variability (Heino et al., 1999).

Prior to use the data for analyses however, the station history (meta data) was examined in more detail. A number of 163 conventional stations can be located which recorded or still record Tmin and/or Tmax over a certain period of time during the 20th century. The stations with incomplete data sets are removed at this point which reduces the number of stations from 163 to 132. Subsequently, the meta data files for these 132 conventional stations (see Figure 2.1) are scrutinised in terms of problems affecting the quality of Tmin and Tmax and the surrounding topography is partially evaluated. An exhaustive list is resulting which figures as *Appendix A*. The reader should be reminded that the meta data is somewhat subjective since the list represents the notes taken by station controllers with different levels of precision. Further, the amount of comments noted to each station is closely linked to the frequency of station inspections. Thus stations with a long list of comments must not necessarily be of poor data quality.

At this point no further stations are removed in order to keep a maximum number of stations involved in the first part of the quantitative analyses. In Chapter 3 (Sections 3.2 and 3.5) however, several tests are made in order to remove the stations with possibly unsatisfactory data homogeneity.

2.3. METHODOLOGICAL PROCEEDING LINKED TO THE NUMBER OF DATA TIME SERIES

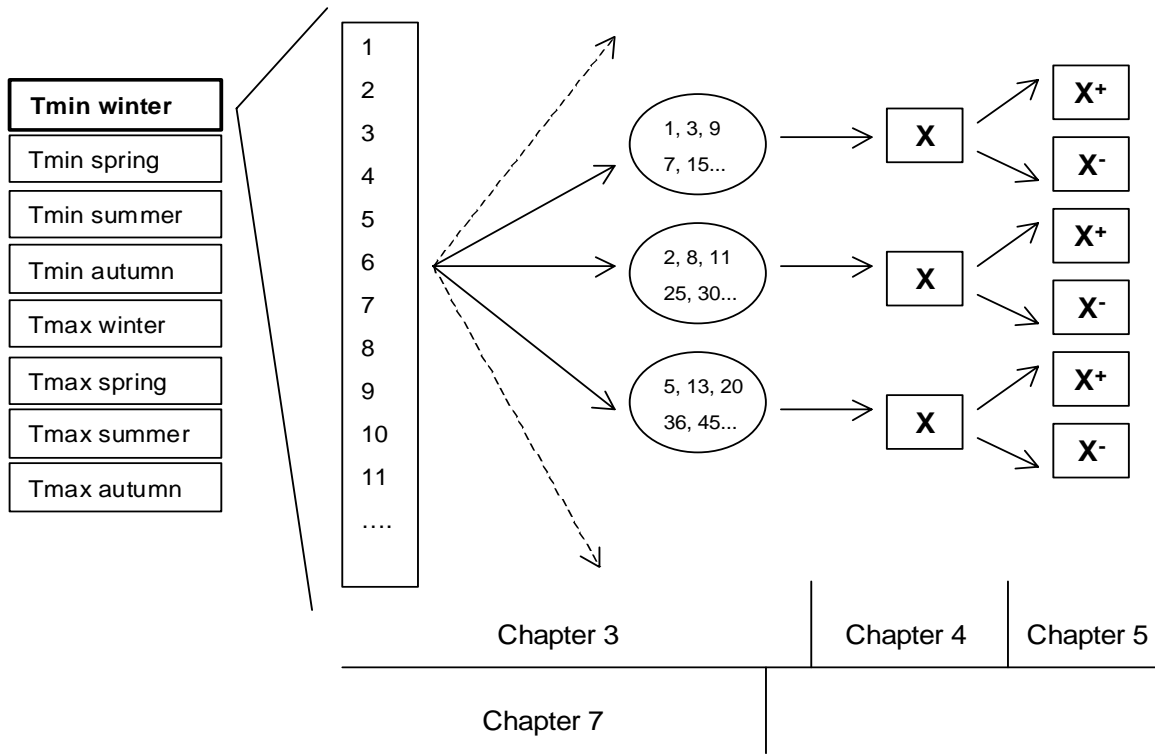
For the global comprehension it might be beneficial at this stage to provide a short preview of the number of station time series included in each working step. In terms of data the nodal points within the methodological proceeding are situated in Chapter 3 and 4 in working steps I, IV and V.

As formulated in working step I a possibly high number of these 132 climatological stations should be included in the first analysis (PCA) of Chapter 3. A condition of this analysis is that all variables (climatological stations in this case) included have equally long time series. Since the 132 operation periods are not of equal length, a time span must be found where a maximum number of these climatological stations are in operation. This reduces the number of climatological stations included in the regionalisation analysis to around 100 per season for Tmin/Tmax. Once the working steps II and III are performed and the stations are fitted into clusters the main interest focuses onto the selection of a number of representative stations per cluster providing qualitatively satisfying data on a possibly long time scale (working step IV). In a first selection several criteria are formulated (Section 3.5.) and the stations meeting these criteria are evaluated from the meta data in *Appendix A*. They are either further taken into consideration as representative stations or excluded from the selection, no data correction is undertaken. Following to this the original time series of these representative stations are correlated with their homogenised time series on a monthly basis. This test assures a good data quality of the representative stations. The homogenised Tmin and Tmax time series were established within the project Norm90 of MeteoSwiss (Bergert et al., 1998). With working step V in Chapter 4 regional mean time series are computed based on the selected representative stations. This reduces the number of time series analysed in Chapter 4 to one per region.

Organigram 2 is a schematic representation of the methodological proceedings, which are conducted in each chapter. It is coded by the number of data time series included in each analysis. In each Chapter this proceeding is performed on Tmin/Tmax in each season, separately (see Organigram 1, Section 1.2.). In Chapter 3, 6 and 7 the analyses are carried out on a daily time scale, in Chapter 4 the time series are spaced interannually and Chapter 5 makes use of both time scales, interannual and daily. Further the temperature data time series used in Chapter 3 are based on standardised values and in Chapter 4 and 5 on anomalies relative to 1961-90.

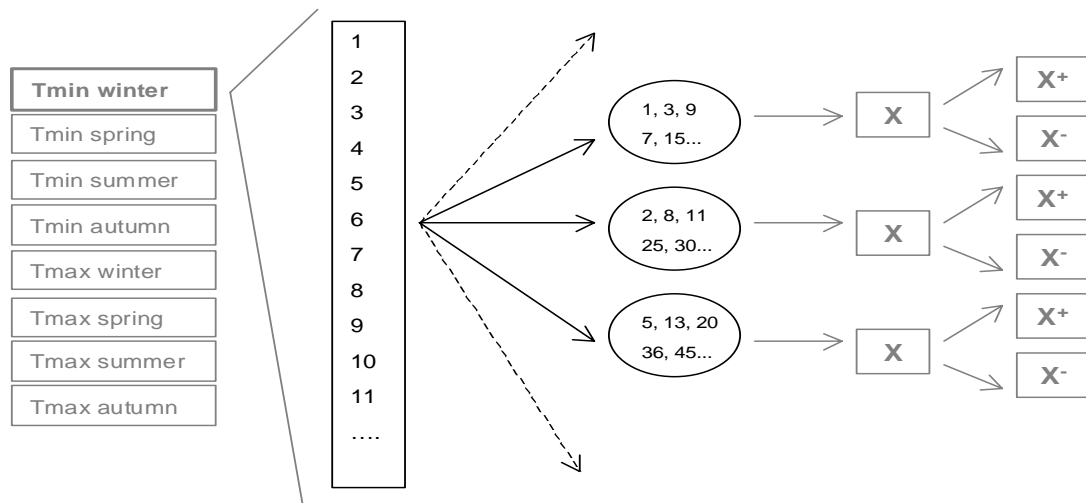
The part of the methodological proceeding performed in Chapter 7 is based on wind gust data, which is assigned either to convective, advective or mixed synoptic weather types

(instead of Tmin/Tmax per season). Chapter 6 does not figure in this organigram because it is based on other data sets and methods with the main purpose to relate the results of Chapter 4 to large and regional scale synoptic circulations.



Organigram 2.1: Methodological proceeding coded by the amount of data time series worked with in each Chapter. The numbers (1, 2, 3, ...) stand for time series of single climatological stations and the “X” signs indicate mean regional time series. The “X +” and “X -“ refer to warm and cold extremes within the Tmin/Tmax time series.

3. CLIMATOLOGICAL REGIONALISATION



The black part of the methodological proceeding organigram is performed in this chapter (see Organigram 2, Section 2.2.) and working steps I to IV are discussed (see Section 1.2.):

- I. *Choosing a period during which a maximum number of Swiss climatological stations are in operation and evaluate their quality by analysing the meta data.*
- II. *Through Principal Component Analysis reduction of data by extracting a number of components explaining the major part of the variance in the original data matrix and assignment of station-related descriptive characteristics to these components.*
- III. *Through Cluster Analysis definition of a number of regions per season as a function of the daily Tmin/Tmax time series of the selected climatological stations and the extracted components.*
- IV. *Selection of representative stations for each region.*

3.1 CHAPTER OUTLINE

In order to undertake the analyses of this chapter a data preparation is necessary. As evoked at the end of Chapter 2 the selected 132 climatological stations recording Tmin and/or Tmax over a certain period of the 20th century, do not share equal time spans of operation. In order to be able to perform the statistical analyses planned in this chapter (PCA/CA) the data strings of the variables included in the analyses have to be of equal length. Thus a period has to be found where a maximum number of the 132 stations, which represent the variables, are in operation. The exigency of a maximum number is related to the aim of this study to analyse temperature variations on the entire territory of Switzerland.

Once this period is determined the exact number of stations recording Tmin/Tmax is verified for each season and the meta data is checked anew in order to exclude stations with obvious problems in their recording. This leaves us with a new number of station time series, which is specified for Tmin and Tmax during each season. Subsequently the time series are standardised since it is a further condition of the PCA/CA to use dimensionless values, e.g. equal values for the standard deviation and the mean in each time series. Several tests for the robustness of the two methods are conducted within this chapter.

Climatological variables are influenced to different degrees by numerous characteristics (station-related, synoptic conditions, local climatology). The type of these characteristics and the degree of their influence on a climatological variable can be similar at various climatological stations distributed in space. Baeriswyl et al. (1997) have worked on methods to regionalise several climate variables and have shown that in Switzerland, characteristics like altitude, topography and regional climate systems are among the most important to influence the climate data. Based on these spatial interrelations, the possibility emerges to perform the regionalisation as a function of Tmin/Tmax and additionally of its degree of dependence upon specific characteristics. Accordingly a PCA is carried out previous to the CA. The PCA is also an appropriate statistical tool to process data in order to meet the technical conditions for a CA. It allows to represent climatological variables through independent principal components. In the present study both, the Tmin and the Tmax time series of each climatological station are considered independently as variables. Based on the component loadings, which indicate the degree of correlation between each station time series and each principal component, “typical members” or “members” of a specific component can be identified. Among the climatological stations classified as “typical members” or “members” it is possible to detect similar station-related

descriptive characteristics; examples are the geographical location, altitude, special site characteristics, topography, population density. The meta data of *Appendix A* is a convenient source in order to carry out this attribution.

Climatological stations with comparable loadings on the same principal component show a similar interannual variability in their temperature time series and can therefore be aggregated into clusters. The station-related descriptive characteristics emerging for each principal component can be linked to each of the resulting clusters since the CA is based on the component loadings. Additionally these characteristics can be used as indicator of coherence between the climatological stations included in each cluster.

This statistical regionalisation method has already been applied successfully by several authors like Goossens (1986) on annual mean temperatures in the Mediterranean region; Klink and Willmott (1989) on surface wind fields in the United States; Jolliffe (1990) on sea-level pressures in the North Atlantic; Baeriswyl and Rebetez (1997) on precipitation in Switzerland; and others.

Subsequent to the clustering of the climatological stations, representative stations of each cluster have to be determined in order to undertake the following working steps. According to a number of criteria representative stations are selected for each of the established clusters. The T_{min}/T_{max} time series of the representative stations are further tested on the data quality by comparing them to their homogenised analogues which were established within the project Norm90 of MeteoSwiss (Bergert et al., 1998).

The reader should be reminded that PCA and CA are repeated for each seasons on both parameters, T_{min} and T_{max}, separately. Thus eight types of divisions, clustering patterns, of Swiss climatological stations are resulting. For further time series analyses (as undertaken in chapter 4), these divisions allow to analyse a limited number of data series (one per cluster) while covering a large, but not necessarily geographically connected, area.

3.2. DATA PREPARATION

In the following analyses the data is processed on a daily time scale in order to retain as much information as possible. Since the Swiss climate is represented by four markedly different seasons, the year is divided into four periods of 3 months each. Winter includes December of the previous year, January and February. Spring includes the months of March, April and May. The summer months are June, July and August and the autumn months are September, October and November.

In order to undertake the analyses on a large number of climatological stations with an equally long and continuous period of operation, different time spans were tested. The period 1983 to 1995 responds best to this demand with about 100 stations that recorded continuously Tmin and/or Tmax data for every season during this 13 year time interval (Table 3.1). As a test of robustness of the statistical methods other periods have been tested (see test 1, Section 3.3.3). The resulting clusters however, do not seem to depend on the length of the period covered by the time series. The meta data in *Appendix A* of the climatological stations which are continuously running during the period 1983 to 1995 is checked anew and stations that are subject to serious problems are removed at this point. An example is the station La Brévine where numerous reading problems are indicated and which is regularly flooded in the 1990s (probably before as well):

La Brévine

1932 (12.11.)	539 400 / 204 500, 1077m	(post office)
1948 (02.02.)	533 960 / 202 400, 1060m	(school, houses in proximity (30m))
1957 (30.01.)		(minimum thermometer changed, the old one measured approx. 2°C too low)
1957 (21.10.)	536 775 / 203 540, 1041m	(presbytery, lowest temperatures)
1958 (24.04.)		(thermometer and minimum thermometer changed)
1962 (24.01.)		(unsatisfactory reading of minimum thermometer)
1964 (20.10.)	536 740 / 203 560, 1042m	(new station observer)
1966		(start of minimum and maximum temperature observations)
1969 (28.05.)		(new station observer)
1991 (23.05.)		(area in depression next to small river, regularly flooded)
1996 (31.12.)		station stop

Additionally, during summer several stations located in proximity to a lake showed a rather unexpected behaviour in terms of cluster membership. Two of these stations had to be excluded from the summer analysis (Montreux - Clarens and Neuchâtel). A probable

explanation could be related to the land-lake breeze system, this however, is only a hypothesis.

Winter Tmin	Winter Tmax	Spring Tmin	Spring Tmax	Summer Tmin	Summer Tmax	Autumn Tmin	Autumn Tmax
104	100	105	104	105	102	105	104

Table 3.1: Number of climatological stations included in each run of the climatological regionalisation process.

Temperature values depend strongly on the altitude and like Jolliffe (1993) stated, often have extremely different variances. Switzerland is characterised by a complex topography and a data transformation is inevitable in order to be able to compare the data of different climatological stations. Applying a standardisation (z-transformation) to the data results in weighting all variables equally, the data is levelled with the arithmetic mean, $\mu = 0$, and the standard deviation, $\sigma_x = 1$. Standardised variables are therefore dimensionless, which is an important requirement for the CA. (Bahrenberg et al., 1990, Jolliffe, 1990, Brown and Katz, 1995). The transformation formula is:

$$z_i = \frac{x_i - \mu}{\sigma_x}$$

where z_i is the i^{th} value of the new z-variable and x_i is the i^{th} value of the original x-variable.

3.3. STATISTICAL METHODS

3.3.1 Principal Component Analysis (PCA)

The PCA is based on a correlation matrix between station temperature time series from 1983 to 1995. Table 3.2 represents an example of the matrix structure where the number of climatological stations, m , previously selected for Tmin/Tmax in each season are considered as variables, V_i , with i going from 1 to m .

winter Tmin	V ₁	V ₂	V ₃	V ₄	...	V _m
01.12.82						
02.12.82						
03.12.82						
...						
28.02.95						

Table 3.2: Structure of the original data matrix covering the period 1983 to 1995 on which the PCA is established. “V” identifies a variable, in this case a station temperature time series, and “m” the number of stations included (see Table 3.1).

The overall variation of the original data matrix can be reproduced in a way that each variable, V , is represented as a linear combination of the computed components, C_l , where l goes from 1 to q . (Bahrenberg et al., 1992). The number of the resulting components equals the number of the stations included ($m = q$). This can be expressed in a global manner:

$$V_i = \alpha_i + \sum_{l=1}^q \beta_{il} C_l$$

where α_i is the constant of V , and β_{il} is the linear equation coefficient of C_l .

The components, C_l , are computed in a way that the first linear combination describes most of the variability in the original data matrix, the second linear combination the next most, though into another dimension, and so forth. It was found to be beneficial to rotate the components. This procedure is widely used in climatology and often facilitates the interpretation of the components, i.e. the attribution of station-related characteristics (VonStorch and Zwiers, 1999). An orthogonal rotation (varimax) is applied through which the components remain uncorrelated and thus independent (SPSS 2, 1999). Consequently, a rotated component matrix emerges from this process with component loadings, denoting the correlation coefficients between each of the q components and each of the m temperature data series with $m = q$ (Table 3.3). The mathematical expression for the computations of any component, C_l , can be expressed as follows:

$$C_l = \alpha_l + \gamma_{l,1} V_1 + \gamma_{l,2} V_2 + \dots + \gamma_{l,m} V_m$$

where γ is the component loading.

	V ₁	V ₂	V ₃	V ₄		V _m
C ₁	γ _{1,1}					
C ₂						
C ₃						
C _q						

Table 3.3: Structure of component matrix. “C” identifies the principal components and “V” the station temperature time series, “m” the number of stations included and “q” the number of principal components extracted, in which $m = q$.

The sum of the squared loadings is called the eigenvalue, λ and the quotient, λ/m , identifies the total variance explained for the entire temperature time series matrix by one principal component (Bahrenberg et al., 1992). A main advantage of the PCA is the ability to explain the major part of the variance in the original data matrix taking only a few of the q principal components into consideration. These components can be determined according to the criterion of Kaiser, where only the components with $\lambda > 1$ should be taken into consideration. Since $\sigma = 1$ for standardised variables, components with $\lambda < 1$ do not contribute more to the explanation of the variance than any normal variable (SPSS 2, 1999). This constitutes an important reduction of data retaining most of the variation in the original data matrix (Bahrenberg et al., 1992). Stating the example of winter Tmin only the first 6 principal components are required to represent the essential information in the original data matrix with $m = 104$ variables. Thus the 104 by 104 rotated component matrix (see Table 3.3) can be replaced by a new 6 by 104 component matrix.

The assignment of the previously (Section 3.1) described attribution of “typical members” or “members” of a specific component to a climatological station is based on the loadings of this new reduced component matrix.

3.3.2. Cluster Analysis (CA)

Bahrenberg et al. (1992) point out that variables used in a CA should be standardised on the one hand be in order to remove scale effects, and on the other hand independent in order to apply appropriate methods to measure distances and similarities between different points and clusters. With the preceding PCA these requirements are fully met. The CA is based on the rotated component matrix (structure depicted in Table 3.3) of the extracted principal components with $\lambda > 1$.

A Cluster Analysis attempts to identify relatively homogeneous clusters of variables (temperature time series of climatological stations in this case), based on selected methods where the difference between two clusters is as large as possible (Bahrenberg et al, 1992). The hierarchical method employed here begins by combining the closest pair of variables as a function of distance and of similarity. The method is hierarchical because once two objects or clusters are joined, they remain together until the final step. The Euclidean distance, which corresponds to the direct distance between two points and is based on the Pythagorean theorem is used as a measure of distance for the stepwise clustering. The similarity between two clusters is determined by measuring the average distance between the centre of two clusters, known as average linkage method (SPSS 2, 1999).

The number of clusters finally taken into account needs to represent a compromise between different degrees of generalisation (Bahrenberg et al, 1992). The intentions are to ensure a certain minimum of clarity and at the same time to limit the loss of information by finding a well explainable clustering pattern of climatological stations and avoiding clusters including only one or two stations. This implies that the clusters are reasonable constructs of climatological stations in terms of geophysical details and regional meteorology. The “agglomeration schedule” resulting out of the CA can be helpful in determining the number of clusters. It indicates the distance between the clusters combined (SPSS 1, 1999). No dendrogram is depicted with this analysis due to the high number of variables included.

3.3.3. Tests

Several tests were made to corroborate the robustness of PCA and CA. The tests all yielded affirmative results, which can be considered as support to the application of these statistical methods to data recorded in complex terrain.

- Test 1 - changing periods and thus size of original data matrix (PCA):
As a test the PCA procedure was additionally run during two other periods than the selected one. The number of climatological stations in operation during 1971 to 1995 (about 65 stations per season), and during 1966 to 1980 (about 50 stations per season) provide the input for two different data matrices. The results are comparable to the selected period 1983 to 1995 with about 100 stations per season; however, the regions are somewhat coarser since the degree of refinement of a region is closely related to the number of input variables.
- Test 2 - several methods (CA):
The robustness of CA was tested applying different methods to measure distance and similarity. Minor changes in the clustering pattern were detected. What proves the robustness of CA.
- Test 3 - missing elements (PCA /CA):
After having run the analyses for a first time one entire cluster was removed and following to this, PCA and CA procedures were run anew. This results in the same clustering pattern as before, with no entirely different structure.
- Test 4 - opposite data (PCA / CA):
Statistical tools do not always recognise opposites as being different entities. PCA and CA are therefore led on composed data series, consisted of exact opposite data. The result of this test assures a separation of those series with contrasting variations.
- Test 5 - time series with comparable trends and different types of short term variability (PCA / CA):
Temperature time series measured at various climatological stations can show a comparable long-term trend although the variability is very different. In this case one station cannot be considered as fully representative of the other. A test undertaken on composed data series has proven that PCA and CA are tools capable of separating the series under these conditions.

All these tests prove the appropriateness of the use of PCA and CA on T_{min} and T_{max} time series.

3.4. RESULTS

Aiming to attribute station-related descriptive characteristics, hereafter referred to as *sr-char.*, to each of the extracted components, the loading matrix is scrutinised. Climatological stations with loadings higher than 0.8 on a component are considered as typical members (tm) of this component and stations with loadings between 0.5 and 0.79

as members (m). The name and the altitude of each climatological station attributed to each cluster are listed in *Appendix B* (comparable to Figure 3.1 to 3.8). These characteristics can be used as indicators of coherence between the climatological stations included in each cluster.

The following statistical analyses have all made use of the software package SPSS (1999).

3.4.1. Establishing clusters in winter

a.) PCA on winter T_{min}

Component	Eigenvalue (λ)	% total variance explained (λ/m)	Cumulative (λ/m)
1	44.2	42.5%	42.5%
2	28.9	27.8%	70.3%
3	9	8.6%	78.9%
4	5.6	5.4%	84.3%
5	4.8	4.6%	88.9%
6	2.7	2.6%	91.5%

Table 3.4: PCA with $m = 104$ stations. Extracted are $q = 6$ principal components with $\lambda > 1$, which explain 91.5% of the original variance. Station-related descriptive characteristics can be attributed to the first 5 components (*bold*).

Component 1:

tm: Stations below 700m situated in the densely populated Plateau and the lower altitudes of the Jura.

m: Stations situated in the eastern Prealps (northern alpine rim) and the higher altitudes of the Jura

sr-char.: northern side of the Alps, low altitude, densely populated areas

Component 2:

tm: Stations above 1400m, most frequently pass or summit sites in the Alps and the Jura.

m: Stations around 1000m, situated in the Prealps of central Switzerland, and the south-eastern part of the Alps.

sr-char.: high altitude, pass or summit sites, sparsely populated areas

Component 3:

m: Stations situated in the south-eastern regions of the Alps located in rather large, SW to NE directed valleys. The second strongest loading is to find without an exception on component 1.

sr-char.: geographical dependency, complex topography, mean population density

Component 4:

m: Stations situated in the southern part of the Alps, in NW to SE directed valleys with small lakes nearby.

sr-char.: geographical dependency, influence of the Mediterranean climate

Component 5:

m: Stations situated on the southern side of the Alps below 400m.

sr-char.: influence of the Mediterranean climate, low altitude, densely populated areas

b.) CA on winter T_{min}

The 9 clusters of climatological stations which can be distinguished are depicted in Figure 3.1. The clusters are likely to reflect the distribution of the typical and very persistent fog and stratus areas during the winter months in Switzerland. Thus the altitude seems to be a main station-related characteristic. For some small clusters uniformity can be observed due to a geographical dependency which can be linked to a strong influence of the Mediterranean climate.

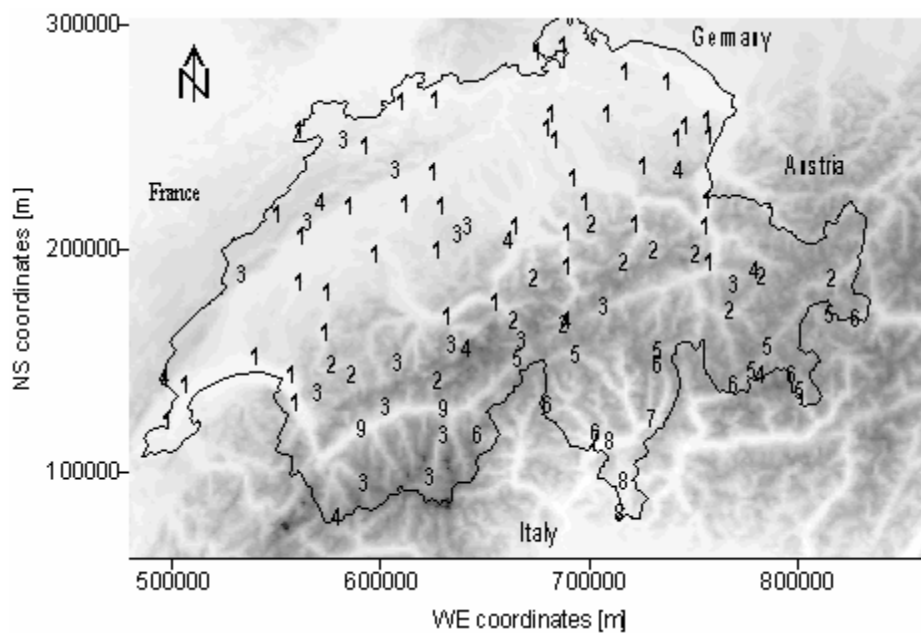


Figure 3.1: Climatological regionalisation of winter Tmin. Each number represents a climatological station attributed to one of the 9 clusters determined.

Cluster 1 – tm and m of component 1. The stations are all situated in the lower parts of the Jura, on the Plateau and at the opening of large alpine valleys onto the Plateau. Each station is subject to the strong and persistent inversion over the Plateau that develops during winter.

Cluster 2 – m of component 1 and 2 and/or 3. The stations are situated on light to medium inclined slopes in the Prealps and in alpine valleys for altitudes generally ranging between 800 and 1000m. These stations are located close to or in villages and are possibly influenced by the winter inversion on days where the inversion layer deepens.

Cluster 3 – tm, m of component 2 and m of component 1. The stations are mostly located in the western Prealps and in alpine valleys, above 1200m, on mean to strongly inclined slopes above glacier terraces. The inversion does not normally reach these stations and due to their location on slopes the cold air generated during the night does not affect the data.

Cluster 4 – tm of component 2. The stations represent summit, ridge or pass sites, situated in the Alps at high altitudes. None of them is placed below 2000m. Especially during winter the high alpine sites can be considered as part of the free atmosphere and thus be linked to the global climate system.

Cluster 5 – m of components 3 and 4. The stations are located in the south-eastern part of the Alps, on valley floors and on weakly inclined slopes close to the valley floor at altitudes within 1000 and 2000m. In this part of the country, the stations are never located under a persistent stratus layer; however night-time inversions are likely to build over the valley floors.

Cluster 6 – m of component 4 and component 2. The stations are situated in the south-eastern part of the Alps in narrow valleys, on south alpine passes and summits. The prevailing altitude is between 1400 and 2300m.

Cluster 7 – m of component 5. The stations are located above 300m in the southern part of Switzerland in areas with low to average slope inclinations, still away from the densely populated areas further south. During the night they are presumably under the influence of the cold air draining from the surrounding mountains.

Cluster 8 – m of component 5. The stations are situated on the southern side of the Alps close to cities and lakes, generally below 300m.

Cluster 9 – tm component 1. The stations are located in the large and densely populated Rhone valley. Although during winter a persistent inversion can develop, fog or stratus layers however, are not generally observed in this region.

c.) PCA on winter T_{max}

Component	Eigenvalue (λ)	% total variance explained (λ/m)	Cumulative (λ/m)
1	41.2	41.2%	41.2%
2	34.5	34.5%	75.7%
3	8	8%	83.7%
4	3.4	3.4%	87.1%
5	2.3	2.3%	89.5%
6	2.3	2.3%	91.7%

Table 3.5: PCA with $m = 100$ stations. Extracted are $q = 6$ principal components with $\lambda > 1$, which explain 91.7% of the original variance. Station-related descriptive characteristics can be attributed to the first 5 components (bold).

Component 1:

tm: Stations generally below 700m situated in densely populated areas of the Plateau, the Jura and the Prealps.

m: Stations around 1000m situated in large alpine valleys.

sr-char.: northern side of the Alps, low altitude, densely populated areas

Component 2:

tm: Stations generally above 1400m, pass or summit sites in the Alps and the Jura.

m: Stations above 1000m in the south-eastern part of Switzerland.

sr-char.: high altitude, pass or summit sites, sparsely populated areas

Component 3:

tm, m: Stations situated on the southern side of the Alps, generally below 400m.

sr-char.: influence of the Mediterranean climate, low altitude, densely populated areas.

Component 4:

tm, m: None. It is to be noted however, that the stations which correlate over 0.3 are all located at the opening of or in large valleys like Rhone, Rhein, Aare, Albula, Sernf and Inn.

sr-char.: large alpine valleys

Component 5:

tm, m: None. All stations with loadings greater than 0.3 on component 5 are located in the south-eastern part of the Alps.

sr-char.: geographical dependency, complex topography

d.) CA on winter T_{max}

The 7 identified clusters of climatological stations are depicted in Figure 3.2. Comparable to the winter T_{min}, altitude appears to be a main clustering factor. The uniformity due to the geographical position or the influence of the Mediterranean climate on the southern regions seem to be more substantial for the winter T_{max}, however. The persistent winter stratus layers over the Plateau frequently exists throughout the day. The cold air pools, which develop during the night at sites located in depressions and alpine valleys, well above the inversion layer over the Plateau, disperse on sunny winter days. Thus the clustering pattern for winter T_{min} and T_{max} can be quite different.

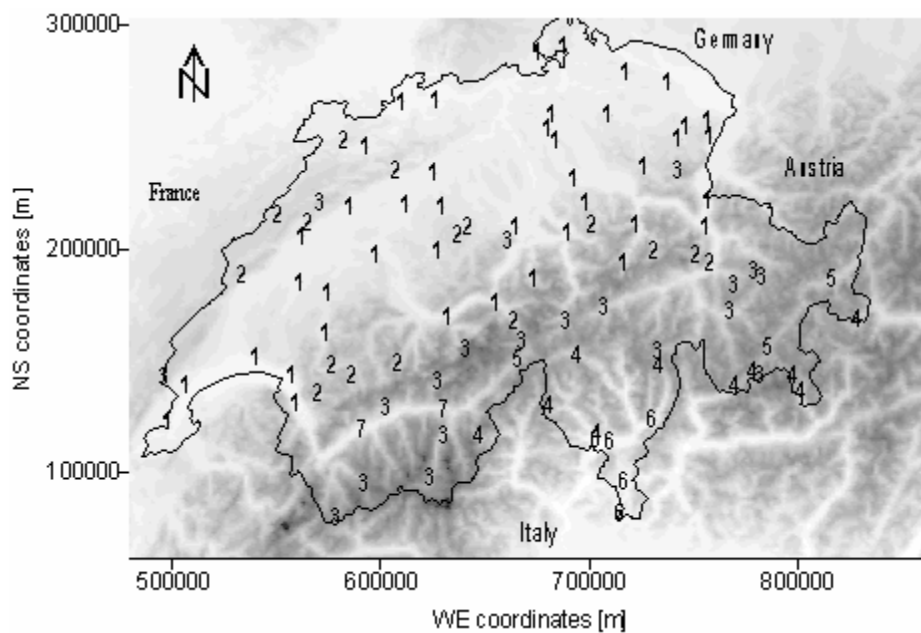


Figure 3.2: Climatological regionalisation of winter T_{max}. Each number represents a climatological station attributed to one of the 7 clusters determined.

Cluster 1 – tm and m of component 1. The stations are located in the lower parts of the Jura, on the Plateau and the Prealps. On typical winter days these stations are all subject to the persistent inversion over the Plateau.

Cluster 2 – tm and m of component 1. The stations are situated at altitudes between 850 and 1400m in the Jura and the Prealps. During sunny days the level of the inversion is becoming lower and stations situated at these altitudes are often above the inversion limit.

Cluster 3 – tm of component 2. The stations are located from 1200 to 3500m in the Alps and on passes and summits of the Jura and the Prealps. These areas are well above the inversion layer over the Plateau.

Cluster 4 – the stations correlate over 0.3 with component 5. They are generally situated at altitudes between 1000 and 2000m, on terrain comparable to the stations of cluster 3.

Cluster 5 – m of component 2 and component 4. The stations are situated on large valley floors at altitudes between 1300 and 1700m. Occasionally the night-time inversion in those valleys is strong enough to last throughout the day.

Cluster 6 – the stations correlate over 0.3 with component 3. They are located below 400m in the south, where the Mediterranean climate and probably the compact population density have an influence on the temperatures.

Cluster 7 – m of component 1. The stations are located in the Rhone valley. In this large valley the inversion often lasts throughout the whole day.

3.4.5. Establishing clusters in spring

a.) PCA on spring Tmin

Component	Eigenvalue (λ)	% total variance explained (λ/m)	Cumulative (λ/m)
1	42	40%	40%
2	37.7	35.9%	75.9%
3	17	16%	92.1%
4	1	1%	93.1%

Table 3.6: PCA with $m = 105$ stations. Extracted are $q = 4$ principal components with $\lambda > 1$, which explain 93.1% of the original variance. Station-related descriptive characteristics can be attributed to the first 3 components (bold).

Component 1:

tm: Stations generally located in the northern part of the Plateau, below 700m.

m: Stations mainly below 1000m, situated on Plateau and at lower in altitude in the Prealps and in large alpine valleys.

sr-char.: northern side of the Alps, low to medium altitude, high to mean population density

Component 2:

tm: High altitude stations on summits and passes, generally above 1600m.

m: Stations above 1000m in the Jura and the Prealps, as well as in the south-eastern and southern Alps.

sr-char.: mean to high altitude, pass or summit sites, influence of the Mediterranean climate, sparsely populated areas

Component 3:

m: Valley stations of the south-eastern Alps at around 1500m and stations in the south below 400m.

sr-char.: influence of the Mediterranean climate, high to mean population density

b.) CA on spring T_{min}

The 8 clusters of climatological stations which can be distinguished are depicted in Figure 3.3. Altitude seems to be a less important clustering factor for spring than for winter temperature data sets, although overnight inversions occasionally develop and affect the T_{min}. Geographical dependency and similarity in the topography seem to be substantial station-related characteristic. This can partly be explained with the turbulent weather situations, which are generally predominant during spring.

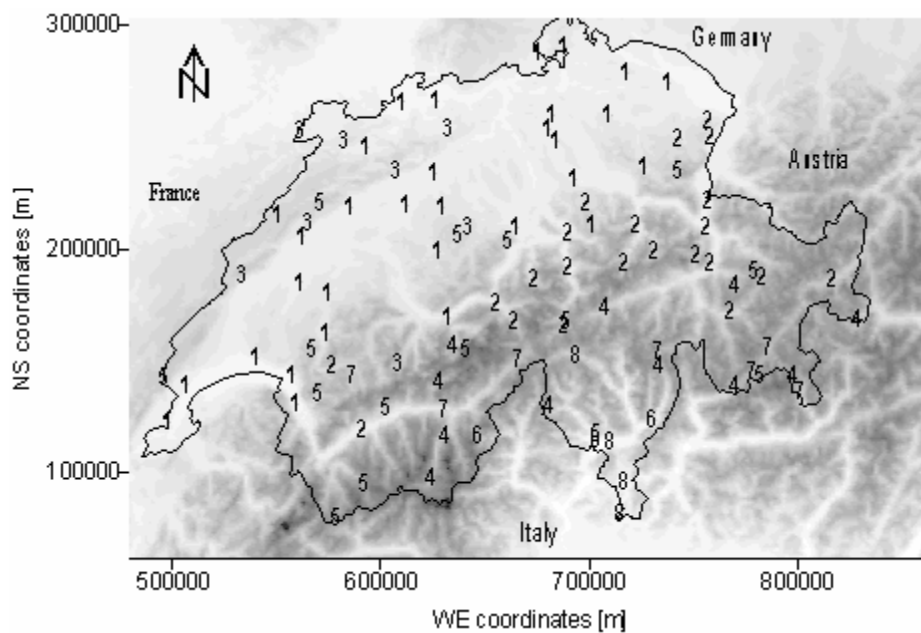


Figure 3.3: Climatological regionalisation of spring T_{min}. Each number represents a climatological station attributed to one of the 8 clusters determined.

Cluster 1 – tm of component 1. The stations are situated at altitudes between 300 and 700m in the Jura, the Plateau and the western Prealps. In those regions an over night inversion frequently develops during the month of March and April and an early morning fog layer can stretch through the Plateau.

Cluster 2 – m of component 1 and weak loadings on components 2 and 4. The stations are mainly located in the eastern and central Prealps in valleys and depressions at

different altitudes. They are probably subject to night-time inversions with a little morning fog.

Cluster 3 – m of component 2. Stations principally located around 1000m in the Jura belong to this cluster. All stations are placed in areas with an average to strong slope inclination where cold air does not accumulate.

Cluster 4 – m of component 2 (loadings lower than cluster 3). Generally the stations are placed in rather narrow alpine valleys with average to strong slope inclinations or on glacier terraces at altitudes between 1200 and 1800m. Like in cluster 3 the cold night air does not accumulate.

Cluster 5 – tm of component 2. Stations located on passes or summits at high altitudes of the Jura, the Prealps and the Alps, between 1400 and 3500m. This cluster can be compared to cluster 4 of the winter Tmin.

Cluster 6 – m of component 2 and loadings lower than 0.5 on component 3. These stations are located at the southern side of the Alps, mainly below 400m and are subject to the influence of the Mediterranean climate.

Cluster 7 – stations, which correlate similarly with components 1, 2, and 3. They are located in rather large alpine valleys generally at altitudes around 1000m, and are probably subject to the nightly formation of cold air pools in depressions or inversions throughout the valley. Moreover, the Mediterranean climate seems to have a certain influence on them.

Cluster 8 - The stations have their strongest loadings on component 3. These sites are located in densely populated areas on the southern side of the Alps at low altitudes. (The exception is Piotta, which presumably has problems with the data quality. It would better fit into cluster 7.)

c.) PCA on spring T_{max}

Component	Eigenvalue (λ)	% total variance explained (λ/m)	Cumulative (λ/m)
1	51.9	49.9%	49.9%
2	25.8	24.8%	74.7%
3	20.9	20.1%	94.7%

Table 3.7: PCA with $m = 104$ stations. Extracted are $q = 3$ principal components with $\lambda > 1$, which explain 94.7% of the original variance. Station-related descriptive characteristics can be attributed to all of the components (bold).

Component 1:

tm: Stations of the north-eastern part of Switzerland (east of the Aare).

m: Stations situated in the western part of Switzerland (loading > 0.7), of the Prealps and Alps (loading < 0.7).

sr-char.: northern side of the Alps

Component 2:

tm: Stations at medium to low altitudes on the southern side of the Alps.

m: Stations above 1000m in the southern part of the Alps.

sr-char.: influence of the Mediterranean climate, geographical dependency, complex topography

Component 3:

m: Pass and summit sites at high altitudes in the Alps and Prealps.

sr-char.: high altitude, pass or summit sites, sparsely populated areas

d.) CA on spring T_{max}

Figure 3.4 represents the 10 identified clusters of climatological stations. Just as for the spring T_{min} geographical dependency and similarity in the topographical features seem to be essential station-related characteristics along with altitude. As mentioned before this can probably be attributed to the rather turbulent weather situation in spring.

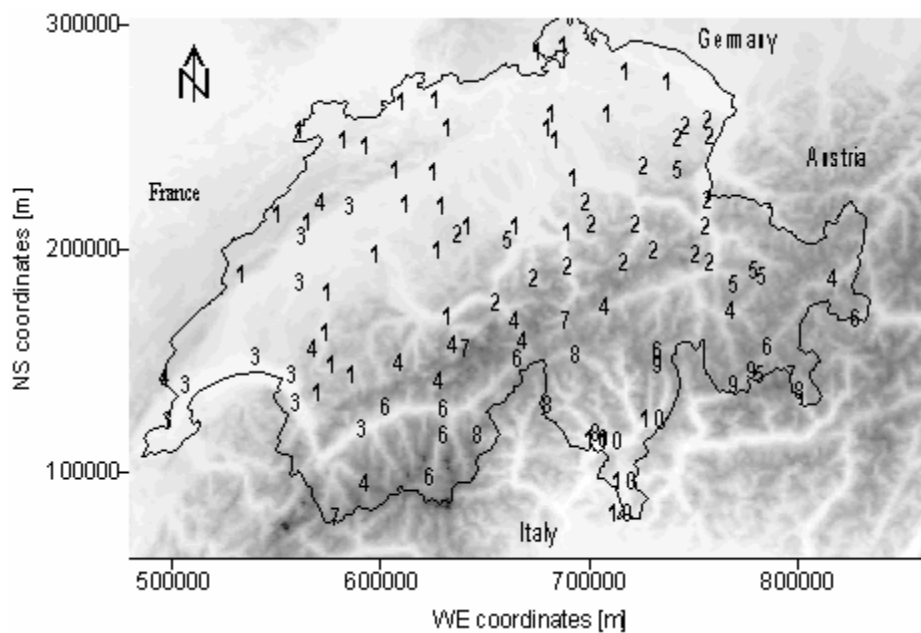


Figure 3.4: Climatological regionalisation of spring Tmax. Each number represents a climatological station attributed to one of the 10 clusters determined.

Cluster 1 – tm and m (loading > 0.7) of component 1. The stations are located in the north-eastern and western part of Switzerland at altitudes below and around 1000m.

Cluster 2 – tm of component 1. The stations are situated in the eastern part of the country, generally at altitudes below 1000m.

Cluster 3 – m (loading > 0.7) of component 1. The stations are situated in the very west of Switzerland at altitudes between 400 and 500m.

Cluster 4 – m (loading < 0.7) of component 1. Stations predominantly situated on glacier terraces in narrow alpine valleys at altitudes between 1000 to 1900m. The areas are frequently on slopes with average to strong slope inclination. Two summit stations in western part of the Jura also fit into this cluster.

Cluster 5 – m of component 3 and 1 (loading < 0.7). Mainly summit stations located in the eastern part of Prealps and Alps at altitudes ranging between 1600 and 3000m.

Cluster 6 – m of component 1 or 2. Stations located in the southern part of the Alps at altitudes between 1300 and 1600m.

Cluster 7 – m of component 3 and 2. High altitude stations of the Alps located on passes or summits at altitudes between 2200 and 3500m.

Cluster 8 – tm of component 2 and m of component 1 (loading < 0.7) or 3. These stations are situated at altitudes between 1000 and 1600m in the southern part of the Alps.

Cluster 9 – m of component 2 and 3. This cluster is comparable to cluster 8 with the exception that the stations are located more to the east, which possibly indicates a strong geographical dependency.

Cluster 10 – tm of component 2. The stations are typical for the southern region, located below 400m in densely populated areas.

3.4.3. Establishing clusters in summer

a.) PCA on summer Tmin

Component	Eigenvalue (λ)	% total variance explained (λ/m)	Cumulative (λ/m)
1	38.7	36.9%	36.9%
2	37.9	36.1%	37%
3	16.8	16%	89%
4	1.2	1.2%	90.2%

Table 3.8: PCA with $m = 105$ stations. Extracted are $q = 4$ principal components with $\lambda > 1$, which explain 90.2% of the original variance. Station-related descriptive characteristics can be attributed to all of the components (bold).

Certain stations located close to a lake have to be excluded from the analyses. No solid explanation can be provided for the link to the cluster they are attributed to. A probable reason is the special land-lake breeze system, which during calm summer nights can affect the shore environment up to 10km (Häckel, 1990).

Component 1:

m: Stations located generally above 1000m in the Jura, the Prealps and the Alps.

sr-char.: medium to high altitude, mean to sparse population density, complex topography

Component 2:

tm, m: Stations situated in the Jura, the Plateau and the Prealps.

sr-char.: northern side of the Alps, low to medium altitude, mean to high population density

Component 3:

m: Stations situated in the south-eastern part of the Alps and in the south of the country at different altitudes.

sr-char.: influence of the Mediterranean climate, complex topography, geographical dependency

Component 4:

No station shows a strong loading on component 4, although stations correlating at around 0.2 with component 4 are without exception located in the western and south-western part of Switzerland.

sr-char.: geographical dependency

b.) CA on summer T_{min}

Figure 3.5 depicts the 7 clusters of climatological stations, which can be distinguished. Altitude, geographical dependency and the influence of the Mediterranean climate are main station-related characteristics. With the geographical dependency of summer T_{min} Switzerland can be divided into roughly 4 sections: the western part, the north-eastern part, the south-eastern part and the high altitude stations.

As mentioned before, several stations located in proximity to a lake had to be excluded probably because of the influence of the land-lake breeze system.

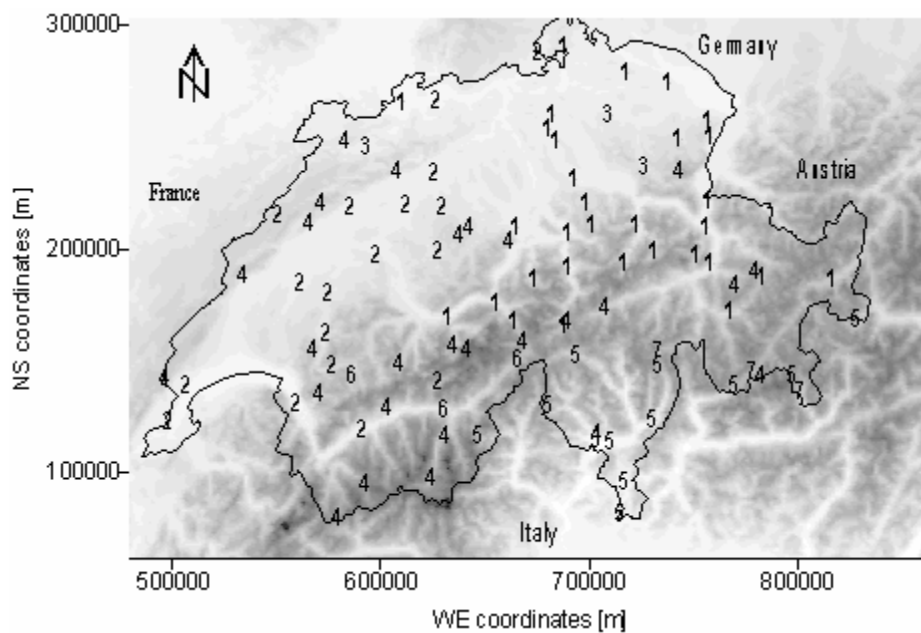


Figure 3.5: Climatological regionalisation of summer Tmin. Each number represents a climatological station attributed to one of the 7 clusters determined.

Clusters 1 and 3 – m of component 2. The stations are situated in the northern and eastern part of Switzerland between the Lake Constance to the northern alpine rim at altitudes among 400 and 1400m. Cluster 3 is a rather strange construction. Judging by the metadata two of the stations do not provide adequate data.

Cluster 2 – tm of component 2 and weak loadings on component 4. The stations are located at altitudes between 400 and 1400m in the west and south-west between the Jura and the Alps.

The first two clusters divide the northern side of the Alps into a western and an eastern section. This supports the hypothesis of a strong geographical dependency of summer Tmin.

Cluster 4 – m of component 1. The stations are located at altitudes between 1000 to 3500m in the Jura, the Prealps and the Alps. In contrast to winter nights, the creation of inversions over a complex terrain is negligible during summer nights. Thus the temperatures at medium to high altitudes in complex terrain show a similar variability.

Cluster 5 – m of component 3. The stations are situated in the southern part of Switzerland at different altitudes and types of terrain.

Cluster 6 and 7 – m of component 2 and 3. The stations are located in a similar topography (valleys) and at similar altitudes (generally above 1000m). The stations of cluster 6 however, are placed in the southwestern part and the ones attributed to cluster 7 in the southeastern part of the Alps. Again the geographical dependency seems to be a very strong station-related characteristic.

c.) PCA on summer T_{max}

Component	Eigenvalue (λ)	% total variance explained (λ/m)	Cumulative (λ/m)
1	50.5	49.5%	49.5%
2	28	27.5%	77%
3	17.4	17.1%	94.1%

Table 3.9: PCA with $m = 102$ stations. Extracted are $q = 3$ principal components with $\lambda > 1$, which explain 94.1% of the original variance. Station-related descriptive characteristics can be attributed to all of the components (bold).

Component 1:

All stations on the northern side of the Alps have their strongest loadings on component 1.

tm: Stations located in the north-eastern part of the Jura and the northern Plateau.

m: Stations placed in the Prealps and the south-western part of the Jura (loading > 0.7).

Stations situated in the northern Alps (loading < 0.7).

sr-char.: northern side of the Alps, geographical dependency

Component 2:

tm, m: Stations located in the southern Alps and on the southern side of the Alps

sr-char.: influence of the Mediterranean climate

Component 3:

tm: Stations located at medium to high altitudes in the south-eastern part of the Alps.

sr-char.: geographical dependency, altitude, influence of the Mediterranean climate

d.) CA on summer T_{max}

The 8 identified clusters of climatological stations are represented in Figure 3.6. The geographical dependency is a major station-related characteristic comparable to summer

T_{min}. A further determining station-related characteristic is the influence of the Mediterranean climate. The characteristic altitude is still present though often overlaps with the geographical dependency factor. During persistently hot summer days the planetary boundary layer (PBL) can grow up to considerable altitudes over the Plateau. Within the PBL the climatological conditions are comparable. Areal links thus become more important than the altitudinal characteristics.

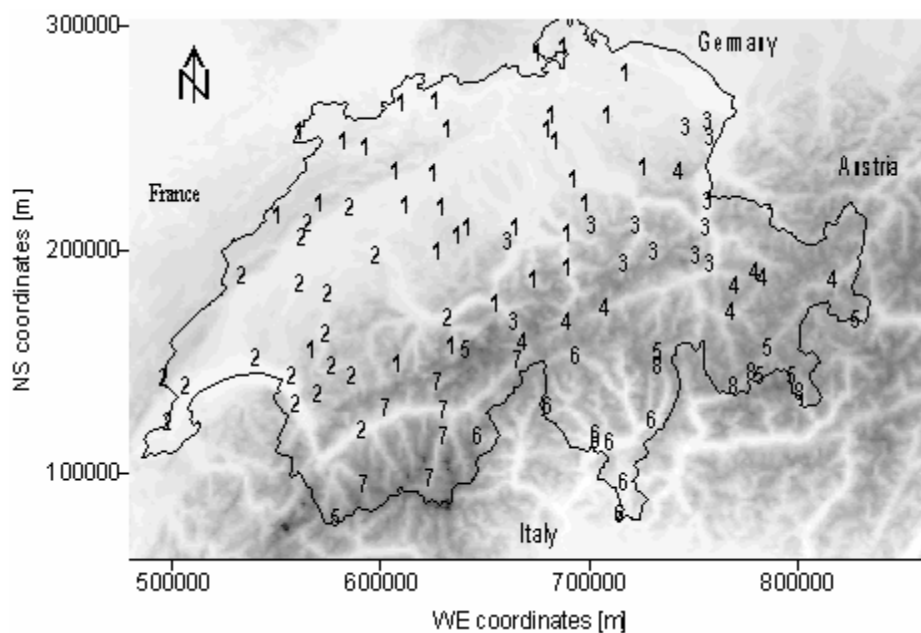


Figure 3.6: Climatological regionalisation of summer T_{max}. Each number represents a climatological station attributed to one of the 8 clusters determined.

Cluster 1 – tm of component 1. The stations are located on the Plateau and in the Jura. The altitude varies between 400 and 1600m.

Cluster 2 – m of component 1 and 2. The stations are concentrated on the western Plateau and in the Jura at altitudes between 400 and 1200m.

Cluster 3 – m of component 1 and 3. The stations are situated in the eastern part of the Plateau, between 400 and 1000m.

Cluster 4 – m of component 1 and 3. The stations are located on passes, summits and in valleys at altitudes between 1100 and 2500m in the central and eastern Alps.

Cluster 5 – m of component 2 and 3. The stations are placed at high altitudes, between 1400 and 3500m, in the south-eastern part of the Alps including the southern most station in the western Alps.

Cluster 6 – tm of component 2. The stations are located in the southern Alps and on the southern side of the Alps. Neither altitude nor topography appear to be important station-related characteristics since the stations are located at altitudes between 200 and 1600m in plains, valleys and on summits. This can perhaps be attributed to the fact that this region is not well ventilated during persistently hot weather. The PBL rises up to high levels and the air cannot be evacuated due to the blocking effect of the Alps to the north.

Cluster 7 – m of component 1 or 2. The stations are located in the south-western part of the Alps generally at altitudes around 1500m.

Cluster 8 – m of component 2. The stations are located at altitudes between 1000 and 1800m in the south-eastern part of the Alps.

3.4.4. Establishing clusters in autumn

a.) PCA on autumn Tmin

Component	Eigenvalue (λ)	% total variance explained (λ/m)	Cumulative (λ/m)
1	47.5	45.3%	45.3%
2	34.6	33%	78.2%
3	15	14.3%	92.5%
4	1.1	1%	93.5%

Table 3.10: PCA with $m = 105$ stations. Extracted are $q = 4$ principal components with $\lambda > 1$, which explain 90.2% of the original variance. Station-related descriptive characteristics can be attributed to the first 3 components (bold).

Component 1:

tm: Stations mainly situated at low altitudes on rather flat terrain in the northern part of Switzerland and the Plateau.

m: Stations located in the Jura, in central Switzerland and in the Prealps (loading > 0.7). Stations situated in large alpine valleys and in the southern part of Switzerland (loading < 0.7).

sr-char.: low altitude, densely populated areas.

Component 2:

tm: High altitude sites located on passes or summits in the Jura, the Prealps and the Alps.

m: Stations situated in the Jura and in alpine valleys (loading > 0.7). Stations in south alpine valleys (loading < 0.7).

sr-char.: medium and high altitude, pass or summit sites, sparsely populated areas.

Component 3:

m: Stations generally located in the southern and south-eastern part of Switzerland.

sr-char.: influence of the Mediterranean climate.

b.) CA on autumn Tmin

Figure 3.7 depicts the 8 clusters of climatological stations, which can be distinguished. The altitude is a major station-related characteristic on the northern side of the Alps, however, less on the southern side of the Alps where the influence of the Mediterranean climate is more important. The nights in autumn can already be considerably cool and therefore night-time inversions and cold air pools in depressions and valleys are a subject to be considered.

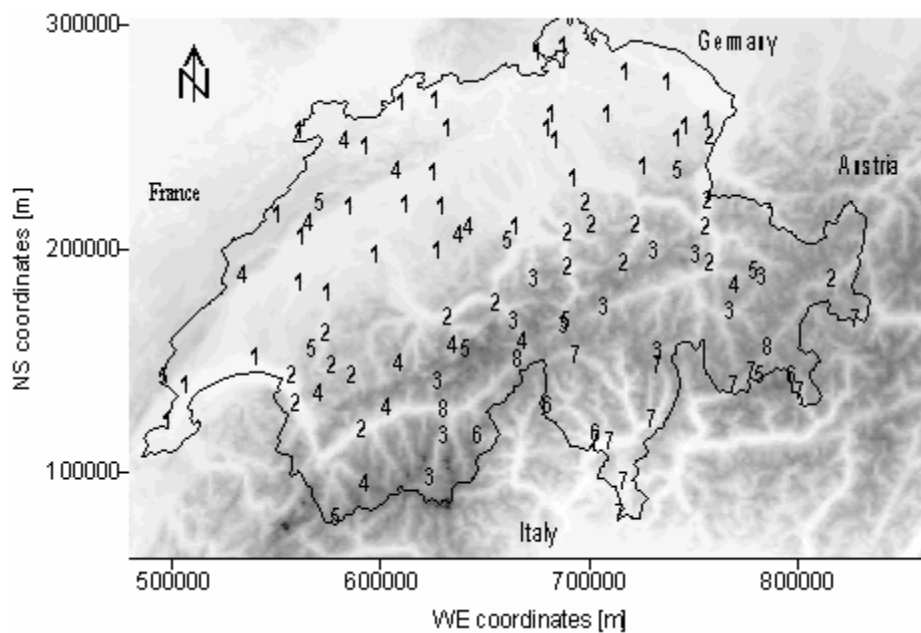


Figure 3.7: Climatological regionalisation of autumn Tmin. Each number represents a climatological station attributed to one of the 8 clusters determined.

Cluster 1 – tm and m of component 1: The stations are located at altitudes between 300 and 600m in the Plateau and the Jura. They are subject to the first inversions and fog layers developing in autumn.

Cluster 2 – m of component 1. The stations are placed at altitudes among 400 and 1000m in the Prealps and large alpine valleys. They are confronted with inversions and first persistent stratus layers only later in autumn.

Cluster 3 – m of component 1 or 2. The stations are located in large alpine valleys at altitudes between 1000 and 1600m.

Cluster 4 – m of component 2. The stations are located at altitudes between 1000 and 1900m in the Jura, the Prealps and the Alps, generally on south exposed, strong inclined slopes and on ridges, passes or summits. Thus, topographic characteristics do not favour an accumulation of cold air.

Cluster 5 – tm of component 2. High altitudes sites, between 1500 and 3500m, on passes and summits in the Jura, the Prealps and the Alps. These stations are possibly in contact with the free atmosphere during the night.

Cluster 6 – m of component 2. The stations are situated in the south-western, the southern and the south-eastern part of the Alps at altitudes of 1500 to 2200m. The two characteristics they have in common are the probable influence of the Mediterranean climate and the altitude.

Cluster 7 – m of component 1 and 3. The stations are located in the southern and south-eastern part of Switzerland at different altitudes.

Cluster 8 – comparable loadings on the components 1 and 3. The stations are situated in large alpine valleys in the south-western and south-eastern part of Switzerland and are probably subject to cold air pools late in autumn.

c.) PCA on autumn T_{max}

Component	Eigenvalue (λ)	% total variance explained (λ/m)	Cumulative (λ/m)
1	39.4	37.8%	37.8%
2	36.3	34.9%	72.7%
3	22.5	21.6%	94.3%

Table 3.11: PCA with $m = 104$ stations. Extracted are $q = 3$ principal components with $\lambda > 1$, which explain 94.3% of the original variance. Station-related descriptive characteristics can be attributed to all of the components (bold).

Component 1:

tm, m: Stations generally below 1000m on the Plateau, the Jura, the Prealps and in large Alpine valleys.

sr-char.: low to medium altitude, northern side of the Alps, high to mean population density

Component 2:

tm: Pass and summit sites in the Jura, the Prealps and the Alps, between 1500 and 2500m.

m: Stations located in the Alps and the Jura above 1000m.

sr-char.: medium to high altitude, complex topography, mean to sparse population density

Component 3:

m: Stations located on the southern side of the Alps regardless to the altitude.

sr-char.: influence of the Mediterranean climate.

d.) CA on autumn T_{max}

Figure 3.8 depicts the 6 identified clusters of climatological stations. Similarly to the autumn T_{min}, the altitude is a major station-related characteristic. During autumn the inversions at low altitudes, in large alpine valleys and in depressions also gain importance during the day.

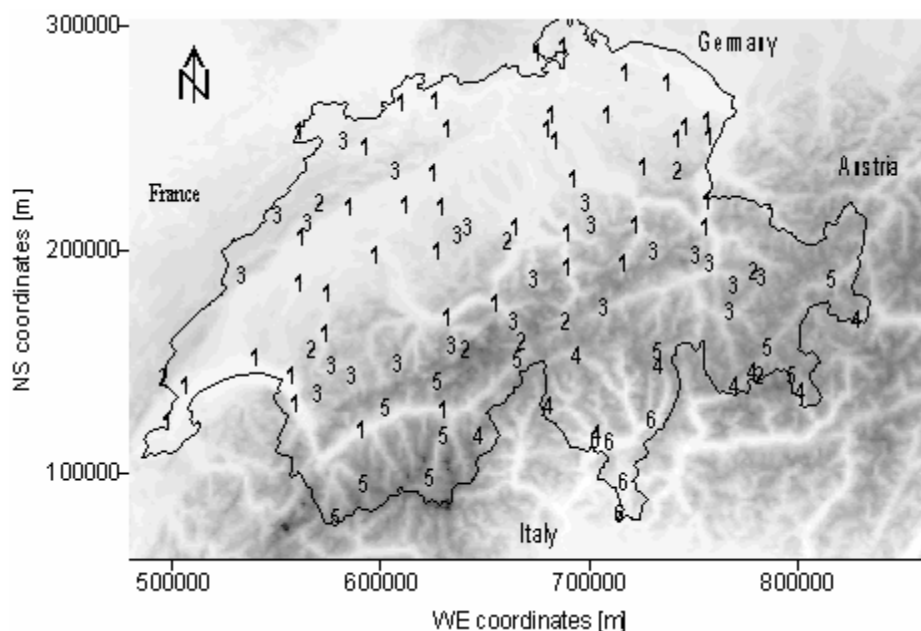


Figure 3.8: Climatological regionalisation of autumn T_{max}. Each number represents a climatological station attributed to one of the 6 clusters determined.

Cluster 1 – tm, m of component 1. The stations are located at low altitudes, below 800m in the Jura, the Plateau and the Prealps. These stations are subject to autumn inversions and fog layers.

Cluster 2 – tm of component 2. The stations are situated on passes and summits in the Jura and the Alps, at high altitudes between 1500 and 3500m.

Cluster 3 – m of component 2 or 1. The stations are generally located at altitudes between 800 and 1600m in the Jura and the Prealps. They are normally not subject to inversions and fog during autumn days.

Cluster 4 – m of component 3. The stations are located at altitudes between 1000 and 1800m and are strongly influenced by the Mediterranean climate.

Cluster 5 – m of component 2. Alpine stations in areas with average to strong slope inclination at altitudes between 1300 and 2500m.

Cluster 6 – m of component 3. Stations located on the southern side of the Alps below 400m.

3.5. REPRESENTATIVE STATIONS PER CLUSTER

The seasonally established clusters of climatological stations for T_{min} and T_{max} are listed in *Appendix B* and their number is indicated in Figure 3.9.

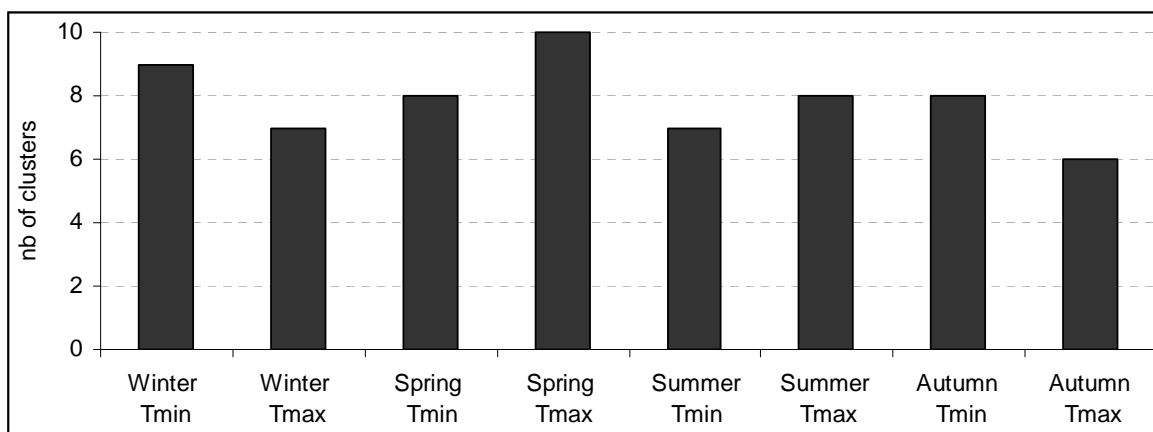


Figure 3.9: Number of clusters established in each season for T_{min} and T_{max}.

In *Appendix B*, the stations printed in bold are selected as representative for the particular region based on the criteria listed below and the comparison to their homogenised analogues over the period 1959 to 1997.

Criteria for representative stations:

- The station has to be in operation at the present time because it is an objective of the study to focus on climate variations during the last decade of the 20th century.

- The station has to provide an as long time series as possible, i.e. observation start 1901, 1931 or latest in 1961, in order to detect climatological trends.
- The meta data in *Appendix A* has to be checked to assure the data quality. Stations, which show various changes in location, instrumentation or station observers, should not be taken into consideration. As mentioned beforehand the meta data is somewhat subjective, however. Some stations are very well documented and consequently figure with many comments whereas others are not so well supervised and therefore figure with fewer comments without necessarily providing a better data quality.

These manipulations results in a selection of a few climatological stations per cluster (final selection shown in Table 3.12). Occasionally only one single station can be selected per cluster and for a small number of clusters none of the criteria applied to any of the climatological stations included. In this case no representative station was selected and thus these regions are not included in the quantitative time series analyses of Chapter 4. The following point denotes the final criteria on which the representative stations are tested:

- The data homogeneity should be satisfactory. Through newly homogenised Tmin and Tmax data sets a test for this criteria on the selected representative stations becomes possible.

In a project of MeteoSwiss, temperature and precipitation data were homogenised applying the tool THOMAS (Tool for the Homogenisation of Monthly Data Series) presented in Bergert et al., (1998). As a result, homogenised monthly Tmin and Tmax data series for most of the climatological stations currently in operation are available for the period 1959 to 1997. Listed in *Appendix B* are the representative stations and the correlation coefficients between the original and the homogenised time series. In most cases the original data series of the selected representative stations show highly significant correlation coefficients (>99%) with the corresponding homogenised data series. Therefore, data homogeneity within the original data sets of representative stations can be assured to a satisfying degree at least for the last 40 years of the 20th century.

Figuring in Table 3.12 is the number of representative stations that is selected for each cluster including the recording period they cover.

Winter Tmin	Winter Tmax	Spring Tmin	Spring Tmax
-------------	-------------	-------------	-------------

Clust.	Stat.	Per.	Clust.	Stat.	Per.	Clust.	Stat.	Per.	Clust.	Stat.	Per.
1	12	01-99	1	10	01-99	1	8	01-99	1	7	01-99
2	2	01-99	2	2	37-99	2	4	01-99	2	3	31-99
3	3	31-99	3	5	01-99	3	-	-	3	2	01-99
4	2	01-99	4	1	61-99	4	2	31-99	4	1	61-99
5	1	61-99	5	-	-	5	2	01-99	5	3	01-99
6	1	31-99	6	2	01-99	6	1	35-99	6	1	31-99
7	1	35-99	7	-	-	7	1	61-99	7	1	61-99
8	1	01-99				8	1	01-99	8	1	61-99
9	-	-							9	-	-
									10	2	01-99

Summer Tmin			Summer Tmax			Autumn Tmin			Autumn Tmax		
Clust.	Stat.	Per.	Clust.	Stat.	Per.	Clust.	Stat.	Per.	Clust.	Stat.	Per.
1	6	01-99	1	4	01-99	1	9	01-99	1	10	01-99
2	3	31-99	2	4	01-99	2	5	31-99	2	2	01-99
3	1	61-99	3	3	31-99	3	2	01-99	3	4	01-99
4	4	01-99	4	4	01-99	4	2	31-99	4	1	61-99
5	2	01-99	5	1	61-99	5	2	01-99	5	1	31-99
6	-	-	6	2	01-99	6	-	-	6	2	01-99
7	1	61-99	7	1	31-99	7	5	01-99			
			8	1	61-99	8	-	-			

Table 3.12: Number of representative stations per cluster with the time span of data recording. The abbreviations "Clust.", "Stat.", "Per.", signify cluster, station, period, respectively. The indications of the years in period are limited to the last two positions, 19XX - 19YY.

3.6. DISCUSSION

The statistical methods used prove to be very convenient tools to divide a large number of climatological stations into clusters of individual stations which all show a comparable day to day variability in Tmin or Tmax. The resulting regions are subject-related constructs, coherent in terms of temperature variability and station-related characteristics. The spatial coherence as such is not a topic in this work.

Using PCA, between 90% and 95% of the variance of the original Tmin/Tmax data matrix can be explained for each season by 3 to 6 principal components. With the division of the stations into “typical members” and “members”, which is related to the degree of correlation between a component and a station, specific characteristics could successfully be attributed to almost every component. Thus, the resulting clusters are not only based on the similar variability in Tmin/Tmax between the time series but also by the station-related descriptive characteristics that can additionally be used as indicators of coherence between the climatological stations included in each cluster. The station-related characteristics most frequently attributed to the components are: altitudinal stages, northern side of the Alps, influence of the Mediterranean climate, complexity of the topography, geographical dependency and population density.

The eight different patterns of clustering resulting out of the eight data sets analysed (see Organigram 1, Section 1.2) show differences related to Tmin and Tmax on the one hand and to the seasons on the other hand. Tmin reflect an image of the night-time temperature distribution in space, where altitudinal stages and topographic features are determining characteristics. Tmax, in contrast, represent the day-time temperature distribution in space, where the geographical dependency seems to be just as significant as the different altitudinal stages. Further, winter and autumn show a similar clustering pattern as well as spring and summer. The winter/autumn pattern is closely related to typical meteorological situations during winter where inversion processes and the formation of a persistent stratus layer over the Plateau are essential. The spring/summer pattern can be associated to typical summer weather situations and regional circulation systems of warm air. With this newly obtained knowledge on seasonal Tmin/Tmax patterns the following concluding points can be formulated:

⇒ T_{min}

Altitude and topography are two essential station-related characteristics influencing the T_{min} clusters in winter and autumn. The clusters of both seasons reflect the extension of the foggy inversion layer over the Plateau, which generally becomes increasingly persistent from autumn to winter. Other climatological stations, which are situated at higher altitudes or at places not affected by this persistent inversion layer over the Plateau, are essentially influenced by the characteristic movements of cold air masses over a complex topography.

Summer and spring T_{min} clusters often show a geographical dependency and the altitude seems to be a less important factor than for winter and autumn T_{min} clusters. In spring however, nocturnal inversions can still develop.

⇒ T_{max}

The clustering pattern of the T_{max} in winter and autumn reflects the typical inversion areas where the persistent stratus layer over the Plateau can last throughout the day. Yet, at higher elevations inversions disperse with the diurnal warming of the air and the stratus layer drops to lower altitudes. Thus at higher altitudes, uniformity due to the geographic situation becomes more important within a cluster of climatological stations. Geographical dependency is the determining station-related characteristic in relation to T_{max} clusters in summer and spring. Over complex topography, regional circulation patterns are decisive for the spatial distribution of warm air.

Analysing the clustering patterns three clusters are emerging which regularly occur within all eight data sets. This is a substantial finding since these three clusters can be associated with the three main station-related characteristics previously attributed to the principal components in Section 3.4: “altitude”, “northern side of the Alps” and “influence of the Mediterranean climate”. These typical characteristics can be linked to the spatial distribution of the climatological stations. Resulting is a relation between the three regularly occurring clusters, a geographic region and a specific altitudinal range. The three clusters can thus be referred to as “low altitudes, north”, “high altitudes” and “low altitudes, south”. These three regions represent the most contrasting climatic areas in Switzerland. The low altitude stations on the northern side of the Alps are generally situated on the Plateau and are influenced by local circulation processes within the densely populated Plateau and by synoptic systems with air masses originating from the Atlantic (W) or the continent (E). The high altitude stations are frequently located on alpine

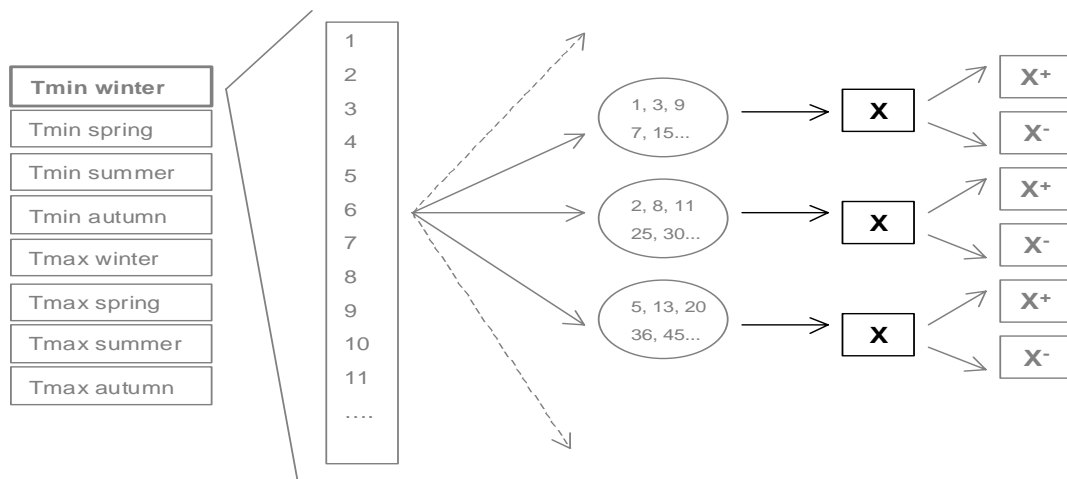
passes and summits. Principally during the cold months, they are assumed to be in contact with the free atmosphere and thus to capture the global sign of climate change (see Section 1.3.2. c). And the climatological stations at low altitudes on the southern side of the Alps are located in the most southern part of Switzerland where the southern alpine slopes merge with the Po basin. The region is subject to an influence of the Mediterranean climate, it is densely populated and in summer heavily polluted air masses, originating from the surrounding area and the Po basin frequently accumulate in this region due to the barrier effect of the Alps. Table 3.13 shows which clusters of each data set correspond to the three regions defined.

	“low altitudes, north”	“ high altitudes”	“low altitudes, south”
Winter Tmin	Cluster 1	Cluster 4	Cluster 8
Winter Tmax	Cluster 1	Cluster 3	Cluster 6
Spring Tmin	Cluster 1	Cluster 5	Cluster 8
Spring Tmax	Cluster 1	Cluster 5	Cluster 10
Summer Tmin	Cluster 1	Cluster 4	Cluster 5
Summer Tmax	Cluster 1	Cluster 4	Cluster 6
Autumn Tmin	Cluster 1	Cluster 5	Cluster 7
Autumn Tmax	Cluster 1	Cluster 2	Cluster 6

Table 3.13: Regularly occurring clusters identified as “low altitudes, north”, “high altitudes” and “low altitudes, south”. The clusters are described in Section 3.4 with their numbers indicated in Figures 3.1 to 3.8.

The remaining, intermediate, clusters are strongly related to the seasonal temperature variability and thus very specific to Tmin/Tmax in one season.

4. SECULAR TRENDS AND INTERANNUAL TO DECADEAL SCALE FLUCTUATIONS IN REGIONAL MEAN TIME SERIES



The black part of the methodological proceeding organigram is performed in this chapter (see Organigram 2, Section 2.2.) and working steps V to VII are discussed (see Section 1.2.):

- V. *Creation of regional mean time series based on the representative stations.*
- VI. *Analysing the secular, the recent 60-year and 40-year trends as well as the interannual and interdecadal variations in T_{min}/T_{max} for the 20th century on regional mean time series.*

4.1 CHAPTER OUTLINE

The focal points of this chapter are to describe and to compare the secular trends and the interannual to decadal fluctuations in secular T_{min}/T_{max} for different regions with an emphasis on the last decade of the 20th century. Based on regional mean time series various quantitative analyses are carried out for each region. In a first approach, linear trends of three phases (1901-99 / 1931-99 / 1961-99) are calculated in order to analyse and evaluate the secular and shorter-term trends. Further, a smoothed curve (moving

averages) describes the interannual fluctuations of the 20th century time series. The subsequent analysis of separate 11-year periods allows to observe on the one hand decadal fluctuations within the time series and on the other hand to compare the last decade (1989-99) to periods of equal length during the century.

In a final point the results are brought into context with comparable studies undertaken in the Alpine countries.

The contents and results of this chapter have recently been published by Jungo and Beniston (2001). This publication is included in my thesis (Section 4.3) and replaces the usual structure of a chapter. Thus closer information about the data and the methods used can be found in chapter 3 of the publication. Chapter 4 of the publication treats winter in detail whereas the analyses of spring, summer and autumn are presented in a more succinct manner. Additional graphical information on these latter seasons may be found in *Appendix D*. The graphs depict the T_{min} and T_{max} distribution of 9 equal periods during 1901-1999.

4.2 PRELIMINARY ANALYSES

4.2.1. Computation of the regional mean time series

The regionalisation procedure discussed in Chapter 3 yielded between 6 and 10 clusters of climatological stations depending on the season. These clusters represent different Swiss climatic regions in terms of T_{min}/T_{max}. The concept of this chapter is based on the quantitative analysis of a regional mean time series computed out of each cluster. In Section 3.5 representative climatological stations were selected within each cluster (see *Appendix B*), which now serve to compute mean time series on a daily basis. In order to scale the single time series on comparable levels their anomalies are calculated relative to the 1961-90 normal period.

Figure 4.1 visualises the regional mean time series for T_{min} in winter, cluster 1, which aggregates most stations located on the Plateau (see Figure 3.1). The mean time series are calculated on a daily time scale, which however, is too small to represent graphically thus the interannual time scale is depicted. Since the clustering of the single station time

series is based on a PCA and CA a high correlation and comparable variability between the single time series is assured. In *Appendix C* the graphs of all regional mean time series are depicted. The graphs show that the regional mean time series adequately represent the single time series of a region.

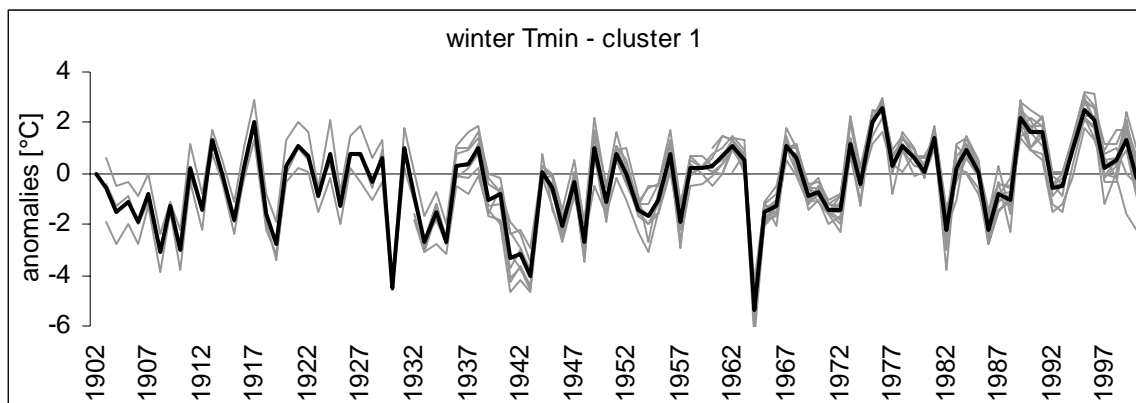


Figure 4.1: Computing of a regional mean time series for cluster 1 of Tmin in winter. The black line represents the mean time series resulting out of 12 time series of individual climatological stations considered as representative for the region (Chapter 3, Section 3.6). The correlation of the mean time series with each of the single time series is over 99% significant.

4.2.2. Limitation of the result description

As evoked at the end on Section 3.6 three typical clusters emerge out of each seasonal data set. They approximately represent the geographical regions of the “Plateau”, the “Alps” and the “South” which are depicted in Figure 1.3. Additionally, the computing of the regional mean time series showed that these typical clusters always have a time series of maximal length (1901-99).

The quantitative analyses, which were carried out on all regional mean time series point to a general link between the regions and this distinct spatial pattern. They showed that the results between the intermediate regions and the main regions are comparable without any exception. However, since the regions depend on the Tmin/Tmax per season and can thus be composed very differently it is not obvious to clearly associate the intermediate regions to the three typical regions in a universal pattern valid for all seasons. For example, a cluster which aggregates stations at around 1000m in alpine valleys can be

associated to the region “low altitudes, north” or to the region “high altitudes” depending on the parameter and the season.

Based on the arguments of comparability and for the sake of clarity it was found to be reasonable to limit the description of the results to these three typical regions hereafter referred to as: “low altitude, north”; “high altitudes”; and “low altitudes, south”. The terms north and south refer to the location of the stations on the northern and on the southern side of the Alps, respectively.

4.3. PAPER BY JUNGO AND BENISTON (2001)

Changes in the anomalies of extreme temperatures in the 20th Century at Swiss climatological stations located at different latitudes and altitudes

SUMMARY

The extreme values of a particular climatological variable determine the thresholds of vulnerability of different environmental systems. Extremes of temperature, beyond a given threshold, may exert irreversible damage on ecosystems, for example, while winds exceeding a given limit will have numerous impacts on vegetation and human infrastructure.

The results of the present study highlight the change in the seasonal temperature limits at different latitudes and altitudes in Switzerland. Winter minimum temperatures at high altitude sites and summer maximum temperatures at low altitude sites in the north, in particular, have changed considerably during the last decade. Since annual extremes are seen to occur either during summer or winter, and much less during the intermediate seasons of spring and autumn, the change in summer and winter extremes are likely to have a significant impact on a number of biospheric, cryospheric, hydrologic and managed systems.

1. Introduction

Over the last few years, there has been an increasing awareness to the fact that a changing climate may have important impacts on natural and socio-economic systems. Prior to the industrial era, climatic change was induced essentially by natural forcings, where the modification of environmental conditions took place at a sufficiently slow pace for the biosphere to adapt. Over the last few decades, however, there is increasing evidence that changes are taking place in an accelerated manner; the global mean temperature is currently about 0.7°C higher than in 1900 (IPCC, 1996; WMO, 1999).

The response to a general warming is likely to lead to an increase in the number of days with extremely high temperatures and less days with extremely low temperatures (IPCC, 1996). For the Northern Hemisphere Karl et al. (1993) found that since the late 1950s an asymmetric evolution in temperature extremes has taken place, expressed in terms of a stronger increase in minimum than in maximum temperatures; more recent work by Dai et al. (1999) based on worldwide satellite data also support this conclusion. This behavior has been confirmed by results from several analyses on the evolution of temperature extremes during the 20th century in the Alpine region (Beniston et al., 1994; Baeriswyl and Rebetez, 1996; Beniston and Rebetez, 1997; Weber et al., 1994, 1997).

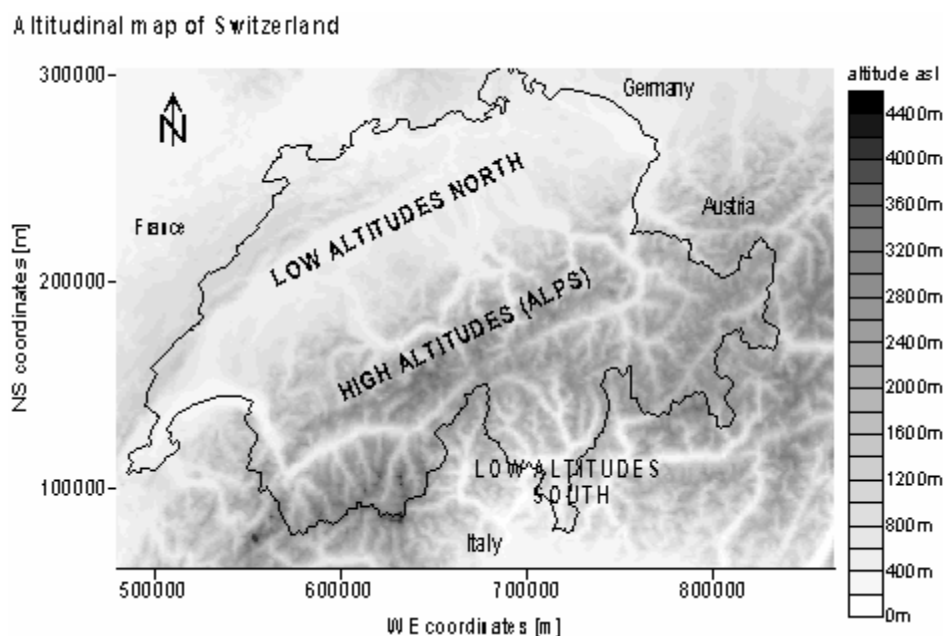


Figure 1: Map of Switzerland. The different latitudinal regions (north and south of the Alps) and the high altitude region are indicated in an approximate manner

It is observed that warming in Switzerland has not taken place in a gradual and continuous manner since the beginning of the 20th century, but rather in separate periods with substantial warming as in the 1940s (Beniston et al., 1994) or in the late 1980s, for example (Beniston and Rebetez, 1996). There is sufficient evidence to link these trends to low-frequency forcing by the North Atlantic Oscillation, as will be seen in Section 5. Furthermore, Baeriswyl and Rebetez (1996) have demonstrated in an analysis carried out over the period from 1901 to 1994 that the minimum tend to rise most during wintertime, at high altitudes (Figure1). Such trends are consistent with regional climate model simulations of current climate; these models show a warming in the Alps, reaching close to 1°C on average, and up to 2°C for individual sites (Marinucci et al., 1995). Studies conducted by Weber et al. (1994, 1997), however, where the annual variations of diurnal temperature range at low and at high elevation sites in the Alpine region are analyzed, are in contradiction with these results. The period considered is 1901 to 1990 and the study concludes that little or no diurnal asymmetry is observed for high altitude stations. Furthermore, the strongest minimum temperature increase has been detected at low-lying stations in the western part of the Alps. These contradictory findings, which basically treat the same set of data but over a shorter length in time, serve to emphasize that an amplification of the global climate signal seems to have occurred over the past decade at high altitudes. The question arises whether alpine regions are more representative of the large-scale, long-term climate change (i.e., of processes taking place in the free troposphere) than a densely populated region located at lower elevations (i.e., where urban and boundary-layer influences are likely to influence climatological trends and characteristics). Especially during late autumn and winter, cold air pools build up over the Swiss Plateau to form a strong and sometimes persistent inversion layer, which essentially decouples the low-level atmosphere from processes above the inversion. As a result of the stability of the atmospheric boundary layer, there is no exchange of air between low and high elevations during wintertime, as has been shown by Baltensberger et al. (1997). Results from a different study undertaken by Jungo (1996) indicate that the ozone concentrations measured at Jungfraujoch during the summer months are comparable to those of the lower free troposphere at about 4000m asl measured by radiosondes over the Swiss Plateau. Consequently high alpine stations can be considered as representative for the free troposphere at most times during winter and summer.

The analyses presented in the present paper focus on the seasonal evolution in minimum and maximum temperatures in Switzerland during the 20th century. They are part of an

extensive study, financed by the Swiss National Science Foundation. This study has the objective to add detailed information and several new aspects to previous work.

The principal aims of the paper are:

- to present the evolution of temperature extremes in the Alpine region for the period 1900-1999 as a whole, referring to seasonally built clusters of Swiss climatological stations.
- to emphasize the most important differences in the 20th century extreme temperature evolution for groups of climatological stations located at different altitudes and latitudes.
- to highlight the unusually fast and important temperature rise that has taken place since the end of the 1980s and its seasonal and regional dependency.

2. Data

2.1. Quality

The data investigated here is provided by the Swiss Meteorological Institute (MeteoSwiss), which manages a dense network of different types of climatological stations distributed throughout Switzerland. The data is not homogenized by MeteoSwiss, however; different tests of plausibility (limits, variability, consistency) are applied and if a correction is necessary, the data series are treated manually (Konzelmann, pers. com.). In 1970, changes in the time of data measurement have been made; yet, no discontinuity, which could have been caused by these time changes can be detected in the 20th century temperature time series (Montmollin, 1993). The meta data (description of the stations' history) is a convenient tool to detect changes in instrumentation and location of each station; however, in most cases overlapping measurements have been made over a certain period in order to ensure data quality. The data homogeneity of the Swiss minimum and maximum temperature time series has been discussed in several publications (Beniston et al., 1994; Weber et al., 1994; Baeriswyl and Rebetez, 1996; Rebetez and Beniston, 1998; Heino et al., 1999). Generally, few inhomogeneities have been brought to light and the Swiss climatological database is considered to be reliable enough for a treatment as such. In a study conducted by Baeriswyl and Rebetez (1996), the homogenized time series of Geneva and Bern are compared to the non-homogenized ones. The findings are that differences in data variability are rarely significant and in the final results, the rare dissimilarities that have been found do not invalidate the results. The temperature bias due to urbanization has been tested for climatological stations close to cities by Weber et al. (1994) and has been found to be negligible. Additionally, it is not

ideal to filter extreme data too rigorously, since real (non-spurious) values would be erroneously eliminated in some cases, even though they express the great temporal and spatial extent of natural variability (Heino et al., 1999).

2.2. Treatment

Based on this knowledge, the daily minimum and maximum temperature database has been used for the analyses of this study. As previously mentioned, many similar studies have been made up until now using the Swiss climatological data set. However, they are all based on the time series of only a reduced set of climatological stations considered as representative for particular and extensive regions. The goal of this current work is to take into consideration a maximum number of stations in order to observe regional changes for each season at fine resolution, since spatial variability is high in mountain regions. Therefore, over 100 climatological stations distributed throughout Switzerland have been evaluated reviewing the meta data. Those which show various changes of placement, instrumentation or observer, were eliminated.

The following statistical analyses have all made use of the commercial software package SPSS (1999).

The time series analyzed are treated using Principal Component Analysis (PCA) and Cluster Analysis, in order to subdivide the large number of climatological stations as a function of the seasonal minimum and maximum temperatures, separately. The resulting groups are clusters of climatological stations, which exhibit comparable variability and highly similar characteristics in their seasonal time series. Differences between the groups can be explained in terms of altitude, topography and other characteristics of regional climate (Baeriswyl and Rebetez, 1996). Moreover, using PCA and Cluster Analysis implies that the time series of the stations within each group show a certain homogeneity in their data; otherwise it would be impossible to obtain well explainable groups. PCA is based on a spatial correlation matrix between the station time series. As explained in Bahrenberg et al. (1992), the entire variation of the original data matrix can be reproduced in such a way that each variable is represented as a linear combination (as in a regression analysis) of the calculated components.

This can be expressed as follows:

$$X_1 = \alpha_1 + \beta_{11}K_1 + \beta_{12}K_2 + \dots + \beta_{1q}K_q$$

$$X_2 = \alpha_2 + \beta_{21}K_1 + \beta_{22}K_2 + \dots + \beta_{2q}K_q$$

$$X_i = \alpha_i + \sum_{l=1}^q \beta_{il} K_l \quad (i = 1, \dots, m)$$

where: K_l = principal component, whereas l continues from 1 to q

X_i = standardized station data

α_i = regression constant of X_i

β_{il} = partial regression coefficient of K_l in the equation for X_i

The number of components normally extracted is far smaller than the number of input variables, which constitutes an important reduction of data while simultaneously retaining most of the variability in the original data. The method however, does not provide a clear separation of the groups, because the variability at a station is explained by more than one component at a time. The following Cluster Analysis attempts to identify homogeneous clusters of climatological stations referring to their minimum and maximum temperatures, separately (as for the PCA). The analysis is based on the correlation matrix between the station time series and the extracted principal components, while the difference between two clusters is as large as possible. Consequently, the resulting groups are aggregates of stations, which exhibit a similar seasonal variability in their data. The hierarchical method employed here begins by finding the closest pair of variables according as a function of distance and combines them to form a cluster. The method is hierarchical because once two objects or clusters are joined, they remain together until the final step. The question concerning the number of clusters that should be taken into account cannot be answered clearly; it needs to represent a compromise between the degrees of generalization. The intentions are to assure a certain minimum of clarity and at the same time to limit the loss of information. (Bahrenberg et al., 1992). The Euclidean distance is used as a measure of distance and the average linkage method as a similarity measure for the stepwise clustering. (SPSS, 1999).

The Euclidean distance corresponds to the distance between two points and is based on the Pythagorean theorem.

$$ED = \sqrt{\sum_{i=1}^m (x_{ij} - x_{ik})^2}$$

where: (x_{ij}) $i = 1, \dots, m$; $j = 1, \dots, n$ (based on a data matrix)

m = number of variables

n = number of objects

ED = Euclidean distance

In the average linkage method, the similarity between different clusters (Cr and Cs) is determined by measuring the average distance between two points in Cr and Cs

$$d_{Cr,Cs} = \frac{1}{n_r} * \frac{1}{n_s} \sum_{j \in Cr} \sum_{k \in Cs} d_{jk}$$

where: d_{jk} = distance measured

$d_{Cr,Cs}$ = similarity of two clusters

3. Methods

For the following analyses, daily absolute extreme temperatures have been used. According to the common usage, the analyses are conducted for temperature anomalies, defined as departures from the 1961 to 1990 climatological period (WMO, 1999). Instead of treating the time series of all stations in each group, it is acceptable to work with the mean time series established for each group. The results of the analysis made for a given mean time series are representative for each station time series of the respective group. The mean values are calculated as the arithmetic mean of all these stations. As a consequence of this procedure, possible irregularities in the data continuity of single stations are smoothed out. The daily anomalies of the mean time series are then averaged over each season, which considerably reduces the amount of data. It is preferable to perform the following statistical tests and analyses on seasonal data, since short-term variations within daily values can distort important large-scale effects.

To analyze the trend behavior of the different groups, a linear regression over three time spans, namely 1901 to 1999, 1931 to 1999 and 1961 to 1999 was carried out. In 1931 and 1961, new stations were added to the MeteoSwiss climatological data network. The three periods have been chosen to illustrate the changes in the strength of temperature warming over the 20th century (Beniston et al., 1994; Beniston and Rebetez, 1996). The significance of the linear trends is determined by running an F-test, which tests the hypothesis that the slope β of the regression line is significantly different from 0 (SPSS, 1999). In addition, for each group and period, a 95 % confidence interval is calculated for the slope β . This allows to determine whether or not the gradients of the regression slopes between the groups differ significantly from each other during one time span. However, linear trends strongly depend on the first and the last values of a series, and in order to ensure the existence of a real trend it is important to analyze the time series more carefully through other types of analysis.

Subsequently, in order to detect long-term fluctuations, a 9-point running mean filter (RM) is used, where the span has been chosen experimentally. The first RM value is set at the end of the first time span. Ideally, the RM span is detected by running an autocorrelation function (ACF), but the temperature time series are subject to a strong trend, which enhances the autocorrelation. In a detrended ACF, no clear repetition periods were found.

In order to obtain better information concerning trend changes over a long period, it is necessary to analyze different periods. Hence, the 99 years are divided into equal time intervals. Based on 11-year spans, the time series are split up into equal groups of 9 periods giving an overall picture of the temperature evolution during the 20th century. It is important that the last decade is depicted as a separate period. Subsequently, analyzing the statistical values of the central tendency (median) and the dispersion (percentiles, min, max, range), it is possible to determine whether the symmetry in the frequency distribution has changed from one period to another, or whether a shift has occurred. Applying a paired samples (dependent) t-test allows to determine whether the shifts between the 9 periods are significant or not. When the calculated differences between two periods diverge significantly from 0, the hypothesis of similarity is rejected within a confidence interval of 95%. [SPSS, 1999].

4. Results

Analyzing the data for both extremes from 1901 to 1999, important differences in terms of temperature rise are found between the seasons. Winter temperatures yield the most striking results. Regional differences, which occur within a season, are generally linked to latitude or altitude. Thus, an exact description will only be given for winter temperatures of three groups representing different latitudes and altitudes with minimum and maximum temperatures (Table 1, Figure 1). The results of the other seasons will only be mentioned briefly.

Low altitudes, north		High altitudes		Low altitudes, south	
Mintemp.	Maxtemp.	Mintemp.	Maxtemp.	Mintemp.	Maxtemp.
Bad Ragaz 496m	Bad Ragaz 496m	Jungfrauoch 3572m	Arosa 1847m	Lugano 276m	Locarno-Monti 379m
Basel 317m	Basel 317m	Säntis 2500m	Davos 1590m		Lugano 276m
Bern 570m	Bern 570m		Disentis 1180m		

Chur 586m	Delémont 416m		Jungfrauoch 3572m		
Delémont 416m	Luzern 456m		Säntis 2500m		
Luzern 456m	Montreux 408m				
Montreux 408m	Neuchâtel 487m				
Neuchâtel 487m	Koppigen 482m				
Koppigen 482m	Schaffhausen 457m				
Rheinfelden 271m	St. Gallen 664m				
Schaffhausen 457m					
St. Gallen 664m					

Table 1: Climatological stations and their elevation, which are included in the calculation of the winter minimum and maximum mean time series representing typically the low altitudes north and south of the Alps as well as the high altitudes.

4.1. Winter

4.1.1. Linear regression over three time spans

LINEAR TREND PER YEAR	1901-99		1931-99		1961-99	
	MIN	MAX	MIN	MAX	MIN	MAX
Low altitude, north	0.018°C <i>(0.005)</i>	not signif.	0.035°C <i>(0.009)</i>	0.020°C <i>(0.009)</i>	0.043°C <i>(0.021)</i>	0.050°C <i>(0.023)</i>
High altitudes	0.014°C <i>(0.005)</i>	0.023°C <i>(0.005)</i>	0.033°C <i>(0.008)</i>	0.032°C <i>(0.008)</i>	0.069°C <i>(0.021)</i>	0.060°C <i>(0.019)</i>
Low altitude, south	0.031°C <i>(0.004)</i>	not signif.	0.052°C <i>(0.005)</i>	0.016°C <i>(0.006)</i>	0.052°C <i>(0.011)</i>	not signif.

Table 2: Linear trends over a variable length in time during the winter month. The trends per year are indicated if the slope β of the regression line is significant i.e., within a 95% confidence interval. The standard errors are provided in italics, within the brackets.

Comparing the gradients of the significant regression slopes individually for each time slice indicated in Table 2, no statistically significant differences can be found between the three groups. The warming of the winter extreme temperatures shows amplification in the second half of the century, especially at high elevations.

4.1.2. Anomaly fluctuations

Through the minimum temperature anomalies, the groups can be separated geographically into a more northern ("low altitude north") or a more southern compartment ("low altitude south"). As shown in Figure 2 from 1972, the temperatures at low altitudes in the north as well as in the south are persistently warmer than normal with dips around 1981/82, 1984 to 87 and 1990/91 and 1999, whereas the positive and negative values are less pronounced in the south. Prior to 1972, the southern stations show only negative anomalies while in the north and at high altitudes they alternate similarly between positive and negative departures from the mean. The maximum temperature anomalies alternate at low altitudes both north and south of the Alps, with more persistent warm phases around 1910-20 and 1940-60. The high altitudes are characterized by mostly cold anomalies until 1970. Between 1970 and 1977 however, a warm phase takes place over the whole country. The years with the most pronounced and persistent warm anomalies in all regions are 1988 to 99 with dips in 1990/91, 1995-96 and 1999. The long-term trend of both extremes changes countrywide to a positive phase around 1990; this is still the case nowadays, more than one decade later.

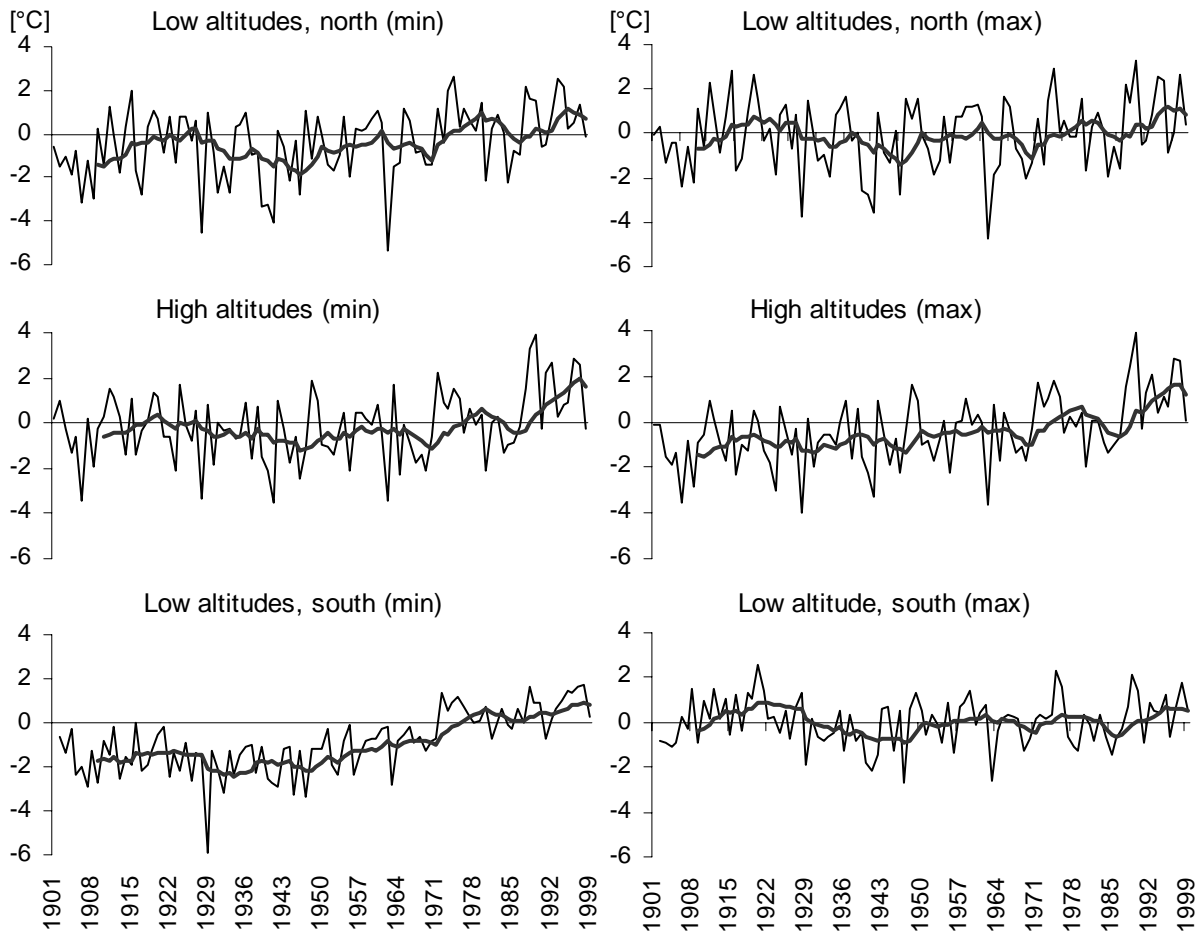


Figure 2: Winter minimum and maximum temperature anomalies from 1901-99 for different latitudes and altitudes in Switzerland. The bold line indicates the 9-point running mean filter.

4.1.3. 9 Periods

Table 3 contains the results of the paired samples t-test, which determines the statistical significance of the shifts in the distributions between the 9 periods. At northern low altitudes, the first (1901-11) and the last (1989-99) period seem to be out of the range compared to the other periods. At high altitudes, the distribution of the most recent period (1998-99) differs significantly from the distributions of all the other periods during the 20th century. The southern low altitudes exhibit a somewhat different behavior. The first 6 periods of the century (1901-66) differ significantly from the remaining 3 periods (1967-99). These conclusions hold especially for the minimum temperatures.

Low altitude, north MIN	Low altitude, north MAX	High altitude MIN	High altitude MAX	Low altitude, south MIN	Low altitude, south MAX
<i>1901-11*1912-22</i>	<i>1901-11*1912-22</i>	<i>1901-11*1989-99</i>	<i>1901-11*1967-77</i>	<i>1901-11*1967-77</i>	<i>1901-11*1912-22</i>
<i>1901-11*1967-77</i>	<i>1901-11*1989-99</i>	<i>1923-33*1989-99</i>	<i>1901-11*1978-88</i>	<i>1901-11*1978-88</i>	<i>1901-11*1989-99</i>
<i>1901-11*1978-88</i>	<i>1934-44*1989-99</i>	<i>1934-44*1989-99</i>	<i>1901-11*1989-99</i>	<i>1901-11*1989-99</i>	<i>1912-22*1923-33</i>
<i>1901-11*1989-99</i>	<i>1945-55*1989-99</i>	<i>1945-55*1989-99</i>	<i>1912-22*1989-99</i>	<i>1912-22*1967-77</i>	<i>1912-22*1934-44</i>
<i>1934-44*1989-99</i>		<i>1956-66*1989-99</i>	<i>1923-33*1967-77</i>	<i>1912-22*1978-88</i>	<i>1912-22*1967-77</i>
<i>1945-55*1989-99</i>		<i>1967-77*1989-99</i>	<i>1923-33*1989-99</i>	<i>1912-22*1989-99</i>	<i>1912-22*1978-88</i>
<i>1956-66*1989-99</i>		<i>1978-88*1989-99</i>	<i>1934-44*1989-99</i>	<i>1923-33*1967-77</i>	<i>1934-44*1989-99</i>
			<i>1945-55*1989-99</i>	<i>1923-33*1978-88</i>	<i>1978-88*1989-99</i>
			<i>1956-66*1989-99</i>	<i>1923-33*1989-99</i>	
			<i>1967-77*1989-99</i>	<i>1934-44*1956-66</i>	
			<i>1978-88*1989-99</i>	<i>1934-44*1967-77</i>	
				<i>1934-44*1978-88</i>	
				<i>1934-44*1989-99</i>	
				<i>1945-55*1967-77</i>	
				<i>1945-55*1978-88</i>	
				<i>1945-55*1989-99</i>	
				<i>1956-66*1967-77</i>	
				<i>1956-66*1978-88</i>	
				<i>1956-66*1989-99</i>	
				<i>1967-77*1989-99</i>	

Table 3: Significant shifts between the distributions of the 9 periods, depicted in the boxplots of Figure 3. When the value wise calculated differences between two periods diverge significantly from 0, the hypothesis of similarity is rejected within a confidence interval of 95%. Periods, which systematically differ significantly from others, are emphasized in italics.

General evaluation of the 9 periods in time:

Figure 3 depicts a first positive shift in the lower tail of the extremes of the minimum temperatures between 1956-66 followed by a first increase of the entire distribution in 1967 and a second one in 1989 for the low altitudes in the north and in the south. The maximum temperatures at low altitudes north and south of the Alps depict a period with highly positive values in 1912-22, then anomalies retrieved and remained rather constant during the following periods to rise again considerably in the upper 75 percentiles of the distribution in 1967. In 1989 the entire distribution experiences a shift towards the positive values. The high altitude stations exhibit a constant evolution for minimum and maximum temperatures until 1989, where the entire distribution shifts significantly towards higher values. The last 11-year period of the 20th century (1989-99) marks a recent warming phase in Switzerland.

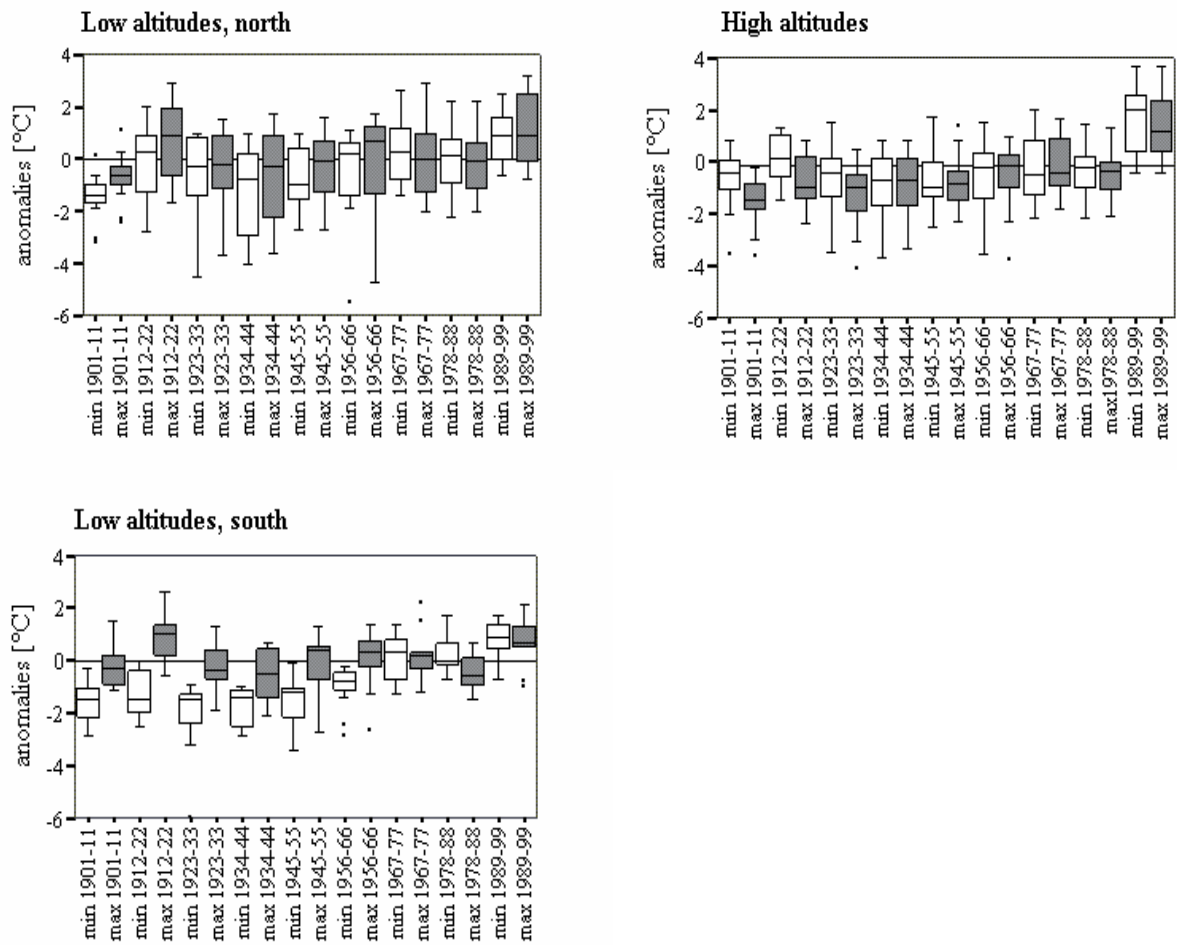


Figure 3: Boxplots of winter minimum (white box) and maximum (gray box) temperature anomalies for different latitudes and altitudes in Switzerland. The period of 1901 to 1999 is divided into 9 periods of equal length. The box comprises 50% of the values, its upper bound defines the 75 percentile, the lower bound the 25 percentile and the black line within the box pinpoints the median. The ends of the vertical lines mark the maxima and the minima respectively, which are not outliers. Outliers (black dots) are defined as values that are more than 1.5 box-lengths away from the 75 or 25 percentiles.

4.2 Spring, summer, autumn

LINEAR TREND PER YEAR	1901-99		1931-99		1961-99	
	MIN	MAX	MIN	MAX	MIN	MAX
Low altitude, north SPRING	0.014°C <i>(0.003)</i>	not signif.	0.019°C <i>(0.005)</i>	not signif.	0.033°C <i>(0.012)</i>	not signif.
Low altitude, north SUMMER	0.009°C <i>(0.002)</i>	not signif.	0.010°C <i>(0.004)</i>	not signif.	0.036°C <i>(0.009)</i>	0.032°C <i>(0.014)</i>
Low altitude, north AUTUMN	0.017°C <i>(0.003)</i>	0.010°C <i>(0.004)</i>	0.015°C	not signif.	not signif.	not signif.
High altitudes SPRING	not signif.	not signif.	not signif.	not signif.	0.043°C <i>(0.016)</i>	not signif.
High altitudes SUMMER	0.009°C <i>(0.003)</i>	not signif.	0.015°C <i>(0.005)</i>	not signif.	0.031°C <i>(0.009)</i>	not signif.
High altitudes AUTUMN	0.012°C <i>(0.005)</i>	0.030°C <i>(0.005)</i>	not signif.	0.030°C <i>(0.007)</i>	not signif.	not signif.
Low altitude, south SPRING	0.026°C <i>(0.003)</i>	-0.010°C <i>(0.004)</i>	0.036°C <i>(0.005)</i>	not signif.	0.039°C <i>(0.01)</i>	not signif.
Low altitude, south SUMMER	0.030°C <i>(0.003)</i>	-0.024°C <i>(0.004)</i>	0.025°C <i>(0.004)</i>	-0.020°C <i>(0.006)</i>	0.034°C <i>(0.008)</i>	not signif.
Low altitude, south AUTUMN	0.026°C <i>(0.003)</i>	not signif.	0.020°C <i>(0.004)</i>	not signif.	not signif.	not signif.

Table 4: Linear trends over a variable length in time during spring, summer and autumn. The trends per year are indicated if the slope β of the regression line is significant i.e. within a 95% confidence interval. The standard errors are provided in italics, within the brackets.

Table 4 shows that the minimum temperatures at low altitudes in the north and at high altitudes have risen mainly during the past 40 years with regard to all seasons except autumn. On the other hand, at southern stations the gradient of the regression slope is continuously strong in all seasons and periods. Only autumn minima indicate a non-significant linear trend at the end of the century in Switzerland. Figure 4 emphasizes that a different evolution in minimum temperatures prior to about 1980 distinguishes the southern low altitude region during spring, summer, and autumn from the northern low altitude regions and the high elevation sites. A persistent period of warm anomalies between 1940 and 1960 characterizes the high altitudes during spring and the entire country during summer. After 1980 however, anomalies become mostly positive in all regions. The most important dips where the minimum temperatures revert to normal or even slightly negative values occur in 1981/82, 1984-87, 1990/91 and 1995/96 for all seasons; the dips are particularly strong, however, since 1990 in autumn at high elevation sites. On a decadal-scale, minimum temperatures are persistently above normal since 1986 in summer and autumn and since 1989 in spring. However, the autumn anomalies at

the high altitudes return to below normal values from 1996 (which is the only period in the latter part of the 20th century where anomalies revert to below-normal values).

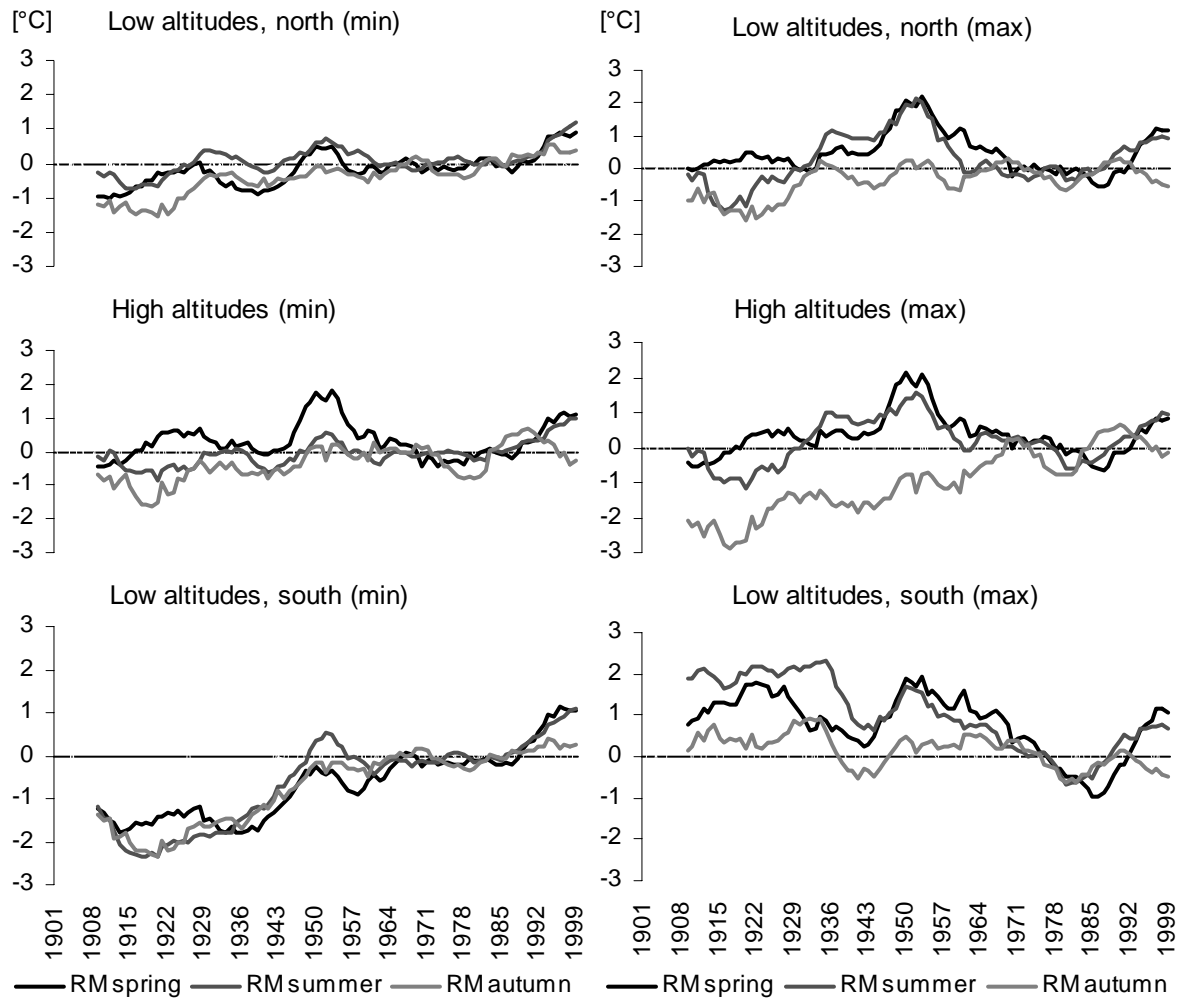


Figure 4: Decadal trend (9-point running mean filter) of spring, summer and autumn minimum and maximum temperature anomalies from 1901-99 for different latitudes and altitudes in Switzerland.

Close inspection of Table 4 highlights the fact that, at low altitudes in the north, summer maximum temperatures have increased significantly during the past 40 years, whereas the autumn temperatures at high altitudes have decreased notably during this period. The day-time maximum temperatures in the south have not changed during autumn during the 20th century, but have rather decreased during spring and summer. The decadal trend in Figure 4 shows that a first strong warming in day-time maximum temperatures occurs from 1940-60 in all regions and seasons, except autumn at high elevation sites. In a

second phase, the values become increasingly positive in all regions during summer and autumn from 1980 onwards, as well as during spring after 1988. In autumn, however, temperatures again drop after 1989. Once more, there are major dips in the persistent warm phase at the end of the century, which are partly comparable between different seasons. The first one in summer is between 1984 and 1987; subsequently, all seasons show lower values in 1990/91 and 1995/96. The decadal trend is persistently positive since 1988 in summer and after 1990 in spring. During autumn, however, the trend is continuously negative from 1994 onward.

5. Discussion

The foregone analyses serve to emphasize that in the alpine region, a new and different behavior in minimum and maximum temperature evolution is emerging in recent decades. The minimum temperatures, however, show more significant results than the maximum temperatures. In the following paragraphs, detailed conclusions concerning the differences in 20th century evolution of extreme temperatures between different latitudes and altitudes in Switzerland are formulated for each season.

- The night-time minimum temperatures show a countrywide significant warming in two main phases during all seasons except autumn. Spring and summer are the first seasons with a shift of the temperatures towards more positive anomalies occurring between 1945 and 1955, followed by winter where the first sign of warming is significant at low altitudes between 1956 and 1977.
- The second set of significantly warmer night-time temperatures is situated between 1989 and 1999, including high elevation sites in winter, which exhibit an exceptionally strong rise. In autumn, only the low altitudes depict significant positive shifts in the temperature distribution, starting in 1945 in the south and in 1978 in the north.
- The warming in maximum temperatures is much weaker than the minima. A warm shift in autumn in 1945 and in winter in 1989 distinguishes the high elevation sites from the other regions. The northern low altitude regions are characterized by two warming phases in spring; the first occurs in 1945 and the second in 1989. During the summer months, a considerable increase in maximum temperatures between 1989 and 1999 at low altitudes in the north can be detected, as well as a cooling between 1934 and 1967, which only concerns the low altitudes in the south.

Linking the phases of strong warming during the last decade of the 20th century to the North Atlantic Oscillation (NAO) can provide a partial explanation to these observations. The NAO represents one of the most important modes of decadal-scale variability of the climate system after ENSO (El Niño/Southern Oscillation), and accounts for up to 50% of sea-level pressure variability in the region (and even over 65% in winter months). It is observed to strongly influence precipitation and temperature patterns on both the eastern third of North America and western and northern Europe; the influence of the NAO is particularly evident during winter months. It has been shown in recent years (Beniston et al., 1994; Hurrell, 1995) that a significant fraction of climatic anomalies observed on either side of the Atlantic are driven by the behavior of the NAO. As highly-positive NAO Index values have been recorded during most of the 1990s, inducing salient changes in the frequency distributions of temperature, moisture and pressure, the highly anomalous nature of temperatures and their extremes discussed in this paper may be, at least in part, explained by the large-scale forcings generated by the NAO. Whether the behavior of the NAO in recent years is linked to global warming is a matter of speculation, although recent work by Paeth et al. (1999) using the German coupled ocean-atmosphere model ECHAM4/OPYC suggests that greenhouse-gas warming may be influencing the behavior of the NAO on time-scales of 60 years or more. However, the causal mechanisms of the “see-saw” in the North Atlantic pressure fields are still not fully elucidated. Nevertheless, it is concluded here that the NAO is a significant driving factor for the climatic anomalies recorded during recent years in the Alpine region.

6. Conclusion

At the beginning of the 20th century, the night-time minimum temperatures have been significantly lower in every season throughout Switzerland. During winter, however, they show the strongest warming with amplification in the second half of the century, especially at high elevations. Additionally, at low altitudes in the north, diurnal summer temperatures have also increased significantly during the past 40 years, whereas the autumn temperatures at high altitudes have diminished notably during this period. Countrywide, the long-term decadal-scale trend of both extremes is persistently positive since the end of the 1980s for all seasons except autumn. The autumn minimum temperature trend reverts to below normal values from 1996 at high altitudes; the autumn maximum temperature trend is continuously negative since 1994 during every season. Generally, the 20th century warming marks the strongest temperature rises around 1945 and 1989.

However, in addition to these two major warming phases, the regions of different latitudes and altitudes do not necessarily show the same temperature evolution during each season. Since the end of the 1980s, though, the climate changes in different regions, and especially at different altitudes, have shown increasingly similar trends. Thus, to a certain extent, low altitudes are also sensitive to the longer-term climate change, even though such change is more evident at high altitudes. The recent periods are completely out of the range of the normal secular trends; this is particularly true for winter night-time minimum temperatures at high altitudes. If this trend were to continue into the 21st century, the ecological and economical consequences resulting from such a change are likely to be quite substantial. The fact that high altitude sites are more sensitive to changing temperatures makes them extremely vulnerable locations. The alpine biosphere, cryosphere and hydrosphere will certainly be affected by such rapid change, which in turn will impact upon mountain communities, which would have to cope with an increase in other predicted impacts of climatic change, such as the increase in natural hazards and their economic consequences.

Acknowledgements

The authors would like to thank M. Rebetez (Swiss Federal Institute for Forest, Snow and Landscape Research - WSL, Lausanne) and C. Collet (Department of Geosciences, University of Fribourg) for helpful comments, discussions and reviewing. Thanks are also extended to two reviewers whose comments helped to improve the original draft substantially. This study is funded by the Swiss National Science Foundation, through Grant NR. 2100-050496.97.

REFERENCES

see References – Section at the end of the work

4.4. COMPARISON WITH EXISTING TEMPERATURE TREND STUDIES IN ALPINE COUNTRIES

It is problematic to compare results on a European or Global scale because the studies conducted for the temperature trends of the 20th century are generally based on different periods, comprising the years only until 1970, 80 or 90. Most of the studies cited in the following paragraphs rely on the result of a linear regression trend, where the length of the period taken into consideration can bias the final result. The trend estimates should thus preferably be compared for similar periods. The direct comparison with studies undertaken on a large scale or at geographically very different regions are especially difficult due to dissimilar conditions, e.g. data recording or synoptic systems. The consistent upward trend in T_{min} and T_{max} resulting out of the quantitative analysis of the present study, however points into the same direction as the studies conducted on mean temperatures over the 20th century cited in Section 1.3.1 “Observed temperature fluctuations in the recent past and the present at different scales and various mountain regions”. Furthermore, the results generally correspond to the findings of various studies conducted in Switzerland present in the introduction to the paper by Jungo and Beniston (2001) and in the following paragraphs.

With an analysis carried out over the period from 1901 to 1994 Baeriswyl et al. (1997) have demonstrated that the T_{min} based on seasonal means tend to rise most during wintertime at high altitudes. Moreover, analysing data of 8 Swiss climatological stations at different altitudes over the period of 1901 – 1996 Rebetez and Beniston (1998a) found that the monthly mean positive trends for T_{min} and T_{max} are greatest in autumn and winter and weakest in late spring and early summer. The results of the present study, emerging from the analyses of seasonal mean T_{min} and T_{max} over the period 1901 – 1999, are in agreement with these findings.

On a somewhat larger geographical scale (Alpine countries) Weber et al. (1997) conducted analyses on seasonal mean T_{min} and T_{max} considering the period 1901 to 1990. For western low-lying stations, which approximately corresponds to the region “low altitude, north” of the present study, the authors found a significant T_{min} increase in all seasons and T_{max} increase in autumn only, with a significantly decreasing diurnal temperature range (DTR) in all seasons. At several European mountain stations a significant T_{min} increase was found in summer and autumn whereas the increase in T_{max} is restricted to autumn. The authors concluded that the DTR at high altitudes was consistent during the period analysed. Furthermore, the trends, though significant, were

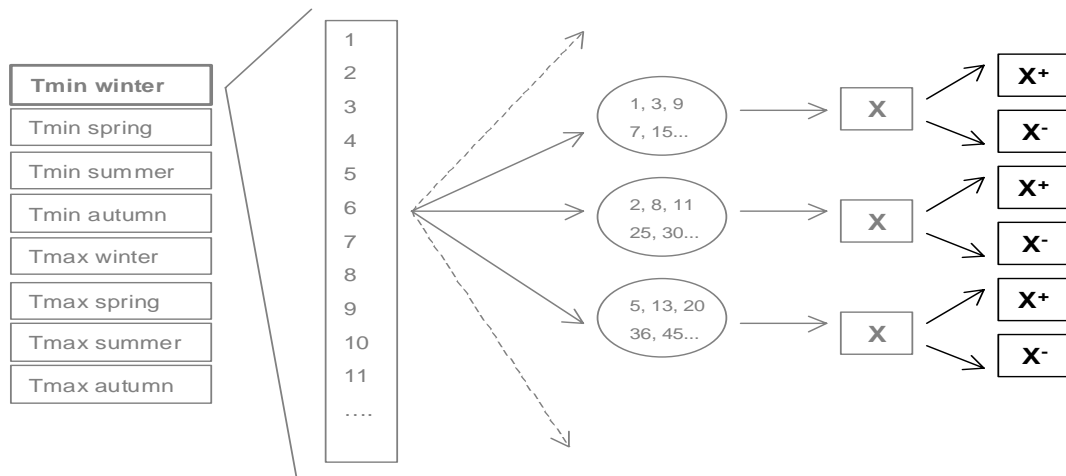
found to be less strong at mountain stations than at low altitudes. Comparing these results to the present study an accordance can be found between the seasonal mean Tmin and Tmax trends of the western low-lying stations (time series 1901-90) and the corresponding results found for the region "low altitudes, north" (time series 1901-99). The DTR in the region "low altitudes, north" however, remains at a constant level over this period. The trends found for the mountain stations are not always comparable to the trends found for the region "high altitudes". Between 1901 and 1999 the Tmin increase significantly in all seasons except spring (not only summer and autumn) and the Tmax increase is not only restricted to autumn, the winter season also shows a significant temperature increase. Additionally, the significant trend estimates calculated on the 1901 to 99 time series are not lower at "high altitudes" than at "low altitudes, north". The consistency found for the DTR is comparable.

These comparisons indicate that the secular warming pattern seems to be changing in recent decades. One of the most important findings of the present study is that if concentrating on the trend estimates emerging for the period 1961 to 1999, a modification in the magnitude of the seasonal warming trends becomes apparent. Autumn temperatures, which show significant secular warming trends in all Swiss regions now remain at a constant level. It was found that the strong secular autumn warming is mainly due to high autumn Tmin and Tmax during the second half of the 1980s which is not extended into the 1990s. The significant positive trends in Switzerland during this recent 1961 to 1999 period are restricted to winter Tmin and Tmax, spring and summer Tmin in all regions and summer Tmax in the region "low altitudes, north". The highest positive trend estimates calculated between 1961 and 1999 emerge in the region "high altitudes" in winter. They amount to +2.7°C for Tmin and +2.3°C for Tmax. Although the Tmin increase stronger than the Tmax, which results in a decreasing DTR, the difference between the increasing trend estimates of Tmin and Tmax over this recent period is not significant in any region nor in any season.

During the last 40 years however, large areas seem to be characterised by a significant decrease in the DTR (IPCC, 1996, Chapter 3). Comparing trends of annual mean Tmin and Tmax between 1950 and 1990 or 1901 and 1996, considering 8 Swiss climatological stations at different altitudes and latitudes, Rebetez and Beniston (1998a) found a decrease in the DTR, which is substantially greater than the average found for the Northern Hemisphere. Analyses based on seasonal or monthly means of the daily-calculated temperature range although rarely provide as obvious results. Several regions show consistent or even increasing DTR. A constant DTR over the period 1951 to 1990

resulted for climatological stations at different altitudes in Austria (Weber et al., 1997). The analysis of two mountain stations in Croatia between 1954 and 1995 showed an increase of the DTR (Gajic-Capka and Zaninovic, 1997). Several Italian stations, though analysed over a long period (1865 to 1996), indicate an increase in the DTR which was found to be greater in the north than in the south of Italy (Brunetti et al, 2000).

5. VARIATIONS IN TEMPERATURE EXTREMES



The black part of the methodological proceeding organigram is performed in this chapter (see Organigram 2, Section 2.2.) and working steps VIII to IX are discussed (see Section 1.2.):

- VIII. *Analysing the secular trend in the warm and cold temperature extremes, exceeding a given threshold within Tmin/Tmax in specific regions.*
- IX. *Relating the results found for the temperature extremes of Tmin/Tmax to the temporal variation of Tmin/Tmax.*

5.1. CHAPTER OUTLINE

In the previous chapter the temporal variations over the 20th century of Tmin and Tmax were evaluated seasonally for three different regions. Resulting are several positive shifts in the Tmin and Tmax distribution, which are becoming more intense during the last decade of the 20th century. The shift of a distribution can be associated with changes, which are more important in either its lower or its upper tail or which are equal in both tails.

The aim of Chapter 5 is based upon the results of Chapter 4 and attempts to describe the observed shifts more closely by analysing the tails of the distributions, i.e., Tmin/Tmax values exceeding a given upper and lower threshold. These values will hereafter be referred to as warm and cold temperature extremes (min+, max+ and min-, max-, respectively).

In order to describe the interannual changes in warm and cold temperature extremes during the 20th century occurring on a seasonal basis in different climatological regions, linear trends are calculated. The interest is focusing on the questions whether the warm and cold temperature extremes have become warmer and if so, which temperature extreme (warm or cold) within the Tmin/Tmax distribution is subject to a stronger secular warming. Further, it is of importance to know whether this warming can be related to a certain point in time. The following three types of comparisons between the trend estimates provide results on the significance of their difference within a 95% confidence bound.

Type I: The warm and the cold extremes within the Tmin or Tmax distribution, e.g. min- with min+ in region A in winter (Figure. 5.1).

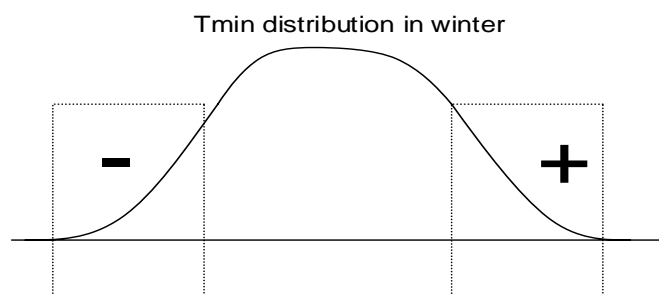


Figure 5.1: Schematic representation of comparison type I.

Type II: Identical extremes between the two regions, e.g. min- in region A with min- in region B in winter (Figure 5.2).

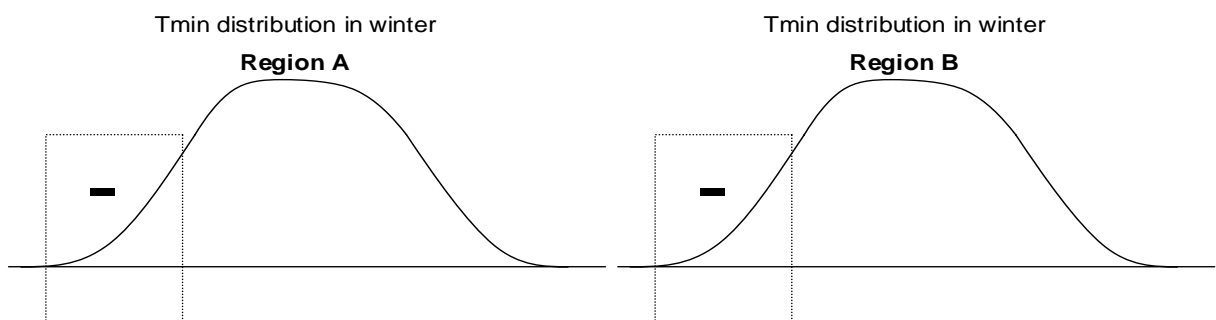


Figure 5.2: Schematic representation of comparison type II.

Type III: Identical extremes and region between the season, e.g. min- in region A in winter with min- in region A in spring (Figure. 5.3).

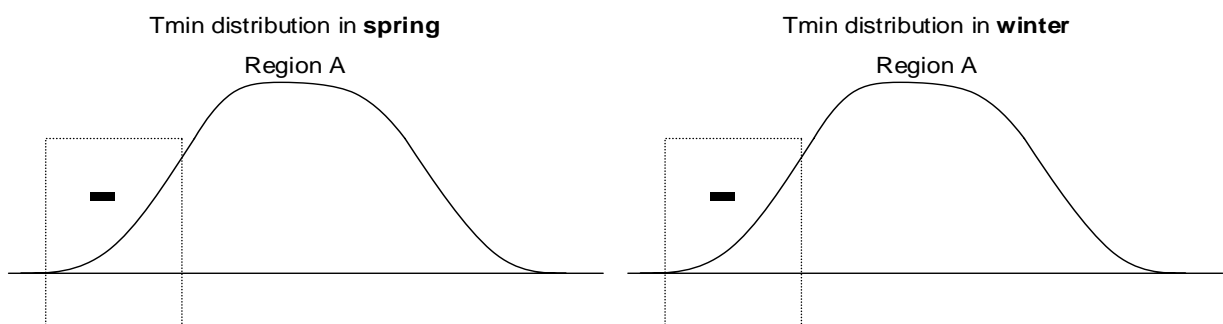


Figure 5.3: Schematic representation of comparison type III.

Secular trend estimates are good indicators for general tendencies, but mask variations on a smaller time scale. Therefore, the frequency count of the temperature extremes occurring during each season is represented graphically on a century time scale. Focusing on the time scale this facilitates to determine on the one hand when possible changes in the warm and cold temperature extremes occurred and on the other hand if they are of a gradual or of an abrupt nature. Additionally, the frequency count graph can visually support the statement resulting out of Chapter 4, that especially in winter the warming observed over the last decade of the 20th century is exceptional compared to other periods of the same length.

The presentation of the results is restricted to the 2 main regions “low altitude, north” and “high altitudes” defined in Chapter 3. The region “low altitude, south”, which has also been analysed in Chapter 4 is no longer included here. According to the meta data of *Appendix A* the data quality of the southern stations, mainly Lugano, was not very high until 1970. The bias, which in this case especially affects the temperature extremes might be too important and hence possibly hides a real tendency.

5.2. METHODS

It is not evident to choose thresholds for extreme values when working with trend statistics. The rarity of an event and the high level of noise in extreme data limits the possibility to detect trends and it is thus recommended to focus the analyses on moderate extremes (Frei and Schär, 2000). The threshold defined in order to conduct the trend analysis of interannual temperature extremes throughout the century is therefore the mean value calculated out of 10% of monthly T_{min} and T_{max} extremes, i.e., the 3 coldest and 3 warmest values per month within both, T_{min} and T_{max}. The secular trend is calculated through a linear regression with an F-test to determine the significance of the inclination of the regression slope, where the level is fixed on 5% (SPSS 1, 1999). A 95% confidence bound for the regression slope is calculated in order to undertake the three types of comparisons formulated in Section 5.1.

A slightly different threshold was used for the frequency count. It although covers a comparable 10% range of the data but it was fixed at the 10th and 90th percentile values of the probability density function (PDF) of the 1961 – 90 climatological mean period. The anomalies used in Chapter 4 were calculated relative to this same reference period. The reason for this selection finds its justification in the constant thresholds, which neither depend on the length of the time series taken into consideration nor on the influence of the warm decade of the 1990s. Hereafter, the cold and warm extremes are often referred to as min- / max- and min+ / max+.

At this point I would like to precise that it is not the purpose of this chapter to calculate occurrence probabilities (used in Chapter 6) or to determine indices for return periods of a rare event, which have destructive potential and are consequential for the ecology and the economy as a single event. These methods are principally applied to wind and

precipitation data or to temperature data in order to detect heat or cold waves. (Progressing literature can be found in Climatic Change 42, 1999 where the results of a workshop on indices and indicators for climate extremes, held in Asheville, USA are published.)

5.3. RESULTS

5.3.1. Winter

WINTER trends /ct	low altitudes, north	high altitudes
Trend Tmin	+1.8°C (0.5)	+1.4°C (0.5)
Trend min-	+2.11°C (0.8)	+1.12°C <i>ns</i> (0.7)
Trend min+	+1.11°C (0.5)	+2.09°C (0.5)
Trend Tmax	+0.8°C <i>ns</i> (0.5)	+2.3°C (0.5)
Trend max-	+1.06°C <i>ns</i> (0.7)	+1.5°C (0.7)
Trend max+	+0.99°C <i>ns</i> (0.6)	+3.16°C (0.5)

Table 5.1: Linear century (ct) trends of Tmin and Tmax and of their cold and warm extremes. “*ns*” = trend estimates not significant on a 5% significance level; “()” = standard error, σ , of the regression slope, with $\pm 1.98\sigma = 95\%$ confidence bound.

Table 5.1 indicates in both of the tested regions a 20th century warming in temperature extremes. Comparing the confidence bounds of the trend estimates of cold and warm extremes within Tmin or Tmax, no significant differences can be found. Therefore, in none of the Tmin or Tmax distributions the values in one tail increase significantly stronger than the values in the other tail. However, a general pattern between the trend estimates of the tails and the two regions can be identified. In the region “low altitudes, north” the cold extremes (min- and max-) show in both cases a stronger warming than the warm extremes (min+ and max+) whereas the exact opposite is true for the region “high altitudes”.

When comparing the confidence bounds of the trend estimates in identical extremes between the two regions one significant difference is found. The Tmax warm values (max+) are characterised by a significantly stronger increase in the region “high altitudes” than in the region “low altitudes, north”. This leads to the conclusion that warm winter days

at high altitudes have been subject to a much stronger warming during the 20th century than at low altitudes.

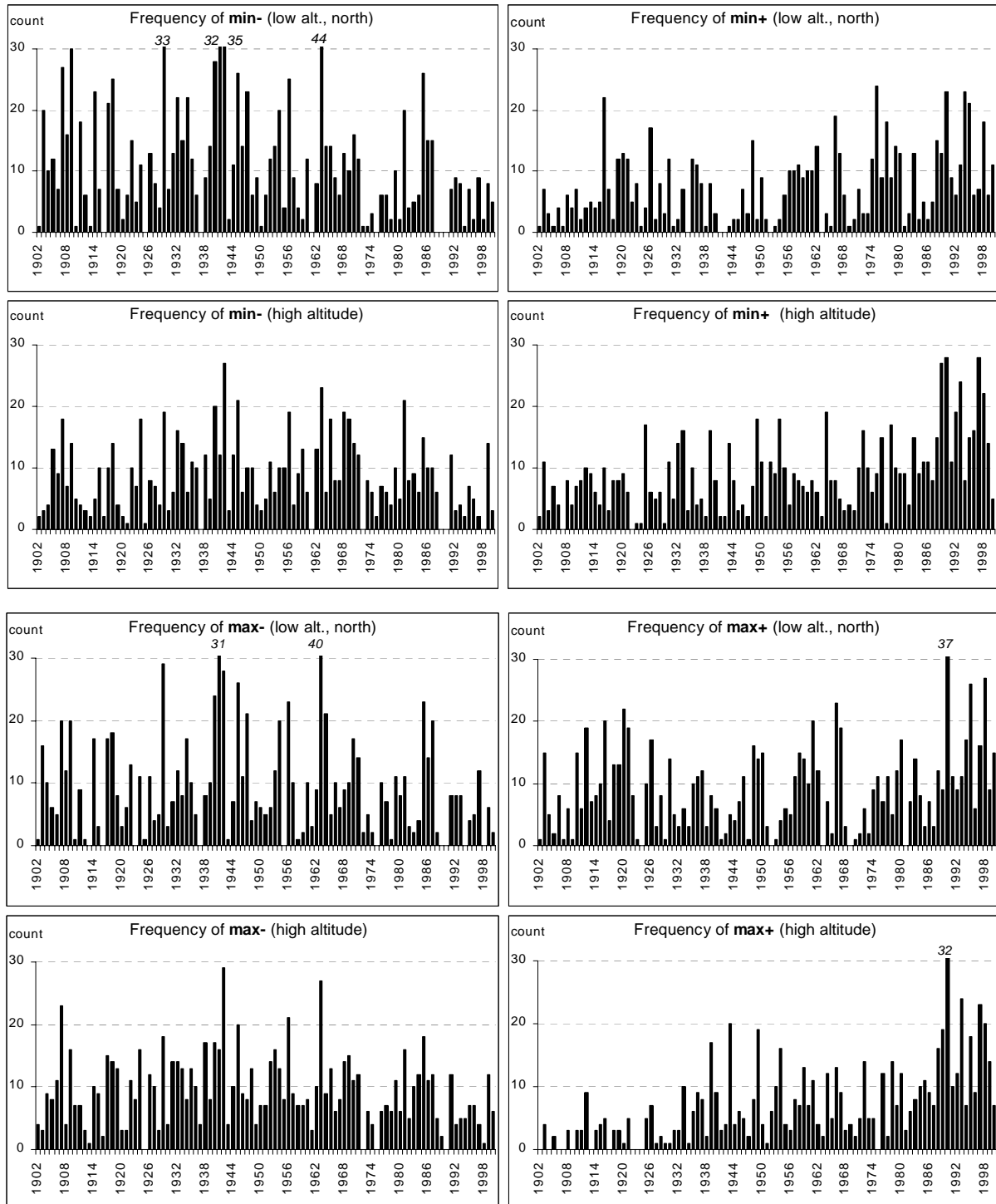


Figure 5.4: Frequency count of winter temperature extremes occurring during each season between 1902-2000.

In Figure 5.4 the occurrence of the temperature extremes exceeding the 10th and the 90th percentiles of the 1961 to 1990 PDF are depicted. Evaluating the interannual frequency count warm phases with a lower number of cold extremes and/or a higher number of warm extremes can be detected. A general change in the frequency of extreme values can be observed after 1990. The T_{min} cold extremes (min-) are partly missing or becoming more rare in both regions. The frequency of the T_{min} warm extremes (min+) on the other hand becomes more important from about 1975 on in the region “low altitudes, north” and in a rather abrupt manner from 1989 on in the region “high altitudes”. This behaviour is in accordance with the results of Chapter 4 where at the end of the century a more gradual increase in T_{min} was found for the region “low altitudes, north” and an abrupt one in the last decade of the century in the region “high altitudes”.

The T_{max} cold extremes (max-) do not show visibly evident changes. Within the warm extremes (max+) however, a clear increase can be observed in both regions from 1990 on. For the region “high altitudes” a first increase in warm winter days occurring in the beginning of the 1940s and a second abrupt one in the 1990s can be identified.

5.3.2. Spring

SPRING trends /ct	low altitudes, north	high altitudes
Trend T_{min}	+1.4°C (0.3)	+0.5°C ns (0.4)
Trend min-	+1.63°C (0.4)	+0.74°C ns (0.6)
Trend min+	+1.21°C (0.3)	+0.71°C (0.4)
Trend T_{max}	+0.3°C ns (0.4)	+0.4°C ns (0.4)
Trend max-	+0.33°C ns (0.5)	+0.06°C ns (0.5)
Trend max+	+0.28°C ns (0.5)	+1.55°C (0.5)

Table 5.2: As Table 5.1.

The linear trends listed in Table 5.2 indicate a general warming tendency within spring temperature extremes, which is not always significant although. Especially T_{max} extremes stayed at comparable levels in the beginning and at the end of the century. The 95% confidence bounds of the trend estimates do neither differ significantly between the warm and cold extremes of a distribution nor when comparing the identical extremes in both regions.

The significant T_{min} increase in spring in the region “low altitudes, north” is characterised by a slightly stronger increase in the min- than in the min+, which resembles the pattern found for winter trend estimates within the tails. A quite high trend estimate results for the T_{max} warm extremes in the region “high altitudes”. A possible explanation can be found in the corresponding graph of Figure 5.5. which depicts mild decades in the 1940s and 1990s where the frequency of the warmest spring days grew especially high.

Figure 5.5 shows that the changes in the occurrence of temperature extremes at the end of the century are not as obvious in spring as they are in winter. The most evident drop in the coldest values and increase in warmest values during the 1990s is shown within T_{min} (min- and min+) of the region “low altitudes, north”. This is in agreement with the significant trend estimates found for the T_{min} distribution in this region (Table 5.2).

In the two regions several mild phases emerge, where the frequency of the warmest night and day values (min+ and max+) is very high. Apart from the 1990s the 1920s and the 1940s can be identified as such.

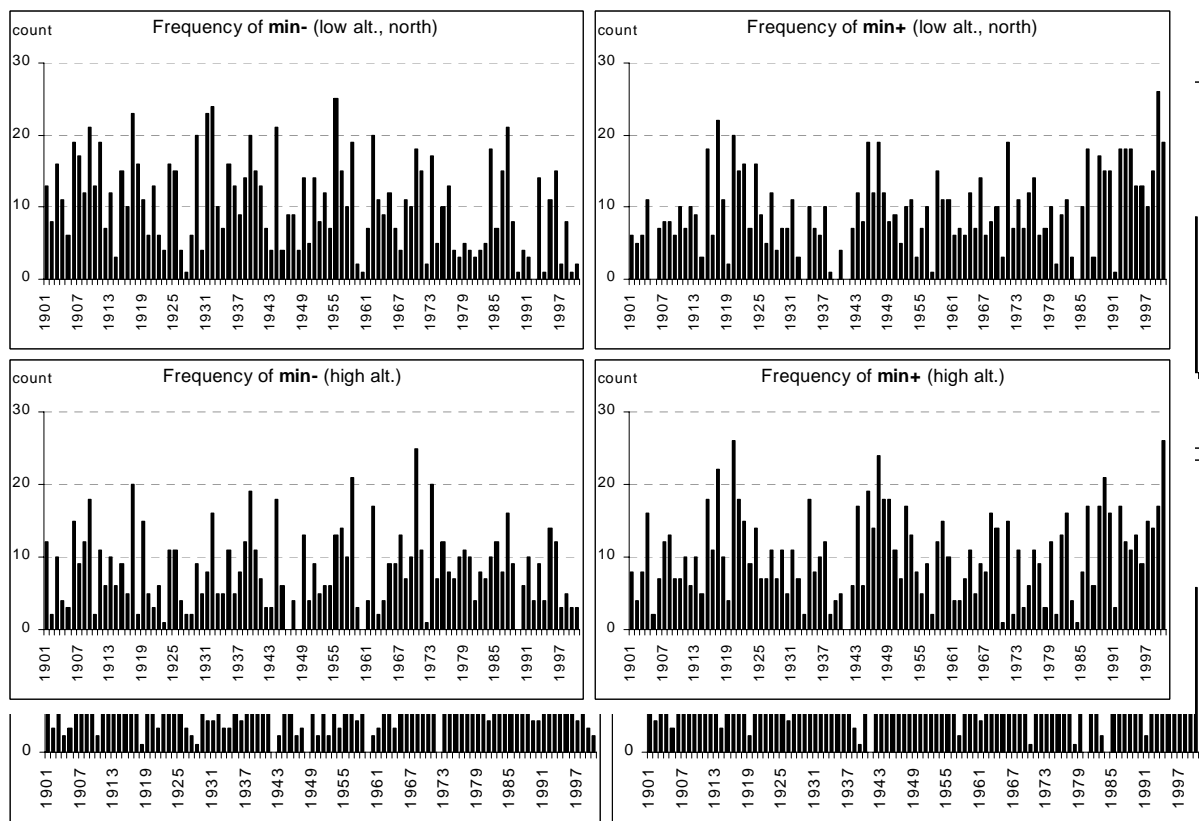


Figure 5.5: As for Figure 5.4 except for spring.

5.3.3. Summer

Summer trends /ct	low altitudes, north	high altitudes
Trend Tmin	+0.9°C (0.2)	+0.9°C (0.3)
Trend min-	+0.71°C (0.3)	+1.03°C (0.4)
Trend min+	+1.31°C (0.3)	+0°C <i>ns</i> (0.4)
Trend Tmax	+0.8°C <i>ns</i> (0.5)	+0.6°C (0.4)
Trend max-	-0.03°C <i>ns</i> (0.5)	-0.52°C (0.5)
Trend max+	+0.55°C <i>ns</i> (0.5)	+1.3°C (0.4)

Table 5.3: As for Table 5.1

As observed for the two previous seasons the summer temperatures also generally tend to rise during the 20th century (Table 5.3). The exceptions are the Tmin warm extremes (min+) in the region “high altitudes”, which remain constant and in the Tmax cold extremes (max-) in both regions, which even show a slightly negative trend. Comparing the 95% confidence bounds of all trend estimates the only significant difference can be found between the Tmax cold and warm extremes (max- and max+) in the region “high altitudes”. The temperatures of the warm extremes increased significantly more compared to the cold extremes. This indicates that the positive century trend in Tmax in the “high altitudes” region is principally due to a strong rise in warmest summer days.

Further, the two regions show a comparable century trend in Tmin. Even though the difference is not significant, the min+ of the region “low altitudes, north” increased slightly more than the min-. For the region “high altitudes” the opposite is true, the cold summer nights are becoming significantly warmer while the warm summer nights remained at a constant level since the beginning of the century. This is in opposition to the pattern found in between the regions and the tails of the winter temperature distributions.

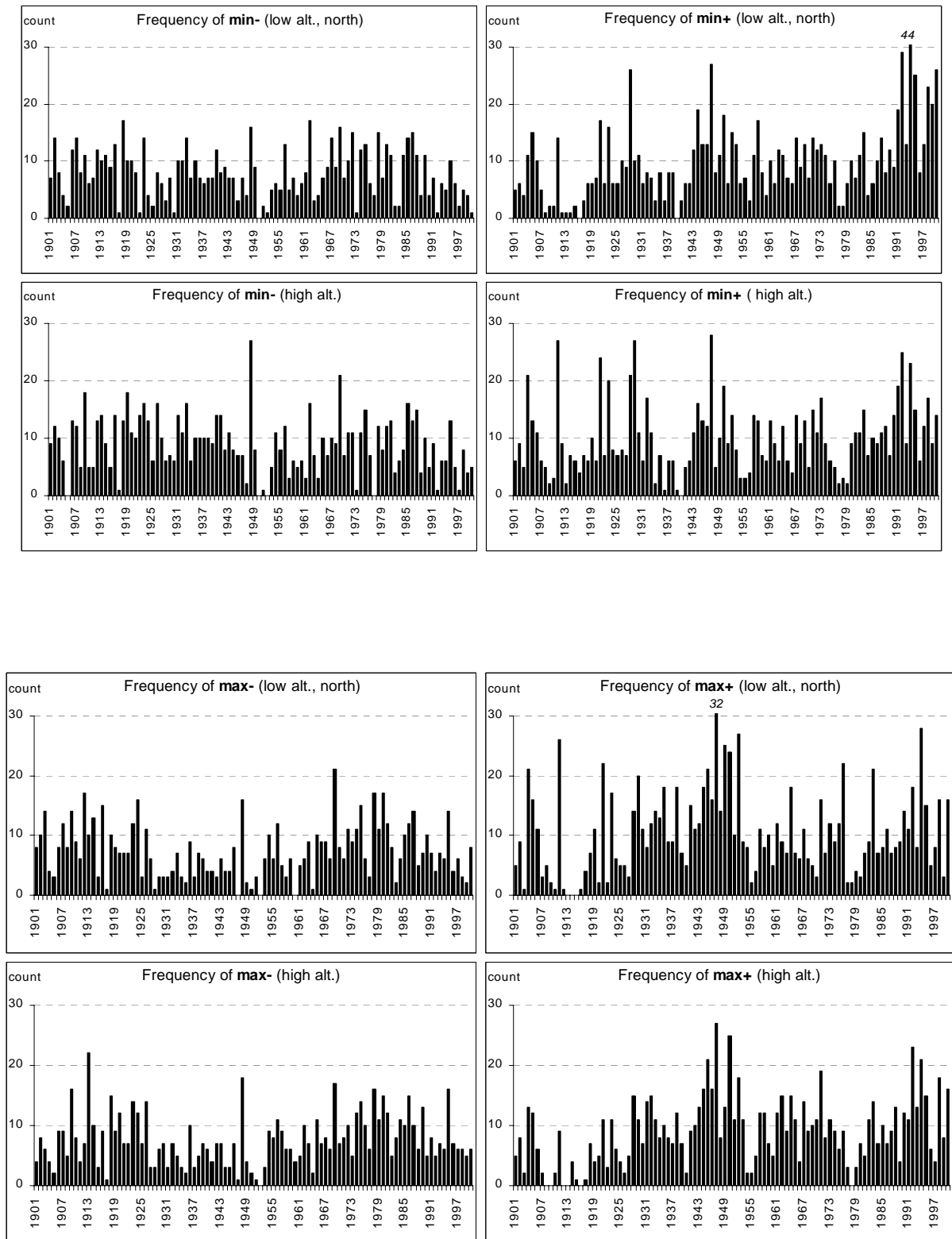


Figure 5.6: As for Figure 5.4 except for summer.

Evaluating the graphs in Figure 5.6, the cold extremes (min- and max-) show a comparable gap in the frequency count of the second half of the 1940s in both regions. The warm extremes (min+ and max+) on the other hand are characterised by a high frequency of warm values during the 1940s and the 1990s, which is comparable to the spring season.

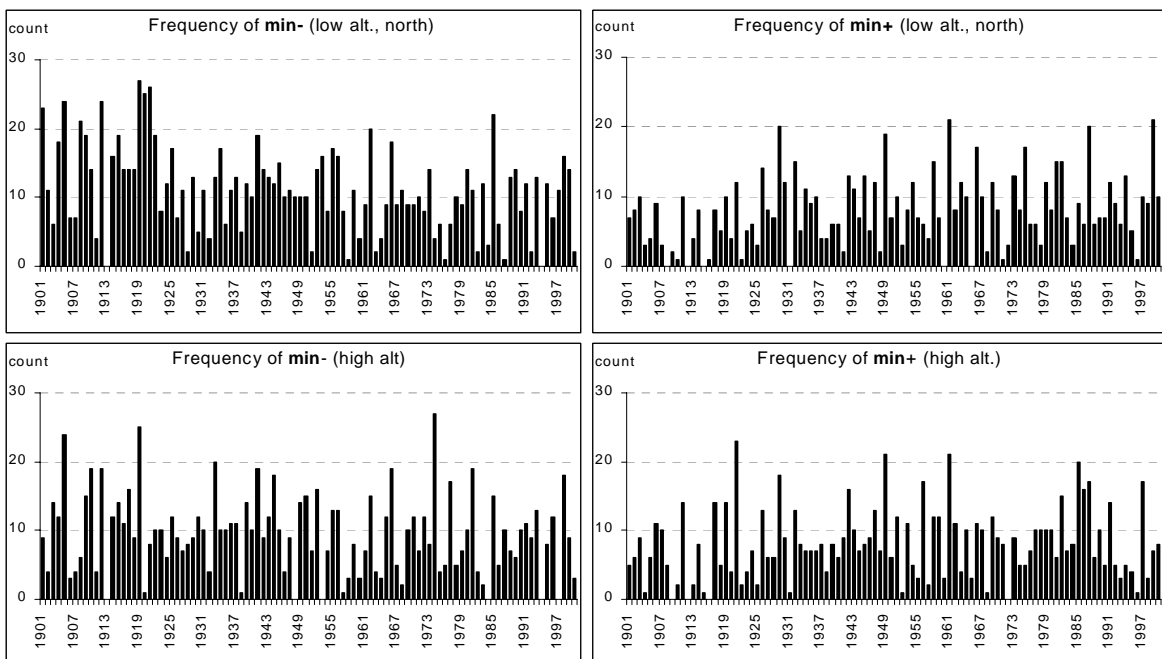
Within Tmin a decrease in the frequency of the cold extremes (min-) can be identified in both regions after 1990. In the region “low altitudes, north” a strong and abrupt rise in the number of Tmin warm extremes (min+) is observable at the beginning to the 1990s. This could be the explanation for the higher trend estimate in the Tmin warm extremes compared to the cold extremes (Table 5.3).

5.3.4. Autumn

<i>Autumn trends /ct</i>	low altitudes, north	high altitudes
Trend Tmin	+1.7°C (0.3)	+1.2°C (0.5)
Trend min-	+1.84°C (0.4)	+0.91°C ns (0.6)
Trend min+	+1.72°C (0.4)	+1.55°C (0.5)
Trend Tmax	+1°C ns (0.4)	+3°C (0.5)
Trend max-	+1.20°C (0.4)	+3.34°C (0.6)
Trend max+	+1.22°C (0.4)	+2.65°C (0.5)

Table 5.4: As for Table 5.1

The autumn temperature extremes are all characterised by a century warming (Table 5.4). The trend estimates are comparably strong to the ones found in winter, however, no pattern emerges as in winter where in one region the stronger trend estimate always corresponds to the same temperature extreme. The 95% confidence bounds of the trend estimates do not differ significantly within the Tmin distributions. A significant difference can be found however, between the Tmax cold extremes (max-) in the two regions. Therefore, the temperature increase within the coldest autumn days is significantly stronger in the region “high altitudes” compared to the region “low altitudes, north”.



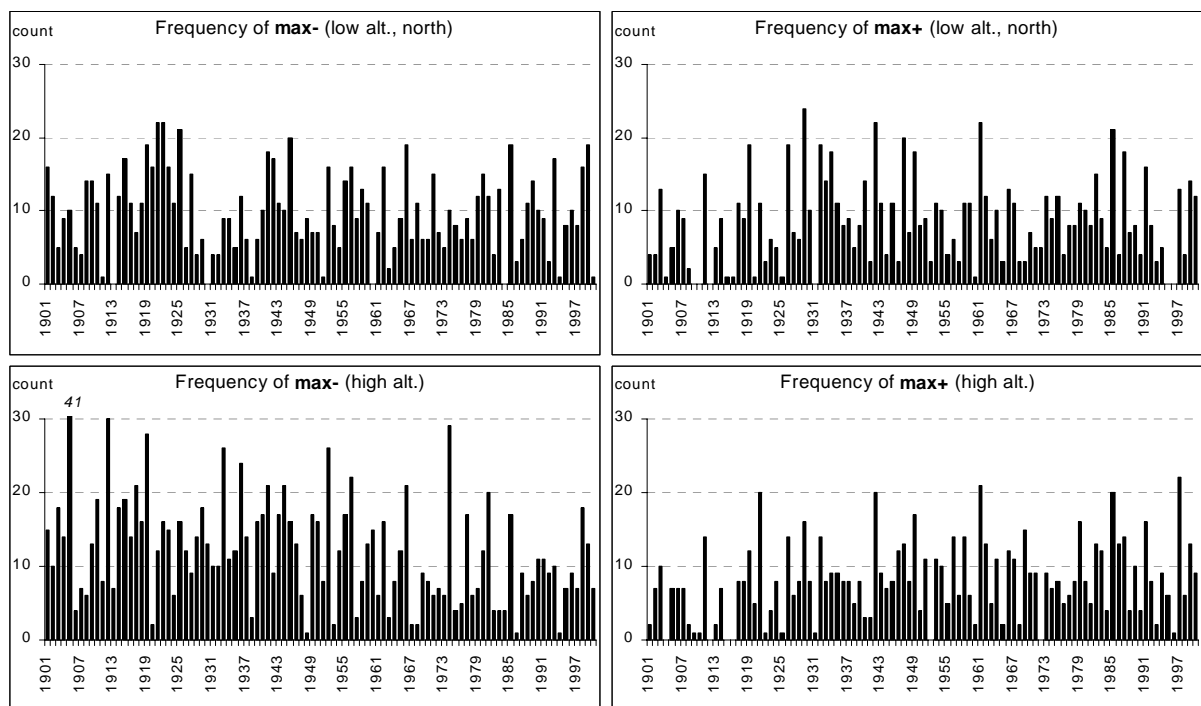


Figure 5.7: as for Figure 5.4 except for autumn.

The frequency count of autumn temperature extremes is unmistakably different compared to winter. Even though the trend estimates of the autumn temperature extremes are also mostly significant positive. The frequency count depicted in Figure 5.7 does not provide clear visual information. The only extremes to show visible changes are the cold extremes in Tmax (max-) in the region “high altitudes” where a continuous decrease since the beginning of the century can be identified. In the same region only few warm extremes in Tmax (max+) occurred in the beginning of the century.

The 1990s do not show a change in frequency counts compared to other periods.

5.4. DISCUSSION

Recalling the most important results of Chapter 4 a general century warming where Tmin often show slightly higher trend estimates than the Tmax, is observed in both regions “low altitudes, north” and “high altitudes”. Further, two sudden warm shifts emerge during the century; a first one between 1940 and 50, which is stronger in Tmax and a second one in the 1990s, visible in Tmin and Tmax and best evident in the region “high altitudes”. The

shift in the middle of the century is restricted to spring and summer whereas the shift at the end of the century concerns spring, summer and especially winter temperatures. A persistently positive long-term trend in Tmin and Tmax since the end of the 1980s can be associated with this warm shift in all seasons except autumn. The autumn temperatures show a strong secular warming, however, are consistent over the period 1961-99 with temperatures during the 1990s, which are inferior compared to the 1980s. These conclusions point to a change in the 20th century seasonal warming pattern in recent decades.

The results of Chapter 5 show that in both of the regions analysed the warming trends observed in Tmin and Tmax can be linked to a temperature increase in both, warm as well as in cold extremes. The frequency count of the warm and cold extremes shows that most of these positive trend estimates in the two extremes can be related to an abrupt and simultaneously increasing number of warm extremes and decreasing number of cold extremes during the 1990s (Figures 5.4-5.7).

Unfortunately the results of Chapter 5 are not as evident with an explicative character as it was hoped for, however, some important findings still are worth noting.

Winter is the only season in which regularity was found. A pattern between the trend estimates in the warm and cold extremes of Tmin and Tmax and the two regions emerges. It needs to be recalled although that the compared trend estimates are not significantly different. There are indications for inverse relations of the observed winter warming in Tmin and Tmax and the warm and cold extremes between the two regions analysed. In the region “low altitudes, north” the stronger secular warming trend is found in cold extremes (min- and max-) whereas in the region “high altitudes” the stronger secular warming emerges for the warm extremes (min+ and max+).

The most important significant differences described in Section 5.1. as types I., II. and III. are listed as follows with a subsequent point of summarising remarks.

Type I:

- In summer the Tmax warm extremes (max+) of the region “high altitudes” are subject to a significantly stronger warming compared to the cold extremes (max-).

Type II:

- In winter the positive trend of the Tmax warm extremes (max+) is significantly stronger in the region “high altitudes” than in the region “low altitudes, north”.
- In autumn the Tmax cold extremes (max-) increased significantly stronger in the region “high altitudes” than in “low altitudes, north”

Type III:

- The warming within the T_{min} and T_{max} warm extremes (min+ and max+) in the region “high altitudes” is significantly higher in winter than in summer.
- The positive trend of the T_{max} cold extremes (max-) increased significantly stronger in autumn compared to spring and summer.

⇒ It is noteworthy that the significantly stronger warming trends concentrate uniquely on the region “high altitudes”. Additionally, they are mainly related to the seasons winter and autumn. The strongest positive trend estimate in winter is found in the T_{max} warm extremes (max+) of the region “high altitudes” whereas in autumn the T_{max} cold extremes (max-) of the region “high altitudes” experienced the strongest warming. At the same time these are the highest trend estimates of all series tested.

Evaluating the frequency counts the decade of the 1990s emerges in both regions as a warm phase in the seasons winter, spring and summer. This is most evident in winter within T_{min} cold and warm extremes (min-, min+) and T_{max} warm extremes (max+). It should be noted though that in winter the region “high altitudes” shows only few T_{max} warm extremes (max+) in the beginning of the century. A first slight increase in their frequency can be identified between 1940 and 1955 and a second, stronger one during the 1990s (Figure 5.4). This possibly illustrates the explanation for the significantly stronger positive trend in winter T_{max} warm extremes (max+) in the region “high altitudes” compared to the “low altitudes, north”.

A further warm phase comparable to the 1990s can be detected in spring and summer extremes during the 1940s. In both seasons an increasing number of T_{min} and T_{max} warm extremes (min+, max+) can be observed whereas in summer the number of the cold extremes (min-, max-) is additionally decreasing (Figures 5.5, 5.6). This warm phase in the middle of the century has obviously a diminishing effect on the positive trend estimates for temperature extremes and consequently the spring and summer trend estimates are lower compared to winter and autumn (Tables 5.1-5.4).

Autumn is the only season in which the 1990s cannot be equated with a warm phase in the temperature extremes. Although, it is worth noting that if compared to other seasons, the autumns in both regions must have been rather cool with a high frequency of T_{min} and T_{max} cold extremes (min-, max-) until the second half of the 1920s (Figure. 5.7). Moreover, resulting out of Chapter 4 is a mild phase during the 1980s for the autumns in the region “high altitudes”. The rather strong trend estimates found for autumn temperature extremes can possibly be linked to these observations.

A direct comparison between the results of my study with other results concerning the temperature extremes is hard to make since extremes are defined and calculated in several ways, often depending on the aim of the study. Additionally, more detailed results are normally strongly linked to the region under observation.

Probably best analysed is the frequency of the cold extremes, which follow a decreasing tendency since the beginning of the 20th century in large areas around the globe. Examples are:

Analysing the 10th and 90th percentiles of Tmin and Tmax anomalies (relative to 1961-90) between 1950 and 1995 on a global data set Folland (1996) found a pronounced rise in warm extremes with a matching reduction in cold extremes during the last decade. In De Gaetano (1996) several thresholds at fixed values were tested between 1951 and 1993 at 22 rural sites distributed over the north-eastern United States. A significant decrease in cold Tmin as well as a significant increase in warm Tmin is resulting. Domonkos (2001) concluded in a Hungarian study of temperature extremes (5th and 95th percentiles) that the period 1967 to 1996 shows clearly less Tmin cold extremes in winter and Tmax warm extremes in summer than the earlier part of the 20th century. Jones et al. (1999) who analysed British temperature extremes (10th and 90th percentiles) of mean temperature anomalies (relative to 1961-90) between 1972 and 1997 found a clear decrease in cold extremes since the late 19th century. The analysis of the frequency distribution of 2 plateau Stations (Chateau d'Oex and Neuchâtel) has shown that the late 1990's have nearly 50 frost days less compared to the beginning of the century (Heino et al. 1999). Analysing the variability in two Swiss temperature time series, situated at different altitudes over the period 1901-99, Rebetez (2001) concluded that especially the winter months are subject to an important loss of minimum temperature cold extremes towards the end of the century.

One of the conclusions made in this chapter that in the region "high altitudes" the winter warm extremes of Tmin and Tmax (min+, max+) show a stronger warming than the cold extremes does not exclude an important reduction in cold extremes. Figure 5.4 of the winter Tmin and Tmax frequency supports these findings concerning the reduction in cold extremes.

6. LINKS BETWEEN TMIN/TMAX, THE NAOI AND ALPINE WEATHER TYPES

In this chapter working steps XII to XIII are discussed (see Section 1.2.):

- X. *Analysing the interdecadal changes in the frequency of alpine weather types since the middle of the 20th century for each season.*
- XI. *Relating the observations of the weather type frequency to the temporal variation of Tmin/Tmax.*

6.1. PAPER BY BENISTON AND JUNGO (2001)

Shifts in the distributions of pressure, temperature and moisture and changes in the typical weather patterns in the alpine region in response to the behavior of the North Atlantic Oscillation

ABSTRACT

An investigation has been undertaken in order to assess the manner in which the North Atlantic Oscillation (NAO) influences not only general, average, climatic conditions, but also the extremes of dynamic and thermodynamic variables. By choosing representative sites in the Swiss Alps, the present study shows that there is a high sensitivity of the extremes of the probability density functions of temperature, moisture and pressure to periods when the NAO index is either highly-positive or strongly negative. When the NAO index is strongly positive, temperatures and pressure shift towards positive anomalies, and there is a general reduction in atmospheric moisture at high elevations. Furthermore, a change in typical alpine winter weather patterns can be detected during strongly positive NAO anomaly phases. The winters of the last decade of the 20th Century (1989-99) are characterized by a substantial decrease in cold advective high pressure situations and simultaneously an important increase in warm convective high pressure systems. These

patterns differ significantly from the weather types, which have been recorded for earlier periods of the 20th Century. As a result of the highly-positive nature of the NAO index in the latter part of the 20th Century, it is speculated here that a significant part of the observed warming in the Alps results from the shifts in temperature extremes induced by the behavior of the NAO. These changes are capable of having profound impacts on snow, hydrology, and mountain vegetation.

1. Introduction

The North Atlantic Oscillation (NAO) is a large-scale alternation of atmospheric pressure fields (i.e., atmospheric mass), whose centers of action are near the Icelandic Low and the Azores High. One mode of the NAO is when sea-level pressure is lower than normal in the Icelandic low-pressure center, it is higher than normal near the Azores, and vice-versa, hence the notion of an oscillatory behavior of the system. Another mode is that pressures may also rise or fall simultaneously in both centers of meteorological activity, but then the NAO signal is not quite as well-defined. The NAO index is a normalized pressure difference between the Azores (an alternate location is Lisbon, Portugal) and Iceland; it is a measure of the intensity of zonal flow across the North Atlantic and the associated position of storm tracks and regions of strongest storm intensity. This flow is itself driven by the temperature (and hence pressure) contrasts between polar and tropical latitudes.

The NAO represents one of the most important modes of decadal-scale variability of the climate system after ENSO (El Niño/Southern Oscillation), and accounts for up to 50% of sea-level pressure variability on both sides of the Atlantic (Hurrell, 1995). It is observed to strongly influence precipitation and temperature patterns on both the eastern third of North America and western half of Europe; the influence of the NAO is particularly conspicuous during winter months. It has been shown in recent years (Beniston et al., 1994 ; Hurrell, 1995; Rogers, 1997; Serreze et al., 1997) that a significant fraction of climatic anomalies observed on either side of the Atlantic are driven by the behavior of the NAO.

Beniston (2000), among others, has shown that temperature, moisture and pressure trends and anomalies at high elevations stand out more clearly than at lower levels, where boundary-layer processes, local site characteristics and urban effects combine to damp the large-scale climate signals. Climatic processes at high elevation sites can thus in

many instances be considered to be the reflection of large-scale forcings, such as the NAO. These findings have been confirmed through numerical experimentation by Giorgi et al. (1997), who have underlined the altitudinal dependency of regional response to large-scale climatic forcings.

A particular feature of the positive phase of the NAO index is that it is invariably coupled to anomalously low precipitation and milder than average temperatures, particularly from late fall to early spring, in southern and central Europe (including the Alps and the Carpathians), while the reverse is true for periods when the NAO index is negative. As an illustration of the impacts of NAO behavior on the seasonality and quantity of snow in the Alps, Beniston (1997) has shown that periods with relatively low snow amounts are closely linked to the presence of persistent high surface pressure fields over the Alpine region during late Fall and to early Spring ; these fields are themselves well in phase with the NAO. Furthermore, since the mid-1980s and up until 1996, the length of the snow season and the general quantities of snow amount decreased substantially in the Alps, as a result of pressure fields which were far higher and more persistent than at any other time during the 20th century (see for example Beniston, 1997).

Because of the exceptional nature of the NAO in the 1990s compared to other periods of the 20th Century (in particular the record high values of the NAO Index observed in the 1990s, and the exceptionally long persistence of the index within the positive range), it is of interest to ascertain to what extent these conditions have determined the highly anomalous behavior of temperatures during the 1990s (Jungo and Beniston, 2001). In particular, it is important to assess the extent to which changes in the NAO are influencing not only average values of temperature or humidity, but also their extremes. This is done by investigating changes in the probability density functions (PDF) of climate variables. In the current debate on global warming, there is increasing awareness that shifts in climatic extremes in a changing climate are likely to impact more significantly on environmental and socio-economic systems than simply changes in means.

A further manner of investigating the relations between the behavior of the NAO and regional climates is through the analysis of typical weather types, using for example the climatological weather classification of Schüepp (1978), which was developed for the Alpine region. The Schüepp classification can be considered to be reliable for Swiss weather conditions, since it includes most of the significant elements that determine the atmospheric conditions over a certain region, i.e., pressure, origin and dynamics of an

airmass, dominant wind direction, etc. The Schüepp classification is based on three main groups, namely convective, advective and mixed weather types, which are further subdivided in relation to the origin of the airmass and the pressure type. Thus 40 weather types emerge from the classification, where 15 are of a convective nature, 24 of an advective nature and 1 of mixed type, the latter occurring when the center of a depression is located just over the Alps. Analyzing the persistency of the European Circulation Types (*Grosswetterlagen* of Hess and Brezowsky) from 1881 to 1992, Wanner et al. (1997) have found out that the zonal flows increased considerably since 1965 and with them the persistence of almost all circulation types. They have also undertaken a short analysis on the persistency of Schüepp weather types, concluding that in an increasing tendency of the 5-day persistency of convective situations with high pressure has occurred in recent years.

2. The influence of the NAO on Alpine climate

2.1 Influence on means

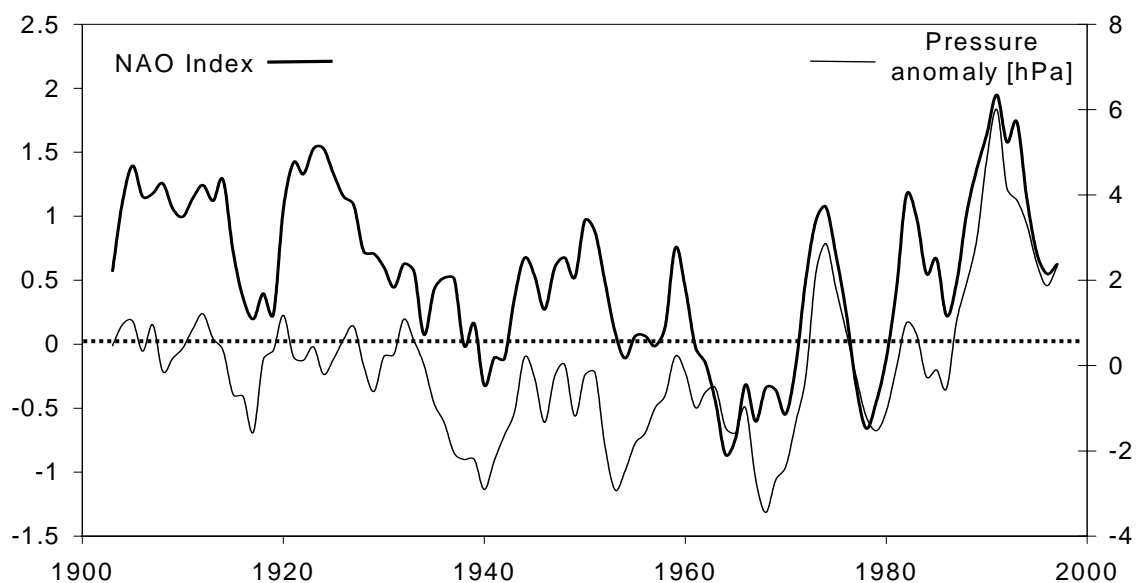


Figure 1: 20th Century time series of the wintertime (DJF) NAO index and surface pressure anomalies at Säntis (2,500 m above sea-level). A 5-point filter is used to eliminate high-frequency oscillations in the series

Figure 1 depicts the time series of the wintertime NAO index during the 20th Century, and the associated surface wintertime (December-January-February) pressure anomalies in Zürich, based on the 30-year climatological average period 1961-1990; a 5-point filter has been applied to both curves in order to remove the higher-frequency fluctuations for the purposes of clarity. Here, wintertime refers to the values averaged for December, January, and February (DJF). Average pressure values, even at a single site, can be considered to be a measure of synoptic-scale conditions influencing the Alpine region, as discussed in Beniston et al. (1994). The pressure measured at Zürich or elsewhere, when averaged on a seasonal or longer time span, is therefore representative of the large-scale pressure field over Switzerland. The very close relationship between the two curves in Figure 1 highlights the subtle linkages between the large-scale NAO forcings and the regional-scale pressure response over Switzerland. When computed for 1901-1999, 56% of the observed pressure variance in Switzerland can be explained by the behavior of the NAO. From 1961-1999, this figure rises to 83%, which is considerable bearing in mind the numerous factors which can determine regional pressure fields. Wanner et al. (1997) speculate that the persistent Alpine high pressure observed in the 1980s and early 1990s is linked to rising NAO index values through a northern shift of the polar front jet axis. When this occurs, the Alps lie to the right exit zone of the diverging jet streamlines, and are thus subject to mass influx and hence positive pressure tendencies.

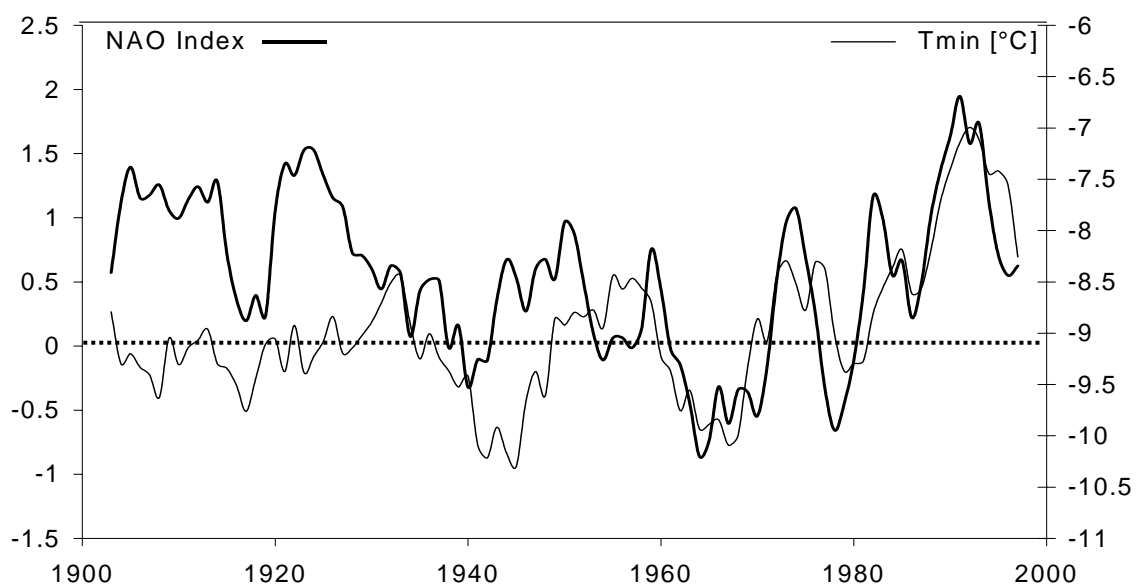


Figure 2: As Figure 1, except for series of NAO and DJF T_{min} temperatures

Figure 2 illustrates the relation between the wintertime NAO index and the DJF temperature time series for Zürich, where both curves are smoothed as in Figure 1. As for pressure trends, the synchronous behavior between temperature and the NAO is striking, particularly in the second half of the 20th Century, where the T_{min} temperature variance which can be accounted for by the NAO fluctuations from 1961-1999 exceeds 72%.

2.2 The influence on the probability density functions of climate variables

In order to highlight the possible relationships of high or low NAO index values with shifts in the frequency distributions of climate variables such as pressure, temperature and moisture, two thresholds for the wintertime NAO index have been chosen, namely the lower and upper 10 percentiles of the NAO index distribution during the 20th Century (i.e., the 10% and 90% thresholds, which correspond roughly to index values around -1.5 and $+2.0$, respectively). These thresholds are representative of two highly contrasting synoptic regimes affecting the Alps, namely above-average pressure and associated positive temperature and negative moisture anomalies when the threshold is above the 90% level, and lower than average pressure and its controls on temperature and humidity when the index is lower than the 10% level.

The probability density functions (PDF) of pressure, maximum and T_{min} temperatures, and relative humidity, have been computed for periods where the NAO index is $\geq 90\%$ threshold, and the temperature PDFs for winters where the NAO anomaly index $\leq 10\%$ threshold. The discussion will focus on the high-elevation site of Säntis, a summit in north-eastern Switzerland which culminates at 2,500 m above sea level (asl), and Zürich, located about 70 km to the west, at 569 m asl. The results presented for these two sites are representative of other high mountain and lower-elevation plain locations in Switzerland. The Säntis data are particularly interesting because the high altitude of this site implies that it is closer to free atmospheric conditions, where the data are less likely to be contaminated by local site features, urban effects or atmospheric boundary-layer influences commonly encountered at lower elevations. In addition, the Säntis climate record is available in digital form on a daily basis from 1901 and is one of the most homogenous data sets at high elevations available in the database of the Swiss Meteorological Service, MeteoSwiss (Bantle, 1989).

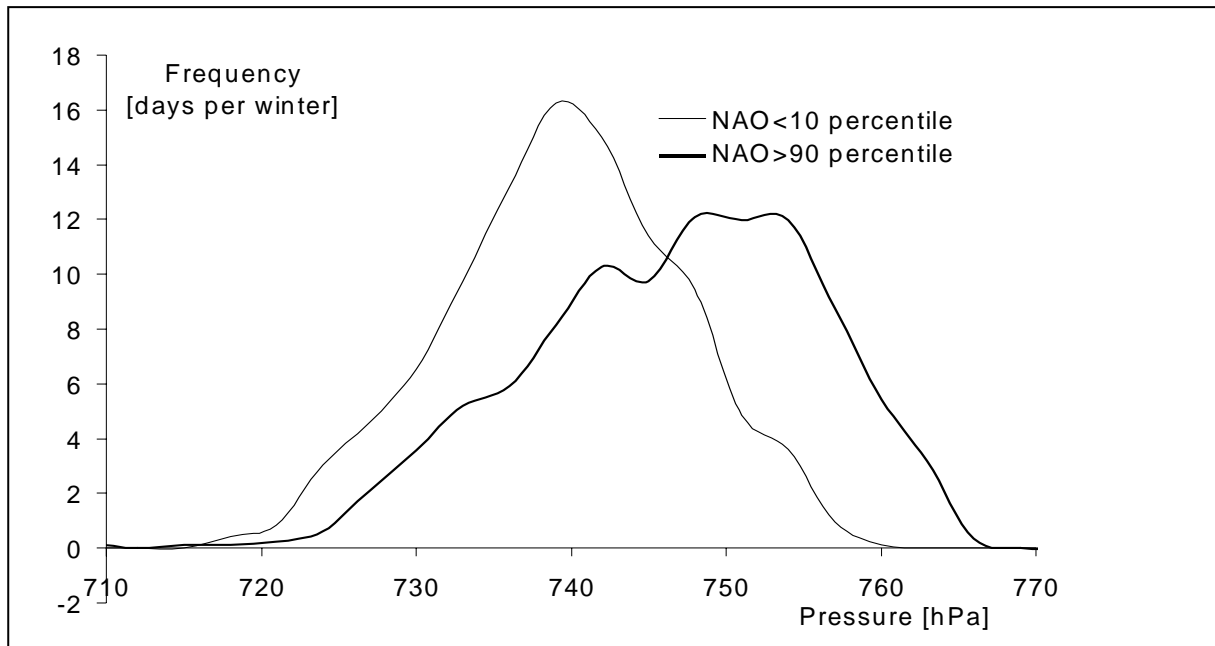


Figure 3: Probability density function of pressure at Säntis for periods when the negative and positive NAO index thresholds are exceeded

Figure 3 illustrates the behavior of the pressure PDFs at Säntis, computed for periods of the 20th Century where the NAO index exceeds the upper threshold (90%), or is inferior to the lower threshold (10%). A substantial shift towards significantly higher pressures is observed for periods when the NAO index exceeds the 90% threshold; the PDF curve is shifted to the right of the diagram, with a change in both the skewness and kurtosis of the distribution. Figure 4 depicts another manner of visualizing the shifts in the pressure PDF from a strongly negative NAO forcing to a highly positive one, namely by mapping the difference in the normalized distribution between high and low thresholds, at both Säntis and Zürich. A normalized distribution is defined here as the departure of pressure from its central value (i.e., the 50-percentile) in the range observed at the two sites. Using the normalized scale enables a direct comparison to be made, which would otherwise not be possible if the absolute pressure values were used, since the pressure difference between Zürich and Säntis is about 200 hPa. The response of the surface pressure extremes to a switch in the NAO index is observed to be a clear transfer from the lower tails of the pressure distribution to its upper tails. In fact, the central values of the PDF of pressure at both the low and the high elevation site appear to be a « pivotal point » around which the shift occurs. It is seen that the integral of less-than-average pressure is practically identical to that of higher-than-average pressure when the NAO index is positive.

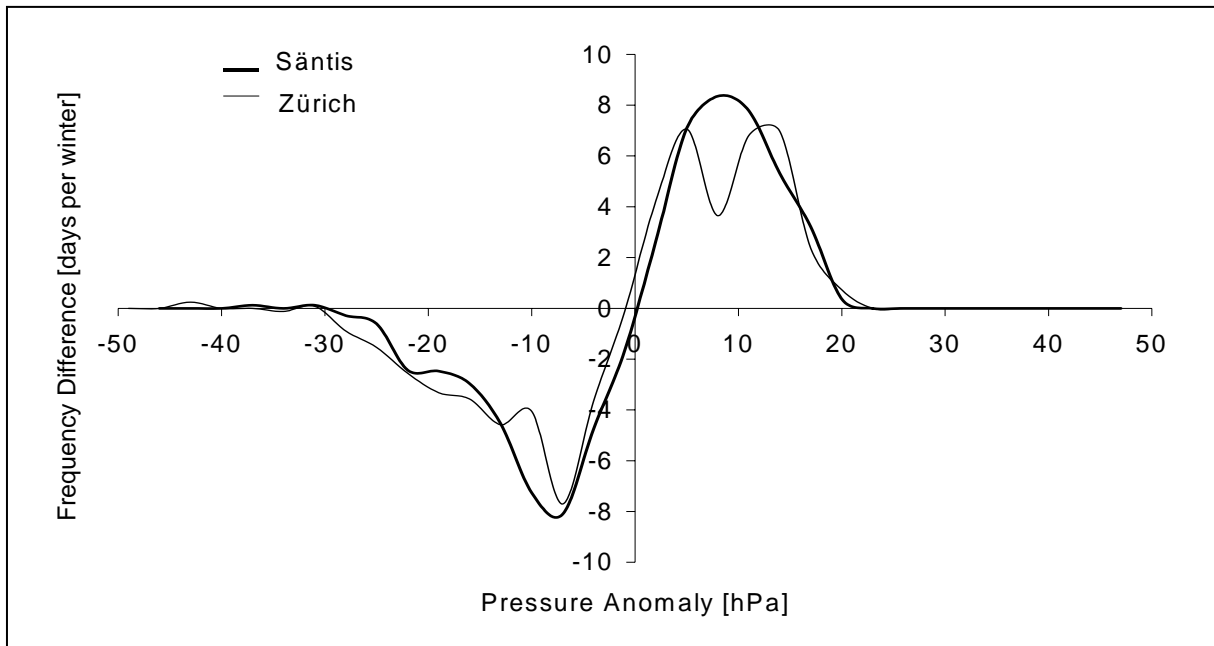


Figure 4: Differences in the normalized probability density functions of pressure between periods where the NAO index ≤ -1.5 and $\geq +2.0$, for Zürich (569 m above sea-level) and Sântis

The forcing of the NAO is thus reflected not just in terms of a change in mean pressure as illustrated in Figure 3 but, indeed, in terms of the entire pressure distribution itself. The changes are by no means negligible, and represent an average shift on the order of 20 hPa at both Sântis and Zürich. When the NAO index at Sântis $\leq 10\%$ level, over 15% of the winter months are concerned by pressures which are less than 730 hPa, while less than 10% are affected by pressures exceeding 750 hPa. When the NAO index $\geq 90\%$ level, on the other hand, the respective figures change to 6% and 54%.

Under such circumstances, it is not surprising that temperature distributions and the extremes of these distributions are also strongly influenced by the behavior of the NAO. Figure 5 shows the response of the T_{min} temperature PDF to these two thresholds.

Figure 5 illustrates the shift in the normalized winter T_{min} temperature distribution as a function of low and high index thresholds for both Sântis and Zürich. Similar to the shifts in pressure PDF illustrated in Figure 4, transfers from the extreme low to the extreme high tails of the distribution occur around a « pivotal point » which is at the center of the range of T_{min} temperatures. The changes are substantial at Sântis, from a peak frequency at

about 12°C below the center of the PDF range when the NAO threshold is low, to about 7°C above the central part of the range when the NAO threshold is high. Comparable shifts in the PDF anomalies are also observed at Zürich ; the respective peak frequencies occur for anomalies of -10°C and +5°C, respectively, around the central part of the range of the Zürich T_{min} distribution. In other words, the extreme low tails of the T_{min} temperature distribution disappear during periods of high NAO index, in favor of much warmer temperatures. Temperatures below -15°C at Säntis, which account for roughly 30% of the winters where the NAO index \leq 10% level, are present only 15% of the DJF months for high NAO values, i.e., the periods with extreme cold conditions are reduced by 50%. Conversely, temperatures at the upper end of the distribution, for example above -5°C represent 12% of the winter days for low NAO values and 23% for high NAO values. The duration of milder temperatures at Säntis is thus almost doubled under conditions during which a high NAO index prevails.

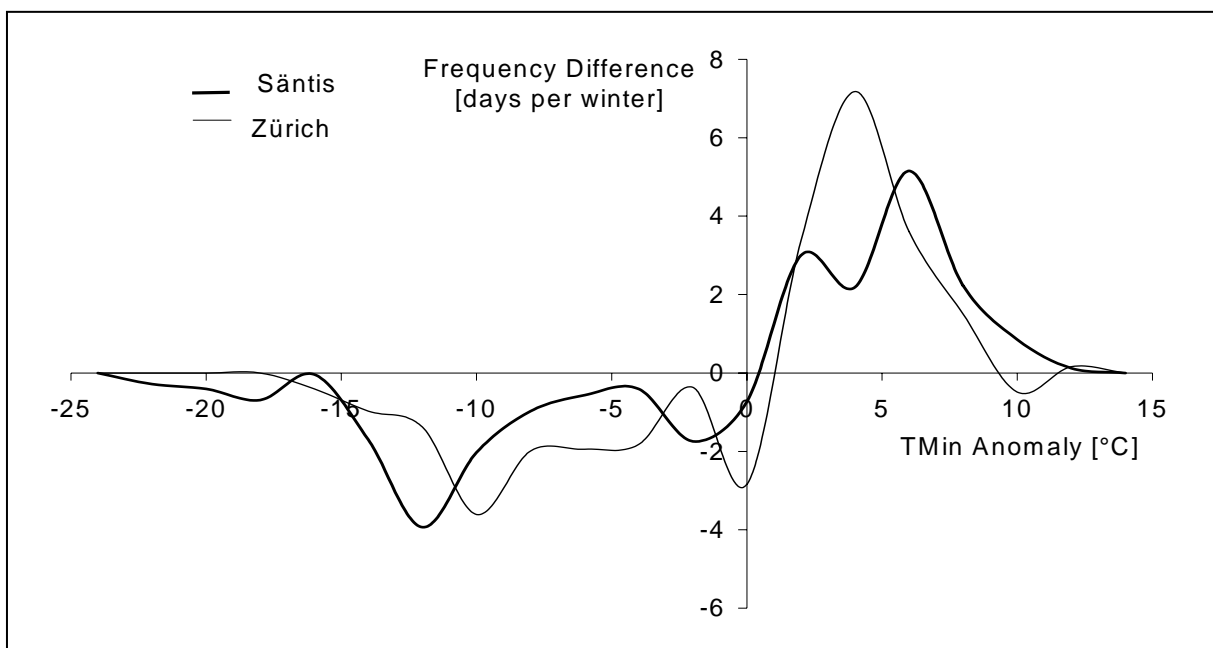


Figure 5: As Figure 4, except for T_{min} temperature

Similar conclusions can be reached for the distribution of T_{max} (Figure 6). This particular figure emphasizes the fact that the number of days in winter in which T_{max} exceeded the freezing point range from 10 days for the lowermost NAO 10-percentile to 25 days for the uppermost NAO 10-percentile. This obviously has implications for physical variables such as snow amount and duration, and biologically-relevant factors such as the start of the vegetation period, as will be mentioned later. Temperatures below the « pivotal point » of

-5°C, which make up 48 days per winter during low NAO index episodes, drop sharply to only 33 days when the index is high.

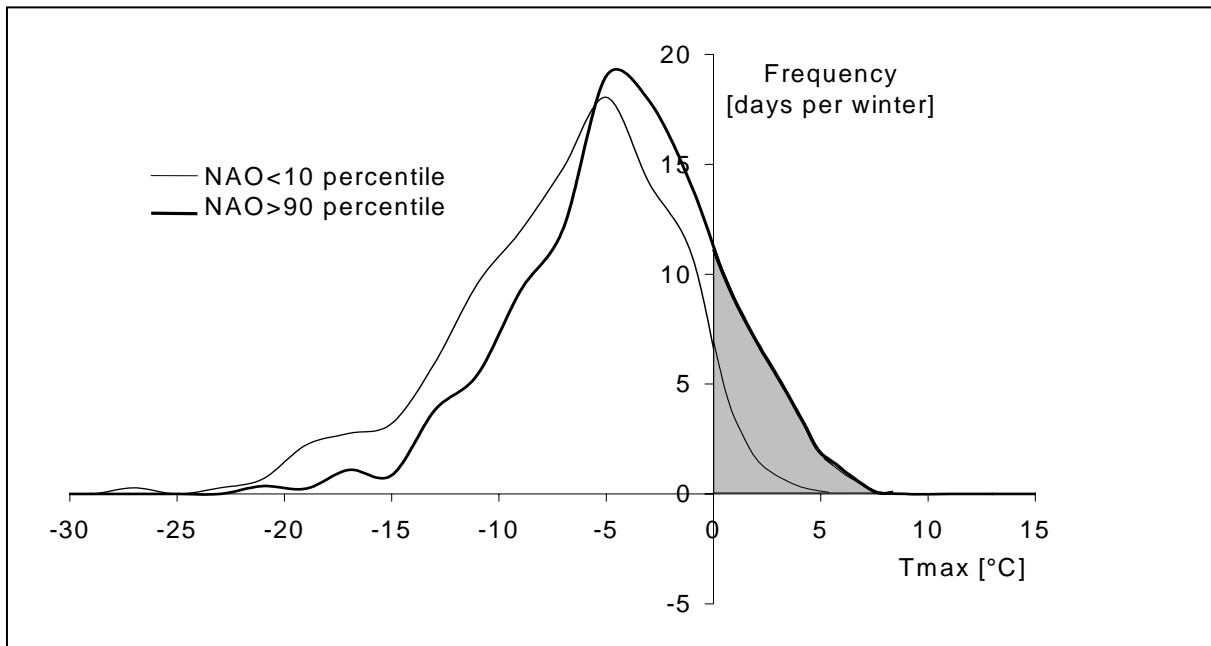


Figure 6: Differences in the probability density function of maximum temperature (absolute values) between NAO index ≤ -1.5 and $\geq +2.0$ (shown here for Säntis only)

Moisture and precipitation in the Alpine region is also influenced by the behavior of the NAO. As an illustrative example, Figure 7 shows the difference in the distribution of relative humidity at Säntis for the two selected thresholds. In the case of the negative index threshold, over 50% of the values recorded in winter exceed 90% relative humidity, while in the case of the positive threshold, the 90% relative humidity is exceeded only during 35% of the winter months. There is thus a clear reduction in ambient moisture at high elevations. Such a substantial drying of the atmosphere is not observed at the lower elevations exemplified by the Zürich observational site; this is because low elevation sites are located within a much moister boundary-layer which, in winter, is often characterized by fog or stratus below 800-1200 m asl when high pressure conditions prevail. The lower levels are essentially decoupled from the higher atmosphere (see for example Beniston and Rebetez, 1996), and as a consequence, the sensitivity of relative humidity to changes in the NAO index is much lower than at higher elevations.

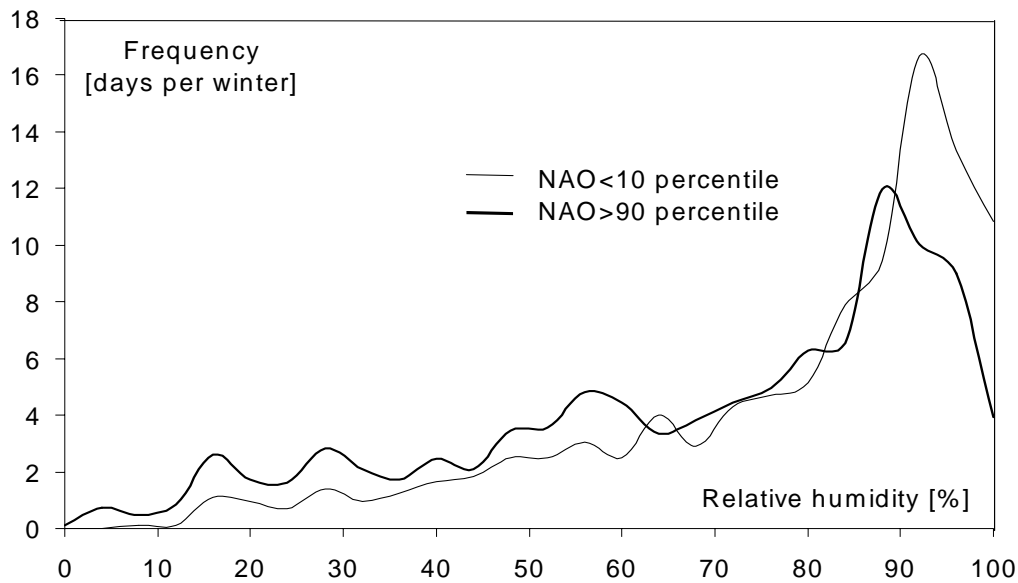


Figure 7: As Figure 3, except for relative humidity

Indeed, the influence of local particularities of climate at low elevations in Switzerland are reflected in Table 1, which expresses the changes in the mean of the PDFs of four variables considered in this study (T_{min} and T_{max}, relative humidity, and precipitation). It is seen that the range of the shift in means is consistently larger at Säntis than at Zürich, whatever the climate variable considered.

Variable	Zürich	Säntis
T _{min} [°C]	0.3	1.3
T _{max} [°C]	0.1	1.1
Relative Humidity [%]	-0.6	-4.7
Precipitation [mm/day]	-0.4 (-12.8%)	-0.9 (-14.7%)

Table 1: Differences in the means of the PDFs of pressure, T_{min} and maximum temperature, and relative humidity, at Zürich and Säntis, between periods when the NAO index ≤ -1.5 and $\geq +2.0$

Although only illustrated here for two sites representative of low and high elevations, respectively, the conclusions from Table 1 hold for other locations in Switzerland,

according to their elevation, i.e., the sensitivity of climatic variables at low elevations to shifts in the sign of the NAO index is systematically lower than at higher elevations.

2.3 The influence on climatological weather types over the alpine region

In a first approach, 5 periods of weather types with an 11-year span (1945-55, 1956-66, 1967-77, 1978-88, 1989-99) are compared. This allows to assess whether the weather types also undergo a change as abrupt as that exhibited by temperature, or if there is a smooth change subsequent to 1970, where the positive NAO tendencies markedly increased and became more in phase with surface pressure at Zürich (Figure 1).

A second point of interest concerns the weather types during the 1990s, taking into account only the extreme 10-percentiles of T_{min} and maximum winter temperatures, hereafter defined as “coldest and warmest winter nights and days”. Figure 4 shows that the winter days become warmer during a phase of extreme positive NAO anomalies. Together with the shift in extreme temperatures, it is seen that during the 1990s, the number of coldest winter nights and days is decreasing while the number of warmest days is increasing. It is thus of interest to determine whether the change in the frequency distribution of extremes can also be detected in terms of weather types in addition to the NAO index. Using the methodology developed by Jungo and Beniston (2001), the 10th and the 90th percentiles of winter T_{min} and maximum temperature anomalies are based on the climatological mean period (1961 to 1990). The statistics are carried out for the mean time series of 3 groups of stations, representing the low altitudes north of the Alps, the Alpine high altitudes and the low altitudes south of the Alps.

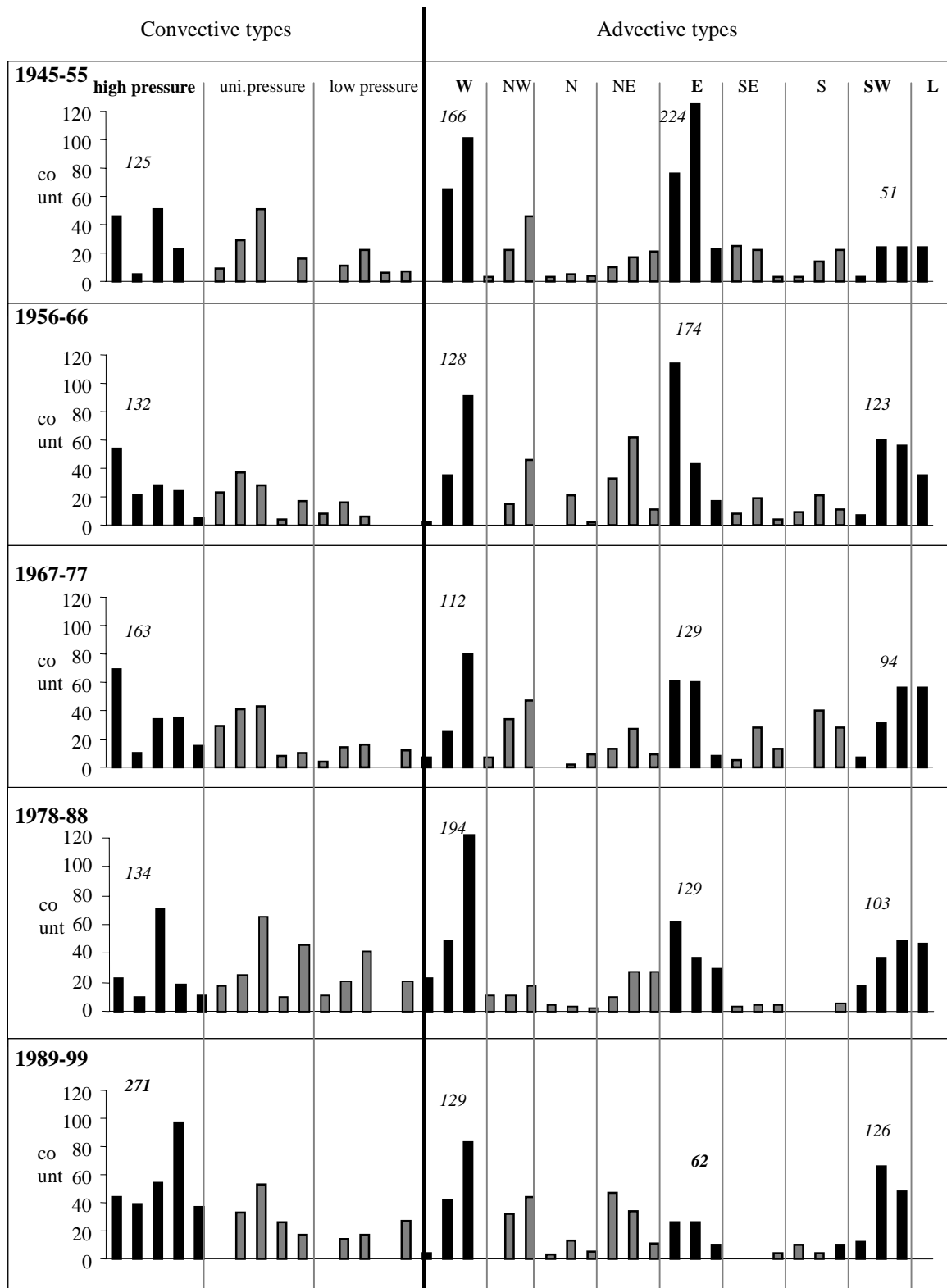


Figure 8: Frequency of the 40 alpine weather types of Schüepp (1978) from 1945 to 1999, divided into five periods of 11 years. The numbers printed into the figure indicate the exact

frequency of the weather types, which show the most important changes in time (black bars). The five single bars of the convective weather type are, from left to right: high or spatially uniform pressure, followed by types originating in the west, north, east, and south. The three bars of each advective type indicate high, uniform or low-pressure.

Figure 8 depicts the frequency of each weather type during 5 sets of winter seasons. There is a clear increase in the frequency of convective situations with high pressure. This weather type has doubled its frequency during the last period (1989-99) compared to the previous periods. As mentioned in Wanner et al. (1997) the 5-day persistency of this weather type also tends to increase. Evident as well is the sharp decrease of eastern advective situations, generally associated with high pressure or situations with reduced pressure gradients (spatially uniform pressure fields), reflecting the typical "Bise" situation, characterized by clear skies, very cold easterly winds and strong infrared radiation loss at night. The western advective situations, with low or uniform pressure have always been numerous and do not change over the different periods considered. However, since 1989 they are seen to be the most frequent advective situations occurring in wintertime, along with the southwesterly low-pressure weather type. The mixed type, where the low-pressure center of a depression is located over the Alps, is practically non-existent in the latter part of the period analyzed. The frequency of the climatological weather types during the last decade of the 20th century is quite different to earlier periods. The recent evolution shows that during winter, warm westerly and southwesterly low-pressure systems under advective conditions and, particularly, high-pressure systems under convective conditions have increased at the expense of cold, high-pressure systems under advective conditions.

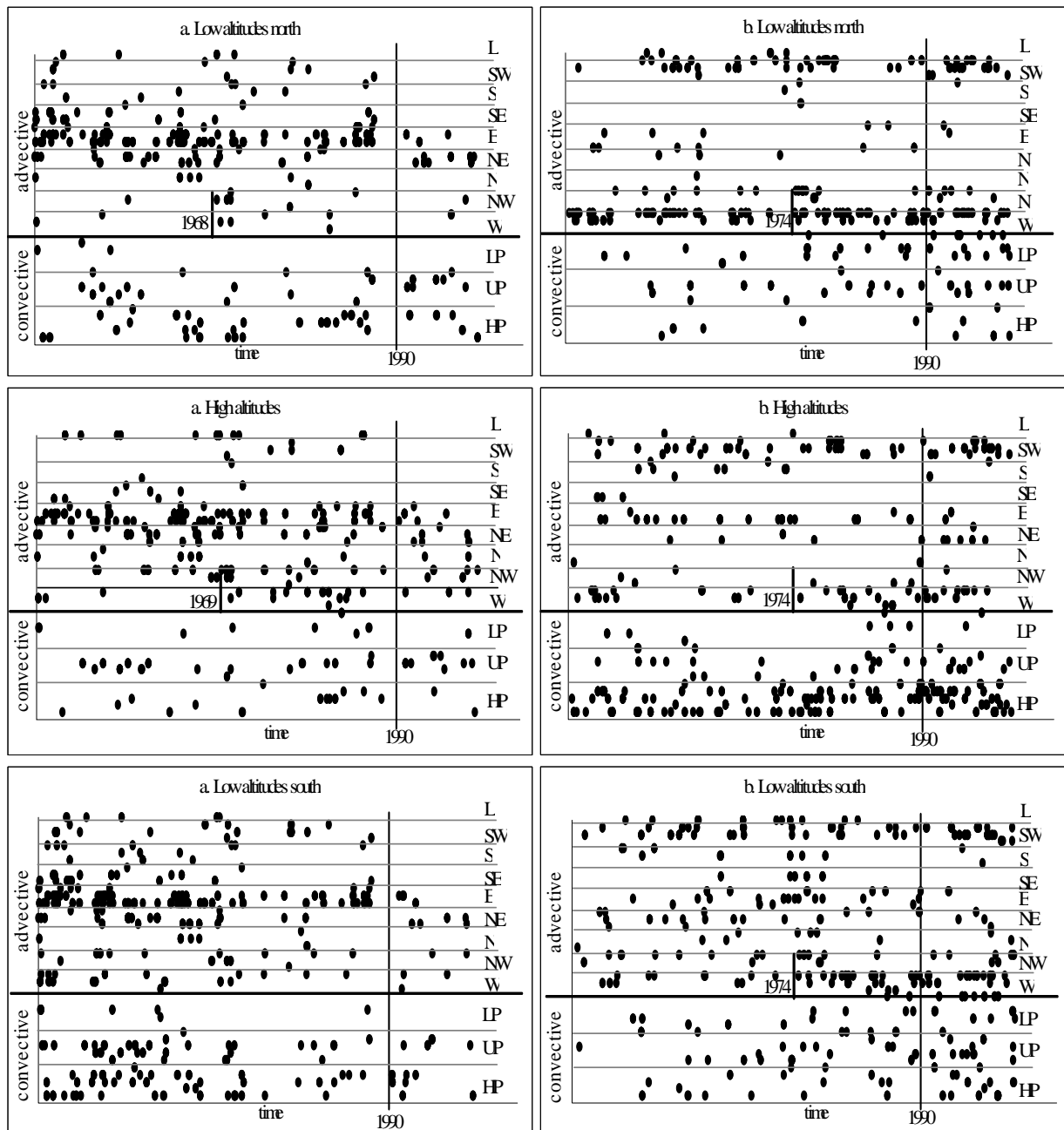


Figure 9 (a, b): Evolution of the 40 alpine weather types of Schüepp (1978) from 1945 to 2000 in different regions of Switzerland for: a) coldest winter nights, b) warmest winter nights.

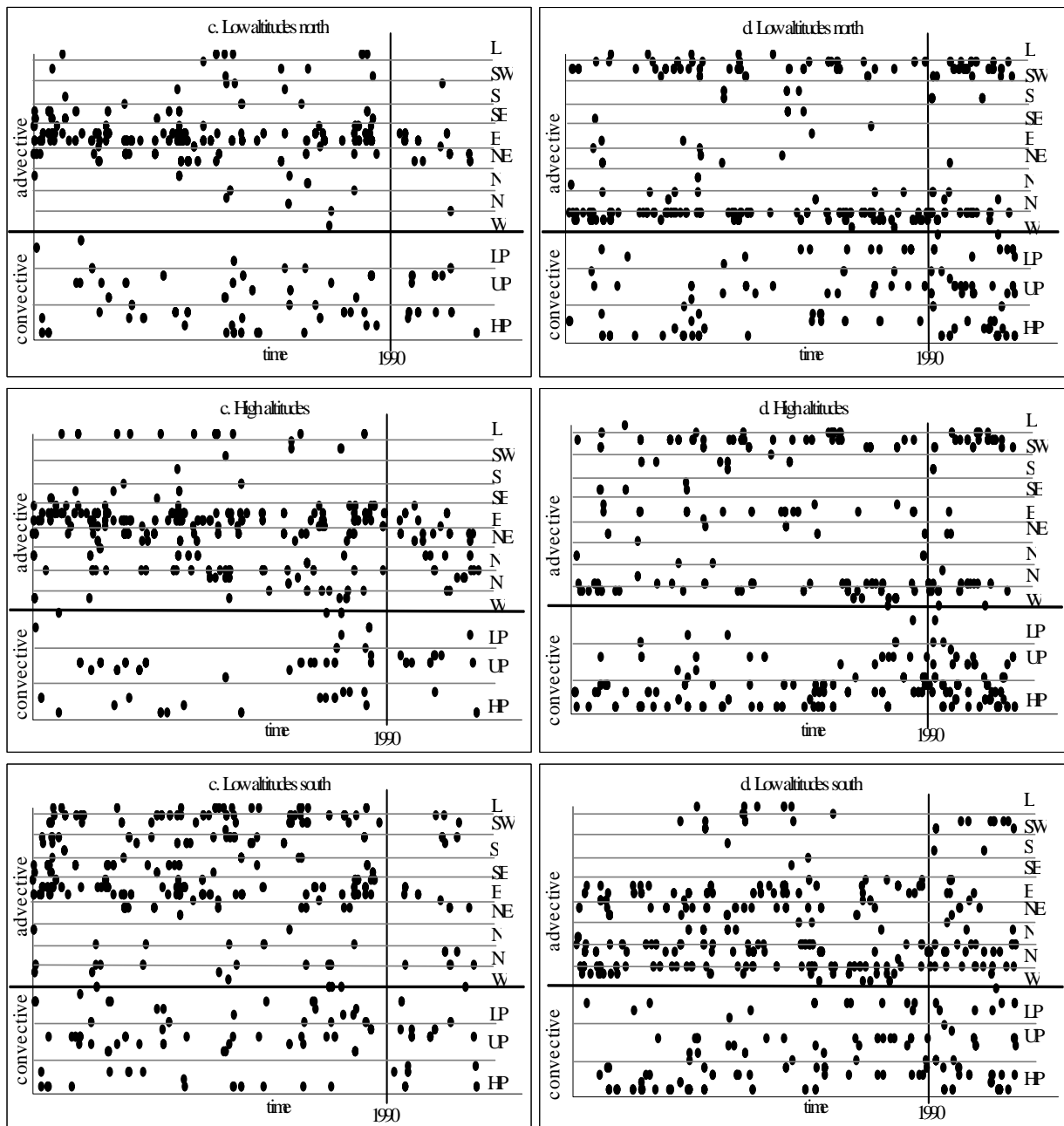


Figure 9 (c,d): As 9 (a, b) except for c) coldest winter days, d) warmest winter days.

Figure 9a illustrates the fact that the coldest winter nights have diminished since 1945, but most occurrences are related to the cold “Bise” situation, i.e., eastern advective situations with high or uniform pressure. After about 1995 there is a slight tendency however, for a shift from eastern to northeastern situations. The 3 sets of regions have further in common that all southern advective situations and the mixed situation, where the low-pressure

center of a frontal systems is located over the Alps, no longer occur after 1990. Figure 9b shows a general increase in the number of warm winter nights towards the end of the 20th century. These occur most frequently during westerly and southwesterly advective situations under low-pressure, particularly north of the Alps and in the south at low elevations. At high altitudes, the convective situations with high-pressure are the most frequent cause for mild temperatures. In all regions, according to the weather classification analysis, the higher number of warm nights is principally related to an intensification of convective situations. This intensification is limited to high-pressure systems at high altitudes (clear skies), whereas at low altitudes north of the Alps, it is more related to low-pressure systems (covered skies).

In Figure 9c it is seen that just as the coldest winter nights, the coldest winter days occurred since 1945 predominantly during cold “Bise” situations. This pattern does not change after 1990, although at high altitudes a slight shift from easterly to northeasterly situations are to be seen. Due to the diminishing number of coldest winter days, the number of weather types after 1990 are limited to just a few types. The cold easterly advective high-pressure systems are frequent, especially at low altitudes north of the Alps and at high altitudes. Furthermore, at northern low altitudes the high-pressure convective types, and at high altitudes, the uniform pressure convective types (covered skies) are rather frequent for coldest winter days. At southern low altitudes the weather types of the coldest winter days are more diverse. Frequent next to the cold eastern advective situation are high and uniform pressure convective systems, western and advective high-pressure systems originating from west, northwest, southwest and south. The influence of the NAO is not clearly visible on the weather types of the coldest winter days.

Figure 9d shows that the number of warm winter days exceeding the 90% distribution threshold increases, principally at low altitudes north of the Alps, as well as at high altitudes. The increase in the warmest winter days, which occur under conditions of westerly advective flow and low-pressure, begins in the 1970s and the intensification of convective high-pressure situations since 1990 is an additional sign of the dominant influence of the NAO on Alpine climates, particularly since the 1970s.

3. Discussion

In the last decade, much interest has focused on the North Atlantic Oscillation, and it is sometimes used as an empirical predictor for precipitation and temperature in regions where climatic variables are well correlated with the NAO index. This is clearly seen to be the case in Northern and Southern Europe, Central Europe and the Alps being generally a pivot around which the forcing of the NAO is amplified with distance north or south of the alpine region. While at low elevations, the NAO signal may be weak or absent in the Alps, higher elevation sites are on the contrary sensitive to changes in NAO patterns (Beniston et al., 1994 ; Beniston and Rebetez, 1996 ; Rebetez and Beniston, 1998 ; Hurrell, 1995 ; Hurrell and van Loon, 1997 ; Giorgi et al, 1997). The processes associated with periods when the NAO index exceeds the 90% level include frequent blocking episodes, where pressure fields over the Alpine area are high, and vertical circulations induce subsiding air with associated compressional warming. Such circulations invariably generate positive temperature anomalies, and reductions in moisture and precipitation. In addition, diurnal warming at high elevations is enhanced by above-average sunshine, since there is a lowering of cloud amount and duration during periods of blocking high-pressures. The reverse is generally true for periods when the NAO index is below the 10-percentile of its distribution. It could be argued that nocturnal cooling should also be stronger in a cloud-free atmosphere, thus leading to lower minimum temperatures; however, in complex terrain, radiative cooling at night will lead to downslope flow and accumulation of cold air in the valleys. The nocturnal cooling effect is, proportionally, not as strong at mountain summits such as Säntis as further down in the valleys.

Such anomalies are not only reflected in the means of the analyzed climatic variables, but also – and perhaps especially – in their extremes. The previous section has shown that there are clear links between strongly positive or negative modes of the NAO, and extremes of pressure, temperature, and moisture ; high NAO values systematically shift the distributions from the lower extremes to the upper extremes.

Since the early 1970s, and up to 1996, the wintertime NAO index has been increasingly positive, indicative of enhanced westerly flow over the North Atlantic. This has led to synoptic situations in recent decades which have been associated with abundant precipitation over Norway, as cyclonic tracks enter Europe relatively far to the north of the continent (Hurrell, 1995). Over the Alpine region, on the other hand, positive NAO indices have resulted in surface pressure fields that have been higher than at any time this

century. Investigations by Beniston et al. (1994) concluded that close to 25% of pressure episodes exceeding the 965 hPa threshold recorded this century in Zürich (approximately 1030 hPa reduced sea-level pressure) occurred in the period from 1980 - 1992, with the four successive years from 1989 - 1992 accounting for 16% of this century's persistent high-pressure in the region.

Period	Tmin (°C)			Tmax (°C)		
	Observed Mean	Mean without NAO \geq 90% level	Bias	Observed Mean	Mean without NAO \geq 90% level	Bias
1901-1999	-8.95	-9.03	0.08	-4.33	-4.42	0.10
1950-1999	-8.66	-8.74	0.13	-3.36	-3.55	0.19
1975-1999	-8.20	-8.38	0.18	-2.74	-2.95	0.21
1989-1999	-7.50	-8.56	1.06	-2.15	-2.50	0.34

Period	Relative Humidity (%)			Precipitation (mm/day)		
	Observed Mean	Mean without NAO \geq 90% level	Bias	Observed Mean	Mean without NAO \geq 90% level	Bias
1901-1999	75.70	76.06	-0.36	7.04	7.10	-0.06 (-0.79%)
1950-1999	73.44	66.76	6.69	6.42	5.81	0.60 (+9.41%)
1975-1999	69.14	69.71	-0.56	6.73	6.90	-0.17(-2.54%)
1989-1999	65.82	75.34	-9.52	8.12	9.76	-1.63(-20.1%)

Table 2: Mean DJF values for minimum temperature, maximum temperature, relative humidity and precipitation for different periods of the 20th Century. The first column represents the mean recorded during each period; the second column represents the mean which would have been observed in the absence of NAO forcing beyond the 90-percentile threshold; the third column represents the bias imposed by NAO index values beyond this threshold (difference between the first two columns).

Table 2 shows an analysis of mean wintertime values for minimum and maximum temperature, relative humidity and precipitation at Säntis for four distinct periods of the

20th Century, namely 1901-1999, 1950-1999, 1975-1999, and 1989-1999. In each case, the observed DJF mean is given, followed by the mean which would have occurred without the influence of highly-positive NAO index (beyond the 90-percentile threshold). The third column for each variable represents the bias which NAO index \geq 90-percentile has imposed on temperature and moisture variables. It is seen in this table that the bias is relatively small when considering the entire 20th Century (1901-1999), but then increases as one approaches the end of the 20th Century. In the last decade, from 1989-1999, the bias for minimum temperatures exceeds 1°C. In the absence of the large forcings imposed by NAO index values \geq 90-percentile, this decade would in fact have been slightly cooler in terms of minimum temperature than the average conditions which prevailed from 1975-1999. Indeed, had there not been such a strong positive NAO forcing in the latter years of the 20th Century, minimum temperatures would not have risen by almost 1.5°C (decadal mean for the 1990s minus century mean from 1901-1999) but by less than 0.5°C, as seen in the second column of the minimum temperature analyses. The bias imposed by strongly-positive NAO thresholds on maximum temperature follows the same trends, but is not as high as for minimum temperatures; even in the absence of the NAO forcing, maximum temperatures would have risen substantially in the latter part of the 20th Century.

In terms of moisture, relative humidity has decreased in winter, with a bias of close to 10% in the period 1989-1999, resulting from the NAO forcing; mean DJF relative humidity would have otherwise remained relatively constant throughout the century. Precipitation is also seen to be considerably marked by the NAO forcing in the last decade of the 20th Century, with a substantial drop of 20% of winter precipitation linked to the high and persistent NAO index recorded during this period.

Because over half of the NAO index values exceeding the 90-percentile have occurred since 1985, it may be concluded that the NAO is a significant driving factor for the climatic anomalies observed in recent years in the Alps. In particular, the highly anomalous nature of temperatures and their extremes that have been observed and discussed in Jungo and Beniston (2001) are largely explained by the large-scale influence on regional climate generated by the recent trends of the NAO. Removal of the biases imposed by high NAO episodes would have resulted in relatively modest increases in Tmin temperatures and reduced rates of maximum temperature warming, thus leading to Alpine-scale warming comparable to global-average warming (Jones et al., 1999).

With the analysis of the Schüepp (1978) weather type classification from 1945 to 1999, divided into five 11-year periods, it has been shown that the frequency of weather types changed rather abruptly during the period 1989-1999. The changes are principally due to an important increase in high-pressure convective systems and an important decrease in cold "Bise" (easterly high-pressure) situations. The most important winter weather types during the last decade of the 20th century were western and southwestern advective situations with low-pressure (covered skies) and convective situations under high-pressure (clear skies). These are all warm winter weather types, clearly influenced by the strong and persistent positive NAO signal during this period, and certainly one cause of the abrupt shifts of the winter Tmin and maximum temperature towards more positive values during the period 1989-1999. The shift is very strong at high altitudes because of the large increase of convective high-pressure situations, which generate anomalously mild weather in the Alps.

The frequencies of the coldest and warmest winter nights and days (previously defined as the 10- and 90-percentile thresholds of temperature) in different regions in Switzerland also exhibit close relations to the NAO index. The most evident influence is found at low altitudes north of the Alps and at high altitudes within the mountains themselves. The number of cold winter days and nights with temperatures below the 10% threshold decreases towards the end of the 20th century. Paradoxically, since the early 1970s, the rather warm westerly advective weather type with low-pressure is more frequently linked to the coldest winter days and nights. This weather type, as well as the southwesterly low-pressure type are, for more obvious reasons, associated with the warmest winter nights since the 1970s; a more recent feature is the influence of convective weather types since 1990, which also exert a determining influence on the warmest winter nights. The number of warmest winter days with temperatures above the 90% threshold increased principally at low altitudes to the north and at high altitudes after 1990. Warm days occurring during the rather cold winter weather types associated with easterly advective situations have always been rare, but they disappeared completely after 1990. For these warm winter days, high-pressure convective weather types have increased in frequency since 1990, and also the westerly and southwesterly advective systems since about 1978.

4. Conclusions

In the context of climatic change forced by enhanced greenhouse-gas concentrations, the anomalously warm winters experienced in recent years have been shown to be driven in large part by the high values of the NAO index which has prevailed in the last 15 years of the 20th Century.

The influence of these high values has been to increase the upper tails of the temperature and pressure probability density functions to a significant degree, and to reduce the relative humidity and precipitation amounts at high elevations. Because of the controls which the NAO can exert over much of the winter season, the combination of higher temperatures and lower moisture is likely to have a number of impacts on the natural environment. In particular, the fact that at high elevations such as Säntis (2,500 m asl), the number of days where diurnal temperatures exceed the freezing point can increase by as much as two weeks during the winter season inevitably has implications for the timing of snow-melt and the amount of snow which remains on the ground throughout the winter. Earlier snowmelt in turn feeds into the hydrological systems, by increasing river discharge earlier in the season compared to « normal » or negative NAO indexes. Warmer temperatures are also associated with liquid rather than solid precipitation falling at higher elevations; when combined with early snowmelt runoff, this can lead to critical hydrological situations, particularly downstream of the mountains, as was experienced for example in early 1995, when the Rhine River overflowed its banks in Germany and The Netherlands.

Less snow and warmer conditions have taken their toll of glacier mass in the Alps, while at the same time in the late 1980s and early 1990s, Norwegian glaciers were advancing because of the excess precipitation in northerly latitudes associated with high NAO indexes. Earlier snow-melt can also trigger the seasonal cycle of mountain plants, as much of the high Alpine vegetation is dependent on snow-pack amount and duration for its metabolic cycles. The reduction of snow amount, which is closely related to the higher NAO indexes, and generally warmer average temperatures, are coincident with an upward migration of plant species, as reported by Grabherr et al. (1994) and Keller et al. (2000). Plants which survive under warmer conditions are progressively invading areas in which only cold-resistant vegetation was present until recently.

It would be difficult to draw more far-reaching conclusions for climate impacts on the basis of the short series of anomalously warm winters experienced in the Alps; this is *inter alia*

the case for ecosystem responses to climate change, which generally occur over longer time-scales. The run of mild winters in the Alps associated with high NAO index values has, however, had a measurable effect on snowline altitude, snow amount and duration, which in turn has influenced flow regimes in a number of hydrological basins originating in the mountains. Perturbations to hydrological regimes in a changed climate will certainly be the norm in the 21st Century (e.g., Gleick, 1987; Krenke et al., 1991; Leavesly, 1994), because of the different timings of the beginning and end of the snow season, and the overall reduction in the duration of the mountain snow-pack. The sparsity of snow has also had significant economic impacts on Swiss mountain communities in the late 1980s and early 1990s, which are largely dependent on winter sports for their income. The conclusion that snow amount and duration has been sensitive to changes in climate since 1985 at altitudes below 1500 - 2000 m is consistent with the rise in average snowline projected under a warmer global climate (IPCC, 1996); these conclusions could already help certain communities in preparing adaptation strategies for the future, for example through diversification of tourism activities rather than relying solely on the ski industry in winter. The conclusions presented here could provide guidance for future environmental and economic planning in the Alps, particularly for activities related to winter tourism, water resource management, and ecosystem studies.

Because of the very significant controls of the NAO on regional climate variables, their means and their extremes, it is vital in the current debate on global warming for general circulation climate models to improve their performance in simulating North Atlantic decadal-scale variability. This would enable an assessment of whether such variability will be as large as during the 20th Century, or whether the system will exhibit systematically positive NAO index values as observed since the 1980s. This would enable climate modelers and climate-impacts specialists to quantify the role of the future behavior of the NAO on climatic extremes in Europe. It is recognized by the IPCC (1996, 1998) that there is now a crucial need by the climate impacts community for climate scenario data which is not only at high spatial resolution, but which includes information on extremes. Extremes, and not changes in means, generally have the strongest bearing on environmental disruption and damage. The conclusions reported in this paper clearly point to the need for more research in order to improve the simulations of the NAO in climate models, and our understanding of the underlying causal mechanisms of the oscillation, since it is without question one of the major controlling factors on regional climate in the Alps.

ACKNOWLEDGEMENTS

The authors would like to thank the anonymous reviewers whose comments have helped improved the original manuscript. Financial support by the Swiss National Science Foundation for one of the authors (Patricia Jungo) is gratefully acknowledged; this funding is linked to contract 20-56732.99.

REFERENCES

see References – Section at the end of the work

6.2. DISCUSSION INCLUDING WEATHER TYPES IN SPRING, SUMMER AND AUTUMN

According to Folland et al. (1999) changing weather patterns may have a substantial influence on Tmin and Tmax and several studies conducted in Switzerland, including the publication presented in Section 6.1., point to important changes in alpine weather types in winter (Beniston et al., 1994; Wanner et al. 1997, 2000; Stefanicki et al., 1998). The important increase of convective high-pressure weather types and decrease of advective eastern weather types in winter during the period 1989-99 seems to be strongly connected with the North Atlantic Oscillation Index (NAOI), which is increasingly positive since the late 1970s. Luterbacher et al. (1999) found out that the alpine weather correlates best with the NAOI in winter and second best in autumn.

In order to complete the analyses additional figures for the seasons spring, summer and autumn depicting the frequency of the weather types during the 5 periods 1945-55, 1956-66, 1967-77, 1978-88 and 1989-99 are included and evaluated in this section. However, none of these seasons show as obvious and through the NAOI well explainable changes in the weather pattern during the last decade of the 20th century as it was found for winter. The analysis of the link between regional temperatures extremes and the alpine weather types (Figures 9a to 9d, Section 6.1.) is therefore limited to the winter season.

Figures 6.1 and 6.2 indicate for spring and summer a rise in the number of convective low and uniform pressure weather types towards the end of the century. In spring these two weather types increase since the end of the 1970s whereas in summer the increase is limited to the uniform pressure systems since the end of the 1980s. In summer as well, the number of convective high-pressure weather types is decreasing continually since the middle of the century and more abruptly at the end of the 1980s. During the summer warm phase of the 1940s the frequency count of the convective high and uniform pressure weather types is about equal in contrast to the warm phase in the 1990s where the uniform pressure types are over three times more frequent than the high-pressure types. Additionally the western advective weather types increase since the end of the 1970s and the eastern advective weather types decrease. This is a sign of increasing humidity in the air and in combination with overall higher temperatures an increase in the number of especially hot and humid summer days on the Swiss Plateau, i.e., in the region “low altitudes, north”, is possible.

Figure 6.3 depicts the autumn weather types. The number of the convective high-pressure weather types is continually increasing during each period until the end of the 1980s where the frequency count is highest. This high frequency is accompanied by a rise in advective western weather types, which is restricted to the period 1978-88. During the 1990s then a drop in the frequency of convective high-pressure and advective western weather types can be observed. These findings can be linked to the warm autumn temperatures during the 1980s and the significantly stronger century trend in autumn T_{max} in the region “high altitudes” than in the region “low altitudes”. The rise in the number of convective high-pressure weather types points to milder day temperatures at high altitudes.

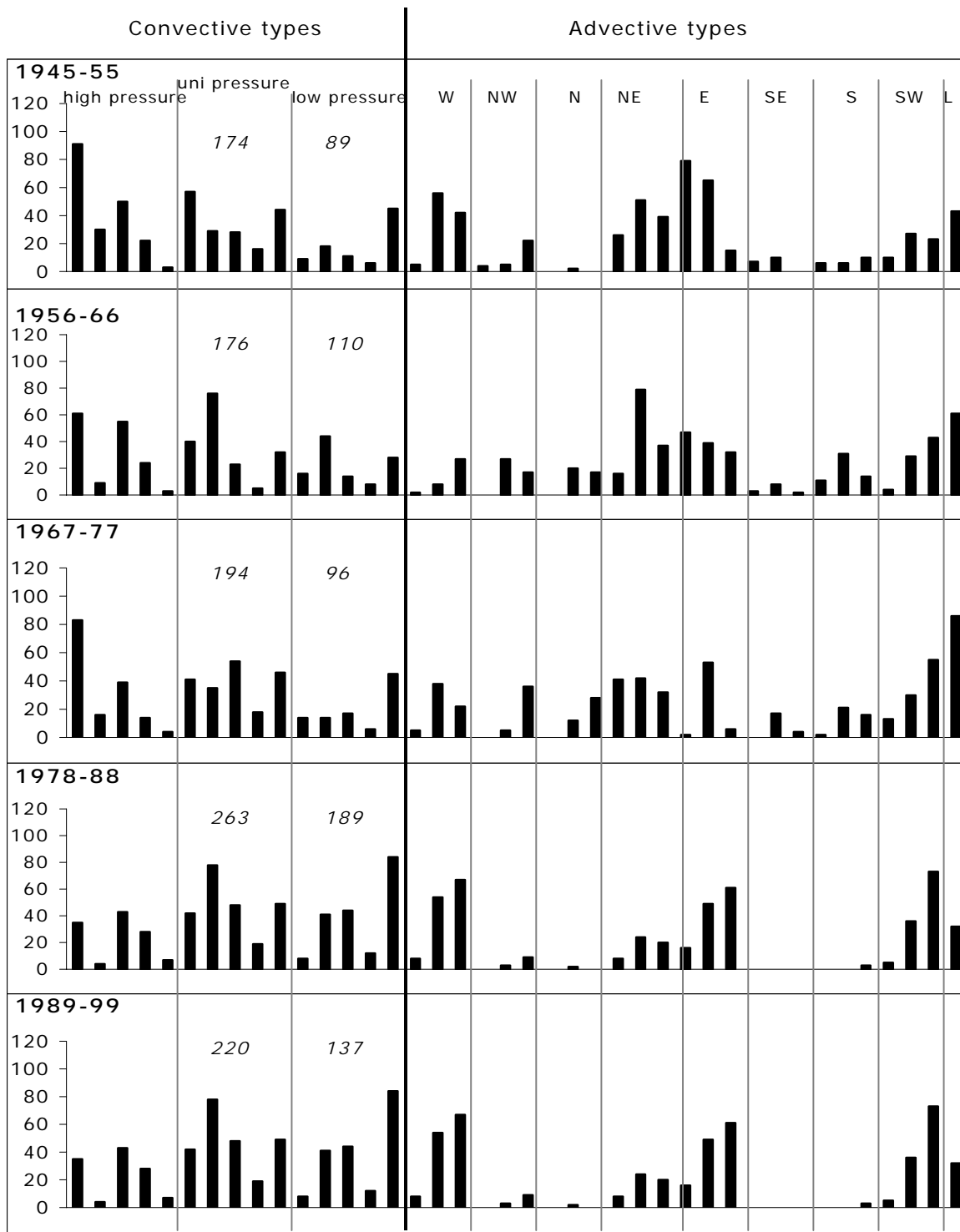


Figure 6.1: Spring - Frequency of the 40 alpine weather types, during 5 equal periods. The numbers printed into the figure indicate the exact frequency of the weather types, which show the most important changes in time. The five single bars of the convective weather type are, from left to right: high or spatially uniform pressure, types originating in the west,

north, east, and south. The three bars of each advective type indicate high, uniform or low-pressure.

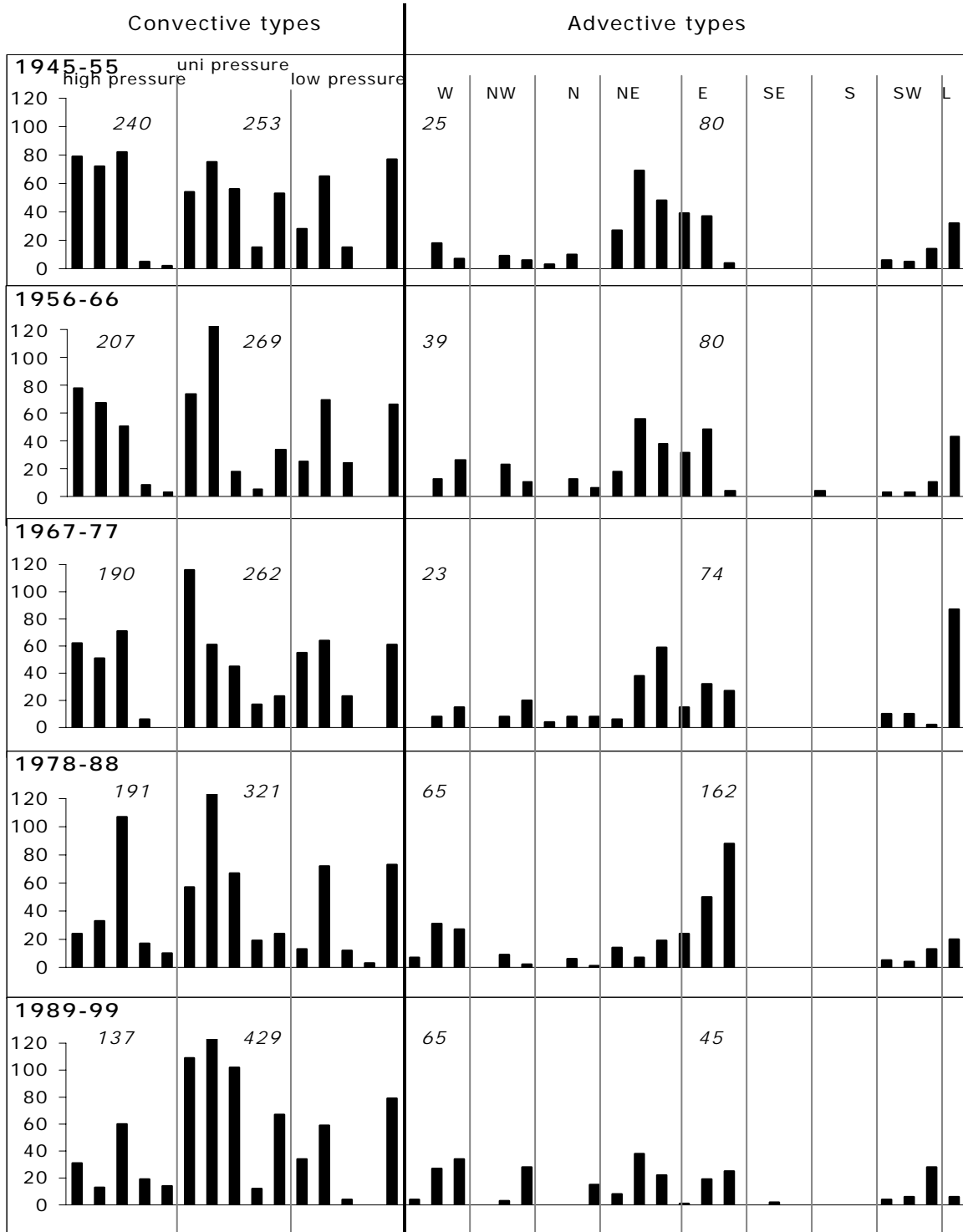


Figure 6.2: As Figure 6.1 except for: Summer

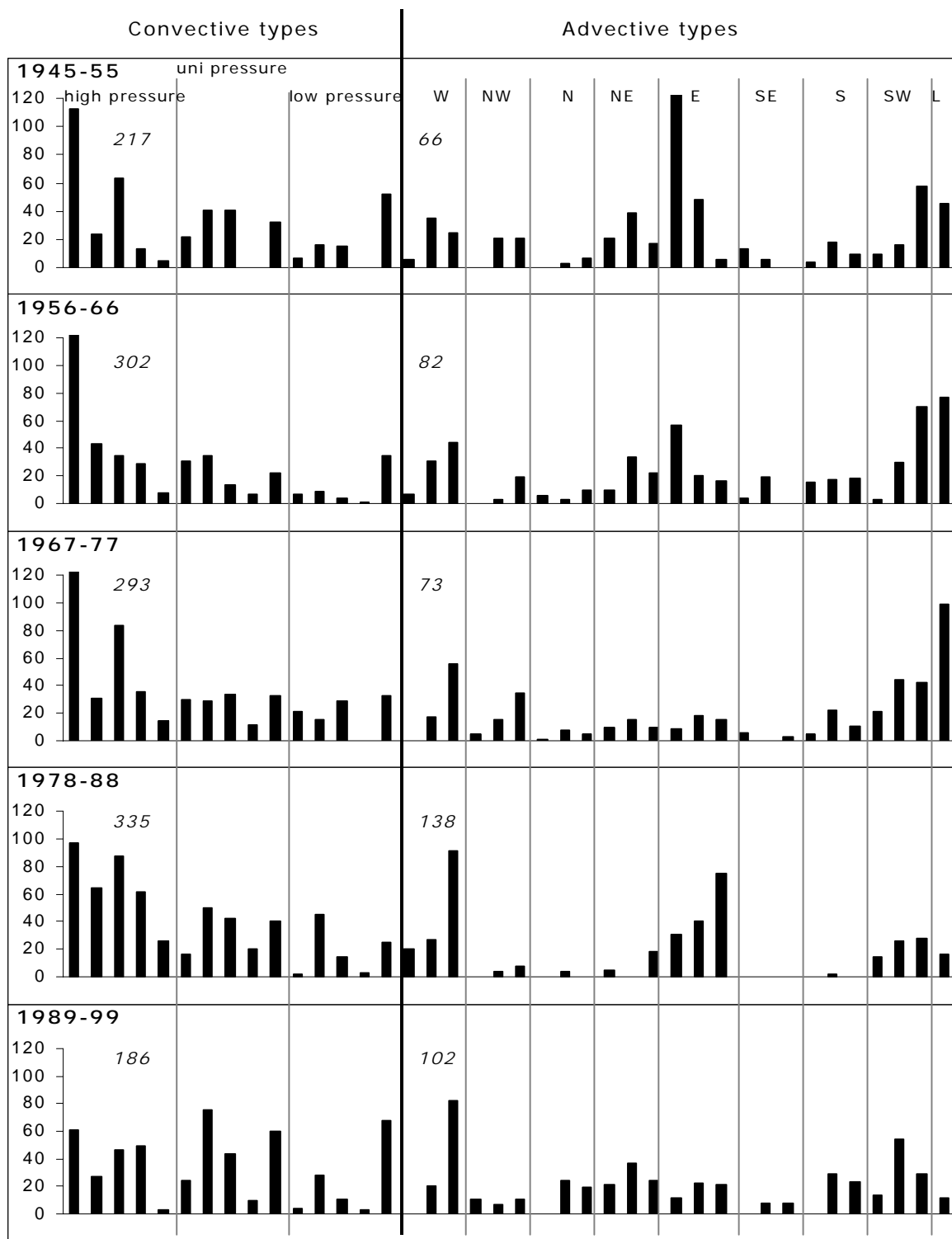


Figure 6.3: As Figure 6.1 except for: Autumn

7. ADDITIONAL APPLICATION OF THE REGIONALISATION METHODS (PCA AND CA) ON WIND GUST DATA

In this chapter working steps XII to XIII are discussed (see Section 1.2.):

XII. Repeating Principal Component and Cluster Analysis on wind speed. Defining a number of regions for different synoptic circulation patterns over the alpine region in function of wind gust data and the extracted components.

XIII. Calculating regional exceeding probabilities for wind gusts.

7.1. PAPER BY JUNGO, GOYETTE AND BENISTON (2001)

Daily wind gust speed probabilities over Switzerland according to three types of synoptic circulation

Abstract

The nowcasting and prediction of strong winds are still far from adequate, using either statistical or numerical modelling approaches. During the last decade, Switzerland has been struck by two extratropical storms, namely the February 1990 storm “Vivian”, and the December 1999 storm “Lothar”, that caused severe damage to infrastructure and to forests. Although numerical weather prediction models captured in both cases the cyclone tracks on the synoptic scale, the severity of local gusts was not properly predicted over the Swiss territory. To help predicting such phenomena, a combined approach to diagnose the wind gust speeds over Switzerland is described. The diagnostics aim at computing the probability of exceeding a gust speed based on the mean wind in relation to the prevailing synoptic weather type for a limited number of groups of climatological stations distributed throughout Switzerland. Based on ten years of Swiss station observations, the computation of this probability uses an empirical gust factor which is a function of the daily gust speed, itself a function of the daily mean wind speed. For this period, each day has been categorised into three weather types according to the Schüepp classification. Principal Component Analysis and Cluster Analysis are performed in order

to group climatological stations having similar characteristics in daily wind gust velocities. The results show that the gust factor provides an accurate method to compute the daily wind gust speeds at each Swiss climatological station for the given period. When combined to the three weather types and group of stations, the proposed diagnostics are an efficient method to predict the distribution of wind gust speeds. The gusts associated with the “Vivian” and “Lothar” storms are then diagnosed for each specific group where more than 85 % of the stations responded similarly to their specific group members, which is highly satisfactory in this case.

KEY WORDS: climate variables; gust factor; complex terrain; winter storms; synoptic weather types; region; statistical techniques.

1. Introduction

The severity and potentially destructive nature of a storm are to a large extent unpredictable, especially over complex terrain. It is assumed that in some cases the frequency of the fluctuation of pressure in wind gusts is close to the natural frequency of different constructions or of trees in a forest, which can provoke a partial or total collapse of the building, the bridge or the trees exposed to these gusts (Beniston, 1999). In a study conducted by Schmidtke and Scherrer (1997) this effect was found to be significant causing extensive damage to forests even if the windspeed is lower than 16 m s^{-1} (Beauford 7), which represent a critical value for damage to be caused. The authors also found that on a local scale, the topography has a strong influence on the gust velocity, and combined with windward slopes and ridges can cause channelling and shooting effects that further accelerates the winds.

Switzerland is characterised by a very complex topography, a mountain range in the northwest (Jura), a plain stretching from the west to the northeast (Plateau), the Alps in the southwestern, central and eastern part and the beginning of the Po plain to the south. Furthermore, winds are influenced by synoptic situations. As investigated by Schüepp (1978), forty weather types may be defined over the Alps which can then be combined into three general groups: convective, advective and mixed. With this information in mind, Schmidtke and Scherrer (1997) presented three basic storm types with destructive character occurring in Switzerland as indicated in Fig. 1 by symbols: west wind storms - W

(advective, generally in winter), Föhn storms - F (south wind) and thunderstorms (convective).

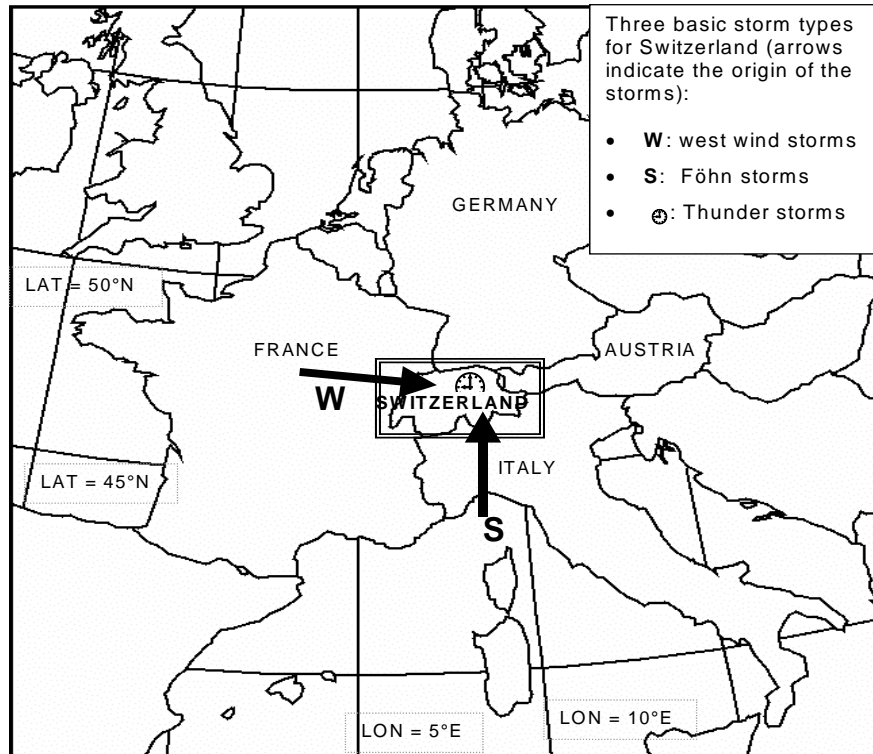
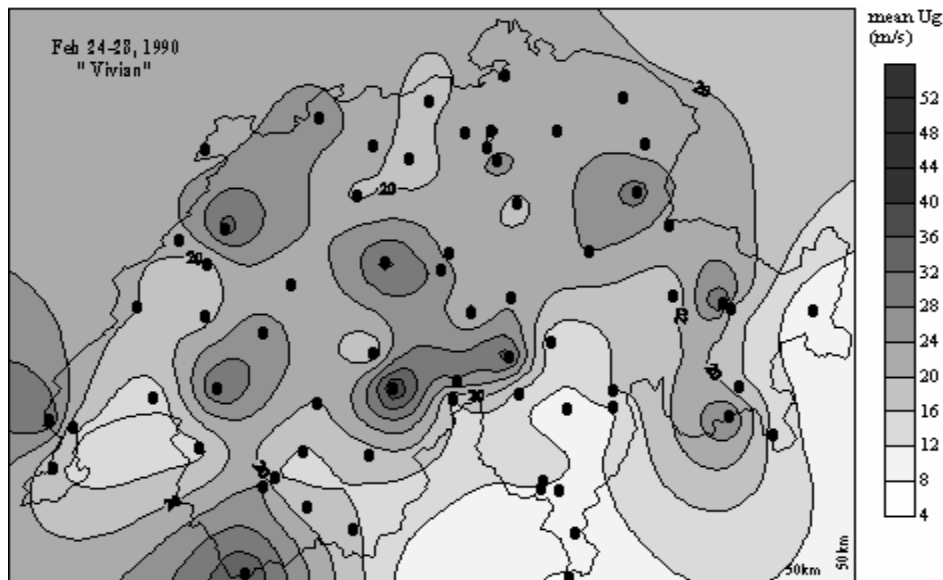


Figure 1: Map of Western Europe. Switzerland is in the insert, which delimits the section of the Swiss maps used in Fig. 2 and 6.

Two thirds of the observed storms in Switzerland since 1500 occurred during winter (October to March) (Pfister, 1999). The last decade was marked by two severe winter storms, namely “Vivian” in February 1990 and “Lothar” in December 1999, which caused serious damage to forests and buildings in different regions and countries of western Europe. In both cases, the local gust speed and the extent of the damage could not be well estimated in advance of the event. Forests in mountainous regions often have a protective function in order to prevent landslides and avalanches; furthermore, on the Swiss Plateau, forestry represents an important economical sector. A better estimation of local wind gust speeds would help insurance companies to define zones of elevated risk, foresters to adapt tree populations in forests to the wind regime, and civil engineers in their construction plans. Although estimates of the largest wind gusts are required by civil engineers, the knowledge of the atmospheric conditions fostering the development of the

gusty nature of the wind is also important for atmospheric scientists. Several studies focused on the stochastic aspects (e.g. Ragwitz and Kantz 2000; Walshaw 2000; Weggel 1999), whereas some others aimed to link the wind gusts with physical processes and/or atmospheric states (e.g. Krayner and Marshall, 1992).

Fig. 2a-b illustrate the distribution of the daily wind gust speeds averaged for the February 1990 “Vivian” and the December 1999 “Lothar” episodes. The strong wind gust centres, which are situated mostly at high altitudes (1600-3600 m) are well identified and share common features in both cases. However, it is not advisable to make predictions for all possible “extremes” since only two severe storms were analysed. It may nevertheless be assumed that under strong synoptic forcing during advective situations the overall response in terms of wind activity is similar.



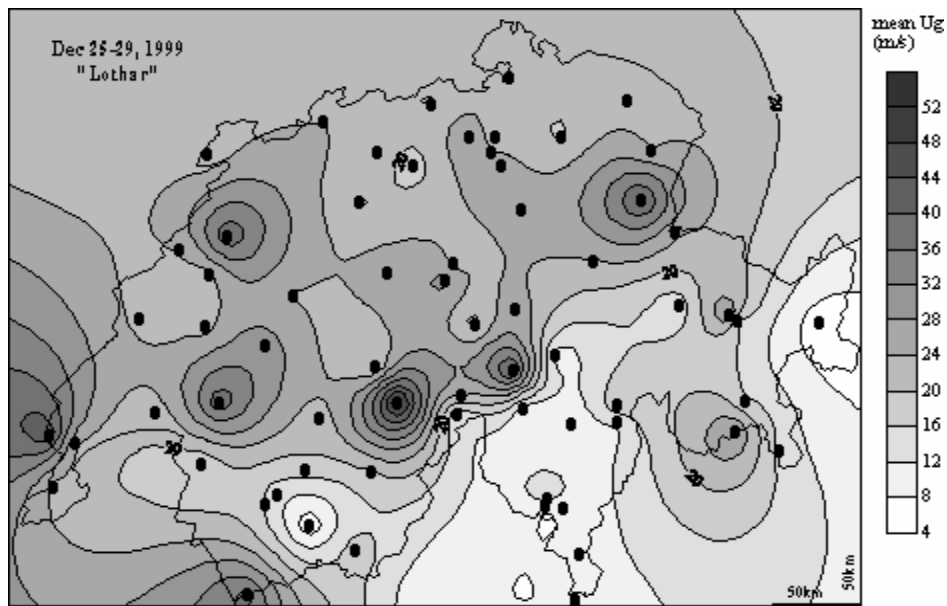


Figure 2: Spatial distribution of the daily wind gust speeds ($m s^{-1}$) averaged over the period of a winter storm over Switzerland **a**: “Vivian” (Feb 24-28, 1990) and **b**: “Lothar” (Dec 25-29, 1999).

Considering the chaotic nature of the weather phenomena together with the observed likeness of the mean wind gust distribution in Switzerland during “Vivian” and “Lothar” a first working hypothesis can be formulated: the wind gust speeds can be estimated over different regions represented as groups of several climatological stations exhibiting similar behaviour in terms of wind gusts.

For example, “Vivian” was a series of 8 strong extratropical cyclones, which swept through Switzerland from February 24-28, 1990. During this period, a deep 968 hPa low-pressure center travelled from southern Iceland to the Barents Sea with a maximum deepening rate of 27 hPa within 12 hours on February 26. On February 27, 1990 large parts of Switzerland were hit by the frontal zone of the cyclone “Vivian”, which produced violent winds causing strong damage to forests. (Schüepp et al., 1994; Schiesser et al., 1997). The maximum gust observed reached more than $75 m s^{-1}$ (Beaufort 12) at the Grand St. Bernard pass station, on the Swiss-Italian border. For other stations located at lower elevations, wind speeds were less intense, but in the range of other observed extreme values (Schüepp et al., 1994). The second severe storm, “Lothar”, occurred from December 25-29, 1999 and consisted of a series of deep cyclones travelling over the Atlantic Ocean. The devastating track of the “Lothar” storm ranged from west to east approximately along $49^{\circ}N$, and travelled with a velocity of about $28 m s^{-1}$ (Beaufort 10).

The irregularities of this cyclone were the strong wind gusts as well as its unusual intensification over land. These phenomena can possibly be linked to an amplified interaction between the geostrophic winds reaching at 9000 m velocities of nearly 400 km h⁻¹ (Beniston, 1999).

The question arises whether observation of extreme events such as “Vivian” and “Lothar” tend to cluster in time. This clustering can either be of a coincidental nature under constant conditions of storm probability or related to a gradual increase in storm probability (Frei et al., 2000). Schiesser et al. (1997) have carried out a study concerning this topic within a project of the Swiss National Science Foundation. Their initial question was whether during the period of 1864 to 1993 the storms in Switzerland (limited to the northern part of the Alps) have become more frequent and more intense towards the end of the century. The conclusions are that 100 years ago the Swiss climate had been stormier than at present and, furthermore, the period before 1940 can be considered as windier than the past few decades. They also concluded, however, that the cyclonic westerly wind situations have increased in number over the past decade. This can be linked to the increasing temperature and pressure gradient between the subpolar and the subtropical regions since the 1980s, generated by the behaviour of the North Atlantic Oscillation (NAO). A further conclusion of Schiesser et al. (1997) is that these westerly wind tracks seem to be shifted northward, hence Switzerland is frequently situated at the southern edge of western storm systems and therefore less affected by severe winds. This shift is also described in the well known report of the Intergovernmental Panel on Climate Change (IPCC) (chap. 6, 1996) where different General Circulation Models (GCM) were used to detect possible long term changes in storminess in a warmer world. However, little agreement was found between the models and conclusions regarding storm events are obviously even more uncertain. Zwiers and Kharin (1998) have evaluated the changes in the wind extremes of the climate simulated by a GCM under double CO₂ conditions; they found that the larger wind extremes occur in high latitudes where sea ice has retreated compared to the control experiment (1xCO₂). However, in the mid-latitudes, the change in return periods of annual wind extremes was found to be marginal at best.

It seems evident that even though research is advancing, it is difficult to predict the location, timing, and frequency of high and devastating wind gust speeds associated with strong storm systems. The fact that many storms occur during westerly wind situations in winter justifies the formulation of a second working hypothesis, which expresses the fact that a more accurate form of gust speed prediction is reached when different synoptic

situations over the alpine region are considered separately. The aim of this study is thus to develop a statistical method to predict the expected value of the daily maximum wind gust speed according to the work of Weggel (1999) in relation with prevailing synoptic weather types for groups of climatological stations distributed in Switzerland.

2. Data

The wind data is provided by the Swiss Meteorological Institute (called MeteoSwiss), which manages a fully automatic network, the Automatisches Netzwerk, (ANETZ) comprising over 70 stations. The data is not homogenised by MeteoSwiss, however, different tests of plausibility (limits, variability, consistency) are applied and if a correction is necessary, the data series are treated manually (Konzelmann, pers. com., June 23, 2000). After an extensive study by Ehinger et al. (1990) the data are considered as reliable and about 98% of the information collected in a year can be exploited. The remaining 2% are lost data due to a malfunctioning of the instrumentation. No aberrant data are being used in this study.

We use hourly mean and maximum wind speed values. Daily mean values as well as daily maximum values have been calculated on the basis of the hourly values. The measures are generally taken at the anemometer level, i.e., about 10 m above the surface.

Data recorded from 1990 to 1999 have been taken into account for this study. This 10-year period is of moderate size for wind analyses and allows to use the data of a maximum number of stations, since many stations of the ANETZ network were not in operation prior to 1990. In addition, the observations of the two severe winter storms “Vivian” in February 1990 and “Lothar” in December 1999 are included.

3. Methods

The present study consists of three parts. It is based on a method developed by Weggel (1999) to predict the expected value of the daily maximum wind gust speed knowing the mean wind, which is now applied to Switzerland (Sect. 3.1). This method is then extended according to the two working hypotheses formulated in the introduction:

Wind gust speeds can be estimated for different regions, represented as groups of several climatological stations having a similar behaviour in daily wind gust speeds (Sect. 3.3).

A more accurate form of gust speed prediction is reached when different synoptic situations over the alpine region are considered separately (Sect. 3.2)

3.1 Wind gust probability

This first part of the analysis is based on the work of Weggel (1999). He developed a method to compute the probability of equalling or exceeding a wind gust of a given magnitude by knowing the daily mean wind. This is very useful since forecasts for extreme values can thus be made quantitatively using the daily mean wind as the only input. The first part of the present work is to validate this method to Swiss station observations. Statistical methods to calculate extreme wind speeds are found in the literature (e.g. Zwiers, 1998). Palutikof et al. (1999) summarized these different methods in a review. In most cases, however, the methods serve the purpose to calculate return periods of violent winds. The current work can be seen as a complement since it is used to evaluate wind gust speed explicitly as a function of daily mean wind speed.

Weggel (1999) based his calculations on the normalised maximum gust speed, which is the ratio between the daily wind gust, U_g , and the daily mean wind, U . He defined a gust factor, G , as:

$$G = \frac{U_g}{U} - 1 \quad (1)$$

which is always greater than 0 since $U < U_g$. The gust factor is an explicit function of the mean wind speed. Therefore the maximum gust is a smaller fraction of the mean wind speed for higher wind speeds, which implies that G decreases with increasing U . Plotting the logarithm of the gust factor, $\log G$, as a function of the logarithm of the mean wind speed, $\log U$, allows to fit a power function to the data to predict a gust factor, namely G_p .

$$G_p = AU^n \quad (2)$$

The loglinear form of Eq. (2) can be expressed as:

$$\log G = n \log A + \log U \quad (3)$$

and allows to calculate the intercept, A , and the slope, n , values for individual stations. As shown in Weggel a linear relationship between A and n can be established in the form $n = \varphi A - \psi$ where the slope φ , and the intercept ψ are parameters of this linear fit. As one may expect, steeper negative slopes correspond to higher intercepts so that φ and ψ are smaller than 0. Furthermore, φ and ψ are station dependent.

The statistical distribution of $\log G$ about its expected value as predicted by the fitted regression is first investigated. The differences between $\log G - \log G_p$, written as X , were ranked and assigned a probability, P , using the plotting position equation:

$$P(X \geq x) = \frac{m}{(N+1)} \quad (4)$$

where x is the ranking variable, m represents the cumulated count of the ranks and N is the number of data points in the time series.

The standardised values for a normal probability distribution are calculated in order to estimate the probability $P(U_g \geq v)$, with which a gust is equalled or exceeded by a given speed, v . The equation of the standardised value, z , can be expressed as follows:

$$z = \frac{\log G - \log G_p}{\sigma_{\log G}} \quad (5)$$

where $\sigma_{\log G}$ is the standard deviation of $\log G$.

3.2 Synoptic weather types

A weather type classification is expected to contain most of the significant elements determining the atmospheric conditions over a certain region i.e. pressure conditions, origin and dynamics of the airmass, main wind direction, etc. The weather type classification of Schüepp (1978) is used in many climatological studies concerning the alpine region and it is reliable for Swiss weather conditions. (Schiesser et al., 1997a). The method characterises weather types based on the altitudinal and the surface pressure conditions at noon in the central alpine region. It is based on three general groups of weather types, namely convective, advective and mixed. These three groups can be further subdivided into 40 weather situations; 15 for the convective type, 20 for the advective type and 5 for the mixed type. Convective situations, normally occurring in summer do not show considerable surface pressure differences and are therefore characterised by generally low wind velocities accompanied by significant vertical movements (convective). Advective situations, normally occurring in winter, in contrast indicate substantial differences in surface pressure and thus strong gradients. Included in the advective weather type are the mostly wind situations, which produce stormy winds during winter. The mixed type is a group of weather situations characterised of significant vertical as well as horizontal winds. (MeteoSwiss, 1985). In order to satisfy the second

working hypothesis and to link the daily gust factor G to different weather situations, a division of the observed days into the three major weather types instead of the 40 situations has been found to be sufficient. The daily wind data series of 1990 to 1999 is partitioned into days of convective, advective or mixed weather situations according to the daily database of weather types of Schüepp, provided by MeteoSwiss.

3.3 Classification of Swiss climatological stations

The first working hypothesis assumes that we can group climatological stations into a few distinct classes. This classification should be linked to the three different weather types defined in Sect. 3.2 and the resulting groups should respond in a similar fashion to a mean wind forcing. Similar grouping was carried out in Jungo and Beniston (2001), where Principal Component Analysis (PCA) and Cluster Analysis (CA) have been applied to a number of Swiss climatological stations in order to group them in function of their interannual minimum and maximum temperature variation. In their study, the PCA and CA have proven to be very convenient grouping tools for climatological stations situated in a complex terrain. For this reason we propose thus such a method to use in the present study. The statistical analyses made use of the software package SPSS (1999).

The PCA and CA are being used in the present study in order to aggregate the 63 ANETZ stations as a function of the daily gust factors, namely logG, which are then linked to the three weather types. As a result groups are aggregates of stations, which exhibit a comparable variability to G and its response to the weather forcing. The geographical distribution of the groups should also depend on the complexity of the terrain.

PCA is based on a correlation matrix between station wind time series from 1990 to 1999. The overall variation of the original data matrix, $\log G_{\text{matrix}}$, can be reproduced in such a way that each variable is represented as a linear combination of the calculated components, C_l , where l goes from 1 to q. (Bahrenberg et al., 1992). This can be expressed as follows:

$$\log G_{\text{matrix}} = \alpha_i + \sum_{l=1}^q \beta_{il} C_l \quad , \quad (i = 1, \dots, m) \quad (6)$$

where α_i is the regression constant of $\log G$, β_{il} is the partial regression coefficient of C_l and m is the number of stations included in data matrix.

The number of components normally extracted is usually smaller than the number of input variables, which constitutes an important reduction of the size of the information while

simultaneously retaining most of the variability in the original data. Since the variability at a station is explained by more than one component at a time the single components indicate typical characteristics that groups of stations have in common, such as the topography, the main wind direction and the location.

The following CA attempts to identify homogeneous clusters of stations, which depend on G and the typical characteristics identified with the PCA beforehand. The method is based on the correlation matrix between G and the extracted principal components, while the difference between two clusters is as large as possible. The hierarchical method employed here begins by finding the closest pair of stations according to a function of distance and combines them to form a cluster. The number of groups finally taken into account needs to represent a compromise between the degrees of generalisation in order to keep coherent groups of stations and to possibly avoid clusters including only one or two stations.

4. Results

Equation (1) described above has been applied to the wind data of 63 climatological stations over a period of 10 years, where G was plotted as a function of U . Fig. 3 is the example for the Grand St. Bernard mountain pass station located at an elevation of 2472m. For each station a lognormal distribution of the wind gust factor G is resulting.

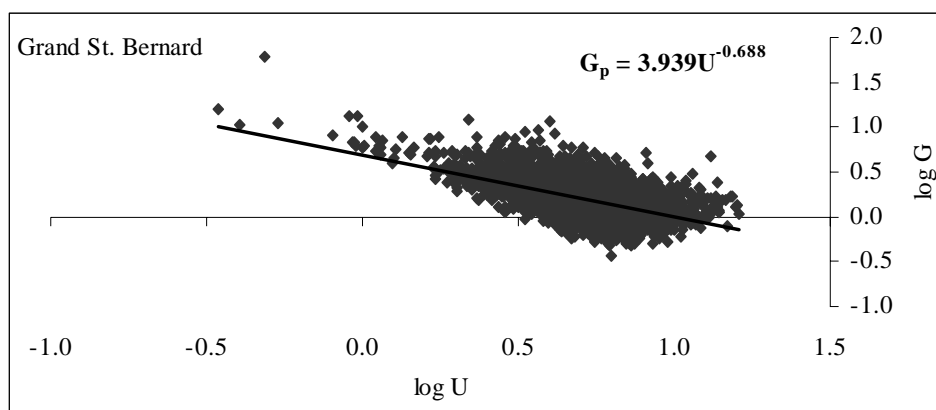


Figure 3: Gust factor as a function of the mean daily wind speed at Grand St. Bernard (2472 m, 07°10" / 45°52") according to Eq. 2.

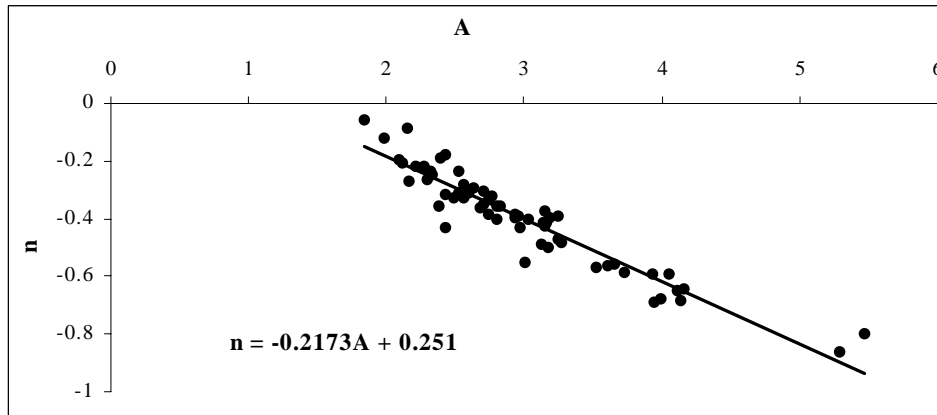


Figure 4: Relationship between A and n coefficients of Swiss ANETZ stations over the period covering 1990 to 1999.

In Fig. 3 the power function is fitted to the data of Grand St. Bernard and applying Eq. (3) the values for A and n can be calculated for all available ANETZ stations. As shown in Fig. 4, data measured over complex terrain still produce a linear relationship between the coefficients A and n . This equation is:

$$n = -0.2173A + 0.251 \quad (7)$$

where $\bar{\varphi} = -0.2173$ and $\bar{\psi} = 0.251$, when the averages $\bar{\varphi}$ and $\bar{\psi}$ are computed for 10 years of stations observations. Again, there is no reason to believe that φ and ψ are universal as shown in Weggel (cf. Eq. (4), 1999). These values could however prove to be useful for further analyses in similar regions with no or insufficient wind data available. In consideration of the high number of stations included (here 63), Eq. (7) is a valid approximation for Switzerland and even for the Alpine region.

To test the statistical distribution of $\log G$ about G_p Eq. (4) is applied to the Swiss data with the result that the difference between $\log G - \log G_p$ at all stations follows a lognormal distribution. Shown as an example in Fig. 5, is the station Grand St. Bernard, which experienced extremely strong winds during the “Vivian” event. The observed cumulative probability computed with Eq. (4) is fitted to a normal cumulative probability distribution. If the resulting dots of the fitting, black in Fig. 5, show a diagonal straight line as the grey model line in Fig. 5, the observed distribution can be accepted as normal. The example in Fig. 5 shows that the cumulative probability distribution of $\log G - \log G_p$ is comparable to a normal cumulative probability distribution. An additional Kolmogorov-Smirnov test was

made where the goodness of fit between observed values and a normal distribution confirms the hypothesis of normality.

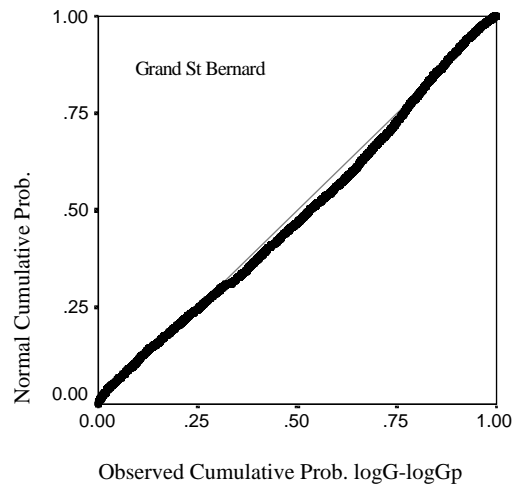


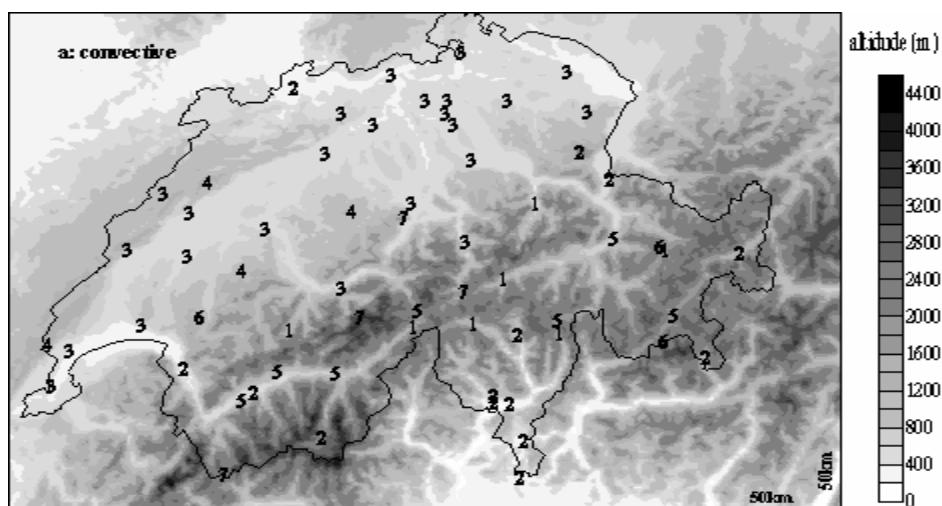
Figure 5: Lognormal distribution of the gust factor (Eq. 4) at Grand St. Bernard. The observed cumulative probability is fitted to the expected normal one. The 1:1 line is shown in light grey, denoting the perfect normal case.

The grouping of Swiss climatological stations linked to the three different weather types of Schüepp is tested in the following. The partitioning results in three different series of various lengths, where 61% of the days are characterised by convective situations, advective situations were predominant in 34% of the days, and 5% of the whole period are mixed situations. PCA and CA are now applied separately to each of these 3 data series. The daily wind gust factors (Eq. 1) of 70 stations between 1990 and 1999 are considered as variables for the PCA. A 70 by 70 data matrix is now defined. Shown in Table 1 are the number of components extracted, C_i , for each synoptic type. For example the major part of the variance (57.3%) of the convective type is represented by only 15 components. A number of components, C_i , are sufficient to explain about 60% of the variance for each of the three weather types.

synoptic type	C_l	variance explained	Nb. of clusters
convective	15	57.3%	7
advective	13	61.4%	6
mixed	18	69.9%	8

Table 1: Results of PCA and CA according to the three synoptic weather types. C_l are the principal components extracted, the second column denotes the total variance explained with these components, and the third column shows the number of clusters identified using CA. Symbol appearing in Eq. (6) is described in the text.

Compared to the analysis made on temperature data (Jungo and Beniston, 2001) where 3 to 6 components explained 90% to 95% of the variance, the wind data is characterised by much more complex characteristics than temperature data. Although its variance is harder to explain wind data still remains adequate for this kind of analysis. The number of clusters identified with CA for each synoptic type is shown in Table 1. As depicted in Fig. 6a-c, the resulting clusters of stations are obviously not randomly distributed. For each weather type, it can be observed that the groups are closely linked to the topography and the location of the stations, to the influence of the Mediterranean climate, which is characteristic of the southern part of Switzerland, and to the main wind direction.



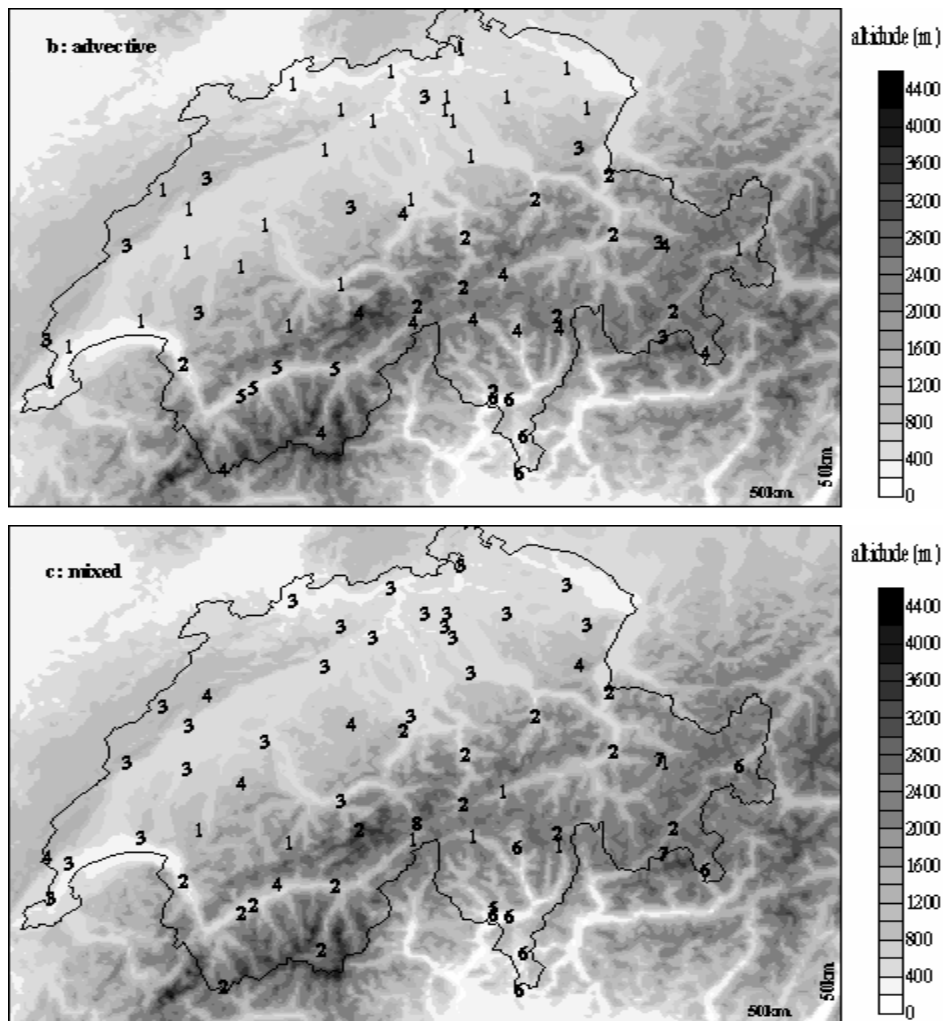


Figure 6: Resulting clusters of ANETZ stations according to the three synoptic weather types, a: convective (7 groups), b: advective (6 groups) and c: mixed (8 groups).

Eq. (5) allows computing the standardised values, z , of a normal probability distribution for single stations. Recalling the objective of this study to calculate the probability of wind gust speeds equalling or exceeding a fixed value during convective, advective or mixed synoptic weather types within different groups of Swiss climatological stations, Eq. (5) must be modified slightly. In order to calculate z for a group of stations, mean values must be applied:

$$z = \frac{-\log G - \overline{\log G_p}}{\sigma_{\log G}} \tag{8}$$

where $\log G$ is based on Eq. (1), and $\overline{\sigma_{\log G}}$ is the arithmetical mean of the standard deviations, σ , of the transformed data at each station included in a group. To compute

$\overline{\log G_p}$, the arithmetical mean of A , and n , namely \bar{A} and \bar{n} are evaluated for each station in a group. Table 2 indicates these mean values computed for each group, which are needed to calculate \bar{z} according to Eq. (8).

synoptic type	group	\bar{A}	\bar{n}	$\overline{\sigma_{\log G}}$
convective	1	3.571	-0.511	0.196
	2	2.579	-0.276	0.168
	3	2.645	-0.329	0.167
	4	2.650	-0.421	0.169
	5	3.577	-0.529	0.179
	6	4.347	-0.652	0.276
	7	6.345	-0.801	0.245
advective	1	2.698	-0.340	0.166
	2	3.233	-0.442	0.173
	3	3.324	-0.501	0.215
	4	4.486	-0.595	0.215
	5	2.741	-0.341	0.163
	6	2.159	-0.136	0.160
mixed	1	3.610	-0.536	0.201
	2	3.859	-0.490	0.187
	3	2.654	-0.332	0.167
	4	2.927	-0.446	0.180
	5	2.118	-0.205	0.158
	6	2.473	-0.238	0.169
	7	4.761	-0.694	0.302
	8	5.289	-0.864	0.238

Table 2: Mean values \bar{A} and \bar{n} and $\overline{\sigma_{\log G}}$ computed for each group according to the three synoptic weather types.

As an example, consider that during an advective weather type we want to determine the skill of the method. The skill is here defined as the percentage of stations included in a group, which actually respond similarly during “Vivian” and “Lothar” episodes. We now assume that the mean wind magnitude $U = 10 \text{ m s}^{-1}$, and then compute the probability, $P(U_g \geq v)$ for group 1, where $v = 25 \text{ m s}^{-1}$ (Beaufort 9) is a measure of the gust speed. Applying Eq. (1), the gust factor gives $G = (25/10) - 1 = 1.5$ and the predicted gust factor computed with Eq. (2) equals $G_p = 2.698 \times 10^{-0.34} = 1.23$. According to Eq. (8) the standardised value results in $\bar{z} = (0.176 - 0.091) / 0.166 = 0.51$. Using a table of a normal

probability distribution (e.g., Bahrenberg et al., 1990), one finds that $F(0.51) = 0.695$ so that $P(U_g \geq v) = 30.5\%$. In other words, the probability that the gust speed exceed 25 m s^{-1} with a mean wind of 10 m s^{-1} is 30.5%, which is quite significant in this context. In addition, the observations measured during the 10 stormy days of “Vivian” and “Lothar” reveals that at 84% of the stations included in group 1, U_g typically equals or exceeds 25 m s^{-1} when $U = 10 \text{ m s}^{-1}$. A range of $\pm 2.5 \text{ m s}^{-1}$ has been used here to capture the variability of the observed hourly average wind speed. Examples of observed gust speeds when $U = 10 \text{ m s}^{-1}$ at single stations out of group 1 are: Geneva airport: 29 m s^{-1} ; Bern 30 m s^{-1} ; Basel 41 m s^{-1} and Zurich airport 30 m s^{-1} . In other words, 84% of the stations included in group 1 exhibit a similar behaviour in response to an advective synoptic situation characterised by explosive cyclogenesis.

group	<i>P</i>	score
1	30.5%	84%
2	26.4%	40%
3	23.6%	100%
4	29.1%	40%
5	31.6%	75%
6	25.8%	100%

*Table 3: Occurrence probability, *P*, of a wind gust during the Feb. 24-28, 1990 “Vivian” and the Dec 25-29, 1999 “Lothar” episodes where for group 1 to 5, $U = 10 \text{ m s}^{-1}$ and $U_g \geq 25 \text{ m s}^{-1}$ and for group 6, $U = 2 \text{ m s}^{-1}$ and $U_g \geq 7 \text{ m s}^{-1}$. The score of the method represents the percentage of stations in a group where observations correspond to these two events.*

The probabilities for each group of stations for which the wind gust speed of 25 m s^{-1} is equalled or exceeded during “Vivian” and “Lothar” are shown in Table 3 and indicated with an asterisk in Fig. 7-1 to 7-6. These results are combined to the scores of stations per group containing real cases corresponding to these theoretical conditions. For group 6, the U and the v values have been modified to 2 m s^{-1} and to 7 m s^{-1} , respectively, because west wind storms generally do not affect the southern part of Switzerland, therefore high wind speeds are not realistic. The highest destruction rate during the storm episodes was found in the regions defined by groups 1 and 5, where a high score is also reached. Group 3 reaching a 100% score, aggregates pass and summit stations, which are frequently exposed to high wind speeds.

A further test of the skill of the method is done in order to quantify the performance of the method in cases during low U and low U_g (Table 4a) as well as with a high U and a high

U_g (Table 4b). First the occurrence probability of these two examples has been calculated separately for each station included in a group and then the mean of all these station probabilities, \bar{P} , and its standard deviation, $\sigma_{\bar{P}}$, was determined. Then, the occurrence probability per group, $P(\bar{A}, \bar{n})$, computed according to Eq. (8), is compared to the mean station probability, \bar{P} . According to Table 4 the difference between both, ΔP , never exceeds one standard deviation of \bar{P} , named $\sigma_{\bar{P}}$. This represents a satisfying result for the skill of the method. Wind gust occurrence probabilities, computed for specific groups of climatological stations, established in this study are as reliable as if they were computed for single stations and then averaged.

synoptic type	group	\bar{P}	$\sigma_{\bar{P}}$	$P(\bar{A}, \bar{n})$	ΔP
convective	1	14.35%	6.33	14.92%	-0.57
	2	5.49%	6.03	5.16%	0.33
	3	5.08%	3.19	4.85%	0.23
	4	3.76%	2.37	3.59%	0.17
	5	11.71%	9.3	12.3%	-0.59
	6	25.58%	12.3	28.1%	-2.52
	7	27.38%	25.5	43.25%	-18.87
advective	1	5.25%	3.16	4.95%	0.3
	2	9.49%	8.65	9.68%	-0.19
	3	12.25%	12.9	14.01%	-1.76
	4	18.55%	16.6	27.43%	-8.88
	5	5.39%	4.72	5.05%	0.34
	6	2.73%	0.96	2.68%	0.05
mixed	1	14.74%	6.31	15.39%	-0.65
	2	12.51%	15.78	19.22%	-6.71
	3	5.05%	3.21	4.75%	0.3
	4	7.3%	8.21	6.68%	0.62
	5	1.62%	0	1.62%	0
	6	5.04%	3.89	4.85%	0.19
	7	30.57%	12.44	33%	-2.43
	8	28.1%	0	28.1%	0

Table 4a: captions see below with Table 4b

synoptic type	group	\bar{P}	$\sigma_{\bar{P}}$	$P(\bar{A}, \bar{n})$	ΔP
convective	1	2.38%	1.77	1.74%	0.64
	2	8.97%	9.35	6.94%	2.03
	3	4.21%	3.52	3.36%	0.85
	4	0.86%	0.8	0.6%	0.26
	5	0.91%	0.65	0.73%	0.18
	6	2.99%	2.37	3.22%	-0.23
	7	0.94%	1.19	1.36%	-0.42
advective	1	3.75%	3.4	3.01%	0.74
	2	2.71%	2.79	1.7%	1.01
	3	3.21%	1.99	2.28%	0.93
	4	2.33%	1.79	2.44%	-0.11
	5	4.95%	7.29	3.01%	1.94
	6	19.66%	10.63	18.41%	1.25
mixed	1	1.82%	1.24	1.43%	0.39
	2	3.08%	4.14	2.94%	0.14
	3	3.98%	3.44	3.22%	0.76
	4	1.28%	1.1	1.07%	0.21
	5	6.3%	0	6.3%	0
	6	12.78%	1.45	9.85%	2.93
	7	3.8%	2.71	4.01%	-0.21
	8	0.16%	0	0.16%	0

Table 4: Occurrence probabilities for wind gusts computed as a mean of single station probabilities \bar{P} , compared to the occurrence probability computed per group, $P(\bar{A}, \bar{n})$. The difference ΔP , should not exceed the standard deviation of \bar{P} , $\sigma_{\bar{P}}$.

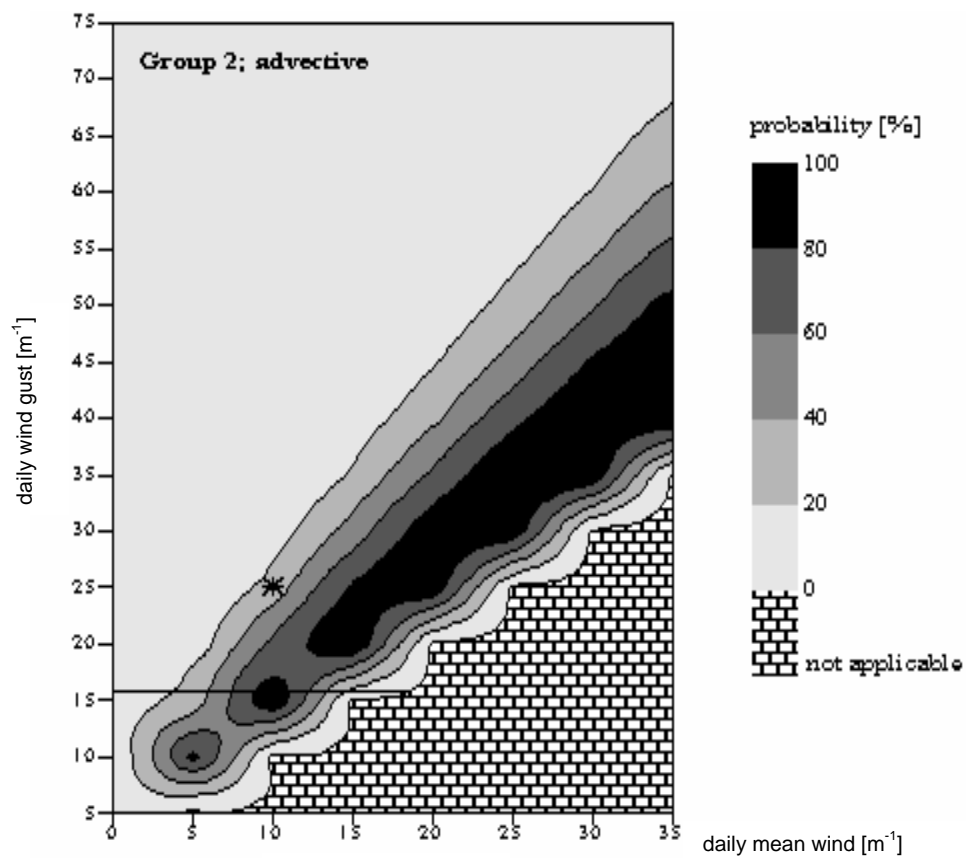
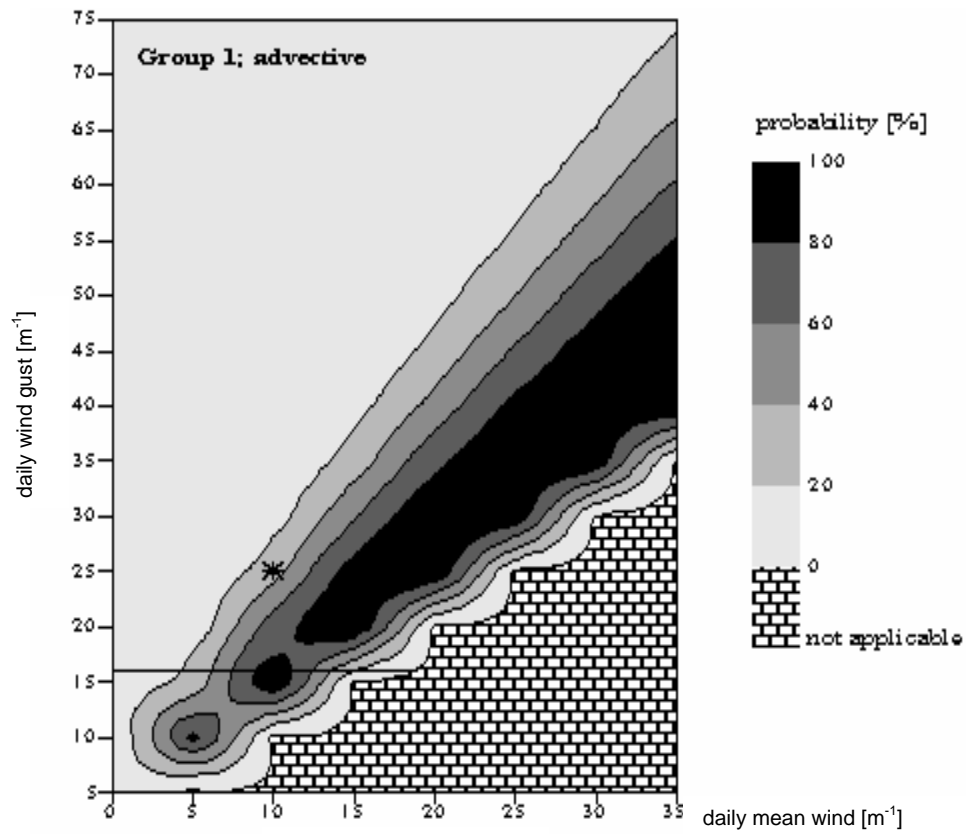
a (upper table): $U = 2 \text{ m s}^{-1}$; $U_g \geq 10 \text{ m s}^{-1}$; b (lower table): $U = 20 \text{ m s}^{-1}$; $U_g \geq 60 \text{ m s}^{-1}$.

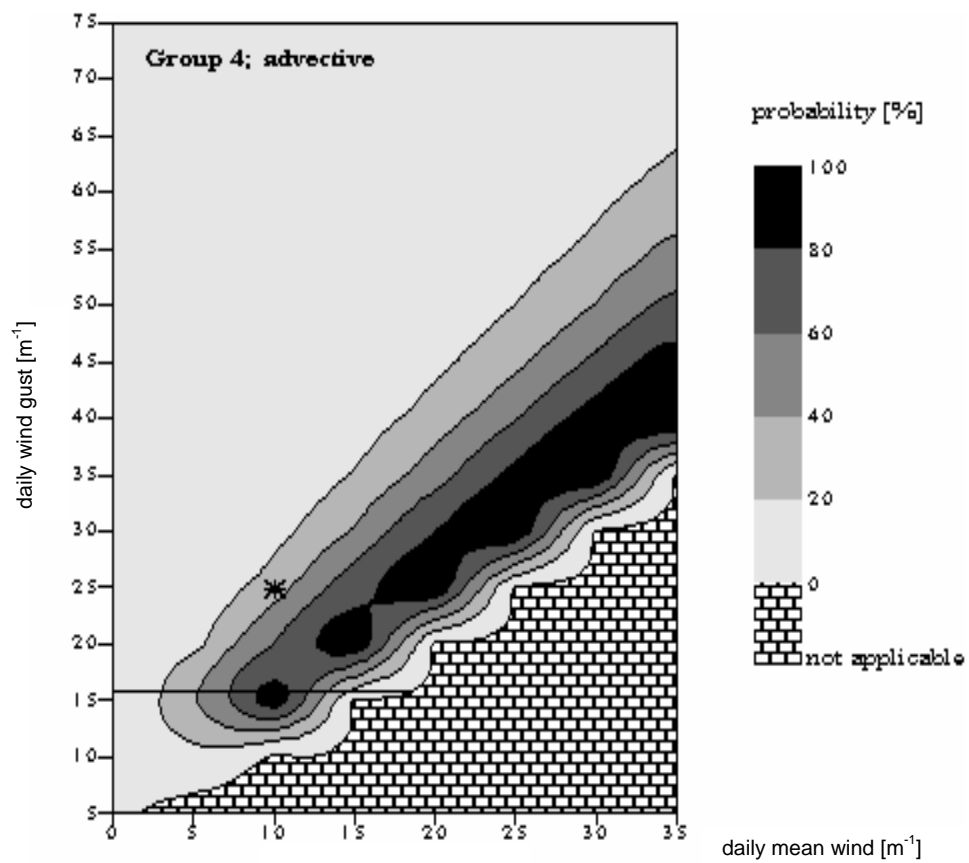
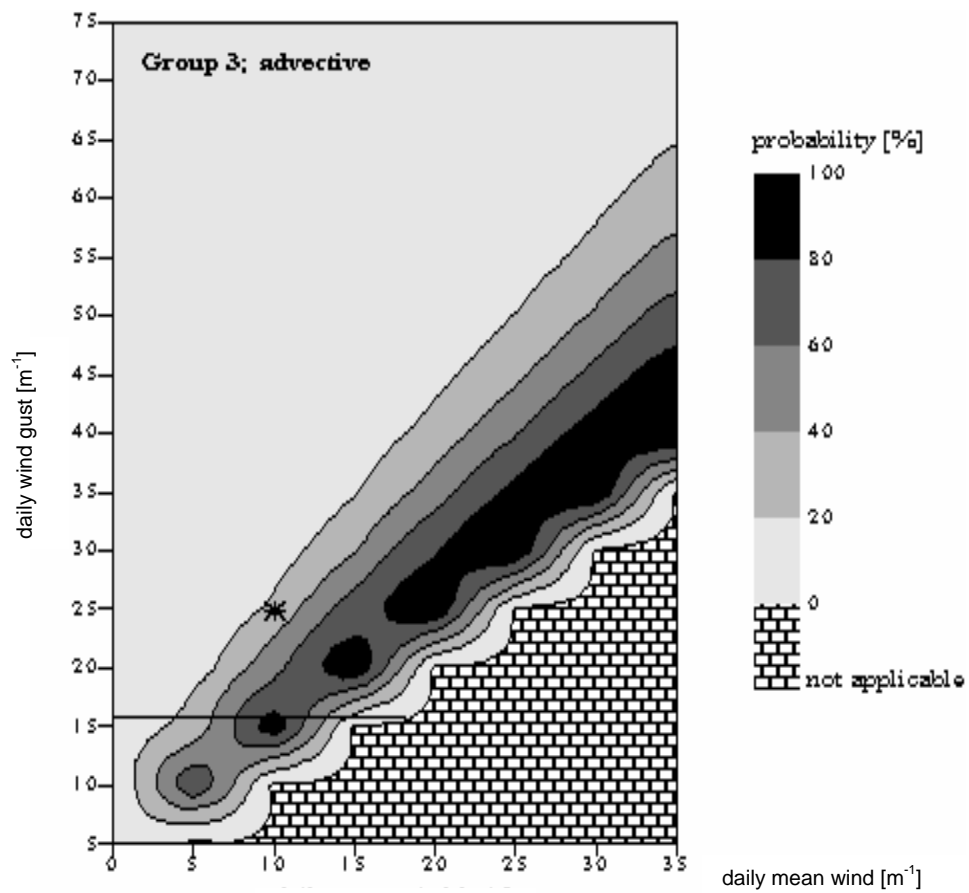
5. Example and Discussion

Summarizing the results given above, a convenient method is now available to compute the probability of occurrence of a wind gust speed for groups of stations over Switzerland, as a response of three different weather types, when the mean wind speed is known. Fig. 7-1 to 7-6 represent the summary of the results for advective situations. This weather type is of major interest since westerly wind storms like “Vivian” and “Lothar” generally occur during the winter months under advective conditions. Fig. 7 shows isolines of the probability of occurrence of gust wind speeds as a function of the mean wind speed for

the six groups (1 – 6) in Switzerland during advective situations. It is expected that these distributions will become smoother as the data series increases. At $U_g = 16 \text{ m s}^{-1}$, a line has been drawn on the graph to indicate the critical gust value for damages. As mentioned earlier, Schmidtke and Scherrer (1997) have observed that gusts of 16 m s^{-1} over complex terrain can cause significant damage to forests. It can be noticed in Fig. 7-1 to 7-6 that there is an 80 to 100% probability for wind gusts to reach 16 m s^{-1} or more if the daily mean wind during advective situations is in the range of 8 and 12 m s^{-1} . As demonstrated with the examples in Sect. 4, daily mean wind speeds around 10 m s^{-1} during stormy situations are frequently observed. The examples with $U = 10 \text{ m s}^{-1}$, $U_g \geq 25 \text{ m s}^{-1}$ for groups 1 to 5 and $U = 2 \text{ m s}^{-1}$, $U_g \geq 7 \text{ m s}^{-1}$ for group 6 are indicated by asterisks. These points are gust speeds that have effectively been observed at most of the climatological stations in Switzerland during “Vivian” and “Lothar”; the scores shown in Table 3 corroborate this.

If we compare Fig. 6b, where the station location is shown per group, with Fig. 2a and 2b, which show the distribution of the mean wind gusts during the “Vivian” and “Lothar” episodes, the strong wind gust centres can be identified as stations belonging to group 3 and 4. The stations in group 3 are mostly situated at passes and summits in the Jura and the Prealps and group 4 unites alpine stations. It can also be noticed in Fig. 7-3 and 7-4, however, that groups 3 and 4 show a modest probability for extremely strong wind gust speeds even though it is precisely these groups that are frequently exposed to strong wind speeds. This can be related to the fact that with Eq. (1) G decreases with increasing wind speed, i.e., the maximum gust is a smaller fraction of the mean wind speed for higher wind speed. Such a behaviour in groups 3 and 4 emphasises the functional form of G .





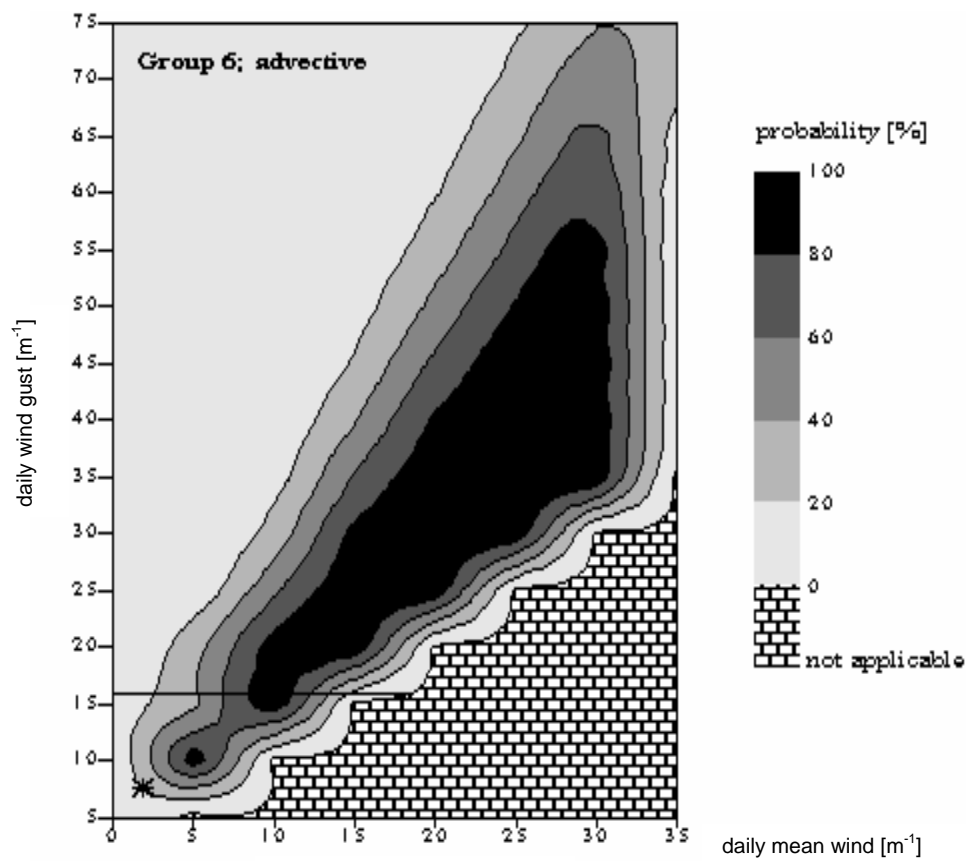
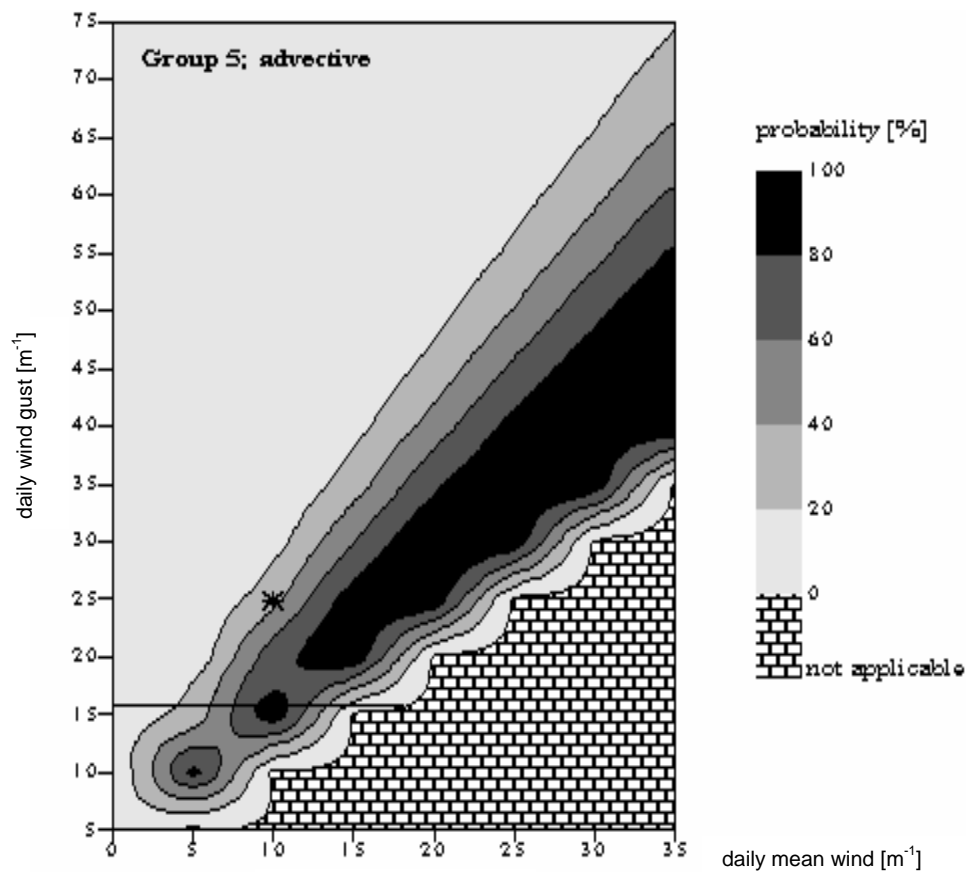


Figure 7: Isolines of the occurrence probability of a daily wind gust speed knowing the daily mean wind speed. Figures 1 to 6 represent the groups 1 to 6 valid for days with advective situations. $U_g = 16 \text{ m s}^{-1}$ denotes a critical gust value over complex terrain for forest damages. The asterisk correspond to the gust probability values during storms, noted in Table 3, with $U = 10 \text{ m s}^{-1}$ and $U_g \geq 25 \text{ m s}^{-1}$ for groups 1 to 5 and $U = 2 \text{ m s}^{-1}$ and $U_g \geq 7 \text{ m s}^{-1}$ for group 6.

6. Conclusion

This paper presents a manner of determining the probability of occurrence of daily wind gusts as a function of daily mean wind speed according to three types of synoptic weather situations within groups of Swiss climatological stations. These results demonstrate that the gust factors between maximum and mean wind speeds, which are measured over the complex terrain of Switzerland follow the lognormal distribution of Weggel (1999) applicable to the United States. The achievement to summarise several single climatological stations into groups for the convective, the advective and the mixed weather types of Schüepp separately, represents a convenient approach to compute the occurrence probability of wind gusts over complex terrain according to forecasts of mean wind. The skill of the method is tested and is found to be satisfactory in quantitative terms. All the computations are based on the period ranging from 1990 to 1999 and the observations of the two severe winter storms “Vivian” (Feb 24-28, 1990) and “Lothar” (Dec 25-29, 1999) are included in the data. Although only 10 years of data has been used, we succeeded in a relatively smooth graphical representation (Fig. 7-1 to 7-6) to predict the occurrence probability of a daily wind gust speed knowing the daily mean wind in relation to prevailing synoptic weather types for groups of climatological stations distributed in Switzerland. With the data of the two storm events included, the validity of these graphical results is particularly high for the decade 1990 to 1999.

With the current warming trend of global climate, it is uncertain however, if these results are valid for future predictions. If the signal of a northward shift of the westerly wind tracks (Schuesser et al., 1997; IPCC 1996, chap. 6) proves to be true then the probability of occurrence of wind gusts may also undergo important changes. Predictions of this kind are becoming more accurate when simulated with Regional Circulation Models (RCM). Goyette et al. (2001) present short-term results of storm simulations on a local scale (1km) where “Vivian” was successfully simulated. The method proposed in this study will

be applied to simulated data in the coming future to investigate the behaviour of the gusty nature of the wind following global climate warming.

Acknowledgements

This study is funded by the Swiss National Science Foundation, through Grant NR. 2100-050496.97

REFERENCES

see References – Section at the end of the work

8. SYNTHESIS

The general structure of this thesis comprises four major parts where different types of analyses are carried out:

A: A *climatological regionalisation* where a maximum number of climatological stations distributed all over Switzerland is aggregated into clusters. The information in order to form the clusters originates out of the daily variability of the Tmin or the Tmax station time series joined with station-related characteristics. (Chapter 3).

B: *Quantitative methods on Tmin and Tmax time series* which serve the purpose to analyse the trends on different time scales during the 20th century as well as the interannual and interdecadal variations.

A secular trend and the frequency analysis of Tmin and Tmax extremes providing a more accurate insight on Tmin and Tmax fluctuations over the 20th century. (Chapter 4 and Chapter 5).

C: A *frequency analysis of small scale synoptic weather types* and the evaluation of their probable *link to the NAO* allows to formulate explanatory hypotheses on the observations made in the previous parts. (Chapter 6).

D: A *test application of the climatological regionalisation method* is undertaken on wind gust data combined with a *probability calculation* for expected wind gust speed values over complex terrain. (Chapter 7).

The climatological regionalisation of Part A represents the actual basis of the work which together with Part B outline the essential issue of this study. The analyses undertaken in Part C are closely linked to the conclusions resulting out of Part A and B and aim to add further explanatory details to these conclusions.

The climatological regionalisation showed that the clustering pattern of climatological stations strongly depends upon the parameter (Tmin or Tmax in this case) to which the method is applied as well as upon the season during which it is performed. Comparing the clustering patterns established for Tmin/Tmax in each season separately, a certain similarity emerges between the patterns in winter and autumn just as between summer and spring. The regions based on Tmin reflect an image of the night-time temperature distribution in space which is strongly influenced by characteristics such as altitude and topographic features. The regions based on Tmax represent the spatial day-time

temperature distribution where next to the altitude the geographical location of a station is determining for the clustering pattern. Although the patterns were found to be specific to a climatological parameter and a season three main regions are regularly occurring regardless to the parameter or season the regionalisation is based upon. They represent the three most contrasting climatic areas in Switzerland and are identified as “low altitudes, north”, “high altitudes”, and “low altitudes, south”. A generally good agreement was detected between the results of the intermediate and the main regions. Hence it was found to be reasonable to limit the description of the results of all further analyses to the three main regions.

With the aim to work on qualitatively satisfying data sets with a maximal temporal extension an interannual mean time series, based on seasonal means was computed for each clusters. The regional mean time series are considered to be representative for each stations time series included in one cluster.

Computing secular trends on the 20th century on these newly established regional mean time series a warming trend becomes apparent which, however, does not manifest itself equally in Tmin and Tmax neither in all seasons nor in all regions. Generally the Tmin which represent night-time temperatures are subject to a stronger warming than the Tmax representing day-time temperatures. It should be noted although that these results are not always statistically significant. Analysing the time series on the decadal scale more details can be added to the temperature variations during the century. The warming observed in winter is mainly concentrating on the 1990s where it is especially strong in the region “high altitudes”. Comparing the period 1989-99 of the region “high altitudes” to other periods of the same length during the century results in a significant difference of this recent period to each of the others. This can be interpreted as a remarkable shift towards milder winter nights at high elevation sites during the 1990s. In summer and spring two increases become apparent. The first one occurs between about 1945 to 1955 and is mainly observed in Tmax of all regions. In Tmin it is limited to spring in the region “high altitudes”. The second warming takes place in a rather abrupt manner in the 1990s, where it is observable for Tmin and Tmax in all regions. The autumn temperatures present a rather contrasting picture compared to the other seasons. Despite the significant and strong secular warming trend observed in autumn temperatures, the long-term trend indicates decreasing tendencies during the 1990s in all regions for Tmin as well as for Tmax. This can be related to a warming in autumn temperatures during the 1980s, which however, is not extended into the 1990s.

The secular warming trends detected in Tmin and Tmax extremes provide a more accurate understanding of the observed warming process of Tmin and Tmax in the course of the 20th century. Generally the Tmin and Tmax warming can be linked to a positive trend in both, cold and warm extremes (min-/max- and min+/max+). However, no striking significant difference was found which would allow to clearly assign the observed Tmin or Tmax warming to a temperature increase in one specific temperature extreme. The frequency analysis of the extremes yielded some supporting conclusions for the 20th century temperature fluctuation. It was found that the Tmin and Tmax warming at the end of the century in the seasons winter, spring and summer is concurrent with an abrupt increase in the number of warm extremes and a simultaneous decrease in cold extremes during the 1990s. The observed mid-century spring and summer warming which is especially apparent in Tmax likewise finds an additional support in the frequency count of the extremes. In spring this is expressed by a higher frequency in Tmax warm extremes whereas in summer the number of both Tmax extremes shows a modification, the warm extremes increase and the cold extremes decrease. The frequency count also shows that in autumn rather cool temperatures with a high frequency of Tmin and Tmax cold extremes were predominant in the beginning of the century. This elevated number of cold extremes between about 1900 and 1925 combined with the lower frequency of Tmin and Tmax cold extremes and the higher frequency of warm extremes during the 1980s most probably leads to the strong secular warming in autumn Tmin and Tmax.

Possible causal mechanisms related to the resulting conclusions of 20th century regional temperature variations are likely to be found in large and small scale synoptic weather patterns. The closer inspection of the North Atlantic Oscillation Index (NAOI) provides supporting evidence for its close relation to the observed winter warming in the 1990s. With the evaluation of the frequency of typical alpine weather types it becomes apparent that especially in winter they need to be considered as a linking element between NAOI and the regional temperatures. The comparison of 11-year periods since 1945 indicates in the period 1989 to 1999 a change in the frequency pattern of the winter weather types. The advective high-pressure systems originating in the east show a strongly decreasing frequency in the last decade of the 20th century and at the same time the frequency of the convective high-pressure systems is increasing at a comparable rate. Both types provide a clear sky the first however, carries cold continental air masses whereas the latter type is considered as rather warm winter weather type influenced by the positive NAOI. Together with the western to southwestern advective weather type, which carries warm and humid

air masses and consequently yield a covered sky, the high-pressure convective type represent the largest share of winter weather types during 1989 to 99. The increase in high-pressure convective weather type is of a principal importance for the region “high altitudes” because it generates anomalously mild conditions in the Alps. This region is always situated above the persistent winter stratus layer, thus the days are warm and sunny and therefore especially mild. These findings are in agreement with the conclusions resulting out of the analysis of Tmin/Tmax extremes where in the region “high altitudes” the Tmin and Tmax warm extremes seem to increase at a higher rate than in the region “low altitudes, north”.

The causes of the 1945 to 1955 summer and spring warmth were most probably of a different nature. The frequency analysis of the summer weather types shows a striking difference between the number of convective weather types occurring in 1945-55 and in 1989-99. The period in the middle of the century is characterised by a comparable number of convective high and indifferent pressure types in contrast to the 1990s where the number of the indifferent pressure type is over three times larger than the number of the high-pressure type. This evolution points to an increase in the number of summer days with a cloud cover over the second half of the century. The warm autumn temperatures during the 1980s can likewise be linked to the weather types. Compared to other periods the period 1978-88 is characterised by the highest number of convective high-pressure weather types which generate mild conditions in autumn often referred to as Indian summer.

A final analysis was undertaken which serves the purpose to estimate wind gust speed probabilities in different regions of Switzerland knowing the mean wind speed and the type of synoptic circulation at a specific moment. The climatological regionalisation method, previously used with Tmin and Tmax data, is applied to wind gust data during days between 1990 to 1999 where either convective or advective or mixed weather types were prevailing. Within this period the data of two winter storms, namely “Vivian” in February 1990 and “Lothar” in December 1999 is included. Testing the skill of the method provides satisfactory results in quantitative terms thus the method is considered as a convenient approach to compute occurrence probabilities of wind gusts over complex terrain.

Merging these results can contribute to generate a basis of source information in order to evaluate the possible climatic influence on concurrent variations observed in the ecosystem such as glacier regression, permafrost occurrence, changes in the water

balance, plant migration, etc.. The results of the present study yield that the extraordinary Tmin and Tmax warming observed at the end of the 20th century is most emphasised in the region "high altitudes". Considered as marginal parameters within the mean temperature distribution Tmin and Tmax primarily affect the margins of the natural tolerance range of the ecosystem. Thus numerous far-reaching socio-economic consequences which are connected to variations in the ecosystem are a realistic scenario for Switzerland and especially for the Alps. It is very likely that within the close future the economic activities in the alpine areas are progressively subject to natural hazards, which correspond to an unusual financial burden for small mountain communities with a limited budget. This supports the hypothesis that a shift in a meteorological parameter can provoke a complex chain of reactions affecting the natural and the anthropogenic systems, especially in complex territories.

These conclusions clearly show the importance and the necessity of climatological studies on the regional scale. The results of this study can be considered as a highly detailed contribution to the description of Swiss 20th century Tmin and Tmax variations on different time scales.

REFERENCES

Ahrens C. D., 1994: *Meteorology today. An introduction to weather, climate, and the environment.* 5th ed. West Publishing Company, Minneapolis, St. Paul. 591pp.

Bader S., Baudraz G., Bergert M., Köhli V., Musa M., Schlegel T., Seiz G., 2000: Regional Climate Variability in Switzerland since 1964. Poster presentation at 3rd European Conference on Applied Climatology, Pisa, Italy, October 2000.

Baeriswyl P.-A., Rebetez M., Winistörfer A., Roten M., 1997: Répartition spatiale des modifications climatiques dans le domaine alpin. Final report NFP 31. Zurich: vdf, Hochsch.-Verl. an der ETH. 236 pp.

Baeriswyl P.-A. and Rebetez M., 1997: Regionalisation of precipitation in Switzerland by means of Principal Component Analysis. *Theor. Appl. Climatol.* 58, 31-41.

Bahrenberg G., Giese E., Nipper J., 1990: *Statistische Methoden in der Geographie 1*, Teubner Studienbücher. 232pp.

Bahrenberg G., Giese E., Nipper J., 1992: *Statistische Methoden in der Geographie 2*, Teubner Studienbücher. 412 pp.

Baltensperger U., Gäggeler H. W., Jost D. T., Lugauer M., Schwikowsko M., Weingartner E., Seibert P., 1997: Aerosol Climatology at the High-Alpine Site Jungfrauoch, Switzerland. *J. Geophys. Res.*, Vol 102, No 16, 19707-19715.

Bantle, H., 1989: *Programmdokumentation Klima-Datenbank am RZ-ETH Zürich*, Swiss Meteorological Institute, Zürich.

Bantle H., 2001: *On-line Benutzeranleitung Klima-Datenbank*. Swiss Meteorological Institute, Zürich.

Barry R. G., 1992: *Mountain Weather and Climate*, 2nd edn. Routledge, London. 392 pp.

Beniston M., 1994: Climate scenarios for mountain regions. In: Beniston, M. (Ed.): *Mountain Environments in Changing Climates*, pp. 136-151. Routledge Publishing Company, London and New York. 492 pp.

Beniston M., Rebetez M., Giorgi F., Marinucci R., 1994: An analysis of regional climate change in Switzerland. *Theor. Appl. Climatol.*, 49, 135-159.

Beniston M., and Rebetez, M., 1996: Regional behavior of minimum temperatures in Switzerland for the period 1979 - 1993. *Theor. Appl. Climatol.* , 53, 231 – 243.

Beniston, M., 1997: *From Turbulence to Climate*. Springer, Heidelberg and New York. 330 pp.

Beniston M. and Rebetez M., 1997: Extreme climatic events and variability. Conference on Global Climate Observing System (GCOS), Asheville, North Carolina, USA, June 1997.

- Beniston M., 1999: Der Sturm «Lothar» vom 26. Dezember 1999. In: Jahresbericht 1999 der kantonalen Gebäudeversicherung Freiburg: Freiburg. 72pp.
- Beniston, M., 2000: Environmental Change in Mountains and Uplands. Arnold/Hodder and Stoughton/Chapman and Hall Publishers, London, UK, and Oxford University Press, New York, USA. 172 pp.
- Berger A., 1992: Le climat de la terre. Un passé pour quel avenir ?. De Boeck University press, Bruxelles. 479 pp.
- Bergert M., Gigoud M., Kegel R., Seiz G., Köhli V., 1998: Operational Homogenization of Long Term Climate Data Series at SMI. Proceedings ECAC, October 1998, Vienna.
- Böhm R., Auer I., Schöner W., 2000: Temperature and Precipitation Variability in the Alps - The Gridded Time Series of Project ALPCLIM. Presentation at 3rd European Conference on Applied Climatology, Pisa Italy October 2000.
- Bradley R. S. and Jones P. D., 1995: Climate since A.D. 1500. Routledge Publishing Company, London and New York. 706pp.
- Bradley R. S., 2000: Past global changes and their significance for the future. Quaternary Science Reviews, 19, 391-402.
- Brunetti M., Buffoni L., Maugeri M., Nanni T., 2000a: Trends of Minimum and Maximum Daily Temperatures in Italy from 1865 to 1996. Theor. Appl. Climatol. , 66, 49 – 60.
- Brunetti M., Maugeri M., Nanni T., 2000: Variations of temperature and precipitation in Italy from 1966 to 1995. Theor. Appl. Climatol. , 65, 165 – 174.
- Brown B. G., Katz R. W., 1995: Regional analysis of temperature extremes : Spatial analog for climate change? Journal of Climate, 8, 108-118.
- Crowley T. J., 2000: Causes of climate change over the past 1000 years. Science, col 289, 270-276.
- Dai, A., Trenberth K. E. and Karl T. R., 1999: Effects of clouds, soil moisture, precipitation and water vapor on diurnal temperature range. Journal of Climate, 12, 2451-2473.
- De Gaetano A. T., 1996: Recent trends in maximum and minimum temperature threshold exceedences in the northeastern United States. Journal of Climate, 9, 1646-1660.
- Diaz H. F. and Bradley R. S., 1997: Temperature variations during the last century at high elevation sites. Climatic Change, 36, 253-279.
- Domonkos P., 1998: Statistical Characteristics of extreme temperature anomaly groups in Hungary. Theor. Appl. Climatol. , 59, 165 – 179.
- Domonkos P., 2001: Temporal accumulations of extreme daily mean temperature anomalies. Theor. Appl. Climatol. , 68, 17 – 32.
- Easterling D. R., Horton B., Jones P. D., Peterson T. C., Karl T. R., Parker D. E., Salinger M. J., Razuvayev V., Plummer N., Jamason P., Folland C. K., 1997: Maximum and Minimum trends for the globe. Science, vol 277, 364-367.

- Ehinger J, Hertig J-A, Alexandrou C, Berney M, Christinat M-O. 1990: Analyse de l'influence de la topographie sur les conditions d'exposition des bâtiments. Ecole Polytechnique Fédérale de Lausanne. Swiss National Science Foundation, Grant No: 20-5189.86. 203 pp.
- Folland C. K., 1996: Temperature anomaly percentiles. In : The Global Climate System Review. World Meteorological Organization, Dec 1993 - May 1996. WMO No 856.
- Folland C. K., Miller C., Bader D., Crowe M., Jones P., Plummer N., Richman M., Parker D. E., Rogers J., Scholefield P., 1999: Breakout group C: Temperature indices for climate extremes. In: Weather and Climate Extremes, changes, variations and a perspective from the insurance industry. Eds. Karl T. R., Nicholls N., Ghazi A., Kluwer Academic Publishers 1999.
- Frei Ch. and Schär Ch., 2000: Detection probability of trends in rare events: Theory and application to heavy precipitation in the Alpine Region. *Journal of Climate*, 14, 1568-1584.
- Frei Ch., Davies H. C., Gurtz J., Schär Ch., 2000: Climate dynamics and extreme precipitation and flood events in Central Europe. *Integrated Assessment* 1, 281-299.
- Gajic-Capka M. and Zaninovic K., 1997: Changes in temperature extremes and their possible causes at the SE boundary of the Alps. *Theor. Appl. Climatol.*, 57, 89-94.
- Giorgi, F., Hurrell, J., Marinucci, M., and Beniston, M., 1997: Height dependency of the North Atlantic Oscillation Index. *Observational and model studies. J. Clim.*, 10, 288 – 296.
- Gisler O., Baudenbacher M., Bosshard W., 1997: Homogenisierung schweizerischer klimatologischer Messreihen des 19. und 20. Jahrhunderts. Final report NFP 31. Zurich: vdf, Hochsch.-Verl. an der ETH. 118pp.
- Gleick, P. H., 1987: Methods for evaluating the regional hydrologic impacts of global climatic changes, *J. Hydrology*, 88, 97-116.
- Goossens Ch., 1986: Regionalization of the Mediterranean Climate. *Theor. Appl. Climatol.* 37, 74-83.
- Goyette S., Beniston M., Caya D., Laprise J. P. R., Jungo P., 2001: Numerical investigation of an extreme storm with the Canadian Regional Climate Model: The case study of windstorm VIVIAN, Switzerland, February 27, 1990. [in press: *Climate Dynamics*].
- Grabherr G., Gottfried M., Pauli H., 1994: Climate effects on mountain plants. *Nature* 369-448.
- Häckel H., 1990: *Meteorologie*. UTB Ulmer Verlag, Stuttgart. 402pp.
- Haeberli W., 1994: Accelerated glacier and permafrost changes in the Alps. In: Beniston, M. (Ed.): *Mountain Environments in Changing Climates*, pp. 91-105. Routledge Publishing Company, London and New York. 492 pp.
- Haeberli W. and Beniston M., 1998: Climate change and its impacts on glaciers and permafrost in the Alps, *Ambio*, 27, 4, 258-265.

Heimann D. and Sept V., 2000: Climate change estimates of summer temperature and precipitation in the alpine region. *Theor. Appl. Climatol.*, 66, 1-12.

Heino R., Brazdil R., Forland E., Tuomenvirta H., Alexandersson H., Beniston M., Pfister C., Rebetz., Rosenhag G., Rösner S., Wibig J., 1999 : Progress in the study of climatic extremes in northern and Central Europe. *Climatic Change*, 42, 151-181.

Hurrell, J. W., 1995: Decadal trends in the North Atlantic Oscillation regional temperatures and precipitation. *Science*, 269, 676 – 679.

Hurrell, J. W., and van Loon, H., 1997: Decadal variations in climate associated with the North Atlantic Oscillation. *Climatic Change*, 36, 301-326.

IPCC, 1996: *Climate Change 1995 - The science of climate change. Contribution of working group I to the second assessment report of the Intergovernmental Panel of Climate Change.* Eds. J. J. Houghton, L. G. Meiro Filho, B. A. Callander, N. Harris, A. Kattenberg and K. Maskell. Cambridge University Press. 572 pp.

IPCC, 1996a: *Climate Change 1995 – Impacts, Adaptations and Mitigations of Climate Change : Scientific-Technical Analyses.* Contribution of working group II to the second assessment report of the Intergovernmental Panel of Climate Change. Eds. R. T. Watson, M. C. Zinyowera, R. H. Moss and D. J. Dokken. Cambridge University Press. 878pp.

IPCC, 1998: *The regional impacts of climate change. An assessment of vulnerability. Special report of working group II.* Eds : Watson R. T., Zingowera M. C., Moss R. H., Dokken D. J.. New York, Cambridge University Press. pp. 517.

IPCC, 2001(TS): *The scientific basis: Technical Summary of the Working Group I Report.* Eds: Joos F., Ramirez-Rojas A., Stone J. M. R., Zillman J., New York, Cambridge University Press. pp. 63.

Jolliffe I. T., 1990: *Principal Component Analysis : A beginner's guide – I. Introduction and application.* *Weather*, 45, 375-382.

Jolliffe I. T., 1993: *Principal Component Analysis : A beginner's guide – II. Pitfalls, myths and extensions.* *Weather*, 48, 246-253.

Jones P. D. and Briffa K. R., 1992: *Global surface air temperature variations during the twentieth century : Part I, spatial, temporal, seasonal details.* *The Holocene*, 2, 2, 165-179.

Jones, P. D., New, M., Parker, D. E., Martin, S. and Rigor, I. G., 1999: *Surface air temperature and its changes over the past 150 years.* *Reviews of Geophysics*, 37, 173-199.

Jungo P., 1996: *Vergleiche zwischen Ozonkonzentrationen auf dem Jungfrauoch und aerologischen Ozon-Sondierungen bei Payerne auf der Höhe des Jungfrauochs, insbesondere während sommerlichen Smoglagen.* Department of Geography, University of Fribourg and Aerological Station Payerne: diploma thesis, 120pp.

Jungo P. and Beniston M., 2001: *Changes in the anomalies of extreme temperature anomalies in the 20th century at Swiss climatological stations located at different latitudes and altitudes.* *Theor. Appl. Climatol.*, 69, 1-12.

- Karl T. R., Jones P.D., Knight R.W., Kukla G., Plummer N., Razuvayev V., Gallo K.P., Lindsey J., Charlson R. J., Peterson T. C., 1993: Asymmetric trends of daily minimum and maximum temperature. *Bulletin of the American Meteorological Society*, 74, 1007-1023.
- Katz R. W., Brown B. G., 1992: Extreme events in a changing climate: Variability is more important than averages. *Climatic Change* 21, 289-302.
- Keller F., Kienast F., and Beniston M., 2000: Evidence of the response of vegetation to environmental change at high elevation sites in the Swiss Alps. *Regional Env. Change*, 2, 70-77.
- Klink K., Willmott C. J., 1989: Principal Components of the surface wind fields in the United States: A comparison of analyses based upon wind velocity, direction and speed. *International Journal of Climatology*, Vol 9, 293-308.
- Krayer W. R., and Marshall RD. 1992: Gust factor applied to hurricane winds. *Bull. Amer. Met. Soc.* 73: 613-617.
- Krenke, A.N., G.M. Nikolaeva, and A.B. Shmakin, 1991: The effects of natural and anthropogenic changes in heat and water budgets in the central Caucasus, USSR, *Mountain Res. Devel.*, 11, 173-182.
- Lamb H. H, 1995: *Climate history and the modern world*. 2nd edition, Routledge. 433 pp.
- Luterbacher J., Schmutz Ch., Gyalistras D., Xoplaki E., Wanner H., 1999 : Reconstruction of monthly NAO and EU indices back to AD 1675. *Geophysical Research Letters*, Vol 26, No 17, pp 2745-2748.
- Leavesley, G. H., 1994: Modeling the effects of climate change on water resources - A review, *Assessing the Impacts of Climate Change on Natural Resource Systems*, K. D. Frederick, and N. Rosenberg, (eds.), Kluwer Academic Publishers, Dordrecht, 179-208.
- Mann M. E., Bradley R. S., Hughes M. K. 1999: Northern Hemisphere Temperatures During the Past Millennium: Inferences, Uncertainties, and Limitations. *Geophysical Research Letters*, 26, 6, 759-762.
- Marinucci M. R., and Giorgi F., 1992: A 2 x CO₂ climate change scenario over Europe generated using a Limited Area Model nested in a General Circulation Model – Part I: present day simulation. *J. Geophys. Res.*, 97, 9 989 - 10009.
- Marinucci M. R., Giorgi F., Beniston M., Wild M., Tschuck P., and Bernasconi A., 1995: High resolution simulations of January and July climate over the Western Alpine region with a nested regional modeling system. *Theor. and Appl. Clim.*, 51, 119-138.
- Maugeri M., Nanni T., 1998: Surface air temperature variations in Italy: recent trends and an update to 1993. *Theor. and Appl. Clim.*, 61, 191 – 196.
- Meehl G. A., Lukas R., Kiladis G. N., Weickmann K. M., Matthews A. J., Wheeler M., 2001: A conceptual framework for time and space scale interactions in the climate system. *Climate Dynamics*, 17, 753-775.

- MeteoSwiss - Schweizerische Meteorologische Anstalt. 1985: Alpenwetterstatistik Witterungskalender, Beschreibung der einzelnen Parameter. Schweizerische Meteorologische Anstalt, Abteilung Forschung: Zürich. 43pp.
- Montmollin (de) A., 1993: Comparaisons de différentes méthodes de calcul de la température journalière dans leurs influences sur les longues séries d'observations. ETH Zurich: phd thesis.
- NFP 31, 1998: Klimaänderungen und Naturkatastrophen / Climate changes and natural disasters. Homepage URL: <http://www.cliris.ch/nfp31/> not existant anymore. Further information URL: <http://proclim.ch>
- Paeth H., Hense A., Glowienka-Hense R., Voss R., Cubasch U., 1999: The North Atlantic Oscillation as an indicator for greenhouse-gas induced regional climate change. *Climate Dynamics*, 15, 953-960.
- Parker D. E., Jones P. D., Folland C. K., Bevan A., 1994: Interdecadal changes of surface temperature since the late nineteenth century. *Journal of Geophysical Research*, Vol 99, No D7, pp 14373-14399.
- Palutikof J. P., Brabson B. B., Lister D. H., Adock S. T. 1999: A review of methods to calculate extreme wind speeds. *Meteorol. Appl.* 6: 119-132.
- Pfister Ch., 1999: *Wetternachhersage, 500 Jahre Klimavariationen und Naturkatastrophen*. Bern: Paul Haupt Verlag, 304 pp.
- Price M. F., 1994: Should mountain communities be concerned about climate change?. In: Beniston, M. (Ed.): *Mountain Environments in Changing Climates*, pp. 431-449. Routledge Publishing Company, London and New York. 492 pp.
- Ragwitz M, and Kantz H., 2000: Detecting non-linear structure and predicting turbulent gusts in surface wind velocities. *Europhys. Let.* 51: 595-601.
- Rebetez M. and Beniston M., 1998a: Changes in temperature variability in relation to shifts in mean temperatures in the Swiss Alpine region this century. In: Beniston M. and Innes J. L. (Eds): *The impacts of Climate Variability on Forests*, pp.49-58. Berlin, Heidelberg: Springer-Verlag 329 pp.
- Rebetez M. and Beniston M., 1998: Changes in sunshine duration are correlated with changes in daily temperature range this century: An analysis of Swiss climatological data. *Geophysical Research Letters*, 25, 19, 3611-3613.
- Rebetez M., 1999: Twentieth century trends in droughts in southern Switzerland. *Geophysical Research letters*, 26, 6, 755-758.
- Rebetez M., 2001: Changes in daily and nightly day-to-day temperature variability during the twentieth century for two stations in Switzerland. *Theor. Appl. Climatol.* 69, 13-21.
- Rogers, J. C., 1997: North Atlantic storm track variability and its association to the North Atlantic Oscillation and climate variability of Northern Europe. *J. Climate*, 10, 1635-1647.
- Schär Ch., Davies T. D., Frei Ch., Wanner H., Widmann M., Wild M., Davies H. C., 1998: *Current Alpine Climate in : Views from the Alps* eds: Cebon P., Dahinden U., Davies H. C., Imboden D., Jaeger C. MIT press Massachusetts. 515pp.

Schiesser HH, Waldvogel A, Schmid W, Willemse S. 1997a: *Klimatologie der Stürme und Sturmsysteme anhand von Radar- und Schadendaten*. Swiss National Science Foundation, NFP 31. vdf – Hochschulverlag AG: ETH Zürich. 132pp.

Schiesser HH, Pfister Ch, Bader J. 1997: *Winter Storms in Switzerland North of the Alps 1864/1865 – 1993/1994*. *Theor. Appl. Climatol.* 58: 1-19.

Schmidtke H, and Scherrer H-U. 1997: *Sturmschäden im Wald*. Swiss National Science Foundation, NFP 31. vdf – Hochschulverlag AG: ETH Zürich. 38pp.

Schönwiese Ch.-D., Rapp J., Fuchs T., Denhard M., Frankfurt M., 1994: *Observed climate trends in Europe 1891 – 1990*. *Meteorol. Zeitschrift, N.F.* 3, 22-28.

Schüepp, M., 1978: *Klimatologie der Schweiz, Band III in: Beiheft zu den Annalen der Schweizerischen Meteorologischen Anstalt: Zürich*. 89pp.

Schüepp M., Schiesser H. H., Huntrieser H., Scherrer H.U., Schmidtke H., 1994: *The Winterstorm “Vivian” of 27 February 1990: About the Meteorological Development, Wind Force and Damage Situation in the Forests of Switzerland*. *Theor. Appl. Climatol.* 49: 183-200.

Serreze, M. C., Carse, F., Barry, R. G., and Rogers, J. C., 1997: *Icelandic low cyclone activity: Climatological features, linkages with the North Atlantic Oscillation, and relationships with recent changes in the Northern Hemisphere circulation*. *J. Climate*, 10, 453-464.

SPSS 1 manual, 1999: *Base 10.0 User’s Guide*. SPSS Inc. Chicago USA. 537pp.

SPSS 2 manual, 1999: *Base 10.0, Applications Guide*. SPSS Inc. Chicago USA. 426pp.

Stefanicki G., Talkner P., and R. O. Weber, 1998: *Frequency Changes of Weather Types in the Alpine Region since 1945*. *Theor. Appl. Climatol.* 60, 47-61.

Stott P. Q., Tett S. F. B., Jones G. S., Allen M. R., Ingram W. J., Mitchell J. F. B., 2001: *Attribution of twentieth century temperature change to natural and anthropogenic causes*. *Climate Dynamics*, 17, 1-21.

Villalba R., Boninsegna J. A., Veblen T. T., Schmelter A., Rubulis S., 1997: *Recent Trends in Tree-Ring Records From high elevation sites in the Andes of northern Patagonia*. *Climatic Change*, 36, 425-454.

Von Storch H., and Zwiers F. W., 1998: *Statistical Analysis in Climate Research*. Cambridge University press: Cambridge. 484pp.

Wanner H., Rickli R., Salvisberg E., Schmutz C., Schüepp M., 1997: *Global climate change and variability and its influence on alpine climate – concepts and observations*. *Theor. Appl. Climatol.* 58, 221-243.

Wanner H., Gyalistras D., Luterbacher J., Rickli R., Salvisberg E., Schmutz Ch., 2000: *Klimawandel in der Schweiz. Final report NFP 31*. Zurich: vdf, Hochsch.-Verl. an der ETH. 283 pp.

- Weber R.O., Talkner P., Stefanicki G., 1994 : Asymmetric diurnal temperature change in the Alpine region. *Geophysical Research Letters*, 21, 8, 673-676.
- Weber R.O., Talkner P., Auer I., Böhm R., Gajic-Capka M., Zaninovic K., Bradzil R., Fasko P., 1997: 20th century changes of temperatures in the mountain regions of Central Europe. *Climatic Change* 36, 327-344.
- Walshaw D., 2000: A model for extreme wind gusts. *Appl. Statist.* 49: 499-508.
- Weggel J. R., 1999: Maximum daily wind gusts related to mean daily wind speed. *Journal of Structural Engineering*. April: 465-468.
- WMO, 1999: WMO statement on the status of the global climate in 1998. Geneva, WMO-Nr. 896. 11 pp.
- Zheng X., Basher R. E. Thompson C.S., 1997: Trend Detection in Regional-Mean Temperature Series : Maximum, Minimum, Mean, Diurnal Range, and SST. *Journal of Climate*, 10, 317-325.
- Zwiers F. W., and Kharin V.V., 1998: Changes in the extremes of the climate simulated by the CCC GCM2 under CO₂ doubling. *J. Climate*. 11: 2200-2222.

ACKNOWLEDGEMENTS

The financial support by the Swiss National Science Foundation is gratefully acknowledged. This funding is linked to the contract 20-56732.99.

I want to thank Prof. Martin Beniston, director of this thesis, who supported as PhD Student and who's deliberate reviews of my manuscripts helped me to improve my work.

I want to express special thanks to Prof. Claude Collet, Dr. Martine Rebetez and Dr. Stéphane Goyette. The opportunity to regularly discuss my ideas and results with them and their constructive criticism were extremely valuable to me. I am also thankful to Prof. Claude Collet for accepting the task as a co-examiner.

I would like to express my gratitude to Dr. Christoph Frei for his readiness to accept the task as a co-examiner as well as for the methodical reviews of my manuscripts and the constructive criticism, which was very beneficial to my work.

I am grateful to Prof. Heinz Wanner for reading and commenting my manuscript and for his readiness to accept the task as a co-examiner.

For the evaluation of the station data quality I needed insight in the meta data archives of the Swiss Meteorological Institute thus I would like to express my gratitude to Mr Ruedy Wyss.

I want to thank the Swiss Meteorological Institute for granting me the access to the data on which the analyses of this study are based.

I am especially grateful to Franziska Keller, Anton Crottet and Sabine Baeriswyl for reviewing my manuscripts, all the helpful comments and the moral support.

Finally I thank Marie and Marcel Jungo, Barbara Schoepfer, Daria Ackermann, Sara Buchs and Marlyse Rauber who supported me in many ways during my dissertation.

APPENDIX A

The station history (meta data) of 132 climatological stations distributed throughout Switzerland has been checked. The list represents the notes taken by station controllers with different levels of precision and a partially and short description of the stations position in the terrain. Focusing mainly on the minimum and maximum temperature the list is incomplete for other parameters. If these two parameters have not been recorded in the database since the operation start of the climatological station, the beginning of the recording is specified.

The first column indicates the year and the date (dd.mm) whenever the station controller has taken a note, in the second column the stations location (km coordinates, altitude) is specified and in the third column figure in brackets, the notes the station controllers have taken.

Aarau

1863 (01.10.)	645 850 / 249 180, 389m	(station start in city centre)
1902 (01.10.)	645 740 / 248 750, 407m	(open situation in residential area)
1931		(start of minimum and maximum temperature observations)
1944 (01.07.)	645 700 / 248 750, 408m	(open situation in residential area)
1970 (13.07.)	645 850 / 246 170, 409m	(new instrumentation)
1985 (28.02.)	station stop	

⇒ Plateau. Open country, densely populated.

Adelboden

1966	609 400 / 148 975, 1320m	(village, SW slope (12°))
1983 (01.12.)	transformation into ANETZ station	

⇒ Alps. Narrow valley, closed to the SW, mean population density.

Aigle

1981 (01.01.)	560 120 / 130 630, 381m;	ANETZ station
---------------	--------------------------	---------------

⇒ Alps. Large and open valley SE to NW, densely populated.

Airolo

1873 (23.04.)	689 780 / 153 590, 1141m	(railway station)
1935 (30.12.)	690 400 / 153 690, 1116m	(outside of village)
1952		(start of minimum temperature observations)
1969	688 930 / 153 450, 1139m	(west of railway station)
1970		(start of maximum temperature observations)
1980 (31.12.)	transformation into precipitation station	

Altdorf

1901		
1909		(start of minimum and maximum temperature observations)
1920	691 570 / 190 300, 453m	(rain captor is moved to east because of trees in proximity)
1933 (27.08.)		(painting of hut)
1955 (01.01.)	691 000 / 191 750, 449m	(station is moved 30m more until 30.09. 1958)
1955 (13.10.)		(planting of a hedge to capture precipitation better)
1978 (01.02.)	690 960 / 191 700, 449m;	transformation into ANETZ station
⇒	Alps. Large and open valley SSE to NNW, lake in the north, densely populated.	

Altstätten

1863 (01.12.)	758 690 / 249 780, 477m	(school building)
1905 (26.10.)	259 100 / 249 650, 449m	(residential area)
1927 (13.07.)	758 800 / 249 900, 427m	(satisfactory area, all instruments are kept together)
1945 (26.03.)	758 820 / 250 010, 467m	(similar situation)
1966 (23.09.)		(new station observer)
1971 (01.04.)		(new station observer, start of minimum and maximum temperature observations)
1970 (25.10.)	758 700 / 250 130, 473m	
1973 (28.02.)		(engl. hut moved into neighbouring garden, less satisfactory area)
1978 (08.11.)		(destruction of instruments, new instruments)
1996 (31.12.)	transformation into precipitation station	

Alvaneu

1972 (22.08.)	768 790 / 172 040, 1176m	(village, exposed terrace on slope)
1981 (20.10.)		(new station observer)
1981 (18.12.)		(new station observer, satisfactory)
1996 (31.12.)	transformation into precipitation station	
⇒	Alps. Narrow valley E to W, village is situated on the south slope, mean population density.	

Andermatt

1963 (01.12.)	688 500 / 165 340, 1443m	(presbytery)
1971		(start of minimum temperature observations)
1972 (04.06.)		(station moved to neighbour house)
1973 (07.05.)		(stations moved back to presbytery, instruments in satisfactory condition)
1970 (16.09.)		(installation of a minimum thermometer, several station observers alternate in turn)
1993		(start of maximum temperature observations)
⇒	Alps. Narrow valley, opening to N, mean population density.	

Arosa

1889	770 550 / 183 150, 1835m	
1900	770 500 / 183 020, 1810m	
1901 (01.07)	770 300 / 183 120, 1854m	(hotel in village, several changes of station observers)
1929 (06. –08.)		(data unsatisfactory)
1930 (01.04.)	770 470 / 183 160, 1864m	(steady observer)
1937 (01.01.)		(change from metal into engl. hut)
1944 (04.05.)		(check in Arosa)
1953 (01.12.)		(new station observer)
1954 (04.05.)	770 800 / 183 450, 1818m	(Sanatorium)
1968		(rain captor moved, sheltered by pine trees)
1973 (01.02.)	770 730 / 183 280, 1846m	(station partially moved, not the rain captor)
1987 (15.04.)		(snow measured on different place, former place is shaded)
1996 (01.12.)	770 730 / 183 320, 1840m	

⇒ Alps. Narrow valley SE to NE, strongly wooded. Village is situated on glacier terrace, with two small lakes, mean population density.

Autumn maximum temperatures are too high until 1960.

Bad Ragaz

1870 (01.06.)	757 140 / 207 600, 517m	(sheltered area)
1938 (27.08.)	757 000 / 207 700, 517m	(sheltered area)
1956 (15.10.)	757 140 / 207 800, 510m	(sheltered area)
1974 (22.03.)	757 240 / 207 870, 510m	(sheltered area)
1978 (29.08.)		(instruments stolen)
1980 (01.01.)	756 920 / 209 400, 498m	
1993 (26.04.)	756 900 / 209 370, 496m	(fruit tree next to station)

Balmberg

1973 (09.10.)	607 750 / 234 980, 1075m	(farm house)
1973 (26.10.)		(formation of bubbles in minimum temperature thermometer, else satisfactory data)
1981 (30.03.) – 1981 (06.04.)		(automatic registration of data, station observer moved away)
1981 (06.04.)		(new station observer)
1990		(medially satisfactory data, often interpolated using the stations Chasseral or Rüneberg)
1995 (31.12.)	station stop	

⇒ Jura. Ridge WNW to ESE. Station situated on south slope behind the ridge.

Basel – Binningen

1901 (01.01.)	610 691 / 267 800, 258m
1929 (01.01.)	610 850 / 265 620, 316m
1978 (01.01.)	transformation into ANETZ station

⇒ Plateau. Open, slightly hilly terrain, river in proximity, densely populated. Area on terrain with minor slope of 2°.

Beatenberg

1863 (01.12.)	626 950 / 171 675, 1148m	(presbytery)
1885 – 1954		(several changes in station observer)
1955 (19.12.)	626 000 / 171 300, 1196m	(new station observer, station more to the W)
1957 (03.12.)	626 350 / 172 080, 1183m	(new station observer)
1961 (15.04.)	627 630 / 172 220, 1180m	(new station observer (unsatisfactory), residential area)
1962 (01.04.)		(new station observer, unsatisfactory)
1969 (14.07)	627 640 / 172 180, 1170m	(new station observer, start of minimum and maximum temperature observations)
1980	station stop	

Bellinzona

1906 (15.10.)	722 600 / 117 250, 228m	
1908 (01.10.)		(minimum thermometer about 3° to low)
1956 (01.01.)		(new station observer)
1962 (18.09.)		(new station observer, satisfactory observations)
1964		(start of minimum temperature observations)
1980 (31.12.)	transformation into precipitation station	

Bernina Hospiz

1915 (17.07.)	798 450 / 142 970, 2256m	(Bernina railway station, several station observers)
1972		(start of minimum and maximum temperature observations)
1975 /76		(unsatisfactory observations)
1990 (27.06.)		(engl. hut in bad shape since 1988)
1993 (22.11.)		(malfunctioning of minimum thermometer)
⇒	Alps. High alpine pass station.	

Bern – Liebfeld

1901 (01.01.)	600 000 / 200 000, 560m	
1958 (24.09.)	599 175 / 200 150, 556m	
1977 (19.12.)	598 610 / 197 470, 565m	
1978 (01.01.)	transformation into ANETZ station	
⇒	Plateau. Open area on slight slope, densely populated.	
	<i>Summer minimum temperatures show a brake in the beginning of 1978. This can probably be related to the change of the site end of 1977 and/or to the transformation of the station into an ANETZ station in the beginning of 1978.</i>	

Bever

1901 (01.06.)	788 080 / 158 800, 1713m	(school)
1915 (15.09.)		(new thermometer)
1919 (09.06.)	788 100 / 158 770, 1710m	(village, new station observer)
1923 (01.07.)	788 020 / 158 700, 1711m	(village centre, not optimal area)
1924 (15.07.)	787 700 / 158 640, 1714m	(end of the village, better area)
1934 (01.09.)	787 960 / 158 660, 1713m	(village, new station observer)

1945 (28.12.) 787 840 / 158 320, 1710m (Räthische Bahn – railway, new station observer)
 1951 (22.09.) (temperature reading too high at times)
 1968 (14.10.) (revision of clockwork)
 1983 station stop

Biel

1917 585 065 / 221 150, 485m
 1920 585 455 / 220 790, 434m
 1931 585 285 / 219 895, 433m (city gardening school)
 1953 (01.01.) 585 665 / 220 565, 435m (city climate with high maximum temperatures)
 1959 (start of minimum and maximum temperature observations)
 1960 (repeatedly wrong reading of temperature extremes)
 1961 (29.04.) (sawing of a lawn for better results of maximum temperature)
 1982 (31.01.) 586 450 / 219 400, 432m
 1988 (unsatisfactory observations)
 1989 (01.02.) 586 260 / 218 840, 433m (new instruments)

Bivio

1951 (24.09.) 769 800 / 148 750, 1768m (outside village)
 1951 (28.12.) 769 750 / 148 750, 1774m (new station observer, area close to small stream)
 1966 (start of minimum temperature observations)
 1953 (04.01.) 769 800 / 148 850, 1770m
 1981 (31.12.) transformation into precipitation station

Bochuz

1938 (01.01.) 532 100 / 176 240, 437m
 1964 (start of minimum and maximum temperature observations)
 1966 (25.03.) (station observer has problems reading extreme temperatures)
 1967 (09.05.) 532 060 / 176 300, 437m (moved 100m further north)
 1968 (08.10.) (unsatisfactory data quality)
 1969 (30.04.) (new station observer (several))
 1970 (06.08.) (unsatisfactory station)
 1970 (01.08.) (new station observer (better))
 1979 (30.09.) (new station observer)
 1979 (26.10.) 532 150 / 176 250, 437m (same area)
 1984 (01.08.) (new station observer)
 1990 (16.01.) transformation into precipitation station

Bosco Gurin

1930 (21.07.) 681 100 / 129 950, 1486m (farm)
 1944 (28.11.) 681 180 / 130 000, 1505m (new station observer, village)
 1952 (15.05.) (new station observer)

1956 (01.09.) (new station observer – has problems reading the thermometer)
 1970 (13.10.) (minimum thermometer cannot be fixed and reset correctly)
 1971 (start of minimum temperature observations)
 1976 (start of maximum temperature observations)
 1978 (01.07.) (new station observer)
 1979 (01.10.) (air bubbles in thermometer)
 1981 (01.07.) (thermometer unusable)
 1995 (31.12.) transformation into precipitation station
 ⇒ Alps. Narrow valley open to W into different (Maggia) valley, sparsely populated

Broc

1969 (15.01.) 574 750 / 162 100, 688m (power station)
 1969 (11.03.) (mistakes within extreme temperatures)
 1978 (01.07.) (interpolation of maximum temperatures)
 1995 (31.12.) transformation into precipitation station

Buffalora

1917 (01.01.) 816 450 / 170 250, 1968m
 1920 (01.06.) (new station observer)
 1940 (07.11) (new station observer)
 1944 (15.12.) (new station observer)
 1976 (12.05. - 07.07.) (new installation of station)
 1983 (31.05.) (instruments wrongly installed)
 1987 (08.07.) (change of minimum thermometer, wrong measurements)
 1988 (19.01.) (new station observer, minimum and maximum temperatures are missing in 1988)
 1988 (26.02.) (air bubbles in thermometer)
 1988 (15.04.) (no station observer until 01.01.1989)
 1990 (01.04.) (medium quality of observations, often mistakes in minimum and maximum temperatures)
 1992 (01.06.) (new station observer - has problems to read maximum temperature until 1993)
 ⇒ Alps. Narrow valley from SE to NW, sparsely populated. Area NE of Ofen pass, next to road

Chables

1963 (10.03.) 551 850 / 186 400, 565m (open area)
 1965 (unsatisfactory data quality, start of minimum and maximum temperature observations)
 1970 (new station observer, data usable from 1971, extreme temperatures only from 1972 on)
 1980 (31.12.) station stop

Changins

1965 (01.01.) 507 180 / 139 220, 435m
 1978 (01.01.) 507 280 / 139 170, 430m; transformation into ANETZ station
 ⇒ Plateau. Close to Lake Léman, open slightly hilly area (2°), densely populated.

Chasseral

1980 (01.09.) 571 290 / 220 320, 1599m; ANETZ station
 ⇒ Jura. Summit station.

Château d'Oex

1879 576 650 / 147 200, 966m
 1887 576 820 / 147 100, 968m
 1907 (01.01.) 576 260 / 146 960, 1021m
 1909 (11.07.) 576 150 / 147 220, 1010m (new station observer)
 1911 (12.07.) 576 390 / 147 490, 1021m (new station observer, area next to river)
 1923 (30.06.) 576 150 / 147 250, 1000m (new station observer, area next to railway station)
 1925 (hut found on floor)
 1931 (start of minimum temperature observations)
 1936 (12.07.) 576 390 / 147 490, 1021m (new station observer, same area as 1911)
 1936 (13.08.) (thermometer adjustment of -0.1°C)
 1937 (start of maximum temperature observations)
 1952 (08.05.) 576 430 / 147 290, 994m (new station observer, area in village)
 1954 (27.08.) (inspection, probably repeated interpolation of readings)
 1969 (22.04.) 576 970 / 147 280, 985m (new station observer, area in Les Bossons)
 1979 (04.07.) 575 700 / 146 660, 957m (new station observer, different set up of rain captor, area in La Frasse)
 1986 577 200 / 147 310, 985m
 ⇒ Prealps (northern alpine rim). Valley from E to W. Area on slope, station installed next to road E of the village, mean population density.

Chaumont

1876 (01.11.) 563 840 / 208 840, 1128m (school, close to summit)
 1879 (01.11.) (new station observer)
 1893 (11.10.) (new station observer)
 1895 (11.11.) (new station observer)
 1906 (01.04.) (new station observer)
 1927 (01.10.) (new station observer)
 1933 (13.10.) 565 040 / 211 220, 1141m (new station observer, open area)
 1963 (29.07.) 565 030 / 211 180, 1141m (moved 60m to the W)
 1964 (start of minimum and maximum temperature observations)
 1982 (11.06.) 565 750 / 211 240, 1073m (new station observer)
 ⇒ Jura. Station on SE slope under ridge. Open country towards rim, wooded towards valley.

Chur

1863	759 120 / 190 680, 590m	(hospital)
1887	759 770 / 190 690, 610m	(Romansch Museum)
1929		(rain captor to close to building, no possibility to change)
1940	759 975 / 190 750, 633m	(school)
1953		(rain captor is moved on top of the building, too much wind)
1956	759 030 / 190 550, 585m	(parallel observations)
1958		(start of minimum and maximum temperature observations)
1962		(installation of Hellmann pluviograph at the height of 170cm)
1978	758 720 / 190 550, 582m	(ASTA building)
1978 (01.12.)	759 460 / 193 170, 555m;	transformation into ANETZ station
⇒ Alps. Large valley, city situated on open river delta of Plessur joining the Rhein at this point. The station is situated in the outskirts between the railway in the E and the road and Rhein in the W. Mean population density.		

Cimetta

1982 (01.01.)	704 370 / 117 515, 1672m	
⇒ Southern alpine rim. Summit station.		

Corvatsch

1978 (01.12.)	783 160 / 143 525, 3315m;	ANETZ station
⇒ Alps. High alpine summit station.		

Davos

1901 (01.01.)	781 900 / 185 700, 1567m	(village)
1962 (01.01.)	781 460 / 185 280, 1580m	
1976 (01.12.)	783 580 / 187 480, 1590m	
1978 (01.01.)	transformation into ANETZ station	
⇒ Alps. Valley, opening up to SW, small lake to NNE, area on slope. Station was moved from village with winter cold air lake to SE slope situated above the winter cold air lake. Mean population density.		

Delemont

1892 (01.08.)	592 760 / 245 740, 410m	
1921 (13.07.)		(new station observer)
1940 (01.03.)		(new station observer)
1958 (01.01.)	592 560 / 245 570, 417m	(new station observer)
1961		(start of minimum and maximum temperature observations)
1967 (29.03.)	593 380 / 245 220, 416m	(new station observer)
1981		(area not satisfactory, too many trees)
1986 (16.05.)		(temperatures too high)

Disentis

1961

1979 (01.07.) 708 200 / 173 800, 1190m; ANETZ station

⇒ Alps. Village situated on glacier terrace in SW to NE valley °), sparsely populated.
Area on SW slope (26°).

Ebnat-Kappel

1879 (01.08.) 727 540 / 235 930, 646m (school)

1882 (01.08.) (new station observer)

1885 (01.12.) (new station observer)

1894 (04.11.) (replacement of thermometer case)

1923 (16.02.) (new station observer)

1954 (03.05.) (for morning temperatures unsatisfactory placement of hut, E-wall.)

1962 (21.09.) (new station observer, better placement of thermometer, NW-wall)

1971 (start of minimum temperature observations)

1975 (01.05.) 726 880 / 236 410, 629m (new station observer, area between railway and river, start of maximum temperature observations)

1993 (26.03.) (generally very quality of observations)

Einsiedeln

1863 (01.10.) 699 750 / 220 350, 910m (several station observers until 1900)

1931 (start of minimum temperature observations)

1935 (new dam lake E of village - Sihlsee)

1969 (start of maximum temperature observations)

1992 (10.09.) 699 790 / 220 375, 910m (thermometer about 5° off)

⇒ Prealps. Area situated in monastery, mean population density.

Elm

1918 (05.03.) 732 090 / 198 260, 962m (railway station)

1936 (09.11.) (new station observer)

1948 (27.02.) 932 050 / 198 225, 965m (other side of the road)

1968 (10.07.) (thermometer case in direct sunlight, observer has major problems with reading)

1972 (01.01.) 732 080 / 197 950, 972m (new station observer, area 250m to S, start of minimum and maximum temperature observations, since 1974 area surrounded by houses)

1987 (15.06.) 732 400 / 198 500, 965m (new station observer, area outside village)

⇒ Prealps. Large valley knee, direction changes from SW to NE into S to N. Area between river and road, mean population density.

Engelberg

1931

1970 (start of minimum and maximum temperature observations)

1982 (01.11.) 674 150 / 186 060, 1035m; transformation into ANETZ station

⇒ Alps. Village situated at end of SE to NW valley, which changes to narrow gorge leading from S to N. Area on SW slope (14°) in monastery; sparsely populated.

Ennetbaden

1962 (01.09.) 665 520 / 259 340, 420m
 1964 (start of minimum and maximum temperature observations)
 1980 (31.12.) station stop

Fahy

1981 (01.01.) 562 460 / 252 650, 596m; ANETZ station
 ⇒ Jura. Area on NW slope, village is situated in SE. Strongly wooded country.

Frauenfeld

1918 (28.04.) 710 250 / 268 550, 433m (residential area)
 1959 (18.03.) 709 530 / 268 250, 409m (new station observer, rooftop of power station, maximum temperature not readable, thermometer is in direct sunlight after 13:30h)
 1964 (01.04.) 708 240 / 268 270, 403m (new station observer, on sugar factory, start of minimum and maximum temperature observations)
 1964 (23.04.) (observations unsatisfactory)
 1980 (31.12.) transformation into precipitation station

Fribourg

1863 578 750 / 183 950 (approx.)
 1882 580 000 / 183 240 (approx.)
 1899. 578 500 / 182 500, 650m (approx.)
 1910. 578 500 / 182 500, 677m (approx., moved to second floor)
 1964 (01.01.) 576 850 / 183 300
 1964 (02.03.) 579 640 / 182 890, 696m
 1965 (start of minimum and maximum temperature observations)
 1970 (01.09.) (temporary observation stop)
 1971 (15.02.) 575 280 / 179 880, 634m (change of instruments, area new in Grange-Neuve)

Grand St. Bernard

1817 579 200 / 079 720, 2472m
 1883 (hourly temperature readings until 1901)
 1901 (parallel readings all year long)
 1917 (rain captor moved, water of roof run partially into it)
 1937 (rain captor moved, higher up)
 1960 (start of minimum temperature observations)
 1965 (start of maximum temperature observations)
 1981 (01.11.) 579 200 / 079 720, 2472m; transformation into ANETZ station.
 (rain captor at unsatisfactory position, not possible to move because of strong winds,

snow and rain can partially run from roof into captor)

⇒ Alps. High alpine pass station.

Genève-Cointrin

1901 station start

1962

(start of minimum and maximum temperature observations)

1979 498 580 / 122 320, 420m; transformation into ANETZ station

⇒ Plateau (area of Lake Léman). Open country, densely populated.

Glarus

1975 station start

1980 723 750 / 210 580, 515m; transformation into ANETZ station

⇒ Alps. Large valley open to N. Area on slope (12°), mean population density.

Göschenen

1875 (10.07.) 688 020 / 168 930, 1106m (railway station)

1959 (01.10.) 687 930 / 169 020, 1127m (data not satisfactory)

1960 (start of minimum and maximum temperature observations)

1968 (01.10.) 687 730 / 169 030, 111m

1983 (29.09.) (important environmental influences)

1983 (31.12.) transformation into precipitation station

1987 (12.11.) 687 475 / 169 090, 1100m (on rim of strongly dropping of N-slope, exposed)

Grächen

1863 (01.12.) 630 850 / 116 050, 1617m (several observers, church)

1967 (20.07.) 630 825 / 116 030, 1617m (new installation on presbytery yard, start of minimum and maximum temperature observations))

1967 (01.09.) (new station observer, satisfactory data)

1985 (15.-19.12.) (minimum thermometer broken)

1985 (26.12.) – 1986 (11.01.) (minimum thermometer broken)

⇒ Alps. Village situated on glacier terrace of NW slope of narrow valley. Forest above, sparsely populated.

Grande Dixence

1955 597 260 / 103 580, 2246m (on dam wall)

1964 (17.10.) 597 272 / 103 546, 2467m (start of minimum and maximum temperature observations)

1985 (30.09.) station stop

Grimsel Hospiz

- 1964 668 580 / 158 210, 1980m
 1971 (start of minimum and maximum temperature observations)
 ⇒ Alps. Station N of Grimsel Lake on a hill, dam wall in NE of hill Glacier to W, Grimsel Pass (approx. 300m higher than station) to S.

Grindelwald

- 1915 (04.06.) 645 560 / 163 840, 1034m (Post office, thermometer in direct sunlight at noon)
 1915 (01.12.) (new station observer)
 1916 (25.08.) (thermometer moved to N, direct sunlight from 16h on)
 1919 (01.06.) 645 340 / 163 750, 1005m (railway station)
 1952 (23.08.) 646 460 / 163 830 (strongly inclined slope, unsatisfactory area)
 1966 (start of minimum and maximum temperature observations)
 1990 (01.01.) transformation into precipitation station

Grono

- 1919 (04.10.) 731 669 / 123 420, 357m (residential area)
 1934 (30.08.) (thermometer calibration of +0.2°C at 20°C)
 1936 (01.04.) (new station observer)
 1970 (27.11.) 731 625 / 123 520, 380m (new station observer)
 1971 (start of minimum and maximum temperature observations)
 1997 (01.08.) 732 100 / 123 700, 382m
 ⇒ Alps (southern rim). Large valley NE to WSW, lateral valley joining in from NW. Station area outside Grono, mean population density.

Gstaad-Grund

- 1981 (09.02.) 587 010 / 142 930 (instruments moved from Saanen, station in depression, forest to S and river to E)
 1986 (28.10.) (thermometer shows wrong values)
 1991 (01.01.) 587 070 / 142 970, 1085m (mean data quality, temperature range occasionally too high)
 ⇒ Prealps. Narrow valley S to N, sparsely populated.

Gütsch

- 1971
 1979 (01.12.) 690 140 / 167 590, 2287m; transformation into ANETZ station
 ⇒ Alps. Double ridge (W-E), station area on slope (19°) of lower, southern ridge.

Guttannen

- 1922 (01.04.) 665 280 / 167 580, 1055m
 1947 (19.06.) (unsatisfactory observations)
 1962 (25.09.) (observations improved)
 1967 (01.12.) (new position of hut)
 1971 (start of minimum temperature observations)

1975 (01.10.) 665 280 / 167 550, 1055m (new station observer, hut a few meters next to previous area, start of maximum temperature observations)
 1990 (29.06.) (renovation of hut)
 1992 (09.04.) (minimum thermometer approx. 5° off)
 1996 (31.12.) transformation into precipitation station
 ⇒ Alps. Large valley SSE to NW. Station outside of Guttannen on SW slope.

Güttingen

1976
 1978 (01.01.) 738 430 / 273 950, 440m; transformation into ANETZ station
 ⇒ Plateau (area of Lake Constance). Area inclined by 2°, densely populated.

Haidenhaus

1889 (01.09.) 717 930 / 278 580, 694m (highest point of area)
 1915 (06.06.) 718 150 / 278 650, 694m
 1916 (minimum thermometer out of order)
 1919 (01.08.) (new station observer)
 1922 (25.05.) (minimum thermometer shattered, no replacement)
 1924 (06.11.) (new station observer)
 1926 (07.04.) (new station observer)
 1928 (01.09.) (new station observer)
 1962 (01.04.) (new station observer, unsatisfactory observations)
 1956 (01.07.) 717 930 / 278 580, 694m (new station observer, at forester's lodge)
 1970 (25.11.) (new minimum thermometer)
 1971 (start of minimum temperature observations)
 1977 (15.09.) 718 900 / 278 900, 702m (new station observer, start of maximum temperature observations)

Hallau

1886 (01.07.) 676 500 / 283 650, 450m
 1913 (25.02.) (new station observer)
 1964 (start of minimum temperature observations)
 1975 (14.06.) 676 480 / 283 560, 435m (start of maximum temperature observations)
 1989 (14.12.) (construction of family house to the W of hut, satisfactory station)
 1992 (01.07.) 676 530 / 283 550, 435m (comparable area, new station observer, satisfactory observations)

Heiden

1887 (10.06.) 758 170 / 256 300, 797m
 1917 (29.04.) 757 940 / 256 500, 795m (residential area)
 1918 (13.01.) 758 140 / 256 260, 799m (school house, new station observer)
 1918 (14.07.) 757 800 / 257 000, 800m (new station observer)
 1930 (04.04.) 757 800 / 257 150, 808m
 1935 (01.03.) (new station observer)
 1938 (30.06.) 757 630 / 256 870, 811m

1959 (start of minimum and maximum temperature observations)
 1970 (07.12.) 758 110 / 256 960, 814m
 1977 (07.07.) 758 110 / 257 120, 800m
 1992 110 / 257 090, 802m (village, from now on values often interpolated with Altstätten or St. Gallen)
 1995 (31.12.) station stop
 ⇒ Plateau (area of Lake Constance). Hilly area N of Lake Constance, densely populated.

Hinterrhein

1968
 1979 (01.03.) 733 900 / 153 980, 1611m; transformation into ANETZ station
 ⇒ Alps. Valley floor NE to SW, station outside of village at the base of NE slope, sparsely populated.

Huttwil

1971 (01.05.) 630 660 / 218 240, 638m
 1979 (23.11.) (minimum thermometer changed, former model had bubbles)
 1987 (01.10.-16.05.) (maximum thermometer broken)
 1989 (01.11.) (station moved 30m to W)
 1990 (23.11.) (minimum thermometer broken)
 1991 (mean temperature data quality)
 1995 (31.12.) transformation into precipitation station

Interlaken

1861 631 860 / 170 500, 563m (city centre, rain captor too close to trees)
 1892 632 550 / 170 750, 567m (castle)
 1902 630 920 / 170 940, 590m
 1931 (start of minimum temperature observations)
 1935 (rain captor 3m moved because of a tree)
 1936 631 250 / 170 380, 568m
 1958 633 170 / 170 350, 570m (start of maximum temperature observations)
 1971 632 700 / 170 680, 568m (minimum and maximum temperatures missing in 1971)
 1977 633 070 / 169 120, 580m; transformation into ANETZ station
 (parallel observations until 1978 former station was located too close to trees and houses)
 ⇒ Prealps. Area in open country between two lakes, densely populated.

Jungfraujoch

1933
 1961 (start of minimum and maximum temperature observations)
 1980 (01.09.) 641 930 / 155 275, 3580m; transformation into ANETZ station
 ⇒ Alps. High alpine pass station.

La Brévine

1932 (12.11.)	539 400 / 204 500, 1077m	(post office)
1948 (02.02.)	533 960 / 202 400, 1060m	(school, houses in proximity (30m))
1957 (30.01.)		(minimum thermometer changed, the old one measured approx. 2°C too low)
1957 (21.10.)	536 775 / 203 540, 1041m	(presbytery, lowest temperatures)
1958 (24.04.)		(thermometer and minimum thermometer changed)
1962 (24.01.)		(unsatisfactory reading of minimum thermometer)
1964 (20.10.)	536 740 / 203 560, 1042m	(new station observer)
1966		(start of minimum and maximum temperature observations)
1969 (28.05.)		(new station observer)
1991 (23.05.)		(area in depression next to small river, regularly flooded)
1996 (31.12.)	station stop	

La Chaux de Fonds (old)

1900	553 950 / 217 240, 989m	(NE part of city)
1929 (29.01.)		(thermometer changed)
1959	553 950 / 217 070, 988m	(city centre)
1942 (08.05.)	553 700 / 217 025, 1010m	
1953 (01.01.)	553 950 / 217 070, 995m	
1959		(start of maximum temperature observations)
1974 (01.12.)	551 060 / 214 040, 1060m	
1981 (31.12.)	station stop	

La Chaux de Fonds (new)

1979 (01.11.) 551 290 / 215 150, 1018m; ANETZ station
 ⇒ Jura. Large valley SW to NE. Area next to small airport SW of the city, densely populated area.

La Dôle

1973
 1978 (01.08.) 497 050 / 142 380, 1670m; transformation into ANETZ station
 ⇒ Jura. Summit station.

La Fretaz

1978 (01.01.) 534 230 / 188 080, 1202m; ANETZ station
 ⇒ Jura. SW to NE ridge. Station next to road on SW slope (9°), sparsely populated.

Langenbruck

1900 (02.05.)	625 000 / 244 170, 703m	(village centre)
1931		(start of minimum temperature observations)
1941 (01.07.)	624 630 / 244 230, 740m	(new station observer)
1946-60		(problems with minimum thermometer)
1975		(start of maximum temperature observations)
1979-85		(problems with all instruments)

1987 (19.06.) 624 600 / 244 220; transformation into precipitation station

Langnau i. E.

1907 (15.01.) 262 500 / 198 900, 680m
 1926 (15.09.) 626 775 / 198 925, 692m (not far from previous place, new station observer)
 1970 (15.12.) 626 850 / 196 790, 695m (new station observer)
 1971 (start of minimum and maximum temperature observations)
 1978 (01.03.) (new station observer)
 1980 (01.02.) 627 520 / 198 710, 700m (new station observer)
 628 070 / 198 830, 755m

Lausanne

1887 (01.01.) 538 700 / 152 750, 553m (open terrace area in the NE part of the city)
 1926 (09.04.) (minimum temperature values too low in 1925)
 1928 (15.07.) (new station observer)
 1931 (start of minimum and maximum temperature observations)
 1935 (01.08.) (new station observer)
 1937 (18.02.) (calibration)
 1954 (01.04.) (station moved by 1km)
 1963 (27.03.) (new station observer)
 1965 (07.09.) 539 000 / 153 000, 605m (on power station, new station observer)
 1980 (31.12.) transformation into precipitation station

Le Brassus

1974 (02.10.) 501 900 / 156 080, 1075m
 1979 (01.05.) (thermometer too low, must be calibrated)
 1980 (25.06.) (temperature observations unsatisfactory)
 1980 (19.12.) (minimum temperature values too high)
 1981 (06.05.) (loose connection in thermometer, values either too high or too low)
 1981 (11.11.) (temperature too high)
 1988 (19.01.) (minimum temperature frequently too high during December)
 1991 (31.12.) station stop

Le Sepey

1977 (01.05.) 570 720 / 135 620, 1267m
 1996 (31.12.) station stop
 ⇒ Alps. Station area on SW slope above the village, sparsely populated.

Les Rangiers

1967 (01.04.) 583 440 / 248 230, 856m
 1977 (start of minimum and maximum temperature observations)
 1978 (04.07.) (minimum thermometer has frequently bubbles)

(01.01.) (satisfactory data quality)

(31.12.) station stop

⇒ Jura. Station area next to road with 4 houses around it.

Löbbia

1976 (08.07.) 770 800 / 138 400, 1420m

1989 (satisfactory data quality)

(31.12.) transformation into precipitation station

⇒ Alps. Narrow N to S valley south of the Maloja pass.

Locarno – Magadino

1978 (01.10.) 711 170 / 113 540, 197m; ANETZ station

⇒ South. Station area on river delta, Lake Maggiore to W, densely populated.

Locarno – Monti

1935 704 220 / 114 370, 366m (Observatorio Ticinese)

1939 (rain captor moved from W to SW of building)

1941 (extension of building, new rain captor on roof terrace and parallel measurements with the old instrument. When strong W and NW winds difference too important, therefore rain captor moved to NE corner of terrace)

1955 (07.06.) (rain captor in garden destroyed by thunderstorm)

1963 (Hellmann Pluviograph moved from roof terrace to garden)

1978 704 160 / 114 350, 366m; transformation into ANETZ station

⇒ South. Station area on SE slope (21°) above Lake Maggiore and Locarno. Wooded area, mean population density.

Summer and Spring minimum temperatures show a brake in 1988.

Lohn

1930 (01.04.) 692 420 / 290 230, 643m

1930 (08.04.) (minimum thermometer broken)

1964 (start of minimum and maximum temperature observations)

1968 (06.05.) 692 150 / 289 990, 621m (new station observer)

1983 (31.12.) transformation into precipitation station

Lugano

1863 717 260 / 095 960, 275m

1901 (start of minimum and maximum temperature observations)

1904 (06.10.) (hut moved by 50m)

1905 (19.01.) 717 880 / 095 890, 275m (parallel observations from 01.10.1904 to 30.07.1905)

1948 (rain captor slightly moved)

1972 (09.05.) (hut moved by 60m)

1977 (05.12.) 717 880 / 095 870, 273m

1978 (01.01.) transformation into ANETZ station

⇒ South. Area in open, large river valley, Lake Lugano in the E, densely populated
All seasons maximum temperature too high until 1970.

Luzern

1979 665 940 / 211 850, 451m

1897 (new Hellman Pluviograph)

1899 (additional thermometer, the original one is badly positioned for the noon temperature)

1919 666 450 / 212 650, 498m (rain captor in cloister, very small)

1931 (start of minimum and maximum temperature observations)

1956 (01.01.) (renovation of building, station moved into garden, rain captor protected and changed end of Mai)

1959 (station moved)

1970 666 920 / 210 500, 437m (rain captor only Dec 1971)

1978 (01.01.) 665 520 / 209 860, 465m; transformation into ANETZ station

⇒ Alps. Lake to the SE, hilly terrain, densely populated

Mauvoisin

1971 (19.11.) 592 520 / 094 610, 1841m

1995 (31.12.) transformation into precipitation station

⇒ Alps. Narrow valley opening to NW, station area on NE slope 100m above dam Lake Mauvoisin.

Meiringen

1989 (01.07.) 657 350 / 175 310, 605m

1951 (11.01.) (new station observer)

1956 (01.02.) (new station observer)

1958 (29.04.) 657 360 / 175 340, 603m

1959 (start of minimum and maximum temperature observations)

1970 (03.09.) (unsatisfactory station)

1971 (07.05.) 657 590 / 175 560, 631m

1981-85 (partially missing observations)

1986 (20.06.) (bad installation of minimum and maximum thermometer, minimum temperatures too low when vibrations)

1990 (mistakes in temperature readings)

1991 (26.03.) 657 110 / 175 260, 595m

⇒ Alps. Large valley SE to NW, station area between river and road, mean population density

Menzberg

1973 (20.07.) 642 430 / 209 660, 1035m (slope below ridge)

1995 (31.12.) station stop

⇒ Prealps. Hilly terrain station area next to small ridge, S slope drops steeply (300m) into gorge.

Moléson

1982 (01.10.) 567 740 / 155 175, 1972m; ANETZ station

⇒ Prealps. Summit station

Montana

1928 (01.01.) 603 150 / 128 400, 1453m

1931

(start of minimum and maximum temperature observations)

1960 (01.11.) 603 580 / 129 150, 1508m

1966 (29.10.) 602 700 / 128 560, 1495m

1970 (01.09.) 603 580 / 129 150, 1508m

1978 (01.08.) transformation into ANEZT station

(rain captor moved slightly, data not satisfactory too many missing values)

⇒ Alps. SE slope (10°) above large valley, little lake in proximity, station area in village, sparsely populated

Monte Bré

1913 (01.04.) 719 860 / 096 470, 905m

1963 (01.07.)

(new station observer)

1970 (01.01.)

(new station observer)

1971

(start of minimum temperature observations)

1976

(start of maximum temperature observations)

1984 (04.-05.)

(minimum thermometer broken)

1987 (31.12.) station stop

Monthey

1953 (01.09.) 563 100 / 122 700, 417m

1965 (29.07.) 563 400 / 122 700, 400m

1966

(start of minimum and maximum temperature observations)

1973 (01.07.) 564 040 / 123 280, 395m

(CIBA)

1982 (31.12.) station stop

Montreux Clarens

1902 (13.01.) 558 240 / 143 340, 376m

1905 (01.01.) 558 460 / 143 360, 377m

1925 (01.01.) 559 540 / 142 880, 412m

(new station observer, station moved from Montreux to Clarens)

1927 (05.01.) 558 570 / 143 600, 410m

(new station observer, area next to cemetery)

1931

(start of minimum and maximum temperature observations)

1934 (17.04.)

(thermometer installed too low in hut)

1934 (23.07.)

(thermometer calibration -0.45°C)

1945 (11.01.) 558 550 / 143 620, 480m

1953 (03.07.) 558 560 / 143 600, 405m

(instruments moved because of renovation)

⇒ Plateau (area of Lake Léman). Station area close to lake shore slope with gradually increasing inclination to N, densely populated.

Mont Soleil

1911	566 260 / 223 170	
1931		(start of minimum and maximum temperature observations)
1935 (27.11.)		(correction (details unknown))
1945 (01.06.)		(thermometer hard to read, has to be changed)
1961 (05.01.)		(new station observer)
1961 (23.11.)	566 020 / 223 800	
1979 (13.05.)		(new station observer)
1984 (01.01.)	station stop	
⇒ Jura. Summit station		

Muri

	668 150 / 235 950, 480m	
1951 (20.12.)	668 700 / 236 350	(presbytery)
1966		(start of minimum and maximum temperature observations)
1981 (01.03.)	667 370 / 235 920, 540m;	transformation into precipitation station

Mürren

1958 (01.05.)	635 140 / 157 040, 1638m	
1966 (18.06.)	634 670 / 156 380, 1638m	
1967		(start of minimum and maximum temperature observations)
1978 (24.08.)		(minimum temperatures too low)
1989 (15.08.)	634 700 / 156 410, 1645m	
1990 (17.01.)		(indications on thermometer outside of tolerance bond)
1995 (31.12.)	transformation into precipitation station	
⇒ Alps. Village on glacier terrace in S to N valley. Station area at E slope next to cable railway), sparsely populated.		

Napf

1978 (01.01.)	638 138 / 206 075, 1406m	
⇒ Plateau. Summit station.		

Neuchâtel

1901 (14.11.)	563 110 / 205 600, 485m	(complete reinstallation)
1977 (05.12.)	563 150 / 205 600, 485m	
1978 (01.01.)	transformation into ANETZ station	
⇒ Jura. Hilly terrain, city between Jura (NW) and Lake Neuchâtel (SE), densely populated. Station area on slope (15°).		

Oberiberg

1885 (16.11.)	702 150 / 210 720, 1126m	
1900 (01.09.)		(new station observer, new thermometer box)
1969 (01.01.)		(new station observer)
1970 (19.11.)		(new minimum thermometer)

1971 (start of minimum temperature observations)
 1972 (start of maximum temperature observations)
 1973 (11.10.) (maximum thermometer broken)
 1975 (13.05.) (occasionally bubbles in minimum thermometer)
 1995 (31.12.) transformation into precipitation station
 ⇒ Prealps. Narrow valley open to N, sparsely populated. Station area probably next to cable railway on NE slope.

Oeschberg

1950 (01.01.) 613 000 / 219 650, 483m (gardening school)
 1961 (start of minimum and maximum temperature observations)
 at present 613 250 / 219 525, 483m

Olivone

1976 (01.01.) 715 440 / 154 050, 905m
 1984 (30.03.) (satisfactory station)
 1987 (31.12.) transformation into precipitation station

Olten

1863 (01.12.) 635 350 / 244 600, 395m
 1903 (24.11.) 635 000 / 244 800, 402m
 1931 (14.06.) (new station observer)
 1954 (02.12.) 636 300 / 246 500, 391m (outside city)
 1959 (start of minimum and maximum temperature observations)
 1968 (02.04.) 634 530 / 243 750, 413m (new station observer)
 1986 (31.12.) station stop

Payerne

1978 (01.01.) 562 150 / 184 855, 490m
 ⇒ Plateau. Station area on hill (inclination 2°) E of the city, Lake Morat to the NW, mean population density

Pilatus

1980 (01.11.) 661 910 / 203 410, 2106m; ANETZ station
 ⇒ Prealps. Summit station.

Piotta

1978 (01.12.) 694 930 / 152 500, 1007m; ANETZ station
 ⇒ Alps (south). Valley NW to SE, station area on valley floor outside of village, sparsely populated.

Pully

1978 (01.01.) 540 820 / 151 500, 461m; ANETZ station
 ⇒ Plateau (area of Lake Léman). Station area close to lake shore, slope (6°) gradually increasing to the N, densely populated.

Rheinfelden

1895 (01.06.) 626 380 / 266 880, 280m (spaced residential area)
 1904 (28.11.) and 1912 (new station observers)
 1945 (14.06.) 627 520 / 267 420, 287m (new station observer, area 1 km of city centre)
 1961 (start of minimum temperature observations)
 1970 (27.07.) 627 510 / 268 200, 272m (new station observer, area 1.3 km of city centre close to Rhein river)
 1971 (01.08.) (new station observer, start of maximum temperature observations)
 1984 (03.10.) 625 990 / 266 130, 300m (new station observer, Feldschlösschen)
 1989 (unsatisfactory temperature data)
 1997 (01.02.) 626 970 / 266 320, 300m

Ried, Lötschental

1974 328 270 / 140 225
 ⇒ Alps. Narrow valley NE to SW, station area next to road close to river, sparsely populated.

Robbia

1961
 1978 (01.04.) 801 850 / 136 180, 1078m
 ⇒ Alps (south). Valley N to SE, dam lake to SE, sparsely populated.

Samedan

1979 (01.07.) 787 150 / 156 040, 1705m; ANETZ station
 ⇒ Alps. Large valley NE to SW. Station area outside of village, sparsely populated.

San Bernardino (village)

1968
 1981 (01.11.) 734 120 / 147 270, 1639m; ANETZ station
 ⇒ Alps. End of narrow valley, pass in NW, dam lake in SW.

Säntis

1887 744 180 / 234 920
 1901 (start of minimum and maximum temperature observations)
 1918 (new counter on clock work)
 1933 (new station observer, the parameter: blown off snow is not observed anymore)
 1974 (18.06.) (station moved)
 1975 (30.07.) (station moved)
 1975 (30.09.) (station moved on terrace of Post)
 1978 (01.01.) transformation into ANETZ station
 1988 (01.12.) 744 100 / 234 900, 2490m (moved on summit)
 ⇒ Prealps. Summit station.

Sarnen

1964 661 550 / 193 680, 479m
 1986 station stop

Schaffhausen

1963 689 940 / 283 375, 398m
 1874 690 375 / 283 650, 451m
 1904 690 375 / 283 960, 451m
 1914 (rain captor moved)
 1931 (start of minimum temperature observations)
 1955 (rain captor moved)
 1960 689 200 / 283 980, 457m (start of maximum temperature observations)
 1970 (unsatisfactory observations)
 1971 688 720 / 282 820, 437m
 1981 (01.07.) 688 700 / 282 800, 437m; transformation into ANETZ station
 ⇒ Plateau. Station area on hilly terrain (slope 12°), densely populated.

Schwyz

1971 691 025 / 207 160, 448m
 ⇒ Prealps. Large valley, open to W. Station area between road and river Muota, mean population density.

Scuol

1880 818 380 / 186 920, 1244m
 1890 (rain captor too close to trees)
 1906 (station moved several times)
 1934 (station moved)
 1940 (rain captor moved because of trees)
 1947 (rain captor moved back to previous place)
 1950 (rain captor moved)
 1950 (construction of house right next to the station area)
 1952 (change of place for snow observations)
 1953 (unsatisfactory observations since 1935, quality does not improve)
 1971 817 470 / 186 600, 1298m (observations satisfactory, start of minimum and maximum temperature observations)
 1980 (01.07.) 817 130 / 186 400, 1298m; transformation into ANETZ station
 ⇒ Alps. Narrow valley from W to NE. Station area on SE slope (18°) outside of village, mean to sparse population density.

Sils Maria

1892 (22.10.) 778 660 / 144 680, 181m (school)
 1904 (15.10.) 778 810 / 144 740, 1814m (new station observer, end of village)
 1914 (15.09.) (thermometers broken because of storm)
 1931 (07.07.) (new station observer)
 1934 (thermometer calibration of +0.6°C)
 1948 778 660 / 144 590, 1818m
 1951 (29.12.) (temperature values too high)

1952 (01.07.) 778 920 / 145 020, 1802m
 1971 (start of minimum temperature observations)
 1977 (20.07.) (renovation of station, new instruments, start
 of maximum temperature observations)
 1990 (01.04.-31.12.) (frequently wrong observation of maximum
 temperature)
 778 975 / 145 025, 1802m
 ⇒ Alps. Valley from NE to SW, before Maloja pass, village between two small lakes,
 sparsely populated.

Simplon Dorf

1971 647 570 / 116 130, 1802m
 1974 (start of maximum temperature observations)
 1997 (01.01.) transformation into precipitation station
 ⇒ Alps. Narrow valley from NW to SE, station area on NE slope above village and below
 dense forest, sparsely populated.

Sion

1864 594 000 / 120 600, 533m
 1868 594 200 / 120 400, 538m
 1873 593 850 / 120 700, 542m (monastery)
 1920-21 (constructions, station temporary moved)
 1942 (rain captor is elevated from 1.5m to 2.2m)
 1946 (rain captor too close to trees)
 1947 (01.04.) (rain captor fixed to roof)
 1959 (only pluviograph working)
 1967 (01.03.) (constructions, temporary movement of
 station)
 1978 station stop

Sion a rodrome

1951 592 200 / 118 625, 482m (parallel observations with station Sion)
 1973 (rain captor moved, more exposed and more
 wind)
 1978 (01.01.) transformation into ANETZ station
 (start of minimum and maximum temperature
 observations)
 ⇒ Alps. Large and open valley from NE to SW. Station area on airfield, densely
 populated.

St. Gallen

1863 746 440 / 254 430, 665m
 1864 746 880 / 255 980, 665m
 1865 745 300 / 254 250, 679m
 1867 746 660 / 255 040, 669m
 1879 746 600 / 255 220, 663m
 1883 744 360 / 254 140, 679m
 1890 746 720 / 255 840, 703m
 1931 (start of minimum temperature observations)
 1973 743 010 / 252 340, 678m

1954 748 500 / 256 300, 664m
 1959 (start of maximum temperature observations)
 1981 (01.08.) 747 940 / 254 600, 779m; transformation into ANETZ station
 ⇒ Plateau (area of Lake Constance). Open, hilly terrain (slope 6°), densely populated.

St. Moritz

1955 (08.03.) 784 550 / 152 750, 1853m
 1959 785 050 / 152 800, 1833m (new station and instruments, start of minimum and maximum temperature observations, minimum temperatures too low)
 1960 784 300 / 152 420, 1832m
 1982 (31.12.) station stop

Stabio

1981 (01.08.) 716 040 / 077 970, 353m; ANETZ station
 ⇒ South. Hilly terrain, densely populated.

Stein am Rhein

1965 744 025 / 249 390, 780m

Sta. Maria

1901 828 700 / 165 500, 1388m
 1902 828 600 / 165 450, 1388m
 1906 828 830 / 165 240, 1408m (summer morning temperature influence of direct sunlight)
 1928 (good position for rain captor)
 1931 (start of minimum temperature observations)
 1943 (rain captor moved, now too close to house)
 1947 (minimum temperature thermometer broken)
 1967 (station observer has problems with snow observations, better from 1968 on)
 1976 (renovation of the station, start of maximum temperature observations)
 1978 828 760 / 165 350, 1390m
 ⇒ Alps. Large river valley open to E, station area on NW slope, sparsely populated.

Tänikon

1971
 1978 710 500 / 259 820, 536m
 ⇒ Plateau. Open terrain, densely populated.

Tierfehd

1969 717 760 / 193 140, 810m
 ⇒ Prealps. End of large valley from S to N, sparsely populated.

Ulrichen

1980 (01.10.) 666 740 / 150 760, 1345m; ANETZ station

⇒ Alps. Valley NE to SW, station area outside of village between the railway line and the river (Rhône), mean to sparse population density.

Vaduz

1978 (01.06.) 757 700 / 221 700, 460m

⇒ Prealps. Large valley, densely populated.

Vättis

1966 752 360 / 197 030, 957m

⇒ Prealps. Narrow valley from SSW to NNE, station on WNW slope between the road and a small river, sparsely populated.

Visp

1979 (01.12.) 631 150 / 128 020, 640m; ANETZ station

⇒ Alps. Large valley from NE to W, station area E of the village, densely populated.

Wädenswil

1981 (01.01.) 693 770 / 230 780, 463m

⇒ Plateau. Hilly terrain (slope 2°), Lake of Zurich in the E, densely populated.

Weissfluhjoch

1959

1971

(start of minimum and maximum temperature observations)

1980 (01.10.) 780 600 / 189 630, 2690m; ANETZ station

⇒ Alps. High alpine summit site.

Wynau

1978 (01.01.) 626 400 / 233 860, 422m; ANETZ station

⇒ Plateau. Very large valley, station area in slightly hilly terrain (slope 6°), densely populated.

Zermatt

1960

1982 (01.01.) 624 350 / 097 550, 1638m (minimum and maximum temperatures missing in 1982)

⇒ Alps. Narrow valley from S to N, glaciers to the S, station area on SW slope (48°), mean population density.

Zurich Kloten

1971

1978 (01.01.) 682 720 / 259 740, 436m; ANETZ station

⇒ Plateau. Station at airport, densely populated.

Zurich Reckenholz

1978 (01.06.) 681 400 / 253 550, 443m

⇒ Plateau. Lake Zurich to the S, densely populated.

Zurich SMA

1901

1903 684 150 / 248 000, 499m

1949 (01.08.) 685 100 / 248 100, 556m (parallel observations with former station until August 1951)

1949 (01.09.) 685 111 / 248 098, 573m (roof)

1977 685 125 / 248 090, 556m

1978 (01.01.) transformation into ANETZ station

⇒ Plateau. Station area in city on a hill above Lake Zurich (slope 7°), densely populated.

APPENDIX B

The following tables show the clusters of single climatological stations resulting out of the Principal Component Analysis and the Cluster Analysis conducted on temperature time series during the period from 1983 to 1995 (Chapter 3). **Written in *italic* are the representative stations, which will be used in chapter 4.** A second set of tables indicates the degree of correlation between the original data series of the representative stations and their homogenised analogues over the period 1957 to 1995.

WINTER

WINTER MINIMUM TEMPERATURE:

CLUSTER/STATION	ALTITUDE	CLUSTER/STATION	ALTITUDE
1/Aigle	381m	3/Adelboden	1355m
1/Altdorf	451m	3/Arosa	1847m
1/Altstätten S.G.	474m	3/Balmberg	1075m
1/Bad Ragaz	496m	3/Chaumont	1141m
1/Basel-Binningen	317m	3/Disentis	1180m
1/Bern-Liebefeld	570m	3/Grächen	1617m
1/Biel	434m	3/Grimmel Hospiz	1950m
1/Broc (Usine)	680m	3/La Fretaz	1202m
1/Changins	435m	3/Le Sepey	1267m
1/Chur	586m	3/Les Rangiers	856m
1/Chx-de-Fonds	1018m	3/Mauvoisin	1841m
1/Delémont	416m	3/Menzberg	1035m
1/Ebnat-Kappel	629m	3/Montana	1495m
1/Einsiedeln	910m	3/Mürren	1639m
1/Fahy (Ajoie)	596m	3/Napf	1408m
1/Fribourg	634m	3/Zermatt	1638m
1/Genève	430m		
1/Glarus	470m	4/Chasseral	1599m
1/Güttingen	438m	4/Corvatsch	3015m
1/Haidenhaus	694m	4/Gd. St. Bernard	2479m
1/Hallau	450m	4/Gütsch	2288m
1/Heiden	811m	4/Jungfrauoch	3572m
1/Huttwil	639m	4/La Dôle	1672m
1/Interlaken	574m	4/Pilatus	2106m
1/Langnau i. E.	695m	4/Säntis	2500m
1/Luzern	456m	4/Weissfluhjoch	2540m
1/Meiringen	832m		
1/Montreux-Clarens	408m	5/Buffalora	1968m
1/Neuchâtel	487m	5/Hinterrhein	1619m
1/Oeschberg	482m	5/Piotta	1007m
1/Payerne	491m	5/Robbia/Poschia	1078m

1/Pully	461m	5/Samedan	1705m
1/Rheinfelden	271m	5/Sils Maria	1802m
1/Schaffhausen	457m	5/Ulrichen	1345m
1/Schwyz (Ibach)	448m		
1/St. Gallen	664m	6/Bosco Gurin	1505m
1/Stein am Rhein	786m	6/Cimetta	1672m
1/Tänikon	536m	6/Löbbia	1420m
1/Vaduz	460m	6/Ospizio Bernina	2256m
1/Wädenswil	463m	6/S. Maria/Müstair	1390m
1/Wynau	422m	6/San Bernardino	1628m
1/Zürich Flughafen	431m	6/Simplon Dorf	1495m
1/Zürich Reck.	443m		
1/Zürich SMA	569m	7/Grono	357m
		7/Locarno-Monti	379m
2/Alvaneu	1175m		
2/Andermatt	1442m	8/Locarno-Magad.	197m
2/Château-d'Oex	980m	8/Lugano	276m
2/Davos	1590m	8/Stabio	353m
2/Elm	962m		
2/Engelberg	1018m	9/Sion-Aérodrome	483m
2/Gstaad-Grund	1085m	9/Visp (ASTA)	640m
2/Guttannen	1055m		
2/Oberiberg	1090m		
2/Ried/Lötschental	1480m		
2/Scuol (Schuls)	1295m		
2/Tierfehd/Linthal	810m		
2/Vättis	948m		

WINTER MAXIMUM TEMPERATURES:

GROUP/STATION	ALTITUDE	GROUP/STATION	ALTITUDE
1/Aigle	381m	3/Alvaneu	1175m
1/Altstätten S.G.	474m	3/Arosa	1847m
1/Bad Ragaz	496m	3/Chasseral	1599m
1/Basel-Binningen	317m	3/Corvatsch	3015m
1/Bern-Liebefeld	570m	3/Davos	1590m
1/Biel	434m	3/Disentis	1180m
1/Broc (Usine)	680m	3/Gd. St. Bernard	2479m
1/Changins	435m	3/Grächen	1617m
1/Delémont	416m	3/Grimsel Hospiz	1950m
1/Ebnat-Kappel	629m	3/Gütsch	2288m
1/Einsiedeln	910m	3/Hinterrhein	1619m
1/Engelberg	1018m	3/Jungfrauoch	3572m
1/Fribourg	634m	3/La Dôle	1672m
1/Genève	430m	3/Mauvoisin	1841m
1/Glarus	470m	3/Montana	1495m
1/Güttingen	438m	3/Pilatus	2106m

1/Haidenhaus	694m	3/Ried/Lötschental	1480m
1/Hallau	450m	3/Säntis	2500m
1/Heiden	811m	3/Weissfluhjoch	2540m
1/Huttwil	639m	3/Zermatt	1638m
1/Interlaken	574m		
1/Langnau i. E.	695m	4/Bosco Gurin	1505m
1/Luzern	456m	4/Cimetta	1672m
1/Meiringen	832m	4/Löbbia	1420m
1/Montreux-Clarens	408m	4/Ospizio Bernina	2256m
1/Neuchâtel	487m	4/Piotta	1007m
1/Oeschberg	482m	4/Robbia/Poschia	1078m
1/Payerne	491m	4/S. Maria/Müstair	1390m
1/Pully	461m	4/San Bernardino	1628m
1/Rheinfelden	271m	4/Sils Maria	1802m
1/Schaffhausen	457m	4/Simplon Dorf	1495m
1/Schwyz (Ibach)	448m		
1/St. Gallen	664m	5/Samedan	1705m
1/Stein am Rhein	786m	5/Scuol (Schuls)	1295m
1/Tänikon	536m	5/Ulrichen	1345m
1/Tierfehd/Linthal	810m		
1/Vaduz	460m	6/Grono	357m
1/Wädenswil	463m	6/Loc-Magadino	197m
1/Wynau	422m	6/Locarno-Monti	379m
1/Zürich Flughafen	431m	6/Lugano	276m
1/Zürich Reckenholz	443m	6/Stabio	353m
1/Zürich SMA	569m		
		7/Sion-Aérodrome	483m
2/Adelboden	1355m	7/Visp (ASTA)	640m
2/Balmberg	1075m		
2/Château-d'Oex	980m		
2/Chaumont	1141m		
2/Chur	586m		
2/Chx-de-Fonds	1018m		
2/Elm	962m		
2/Gstaad-Grund	1085m		
2/Guttannen	1055m		
2/La Fretaz	1202m		

COMPARISON TO HOMOGENISED DATA SETS IN WINTER:

T _{min}		T _{max}	
<i>Cluster/Station</i>	<i>/ Corr.</i>	<i>Cluster/Station</i>	<i>/ Corr.</i>
1/Bad Ragaz	0.99	1/Bad Ragaz	0.99
1/Basel	0.99	1/Basel	0.99
1/Bern	0.92	1/Bern	0.99
1/Chur	0.94	1/Delémont	0.99
1/Delémont	0.99	1/Luzern	0.99
1/Luzern	0.97	1/Montraux - Clarens	0.99
1/Montreux - Clarens	0.99	1/Neuchâtel	0.99
1/Neuchâtel	0.99	1/Oeschberg	0.99
1/Oeschberg	0.99	1/Schaffhausen	0.99
1/Rheinfelden	0.96	1/St. Gallen	0.99
1/Schaffhausen	0.99	2/Chur	0.99
1/St. Gallen	0.99	2/Château d'Oex	0.99
2/Château d'Oex	0.99	3/Disentis	0.97
2/Davos	0.99	3/Davos	0.98
3/Arosa	0.99	3/Arosa	0.98
3/Disentis	0.97	3/Säntis	0.98
3/Montana	0.97	3/Jungfrauoch	0.99
4/Jungfrauoch	0.98	4/Robbia	0.99
4/Säntis	0.99	5/ Locarno - Monti	0.99
5/Robbia	0.92	5/Lugano	0.93
6/Sta. Maria	0.92		
7/Locarno – Monti	0.99		
8/Lugano	0.99		

SPRING

SPRING MINIMUM TEMPERATURES:

GROUP/STATION	ALTITUDE	GROUP/STATION	ALTITUDE
1/Aigle	381m	3/Adelboden	1355m
1/Basel-Binningen	317m	3/Balmberg	1075m
1/Bern-Liebefeld	570m	3/Chaumont	1141m
1/Biel	434m	3/Fahy (Ajoie)	596m
1/Broc (Usine)	680m	3/La Fretaz	1202m
1/Changins	435m	3/Les Rangiers	856m
1/Chx-de-Fonds	1018m	3/Menzberg	1035m
1/Delémont	416m	3/Rueneberg	610m
1/Ebnat-Kappel	629m		
1/Fribourg	634m	4/Arosa	1847m
1/Genève	430m	4/Bosco Gurin	1505m
1/Güttingen	438m	4/Disentis	1180m
1/Haidenhaus	694m	4/Grächen	1617m
1/Hallau	450m	4/Löbbia	1420m
1/Huttwil	639m	4/Mürren	1639m
1/Interlaken	574m	4/Ospizio Bernina	2256m
1/Langnau i. E.	695m	4/Ried/Lötschental	1480m
1/Luzern	456m	4/S. Maria/Müstair	1390m
1/Montreux-Clarens	408m	4/San Bernardino	1628m
1/Neuchâtel	487m	4/Zermatt	1638m
1/Oberiberg	1090m		
1/Oeschberg	482m	5/Chasseral	1599
1/Payerne	491m	5/Cimetta	1672m
1/Pully	461m	5/Corvatsch	3015m
1/Rheinfelden	271m	5/Gd. St. Bernard	2479m
1/Schaffhausen	457m	5/Grimmel Hospiz	1950m
1/Tänikon	536m	5/Gütsch	2288m
1/Wädenswil	463m	5/Jungfrauoch	3572m
1/Wynau	422m	5/La Dôle	1672m
1/Zürich Flughafen	431m	5/Le Sepey	1267m
1/Zürich Reckenholz	443m	5/Mauvoisin	1841m
1/Zürich SMA	569m	5/Moleson	1972m
		5/Montana	1495m
2/Altdorf	451m	5/Napf	1408m
2/Altstätten S.G.	474m	5/Pilatus	2106m
2/Alvaneu	1175m	5/Säntis	2500m
2/Andermatt	1442m	5/Weissfluhjoch	2540m
2/Bad Ragaz	496m		
2/Château-d'Oex	980m	6/Grono	357m
2/Chur	586m	6/Locarno-Monti	379m
2/Davos	1590m	6/Simplon Dorf	1495m
2/Einsiedeln	910m		
2/Elm	962m	7/Gstaad-Grund	1085m

2/Engelberg	1018m	7/Hinterrhein	1619m
2/Glarus	470m	7/Robbia/Poschia	1078m
2/Guttannen	1055m	7/Samedan	1705m
2/Heiden	811m	7/Sils Maria	1802m
2/Meiringen	832m	7/Ulrichen	1345m
2/Schwyz (Ibach)	448m	7/Visp (ASTA)	640m
2/Scuol (Schuls)	1295m		
2/Sion-Aérodrome	483m	8/Locarno-Magad.	197m

SPRING MAXIMUM TEMPERATURES:

GROUP/STATION	ALTITUDE	GROUP/STATION	ALTITUDE
1/Balmberg	1075m	3/Aigle	381m
1/Basel-Binningen	317m	3/Biel	434m
1/Bern-Liebefeld	570m	3/Changins	435m
1/Broc (Usine)	680m	3/Genève	430m
1/Château-d'Oex	980m	3/Montreux-	408m
1/Chaumont	1141m	3/Neuchâtel	487m
1/Chx-de-Fonds	1018m	3/Payerne	491m
1/Delémont	416m	3/Pully	461m
1/Fahy (Ajoie)	596m	3/Sion-Aérodrome	483m
1/Fribourg	634m		
1/Gstaad-Grund	1085m	4/Adelboden	1355m
1/Güttingen	438m	4/Alvaneu	1175m
1/Haidenhaus	694m	4/Chasseral	1599m
1/Hallau	450m	4/Disentis	1180m
1/Huttwil	639m	4/Grimsel Hospiz	1950m
1/Interlaken	574m	4/Guttannen	1055m
1/La Fretaz	1202m	4/La Dôle	1672m
1/Langnau i. E.	695m	4/Mauvoisin	1841m
1/Le Sepey	1267m	4/Moleson	1972m
1/Les Rangiers	856m	4/Mürren	1639m
1/Luzern	456m	4/Ried/Lötschental	1480m
1/Menzberg	1035m	4/Scuol (Schuls)	1295m
1/Oeschberg	482m		
1/Rheinfelden	271m	5/Arosa	1847m
1/Rueneberg	610m	5/Corvatsch	3015m
1/Schaffhausen	457m	5/Davos	1590m
1/Schwyz (Ibach)	448m	5/Pilatus	2106m
1/Tänikon	536m	5/Säntis	2500m
1/Wädenswil	463m	5/Weissfluhjoch	2540m
1/Wynau	422m		
1/Zürich Flughafen	431m	6/Grächen	1617m
1/Zürich Reckenholz	443m	6/Hinterrhein	1619m
1/Zürich SMA	569m	6/Montana	1495m
		6/S. Maria/Müstair	1390m
2/Altdorf	451m	6/Samedan	1705m

2/Altstätten S.G.	474m	6/Ulrichen	1345m
2/Bad Ragaz	496m	6/Visp (ASTA)	640m
2/Chur	586m	6/Zermatt	1638m
2/Ebnat-Kappel	629m		
2/Einsiedeln	910m	7/Gd. St. Bernard	2479m
2/Elm	962m	7/Gütsch	2288m
2/Engelberg	1018m	7/Jungfrauoch	3572m
2/Glarus	470m	7/Ospizio Bernina	2256m
2/Heiden	811m		
2/Meiringen	832m	8/Bosco Gurin	1505m
2/Napf	1408m	8/Cimetta	1672m
2/Oberiberg	1090m	8/Piotta	1007m
2/St. Gallen	664m	8/Robbia/Poschia	1078m
2/Stein am Rhein	786m	8/Simplon Dorf	1495m
2/Tierfehd/Linthal	810m		
2/Vaduz	460m	9/Löbbia	1420m
2/Vättis	948m	9/San Bernardino	1628m
		9/Sils Maria	1802m
		10/Grono	357m
		10/Locarno-Magad.	197m
		10/Locarno-Monti	379m
		10/Lugano	276m
		10/Stabio	353m

COMPARISON TO HOMOGENISED DATA SETS IN SPRING:

T _{min}		T _{max}	
<i>Cluster/Station</i>	<i>/ Corr.</i>	<i>Cluster/Station</i>	<i>/ Corr.</i>
1/Basel	0.98	1/Basel	0.92
1/Bern	0.74	1/Bern	0.97
1/Delémont	0.96	1/Château d'Oex	0.94
1/Luzern	0.91	1/Delémont	0.99
1/Montreux - Clarens	0.99	1/Luzern	0.96
1/Neuchâtel	0.97	1/Oeschberg	0.99
1/Oeschberg	0.94	1/Schaffhausen	0.98
1/Schaffhausen	0.99	2/Bad Ragaz	0.97
2/Bad Ragaz	0.98	2/Chur	0.99
2/Château d'Oex	0.85	2/St. Gallen	0.81
2/Chur	0.83	3/Montreux - Clarens	0.99
2/Davos	0.99	3/Neuchâtel	0.97
4/Arosa	0.99	4/Disentis	0.95
4/Disentis	0.89	5/Arosa	0.96

5/Jungfrauojoch	0.98	5/Davos	0.97
5/Säntis	0.99	5/Säntis	0.98
6/Locarno – Monti	0.99	6/Montana	0.96
7/Robbia	0.88	7/Jungfrauojoch	0.97
8/Lugano	0.99	8/Robbia	0.98
		10/Locarno - Monti	0.99
		10/Lugano	0.79

SUMMER

SUMMER MINIMUM TEMPERATURES:

GROUP/STATION	ALTITUDE	GROUP/STATION	ALTITUDE
1/Altdorf	451m	4/Adelboden	1355m
1/Altstätten S.G.	474m	4/Arosa	1847m
1/Alvaneu	1175m	4/Balmberg	1075m
1/Andermatt	1442m	4/Chasseral	1599m
1/Bad Ragaz	496m	4/Chaumont	1141m
1/Basel-Binningen	317m	4/Cimetta	1672m
1/Chur	586m	4/Corvatsch	3015m
1/Davos	1590m	4/Disentis	1180m
1/Einsiedeln	910m	4/Gd. St. Bernard	2479m
1/Elm	962m	4/Grächen	1617m
1/Engelberg	1018m	4/Grimmel Hospiz	1950m
1/Glarus	470m	4/Gütsch	2288m
1/Guttannen	1055m	4/Jungfrauojoch	3572m
1/Güttingen	438m	4/La Dôle	1672m
1/Haidenhaus	694m	4/La Fretaz	1202m
1/Heiden	811m	4/Le Sepey	1267m
1/Interlaken	574m	4/Les Rangiers	856m
1/Luzern	456m	4/Mauvoisin	1841m
1/Meiringen	832m	4/Menzberg	1035m
1/Oberiberg	1090m	4/Moleson	1972m
1/Schaffhausen	457m	4/Montana	1495m
1/Schwyz (Ibach)	448m	4/Mürren	1639m
1/Scuol (Schuls)	1295m	4/Napf	1408m
1/Stein am Rhein	786m	4/Pilatus	2106m
1/Tierfehd/Linthal	810m	4/Säntis	2500m
1/Vaduz	460m	4/Weissfluhjoch	2540m
1/Vättis	948m	4/Zermatt	1638m
1/Wädenswil	463m		
1/Zürich Flughafen	431m	5/Bosco Gurin	1505m
1/Zürich Reckenholz	443m	5/Grono	357m

1/Zürich SMA	569m	5/Löbbia	1420m
		5/Locarno-Magad.	197m
2/Aigle	381m	5/Locarno-Monti	379m
2/Bern-Liebefeld	570m	5/Lugano	276m
2/Biel	434m	5/Ospizio Bernina	2256m
2/Broc (Usine)	680m	5/Piotta	1007m
2/Changins	435m	5/S. Maria/Müstair	1390m
2/Château-d'Oex	980m	5/San Bernardino	1628m
2/Chx-de-Fonds	1018m	5/Simplon Dorf	1495m
2/Fribourg	634m	5/Stabio	353m
2/Genève	430m		
2/Hallau	450m	6/Gstaad-Grund	1085m
2/Huttwil	639m	6/Ulrichen	1345m
2/Langnau i. E.	695m	6/Visp (ASTA)	640m
2/Oeschberg	482m		
2/Payerne	491m	7/Hinterrhein	1619m
2/Rheinfelden	271m	7/Robbia/Poschia	1078m
2/Ried/Lötschental	1480m	7/Sils Maria	1802m
2/Sion-Aérodrome	483m		
2/Wynau	422m		
3/Delémont	416m		
3/Ebnat-Kappel	629m		
3/Tänikon	536m		

SUMMER MAXIMUM TEMPERATURES:

GROUP/STATION	ALTITUDE	GROUP/STATION	ALTITUDE
1/Adelboden	1355m	3/Altstätten S.G.	474m
1/Altdorf	451m	3/Bad Ragaz	496m
1/Balmberg	1075m	3/Chur	586m
1/Basel-Binningen	317m	3/Elm	962m
1/Chasseral	1599m	3/Glarus	470m
1/Chx-de-Fonds	1018m	3/Guttannen	1055m
1/Delémont	416m	3/Heiden	811m
1/Ebnat-Kappel	629m	3/Oberiberg	1090m
1/Einsiedeln	910m	3/Pilatus	2106m
1/Engelberg	1018m	3/St. Gallen	664m
1/Fahy (Ajoie)	596m	3/Tierfehd/Linthal	810m
1/Haidenhaus	694m	3/Vaduz	460m
1/Hallau	450m	3/Vättis	948m
1/Huttwil	639m		
1/Langnau i. E.	695m	4/Alvaneu	1175m
1/Les Rangiers	856m	4/Arosa	1847m

1/Luzern	456m	4/Davos	1590m
1/Meiringen	832m	4/Disentis	1180m
1/Menzberg	1035m	4/Grimsel Hospiz	1950m
1/Moleson	1972m	4/Gütsch	2288m
1/Mürren	1639m	4/Säntis	2500m
1/Napf	1408m	4/Scuol (Schuls)	1295m
1/Oeschberg	482m	4/Weissfluhjoch	2540m
1/Rheinfelden	271m		
1/Rueneberg	610m	5/Corvatsch	3015m
<i>1/Schaffhausen</i>	<i>457m</i>	5/Gd. St. Bernard	2479m
1/Schwyz (Ibach)	448m	5/Hinterrhein	1619m
1/Tänikon	536m	5/Jungfrauoch	3572m
1/Wädenswil	463m	5/Ospizio Bernina	2256m
1/Wynau	422m	5/S. Maria/Müstair	1390m
1/Zürich Flughafen	431m	5/Samedan	1705m
1/Zürich Reckenholz	443m		
1/Zürich SMA	569m	6/Bosco Gurin	1505
		6/Cimetta	1672
2/Aigle	381m	6/Grono	357
2/Bern-Liebefeld	570m	6/Locarno-Magad.	197
2/Biel	434m	6/Locarno-Monti	379m
2/Broc (Usine)	680m	6/Lugano	276m
2/Changins	435m	6/Piotta	1007m
2/Château-d'Oex	980m	6/Simplon Dorf	1495m
2/Chaumont	1141m	6/Stabio	353m
2/Fribourg	634m		
2/Genève	430m	7/Grächen	1617m
2/Gstaad-Grund	1085m	7/Mauvoisin	1841m
2/Interlaken	574m	7/Montana	1495m
2/La Dôle	1672m	7/Ried/Lötschental	1480m
2/La Fretaz	1202m	7/Ulrichen	1345m
2/Le Sepey	1267m	7/Visp (ASTA)	640m
2/Montreux-Clarens	408m	7/Zermatt	1638m
2/Neuchâtel	487m		
2/Payerne	491m	8/Löbbia	1420m
2/Pully	461m	8/Robbia/Poschia	1078m
2/Sion-Aérodrome	483m	8/San Bernardino	1628m
		8/Sils Maria	1802m

COMPARISON TO HOMOGENISED DATA SETS IN SUMMER:

T _{min}		T _{max}	
<i>Cluster/Station</i>	<i>/ Corr.</i>	<i>Cluster/Station</i>	<i>/ Corr.</i>
1/Bad Ragaz	0.96	1/Basel	0.88
1/Basel	0.93	1/Delémont	0.98
1/Chur	0.62	1/Luzern	0.91
1/Davos	0.88	1/Oeschberg	0.99
1/Luzern	0.88	1/Schaffhausen	0.98
1/ Schaffhausen	0.94	2/Bern	0.97
2/Château d'Oex	0.98	2/Château d'Oex	0.93
2/Oeschberg	0.96	2/Montreux - Clarens	0.99
2/Rheinfelden	0.87	2/Neuchâtel	0.98
3/Delémont	0.96	3/Bad Ragaz	0.97
4/Arosa	0.99	3/Chur	0.98
4/Disentis	0.64	3/St. Gallen	0.63
4/Jungfrauoch	0.98	4/Arosa	0.96
4/Säntis	0.99	4/Davos	0.83
5/Locarno – Monti	0.96	4/Disentis	0.91
5/Lugano	0.97	4/Säntis	0.98
7/Robbia	0.48	5/Jungfrauoch	0.96
		6/Locarno - Monti	0.99
		6/Lugano	0.51
		7/Montana	0.98
		8/Robbia	0.99

AUTUMN**AUTUMN MINIMUM TEMPERATURES:**

GROUP/STATION	ALTITUDE	GROUP/STATION	ALTITUDE
1/Basel-Binningen	317m	3/Alvaneu	1175m
1/Bern-Liebefeld	570m	3/Andermatt	1442m
1/Biel	434m	3/Davos	1590m
1/Changins	435m	3/Disentis	1180m
1/Chx-de-Fonds	1018m	3/Elm	962m
1/Delémont	416m	3/Engelberg	1018m
1/Ebnat-Kappel	629m	3/Grächen	1617m
1/Fahy (Ajoie)	596m	3/Guttannen	1055m
1/Fribourg	634m	3/Hinterrhein	1619m
1/Genève	430m	3/Ried/Lötschental	1480m
1/Güttingen	438m	3/Vättis	948m
1/Haidenhaus	694m	3/Zermatt	1638m

1/Hallau	450m		
1/Heiden	811m	4/Adelboden	1355m
1/Huttwil	639m	4/Arosa	1847m
1/Langnau i. E.	695m	4/Balmberg	1075m
1/Luzern	456m	4/Chaumont	1141m
1/Neuchâtel	487m	4/Grimsel Hospiz	1950m
1/Oeschberg	482m	4/La Fretaz	1202m
1/Payerne	491m	4/Le Sepey	1267m
1/Pully	461m	4/Les Rangiers	856m
1/Rheinfelden	271m	4/Mauvoisin	1841m
1/Rueneberg	610m	4/Menzberg	1035m
1/Schaffhausen	457m	4/Montana	1495m
1/St. Gallen	664m	4/Mürren	1639m
1/Stein am Rhein	786m	4/Napf	1408m
1/Tänikon	536m		
1/Wädenswil	463m	5/Chasseral	1599m
1/Wynau	422m	5/Corvatsch	3015m
1/Zürich Flughafen	431m	5/Gd. St. Bernard	2479m
1/Zürich Reckenholz	443m	5/Gütsch	2288m
1/Zürich SMA	569m	5/Jungfrauoch	3572m
		5/La Dôle	1672m
2/Aigle	381m	5/Moleson	1972m
2/Altdorf	451m	5/Pilatus	2106m
2/Altstätten S.G.	474m	5/Säntis	2500m
2/Bad Ragaz	496m	5/Weissfluhjoch	2540m
2/Broc (Usine)	680m		
2/Château-d'Oex	980m	6/Bosco Gurin	1505m
2/Chur	586m	6/Cimetta	1672m
2/Einsiedeln	910m	6/Ospizio Bernina	2256m
2/Glarus	470m	6/Simplon Dorf	1495m
2/Gstaad-Grund	1085m		
2/Interlaken	574m	7/Grono	357m
2/Meiringen	832m	7/Löbbia	1420m
2/Montreux-Clarens	408m	7/Locarno-	197m
2/Oberiberg	1090m	7/Locarno-Monti	379m
2/Schwyz (Ibach)	448m	7/Lugano	276m
2/Scuol (Schuls)	1295m	7/Piotta	1007m
2/Sion-Aérodrome	483m	7/Robbia/Poschia	1078m
2/Tierfehd/Linthal	810m	7/S. Maria/Müstair	1390m
2/Vaduz	460m	7/San Bernardino	1628m
		7/Sils Maria	1802m
		7/Stabio	353m
		8/Samedan	1705m
		8/Ulrichen	1345m
		8/Visp (ASTA)	640m

AUTUMN MAXIMUM TEMPERATURES:

GROUP/STATION	ALTITUDE	GROUP/STATION	ALTITUDE
1/Aigle	381m	3/Adelboden	1355m
1/Altdorf	451m	3/Alvaneu	1175m
1/Altstätten S.G.	474m	3/Arosa	1847m
1/Bad Ragaz	496m	3/Balmberg	1075m
1/Basel-Binningen	317m	3/Château-d'Oex	980m
1/Bern-Liebefeld	570m	3/Chaumont	1141m
1/Biel	434m	3/Chur	586m
1/Broc (Usine)	680m	3/Chx-de-Fonds	1018m
1/Changins	435m	3/Davos	1590m
1/Delémont	416m	3/Disentis	1180m
1/Ebnat-Kappel	629m	3/Einsiedeln	910m
1/Fahy (Ajoie)	596m	3/Elm	962m
1/Fribourg	634m	3/Engelberg	1018m
1/Genève	430m	3/Gstaad-Grund	1085m
1/Glarus	470m	3/Guttannen	1055m
1/Güttingen	438m	3/La Fretaz	1202m
1/Haidenhaus	694m	3/Le Sepey	1267m
1/Hallau	450m	3/Les Rangiers	856m
1/Heiden	811m	3/Menzberg	1035m
1/Huttwil	639m	3/Mürren	1639m
1/Interlaken	574m	3/Napf	1408m
1/Langnau i. E.	695m	3/Oberiberg	1090m
1/Luzern	456m	3/Vättis	948m
1/Meiringen	832m		
1/Montreux-Clarens	408m	4/Bosco Gurin	1505m
1/Neuchâtel	487m	4/Cimetta	1672m
1/Oeschberg	482m	4/Löbbia	1420m
1/Payerne	491m	4/Piotta	1007m
1/Pully	461m	4/Robbia/Poschia	1078m
1/Rheinfelden	271m	4/S. Maria/Müstair	1390m
1/Rueneberg	610m	4/San Bernardino	1628m
1/Schaffhausen	457m	4/Sils Maria	1802m
1/Schwyz (Ibach)	448m	4/Simplon Dorf	1495m
1/Sion-Aérodrome	483m		
1/St. Gallen	664m	5/Gd. St. Bernard	2479m
1/Stein am Rhein	786m	5/Grächen	1617m
1/Tänikon	536m	5/Hinterrhein	1619m
1/Tierfehd/Linthal	810m	5/Mauvoisin	1841m
1/Vaduz	460m	5/Montana	1495m
1/Visp (ASTA)	640m	5/Ospizio Bernina	2256m
1/Wädenswil	463m	5/Ried/Lötschental	1480m
1/Wynau	422m	5/Samedan	1705m
1/Zürich Flughafen	431m	5/Scuol (Schuls)	1295m
1/Zürich Reckenholz	443m	5/Ulrichen	1345m
1/Zürich SMA	569m	5/Zermatt	1638m
2/Chasseral	1599m	6/Grono	357m

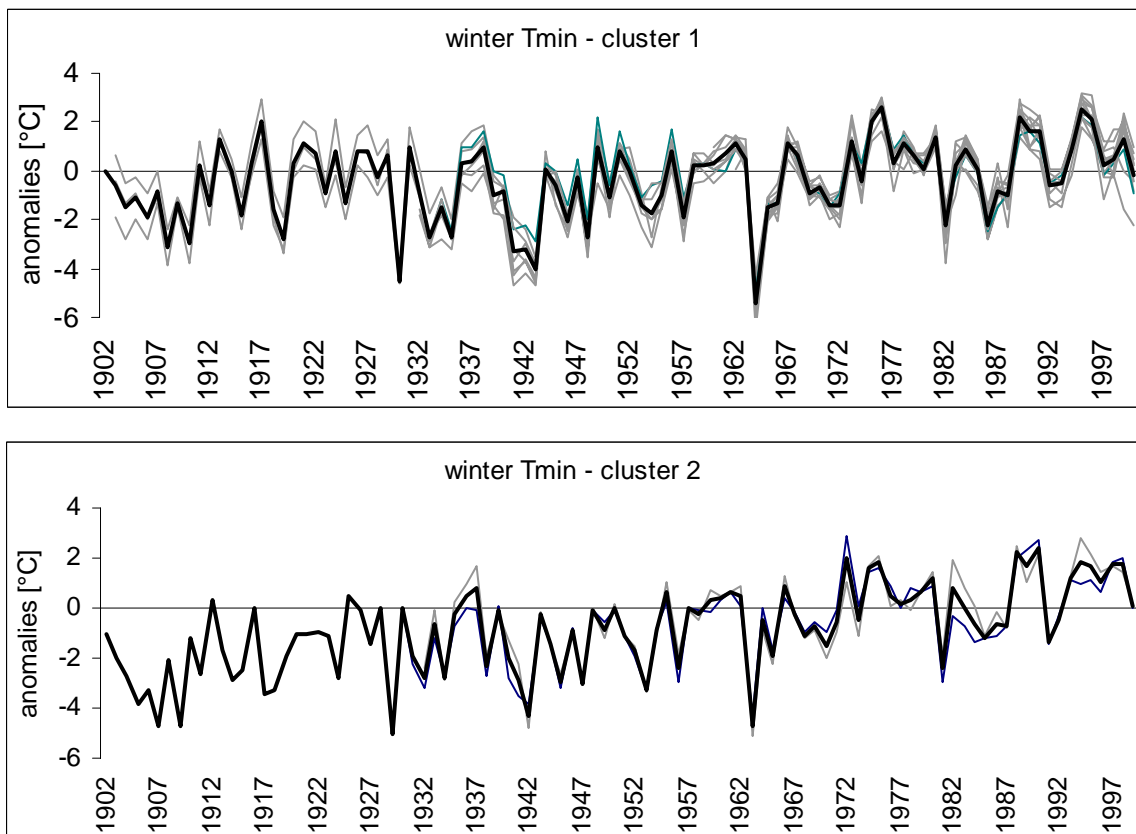
2/Corvatsch	3015m	6/Locarno-Magad.	197m
2/Grimsel Hospiz	1950m	6/Locarno-Monti	379m
2/Gütsch	2288m	6/Lugano	276m
2/Jungfrauoch	3572m	6/Stabio	353m
2/La Dôle	1672m		
2/Moleson	1972m		
2/Pilatus	2106m		
2/Säntis	2500m		
2/Weissfluhjoch	2540m		

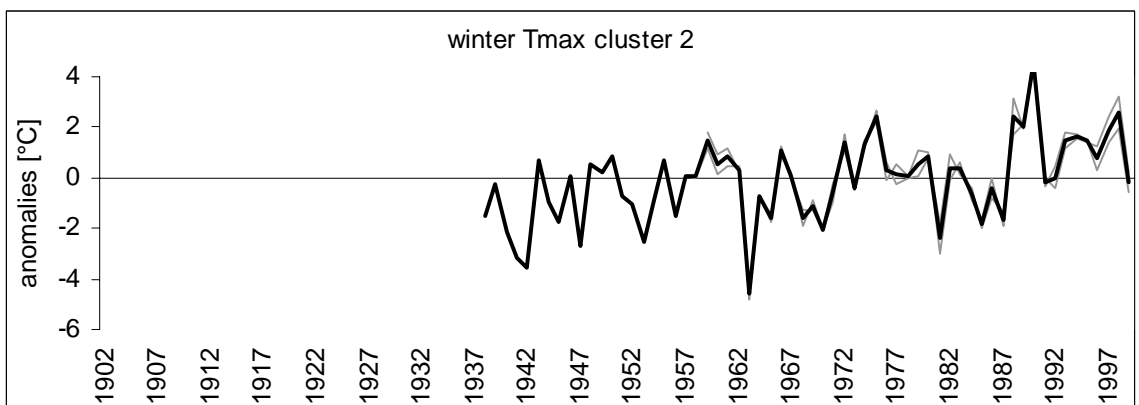
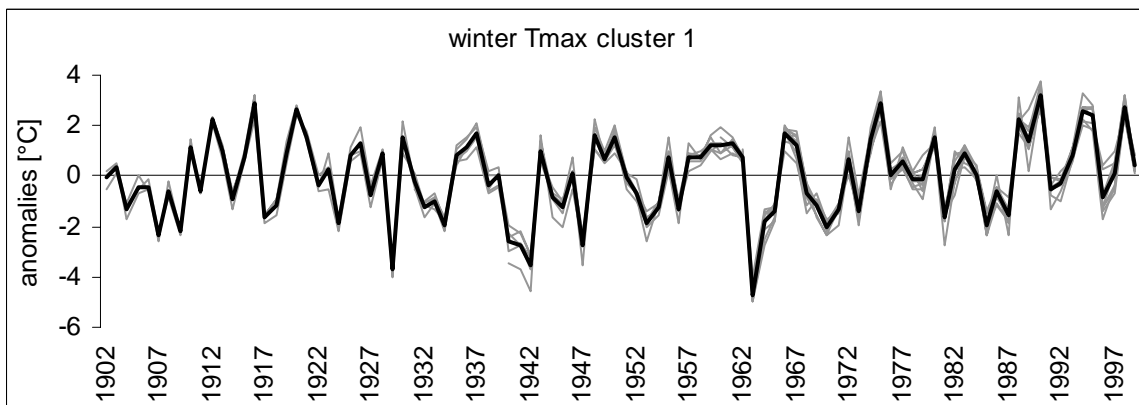
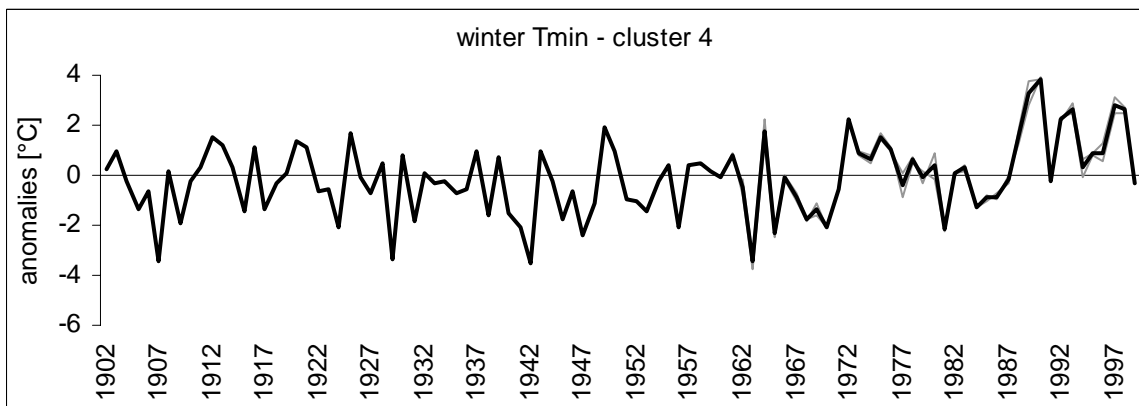
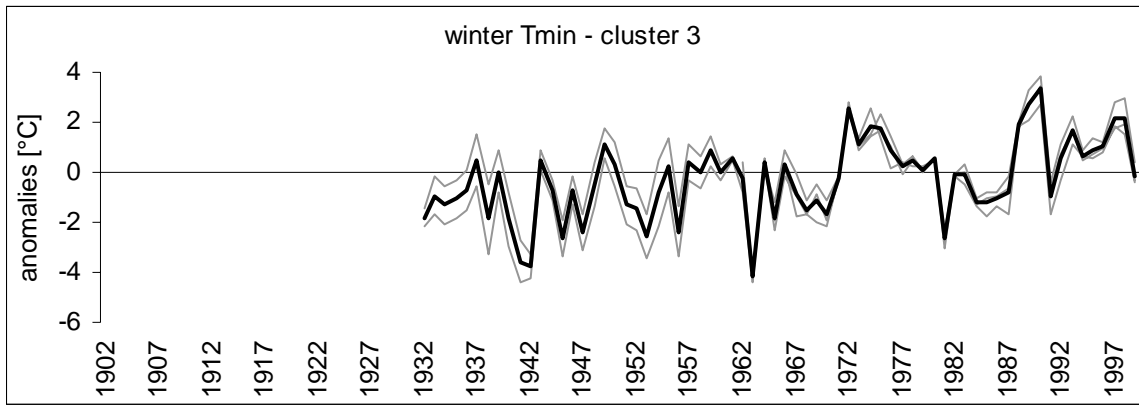
COMPARISON TO HOMOGENISED DATA SETS IN AUTUMN:

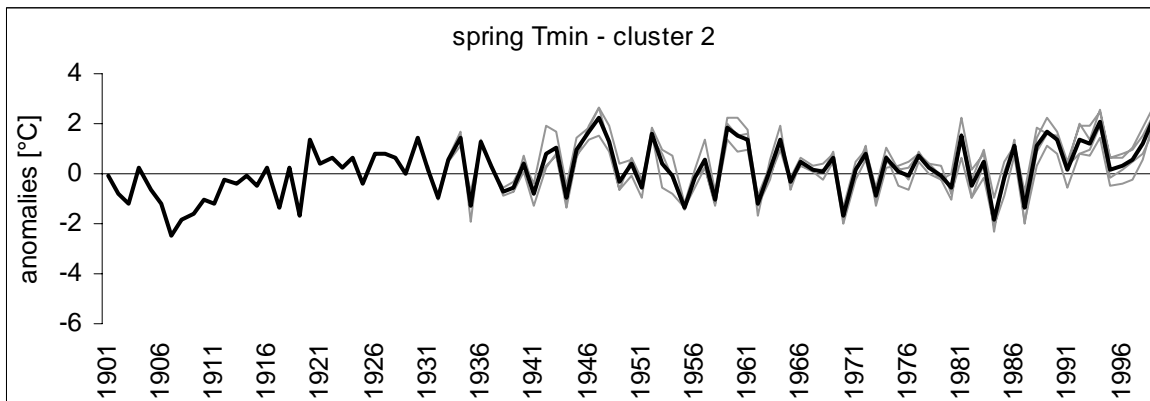
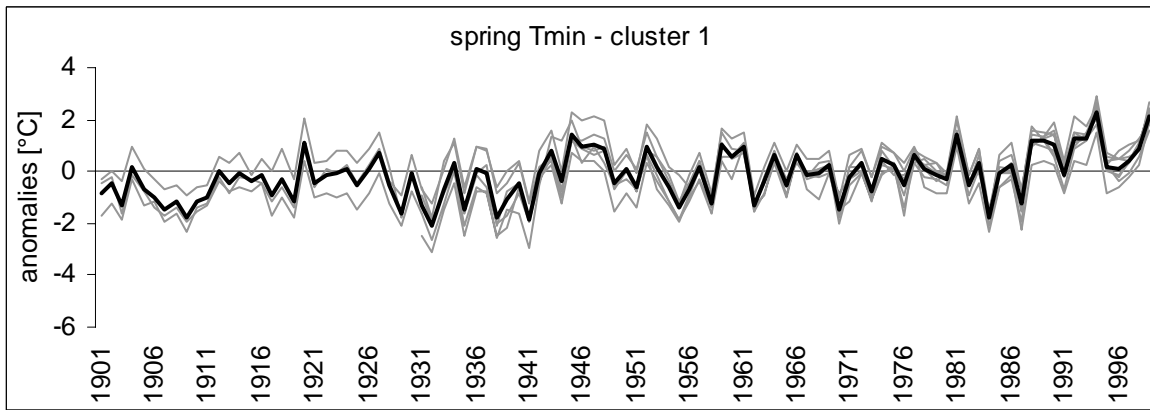
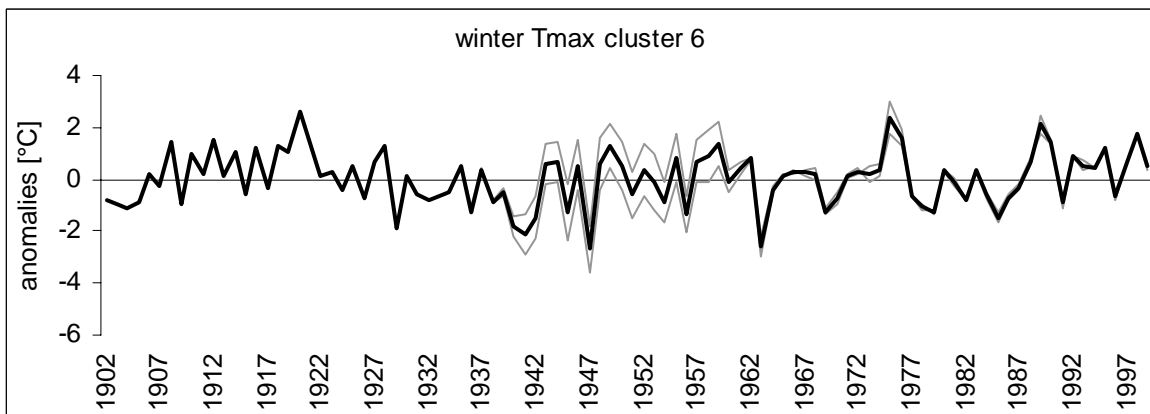
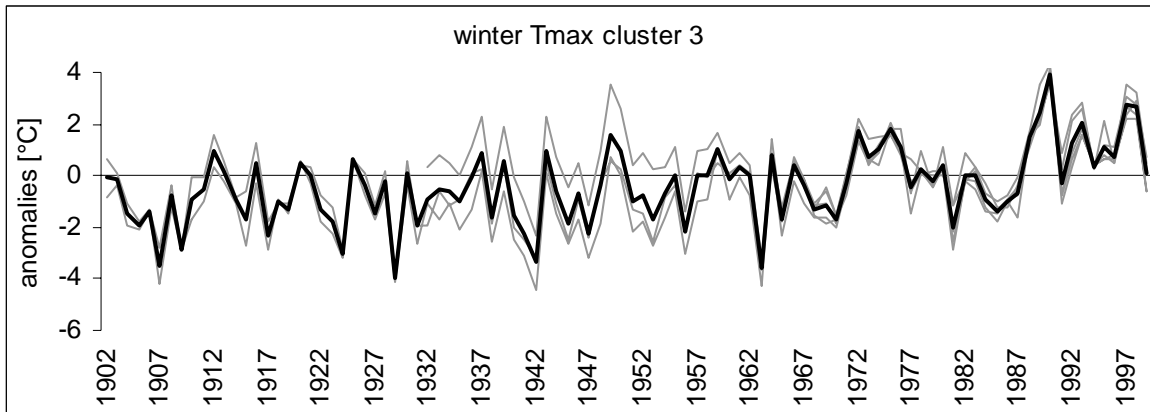
T _{min}		T _{max}	
<i>Cluster/Station</i>	<i>/ Corr.</i>	<i>Cluster/Station</i>	<i>/ Corr.</i>
1/Basel	0.98	1/Bad Ragaz	0.96
1/Bern	0.64	1/Basel	0.93
1/Delémont	0.99	1/Bern	0.99
1/Luzern	0.89	1/Delémont	0.99
1/Neuchâtel	0.97	1/Luzern	0.93
1/Oeschberg	0.99	1/Montreux - Clarens	0.99
1/Rheinfelden	0.93	1/Neuchâtel	0.98
1/Schaffhausen	0.97	1/Oeschberg	0.99
1/St. Gallen	0.97	1/Schaffhausen	0.92
2/Bad Ragaz	0.98	1/St. Gallen	0.84
2/Château d'Oex	0.99	2/Jungfrauoch	0.98
2/Chur	0.99	2/Säntis	0.98
2/Montreux - Clarens	0.99	3/Château d'Oex	0.97
3/Davos	0.94	3/Chur	0.97
3/Disentis	0.84	3/Davos	0.89
4/Arosa	0.99	3/Disentis	0.95
4/Montana	0.97	4/Robbia	0.96
5/Jungfrauoch	0.99	5/Montana	0.96
5/Säntis	0.99	6/Locarno - Monti	0.97
7/Locarno - Monti	0.51	6/Lugano	0.67
7/Lugano	0.99		
7/Robbia	0.81		

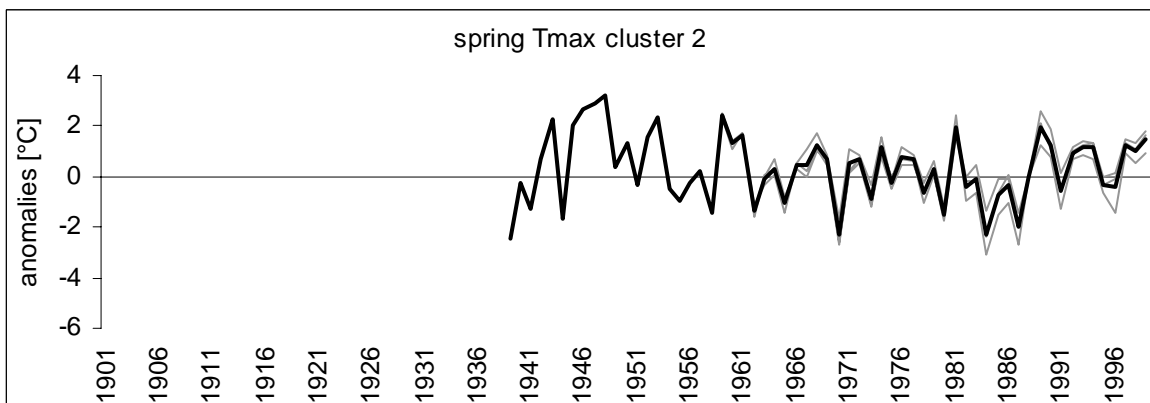
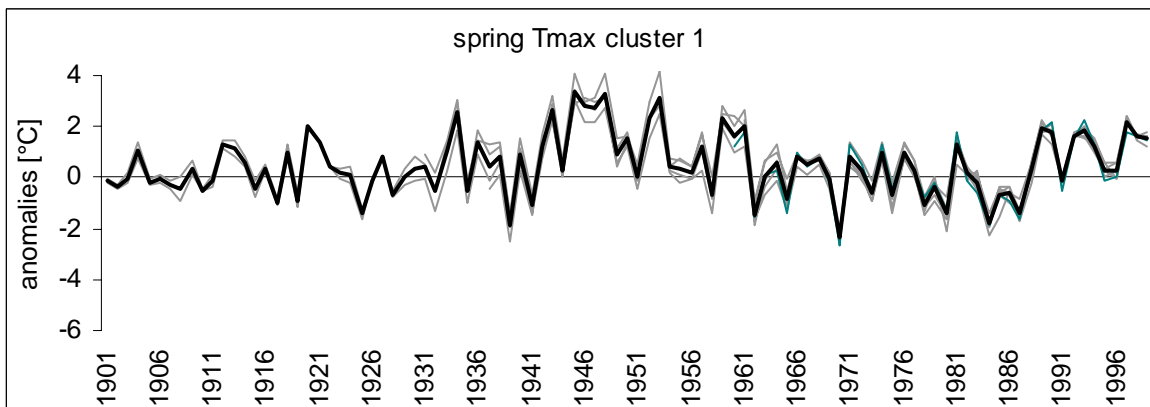
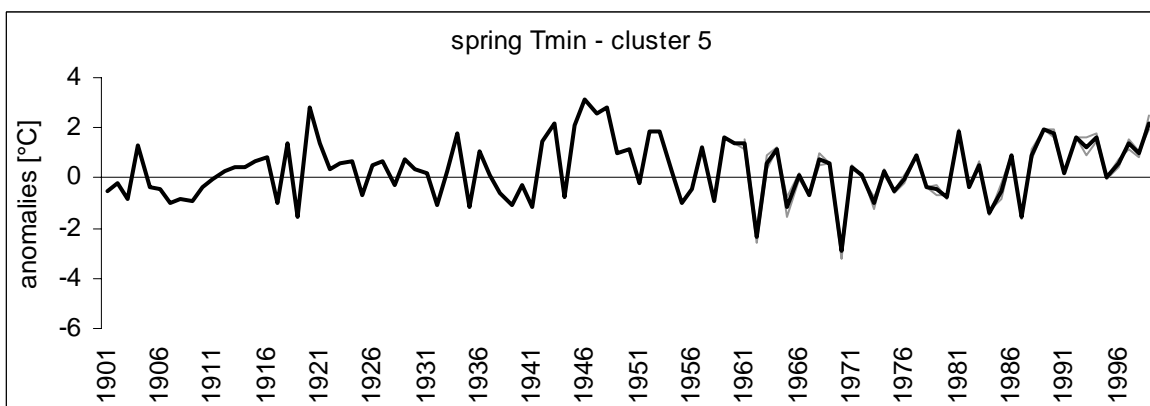
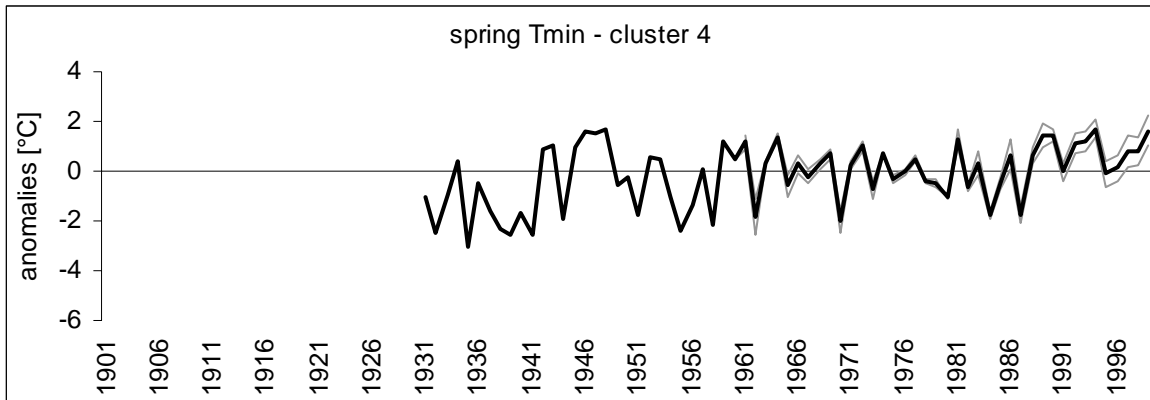
APPENDIX C

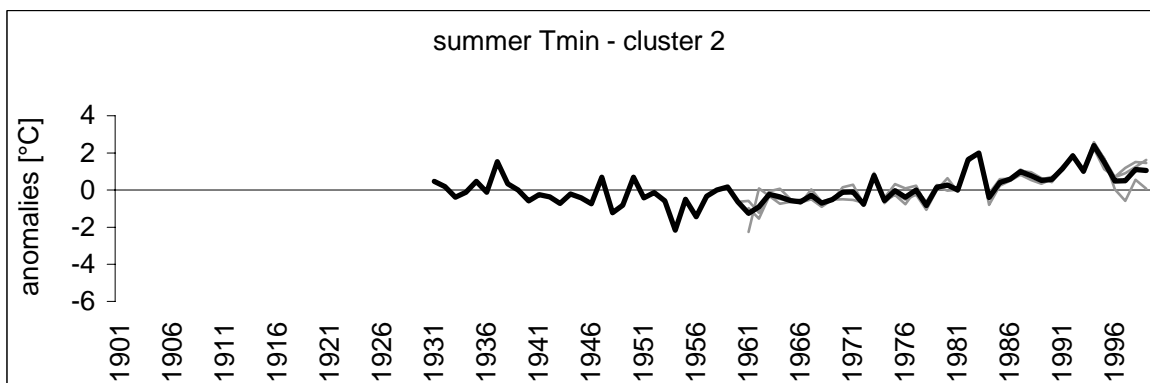
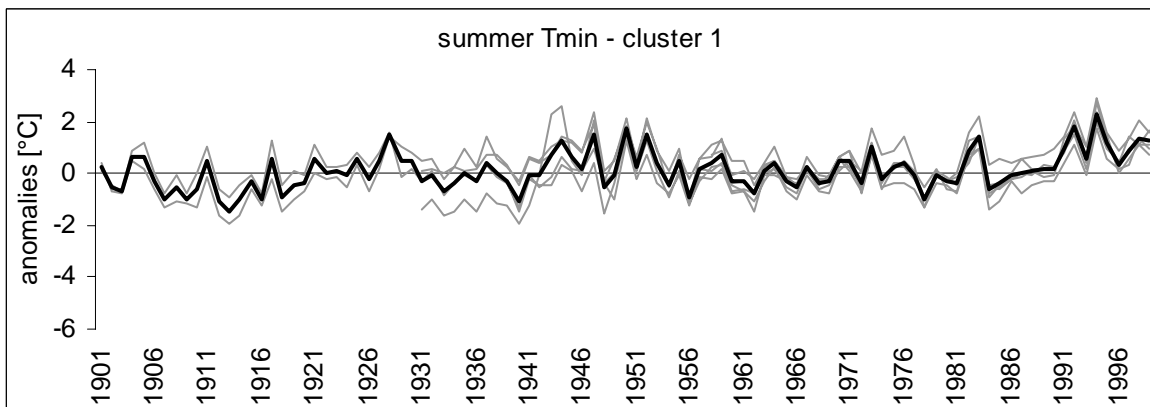
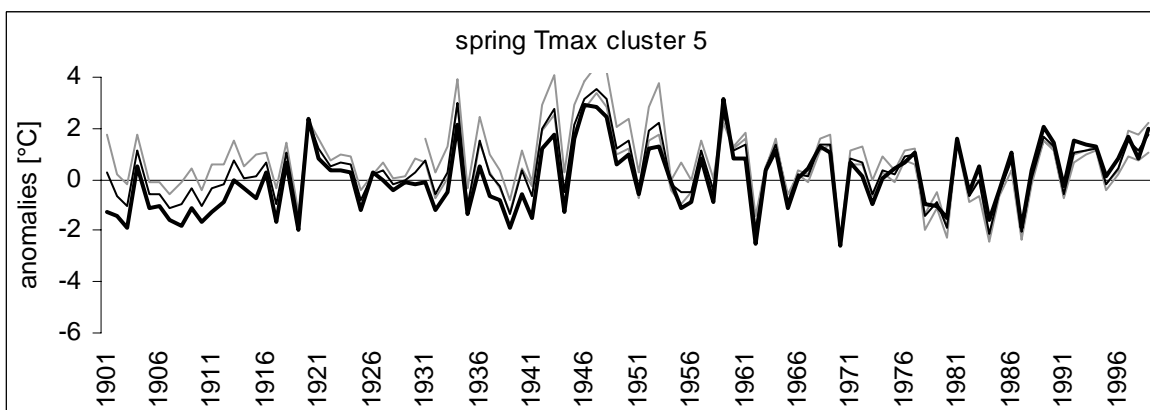
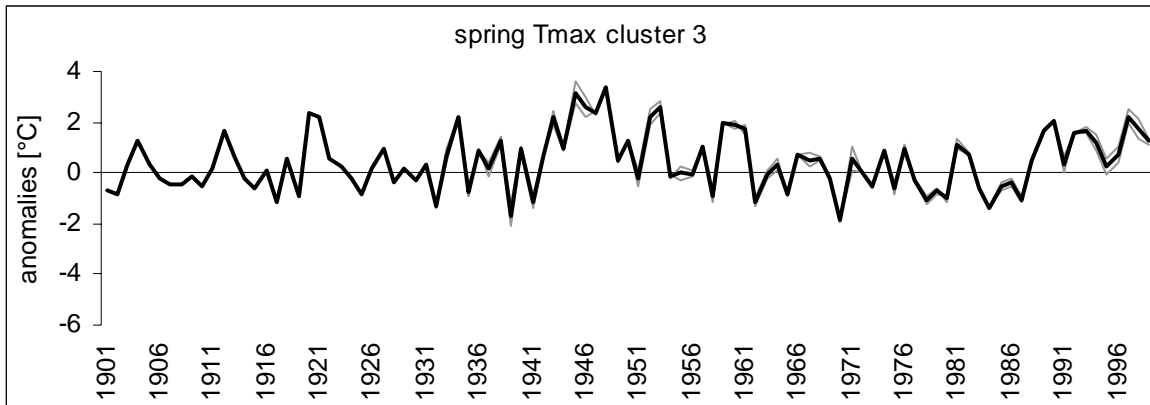
Mean time series for each of the regions established, which include more than one representative station. The black line represents the mean time series resulting out the time series of individual climatological stations (grey lines) considered as representative for the region (Chapter 3, Section 3.6). The mean time series are calculated on a daily time scale, which however, is too small to represent graphically thus the interannual time scale is depicted. Since the grouping of the single station time series is based on a PCA and CA a high correlation and comparable variability between the single time series is assured. In each cluster a highly significant correlation (over 99%) between the mean time series and each of the single time series results.

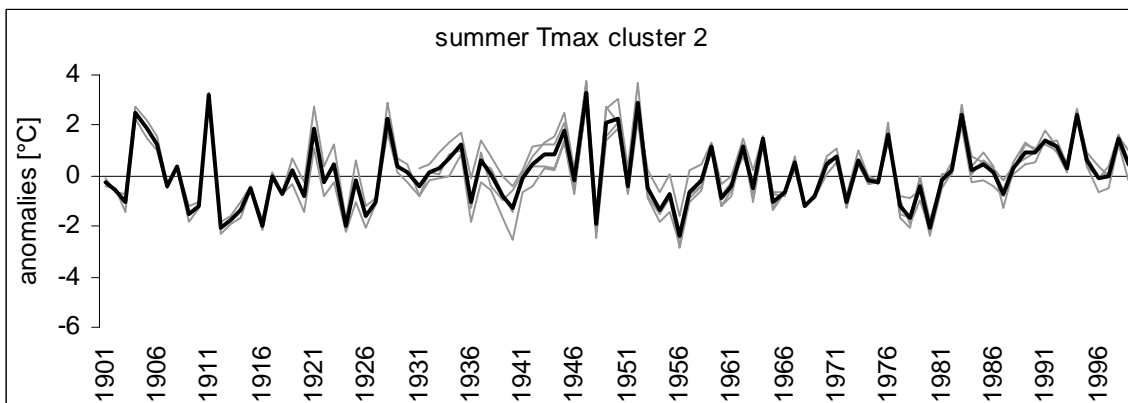
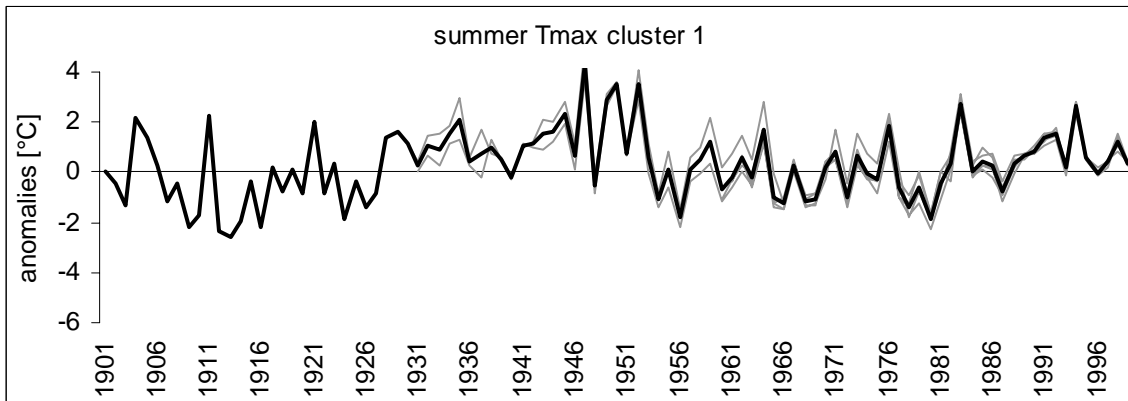
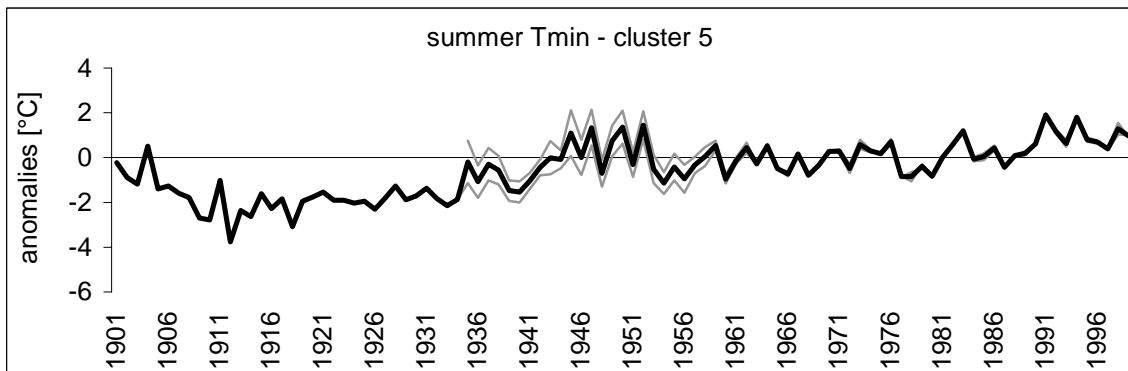
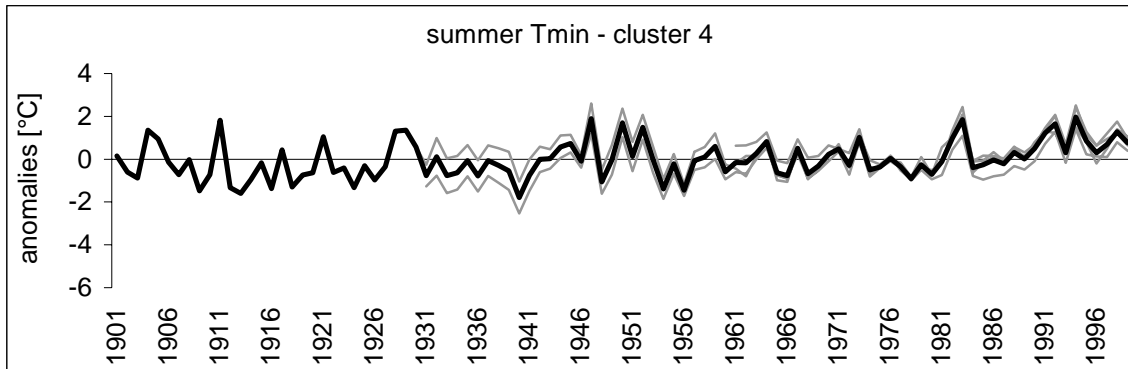


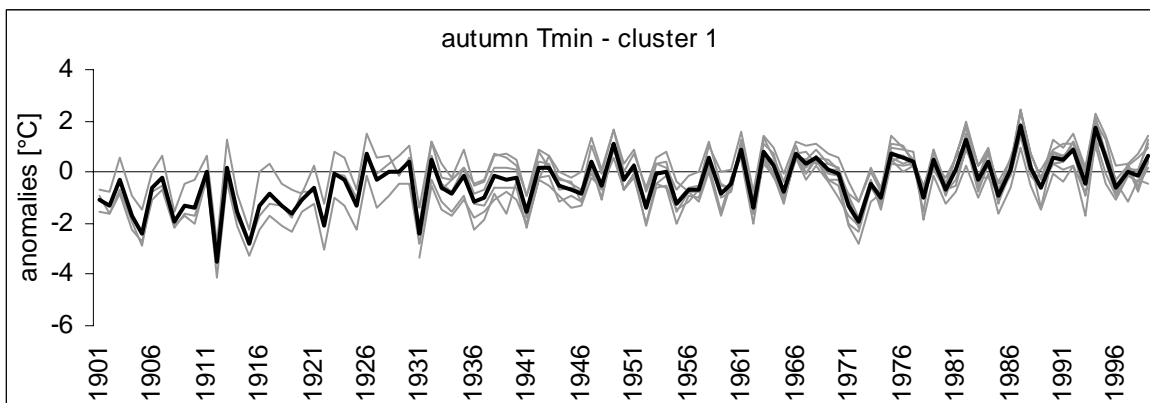
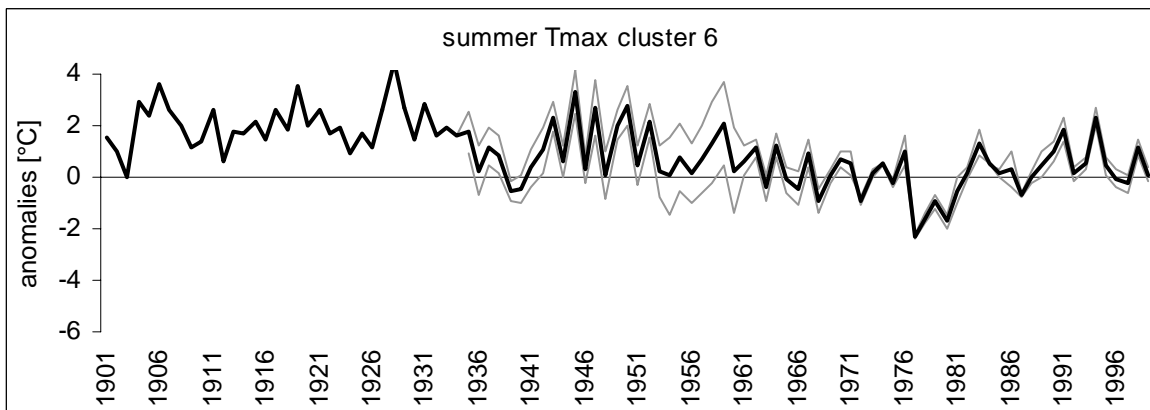
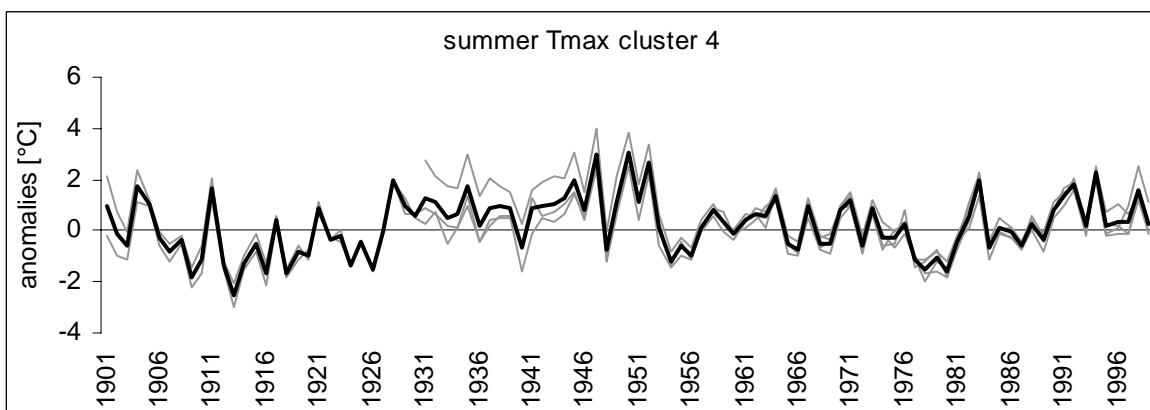
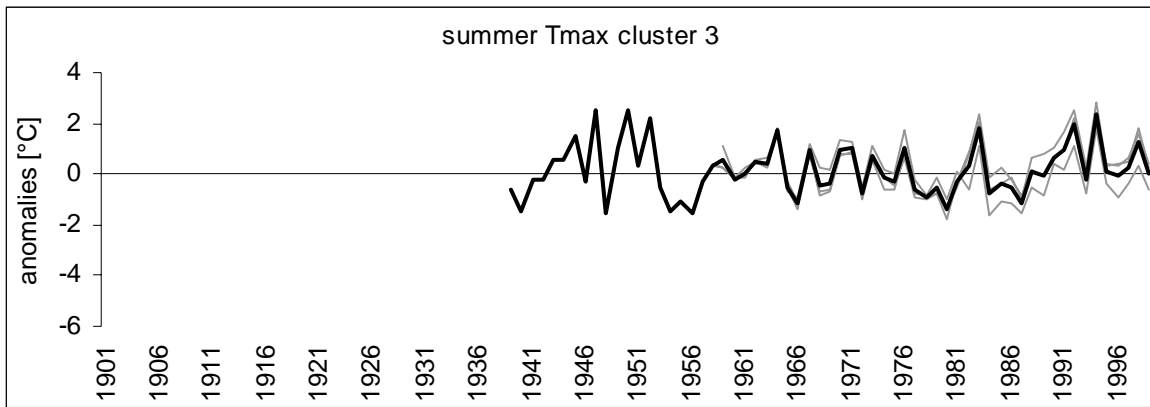


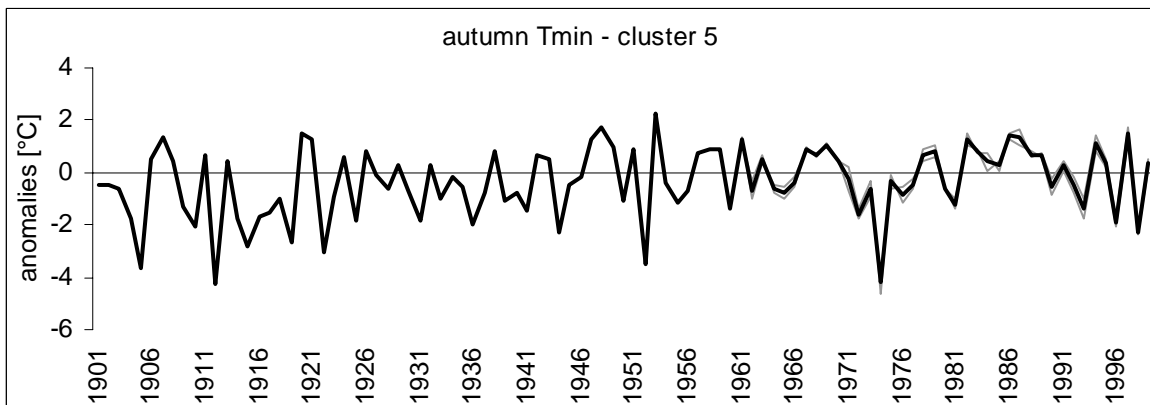
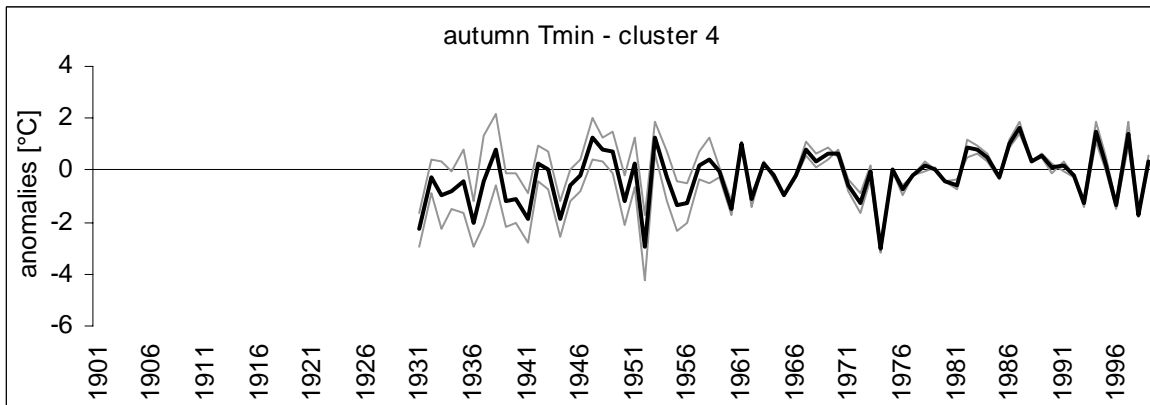
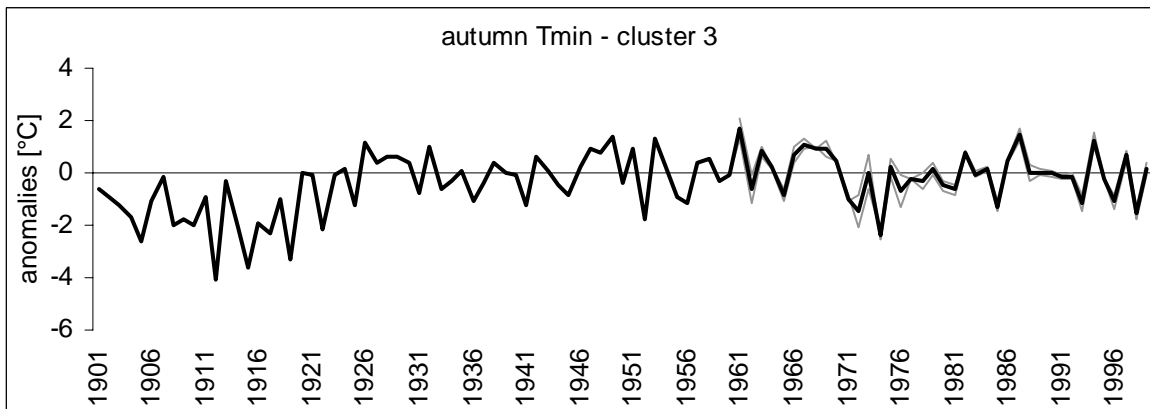
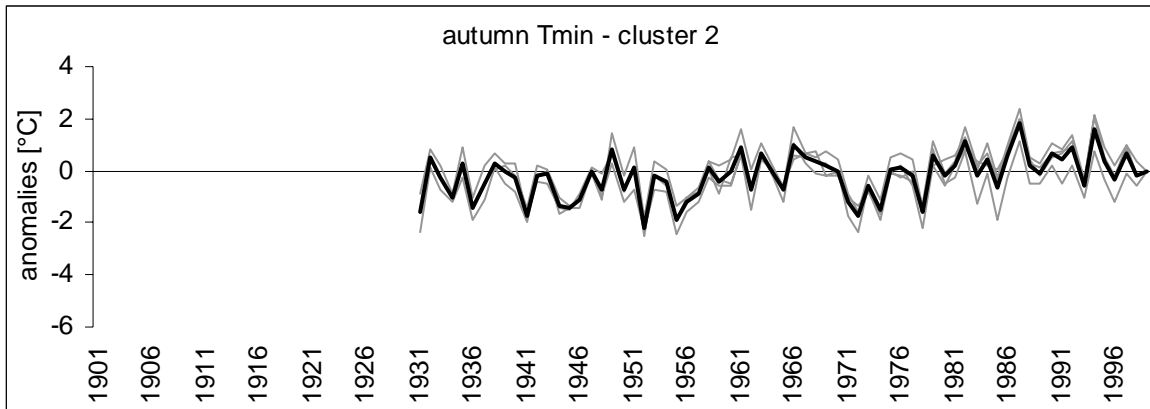


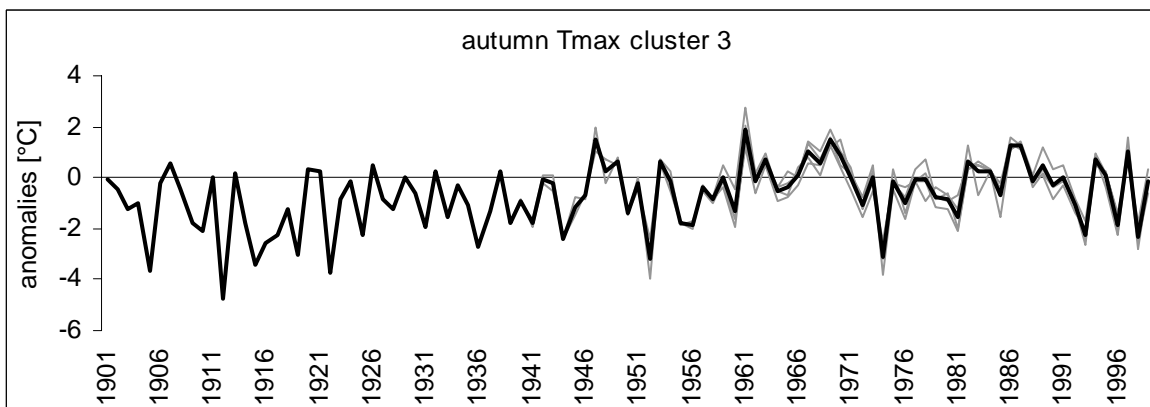
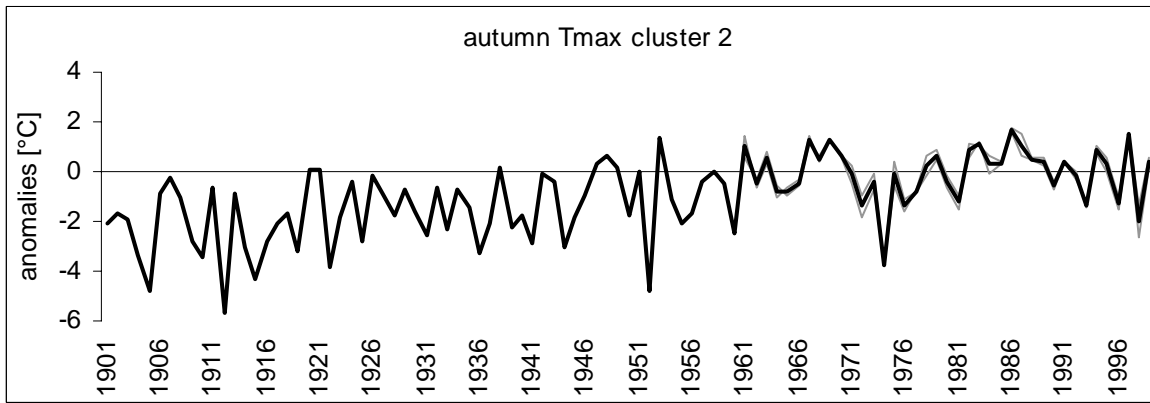
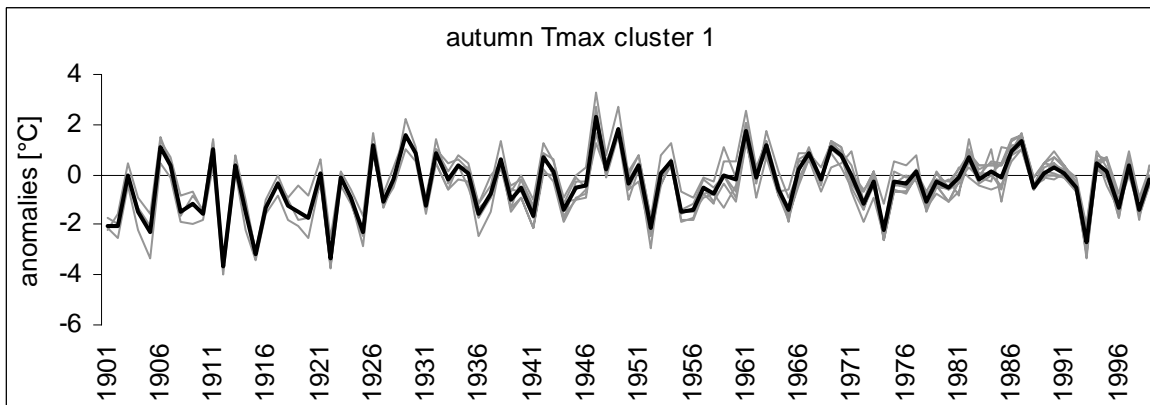
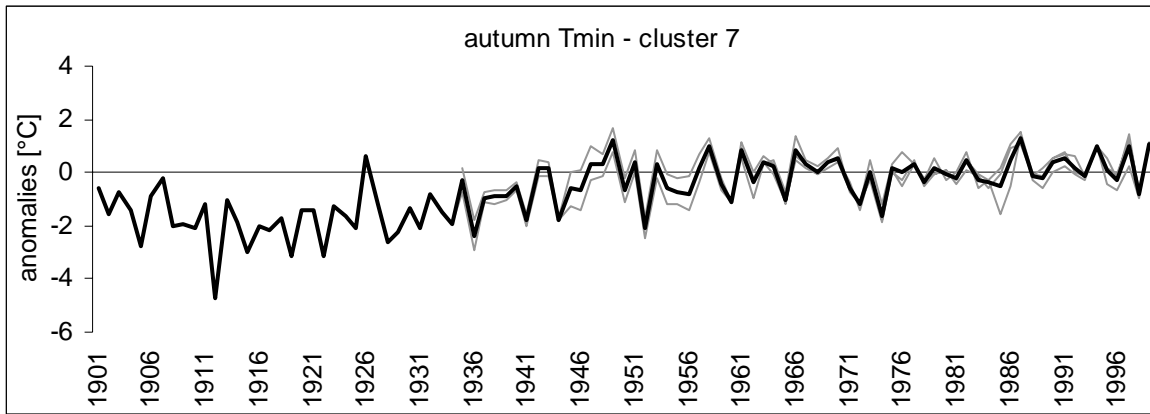


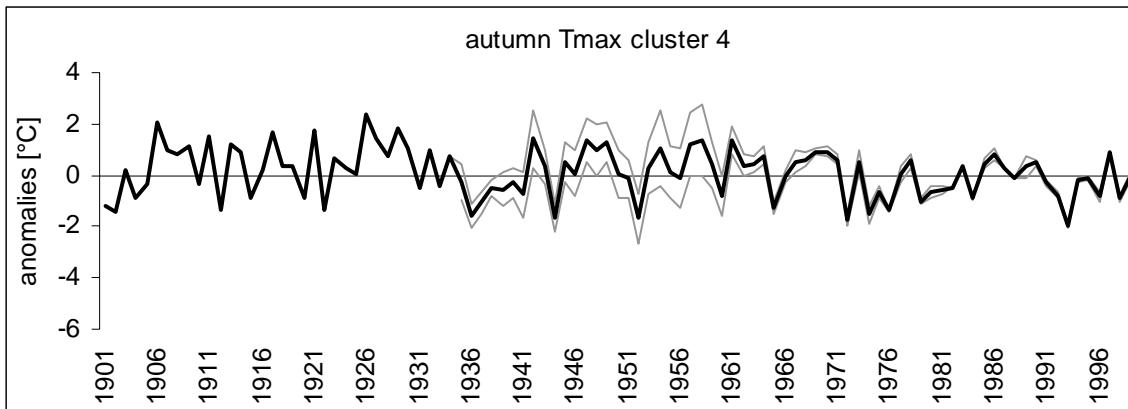










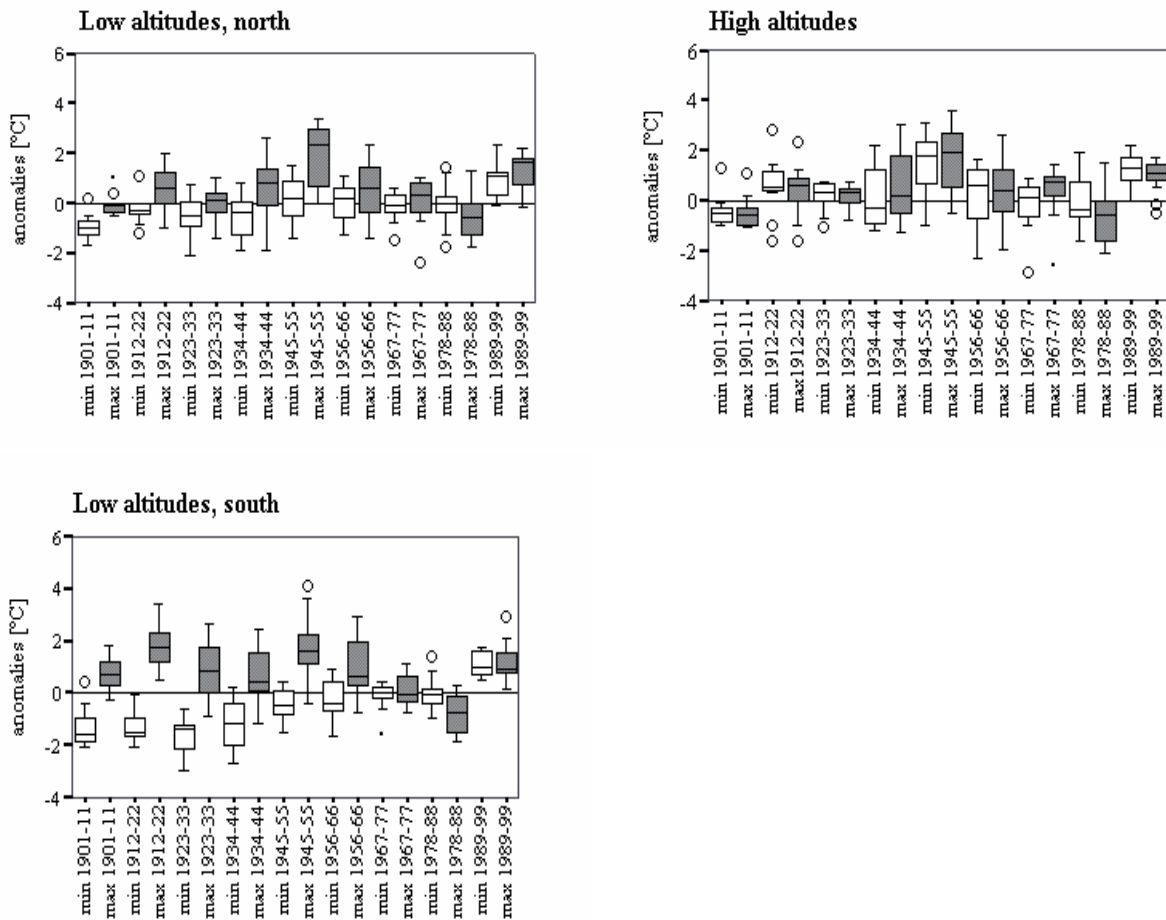


APPENDIX D

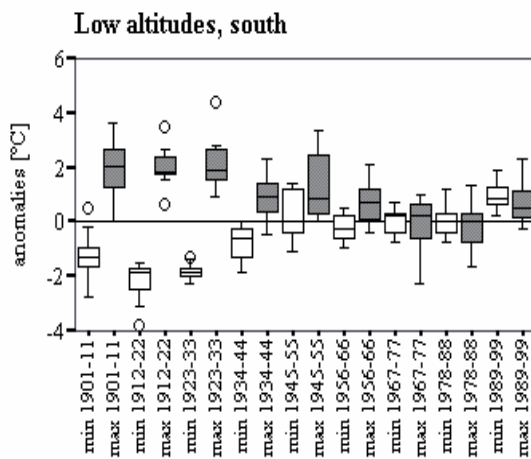
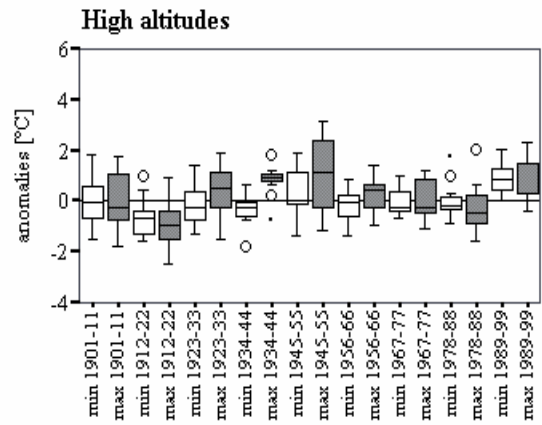
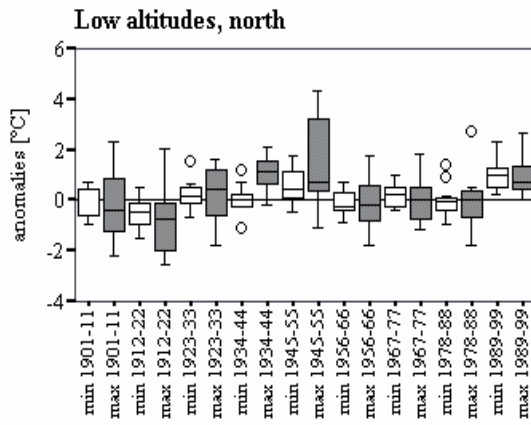
Boxplots of spring, summer, autumn minimum (white box) and maximum (grey box) temperature anomalies for different latitudes and altitudes in Switzerland. The period of 1901 to 1999 is divided into 9 periods of equal length.

The box comprises 50% of the values, its upper bound defines the 75 percentile, the lower bound the 25 percentile and the black line within the box pinpoints the median. The ends of the vertical lines mark the maximum and the minimum, which are not outliers. Outliers (black dots) are defined as values that are more than 1.5 box-lengths away from the 75 or 25 percentiles line.

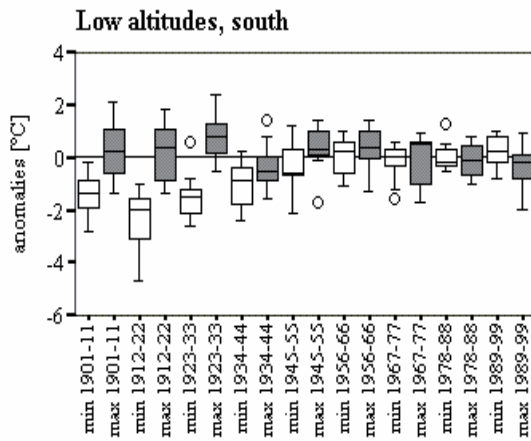
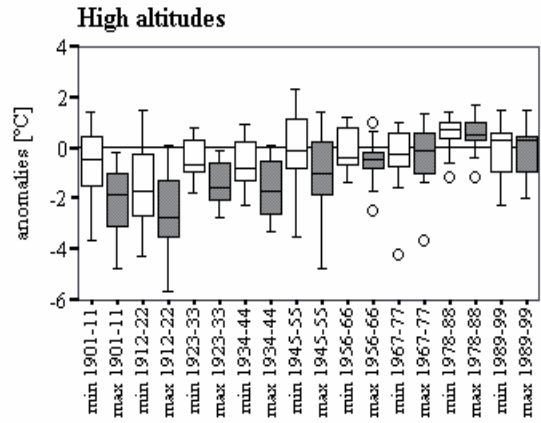
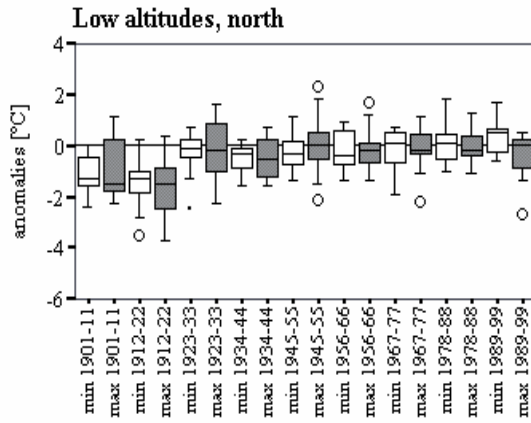
SPRING:



SUMMER:



AUTUMN:



CURRICULUM VITAE

Name: Patricia Jungo

Date and place of birth: October 1st, 1972 in Fribourg, Switzerland

Current Address: Chemin Monséjour 17, 1700 Fribourg

Citizenship: Düdingen and Fribourg

SCHOLAR FORMATION AND DIPLOMA OBTAINED:

01.10.97 – 30.09.01: PhD student under the supervision of Prof. Martin Beniston at the Institute of Geography, Dept. of Geoscience, University of Fribourg.

Title of the Dissertation: 20th century minimum and maximum temperature variations analysed on a regional scale in Switzerland. Statistical analyses of observational data.

October 1996: Diploma in geography, University of Fribourg

1992 – 1996: 8 semesters at the University of Fribourg. Principal branch: Geography; secondary branch I: Geology; secondary branches II: Physics and Computer Science; secondary branches III: Mineralogy and Computer Science.

Diploma Thesis at the aerological Station at Payerne directed by Mr P. Jeannet. Titel: Vergleiche zwischen Ozonkonzentrationen auf dem Jungfrauoch und aerologischen Ozonsondierungen bei Payerne auf der Höhe des Jungfrauochs, insbesondere während sommerlichen Smoglagen.

July 1992: Bac à l'aureat diploma Type E, Collège St. Michel, Fribourg

June 1989: High-School diploma, Western Boone High School, Indiana (USA)

1988 – 1992: High-School/College at Collège St. Michel in Fribourg

1979 – 1988: Elementary school at Schmitten and Tafers